



University
of Glasgow

von Thun, Anne (2012) *The role of ERK2 in controlling tumour cell invasion*. PhD thesis.

<http://theses.gla.ac.uk/3176/>

Copyright and moral rights for this thesis are retained by the Author

A copy can be downloaded for personal non-commercial research or study, without prior permission or charge

This thesis cannot be reproduced or quoted extensively from without first obtaining permission in writing from the Author

The content must not be changed in any way or sold commercially in any format or medium without the formal permission of the Author

When referring to this work, full bibliographic details including the author, title, awarding institution and date of the thesis must be given

The role of ERK2 in controlling tumour cell invasion

Anne von Thun, B.Sc. (Hons)

Thesis submitted to the University of Glasgow for the degree of
Doctor of Philosophy

September 2011

Beatson Institute for Cancer Research
Garscube Estate
Switchback Road
Glasgow, G61 1BD

Abstract

Upregulation of the extracellular signal-regulated kinase (ERK) pathway has been shown to contribute to tumour invasion and progression. Since the two predominant ERK isoforms (ERK1 and ERK2) are highly homologous and have indistinguishable kinase activities *in vitro*, both enzymes were believed to be redundant and interchangeable. To challenge this view, here we show that ERK2 silencing inhibits invasive migration of MDA-MB-231 cells, and re-expression of ERK2 (but not ERK1) restores the normal invasive phenotype. A detailed quantitative analysis of cell movement on 3D matrices indicates that ERK2 knockdown impairs cellular motility by decreasing the migration velocity as well as increasing the time that cells remain stationary. We used gene expression arrays to identify *rab17* and *liprin-β2* as genes whose expression was increased by knockdown of ERK2 and restored to normal levels following re-expression of ERK2 (but not ERK1). Moreover, we established that both Rab17 and Liprin-β2 play inhibitory roles in the invasive behaviour of three independent cancer cell lines, indicating a suppressive role for these proteins in tumour progression. Importantly, knockdown of either Rab17 or Liprin-β2 restores invasiveness of ERK2-depleted cells, indicating that ERK2 drives invasion of MDA-MB-231 cells by suppressing expression of these genes.

Taken together, our data provides evidence that true functional disparities between ERK1 and ERK2 exist with regards to cell migration and identifies Rab17 and Liprin-β2 as two novel motility suppressors downstream of ERK2.

Table of contents

ABSTRACT	2
TABLE OF CONTENTS	3
LIST OF FIGURES	7
AUTHOR'S DECLARATION	9
ACKNOWLEDGEMENTS	10
ABBREVIATIONS	11
1 INTRODUCTION	15
1.1 THE NATURE OF CANCER	15
1.1.1 <i>Hallmarks of malignancy</i>	15
1.1.2 <i>Invasion-metastasis cascade</i>	18
1.1.3 <i>Modes of tumour cell migration</i>	21
1.1.3.1 Amoeboid migration	21
1.1.3.2 Mesenchymal migration	23
1.1.3.3 Collective cell migration.....	23
1.1.3.4 Plasticity in tumour cell migration	24
1.2 MAMMALIAN MAPK PATHWAYS	27
1.2.1 <i>The history of the MAPK cascade</i>	27
1.2.2 <i>Overview of the six distinct mammalian MAPK pathways</i>	27
1.2.2.1 c-Jun N-terminal kinases (JNKs)/stress-activated protein kinases (SAPK)	29
1.2.2.2 p38 kinases.....	30
1.2.2.3 ERK5	32
1.2.2.4 ERK3/4.....	33
1.2.2.5 ERK7	34
1.2.3 <i>MAPK docking sites</i>	35
1.2.3.1 Common docking site.....	35
1.2.3.2 ERK docking site	38
1.2.3.3 FXFP binding site	38
1.2.3.4 Other MAPK-binding domains	38
1.2.3.5 Kinase inhibitor binding sites	39
1.3 THE ERK-MAPK PATHWAY	40
1.3.1 <i>ERK1/2 isoforms and splice variants</i>	41
1.3.2 <i>ERK signalling specificity</i>	45
1.3.2.1 Regulation of ERK activity through protein phosphatases.....	45
1.3.2.2 Regulation of ERK activity through upstream and downstream scaffold proteins	49
1.3.2.3 Localising ERK activity to specific subcellular compartments	56
1.3.2.4 Regulating ERK activity through feedback loops.....	57
1.4 THE ERK-MAPK PATHWAY IN CANCER	60
1.4.1 <i>Activating mutations of the ERK-MAPK pathway</i>	60
1.4.2 <i>The role of ERK in growth and proliferation</i>	62
1.4.3 <i>The role of ERK in cell survival</i>	65
1.4.4 <i>The role of ERK in cell migration</i>	67
1.4.5 <i>The role of ERK in angiogenesis</i>	70
1.4.6 <i>ERK-MAPK pathway and multi-drug resistance</i>	71
1.4.7 <i>Inhibiting ERK signalling as a therapeutic strategy</i>	73
1.5 PROJECT AIMS.....	75
2 MATERIALS AND METHODS	76
2.1 MATERIALS	76
2.1.1 <i>Reagents</i>	76
2.1.2 <i>Solutions</i>	79
2.1.3 <i>Antibodies and dyes</i>	80
2.1.4 <i>Enzymes and kits</i>	81
2.1.5 <i>Primers for qPCR</i>	82
2.1.6 <i>Tissue culture plastic ware</i>	83
2.2 METHODS	84
2.2.1 <i>Molecular biology</i>	84

2.2.1.1	Polymerase chain reaction (PCR)	84
2.2.1.2	Agarose gel electrophoresis.....	85
2.2.1.3	Restriction digestion	85
2.2.1.4	Ligation of DNA	85
2.2.1.5	Recombination.....	86
2.2.1.6	Site-directed mutagenesis	88
2.2.1.7	Bacterial strains.....	88
2.2.1.8	Heat-shock transformation of competent bacteria	88
2.2.1.9	Plasmid preparation (Miniprep).....	89
2.2.1.10	Plasmid preparation (Maxiprep).....	89
2.2.2	Tissue Culture	89
2.2.2.1	Cell origin	89
2.2.2.2	Cultivation of cells.....	90
2.2.2.3	Freezing and thawing of cells.....	90
2.2.2.4	Transfection using the Amaxa™ Nucleofector™	91
2.2.2.5	Transfection using HiPerFect	91
2.2.2.6	Cell proliferation assays	92
2.2.2.7	Inverted invasion assay.....	92
2.2.2.8	Generation of cell-derived matrix.....	93
2.2.2.9	Migration on cell-derived matrix	94
2.2.2.10	Scratch wound assays	94
2.2.2.11	Immunofluorescence	94
2.2.3	Protein biology	95
2.2.3.1	Cell lysis.....	95
2.2.3.2	Protein quantification	97
2.2.3.3	Co-immunoprecipitation.....	97
2.2.3.4	SDS-PAGE and Coomassie staining	97
2.2.3.5	Western Blotting.....	98
2.2.4	Microarray screen and validation	98
2.2.4.1	RNA extraction and quality control.....	98
2.2.4.2	RNA labelling for the microarray screen	98
2.2.4.3	Microarray data analysis.....	99
2.2.4.4	First strand cDNA synthesis.....	99
2.2.4.5	qPCR.....	100
2.2.4.6	Statistical analysis	101
3	ERK2 BUT NOT ERK1 CONTRIBUTES TO INVASIVE CELL MIGRATION	102
3.1	INTRODUCTION	102
3.1.1	<i>Common features of ERK1 and ERK2</i>	102
3.1.2	<i>ERK isoforms in whole animal studies</i>	104
3.1.3	<i>ERK isoforms in cell culture studies</i>	105
3.1.4	<i>ERK isoforms and tumourigenesis</i>	106
3.2	RESULTS	107
3.2.1	<i>The invasive phenotype of A2780-Rab25 cells is dependent on ERK signalling</i>	107
3.2.2	<i>Silencing of ERK2 impairs invasion into Matrigel</i>	109
3.2.3	<i>Transient knockdown of ERK does not induce apoptosis or alter proliferation in A2780-Rab25 cells</i>	112
3.2.4	<i>Both ERK isoforms contribute to migration on plastic surfaces</i>	115
3.2.5	<i>Knockdown of ERK2 impairs migration on cell-derived matrices</i>	118
3.2.6	<i>ERK2 promotes invasion in the breast cancer cell line MDA-MB-231</i>	123
3.2.7	<i>Transient ERK silencing in MDA-MB-231 cells has no effect on apoptosis or proliferation</i>	125
3.2.8	<i>Migration of MDA-MB-231 cells on plastic surfaces is impaired following knockdown of ERK2</i>	127
3.2.9	<i>Silencing of ERK2 impairs migration on CDM in MDA-MB-231 cells</i>	129
3.2.10	<i>Expression of recombinant ERK2 (but not ERK1) restores the migratory characteristics of MDA-MB-231 cells after ERK2 knockdown</i>	132
3.3	DISCUSSION	136
3.3.1	<i>Summary</i>	136
3.3.2	<i>Discrepancy between migration in 2D and 3D in A2780-Rab25 cells</i>	136
3.3.3	<i>Roles of ERK in tumour cell migration</i>	137
3.3.4	<i>Isoform-specific functions for ERK1 and ERK2</i>	138
4	ERK2 REGULATES EXPRESSION OF CSF2, RAB17 AND LIPRIN-B2 IN 3D MICROENVIRONMENTS	142

4.1	INTRODUCTION	142
4.1.1	<i>Regulation of gene expression through ERK1/2</i>	142
4.1.2	<i>Nuclear translocation of ERK1/2</i>	144
4.1.3	<i>The role of extracellular matrix adhesions on nuclear ERK signalling</i>	145
4.1.4	<i>Experimental paradigm</i>	146
4.2	RESULTS	148
4.2.1	<i>Microarray analysis identified an ERK2-specific gene expression signature</i>	148
4.2.1.1	Quality control of microarray samples.....	148
4.2.1.2	Normalisation of microarray data yields good clustering of experimental replicas	151
4.2.1.3	Microarray analysis identifies genes whose expression is down-regulated following ERK2 knockdown.....	153
4.2.1.4	Microarray analysis identifies genes whose expression is up-regulated following ERK2 knockdown.....	156
4.2.2	<i>Validation of ERK2-dependent gene expression using qRT-PCR</i>	159
4.2.2.1	qRT-PCR primer pairs amplify a single product in a linear manner over a range of cDNA concentrations	159
4.2.2.2	ERK2 (but not ERK1) regulates the expression of CSF2, Rab17 and Liprin- β 2 in cells attached to CDM	163
4.2.2.3	Single siRNA oligos confirm an induction of Rab17 and Liprin- β 2 expression following ERK2 depletion.....	168
4.2.2.4	ERK2 also acts to suppress Rab17 and Liprin- β 2 when cells are grown on plastic	170
4.2.2.5	Regulation of CSF2, Rab17 and Liprin- β 2 is dependent on MEK activity	172
4.2.2.6	Rab17 and Liprin- β 2 transcription is suppressed by CSF2	174
4.3	DISCUSSION	176
4.3.1	<i>Summary</i>	176
4.3.2	<i>ERK2 as a regulator of transcriptional initiation</i>	176
4.3.3	<i>Post-transcriptional regulation of gene expression</i>	179
4.3.4	<i>ERK signalling differs between 2D and 3D microenvironments</i>	180
4.3.5	<i>Correlation between mRNA abundance and protein levels</i>	180
4.3.6	<i>Other potentially interesting microarray hits</i>	181
5	RAB17 AND LIPRIN-B2 ARE INHIBITORS OF TUMOUR CELL MIGRATION AND INVASION.....	183
5.1	INTRODUCTION	183
5.1.1	<i>Rab17 - a member of the RAB family of GTPases</i>	183
5.1.2	<i>Liprins – a family of LAR-interacting proteins</i>	187
5.2	RESULTS	191
5.2.1	<i>Knockdown of Rab17 and Liprin-β2 promotes tumour cell invasion of MDA-MB-231 cells</i>	191
5.2.2	<i>Depletion of Rab17 and Liprin-β2 promote invasion of A2780-Rab25 and BE cells</i>	194
5.2.3	<i>Overexpression of Rab17 and Liprin-β2 impairs invasion into Matrigel and migration on cell-derived matrix</i>	196
5.2.4	<i>ERK2 drives invasive cell migration of MDA-MB-231 cells by suppressing expression of Rab17 and Liprin-β2</i>	199
5.2.5	<i>ERK2 drives migration on plastic surfaces but not through Rab17 and Liprin-β2</i>	203
5.2.6	<i>Rab17 localises to early and recycling endosomes</i>	205
5.2.7	<i>Rab17 vesicles are positive for β1 integrin</i>	207
5.3	DISCUSSION	209
5.3.1	<i>Summary</i>	209
5.3.2	<i>Rab17 – a novel suppressor of cell motility</i>	209
5.3.3	<i>Liprin-β2 – a novel inhibitor of cell motility</i>	210
5.3.4	<i>Rab17 and Liprin-β2 - members of the same signalling circuit</i>	211
5.3.5	<i>Rab17 and Liprin-β2 and their potential roles in cancer</i>	214
6	SUMMARY AND FUTURE DIRECTIONS.....	216
6.1	FINAL SUMMARY	216
6.2	FUTURE DIRECTIONS	217
	LIST OF REFERENCES.....	222

List of tables

Table 1-1 Overview of all Mammalian MAPK identified	28
Table 1-2 Overview of the common and divergent features of the 6 distinct mammalian MAPK pathways	31
Table 1-3 Overview of proposed D-motifs of various MAPK substrates.....	36
Table 1-4 Common and distinct features of the alternatively spliced ERK1 isoforms.....	44
Table 1-5 Overview of the different groups of ERK phosphatases	46
Table 1-6 Mammalian scaffold proteins for the ERK-MAPK pathway	51
Table 1-7 <i>Bona fide</i> ERK substrates grouped according to their biological functions	63
Table 2-1 List of all reagents	78
Table 2-2 List of all solutions	79
Table 2-3 Antibodies and dyes.....	80
Table 2-4 List of kits	81
Table 2-5 List of Qiagen Quantitect primers	82
Table 2-6 List of plastic ware and supplier	83
Table 2-7 Comparison of different lysis buffers: Composition and Application	96
Table 5-1 Overview of known and putative Rab17 interaction partners as determined by high-throughput experiments	186
Table 5-2 Overview of known and putative Liprin- β 2 interaction partners as determined by high-throughput experiments	190

List of figures

Figure 1-1 Nine hallmarks acquired by cancer	16
Figure 1-2 The invasion-metastasis cascade	19
Figure 1-3 Characteristics of different modes of migration.....	22
Figure 1-4 Plasticity of tumour cell migration.....	26
Figure 1-5 MAPK docking sites	37
Figure 1-6 Structural differences between ERK1b and ERK1c	42
Figure 1-7 ERK signalling is regulated by cytoplasmic and nuclear phosphatases.....	47
Figure 1-8 Subcellular localisation of ERK activity through scaffold proteins.....	50
Figure 1-9 ERK pathway regulation by feedback loops	58
Figure 1-10 Role of ERK in cell contractility and focal adhesion disassembly	69
Figure 2-1 Schematic outline of the Gateway®-system	87
Figure 3-1 Sequence comparison of human ERK1 and ERK2	103
Figure 3-2 The invasive phenotype of A2780-Rab27 cells is dependent on ERK signalling	108
Figure 3-3 Suppression of ERK2 levels reduces invasiveness of A2780-Rab25 cells	110
Figure 3-4 siRNA of ERK2 opposes invasion into matrigel	111
Figure 3-5 siRNA of ERK1 or ERK2 does not induce apoptosis or inhibit proliferation.....	113
Figure 3-6 Both ERK isoforms contribute towards migration on plastic in A2780-Rab25 cells.....	116
Figure 3-7 Cell-derived matrices (CDM) represent a 3D-like environment.....	119
Figure 3-8 siRNA of ERK2 reduces migration of A2780-Rab25 cells on CDM	120
Figure 3-9 Knockdown of ERK2 decreases the momentary velocity and increases cellular resting	122
Figure 3-10 ERK2 opposes invasion in MDA-MB-231 cells.....	124
Figure 3-11 siRNA of ERK1 or ERK2 does not induce apoptosis or inhibit proliferation	126
Figure 3-12 ERK2 silencing inhibits migration of MDA-MB-231 cells on plastic.....	128
Figure 3-13 siRNA of ERK2 reduces migration of MDA-MB-231 cells on CDM.....	130
Figure 3-14 Knockdown of ERK2 decreases the momentary velocity and increases cellular resting	131
Figure 3-15 ERK expression vectors	133
Figure 3-16 Ectopic expression of ERK2 but not ERK1 restores invasion of ERK2 knockdown cells	134
Figure 3-17 Ectopic expression of ERK2 but not ERK1 restores invasion of ERK2 knockdown cells	135
Figure 4-1 Experimental paradigm	147
Figure 4-2 Quality control of the microarray samples	149
Figure 4-3 Normalisation results in good clustering of experimental replicas	152
Figure 4-4 List of genes down-regulated upon ERK2 silencing.....	154
Figure 4-5 List of genes up-regulated upon ERK2 silencing.....	157

Figure 4-6 qRT-PCR primer pairs amplify in a linear manner over a range of cDNA concentrations	161
Figure 4-7 CSF2 expression is reduced upon ERK2 silencing	164
Figure 4-8 Rab17 expression is induced upon ERK2 silencing.....	166
Figure 4-9 Liprin- β 2 expression is induced upon ERK2 silencing	167
Figure 4-10 Validation of ERK2-dependent gene expression using single siRNA oligos for ERK1 and ERK2	169
Figure 4-11 Knockdown of ERK2 induces Rab17 and Liprin- β 2 expression in 2D	171
Figure 4-12 Expression of CSF2, Rab17 and Liprin- β 2 is dependent on ERK2's kinase activity	173
Figure 4-13 Rab17 and Liprin- β 2 expression is suppressed by CSF2.....	175
Figure 4-14 ERK2 as a regulator of gene expression	178
Figure 5-1 Schematic illustration of Liprin domain organisation and proposed complex formation	189
Figure 5-2 Suppression of Rab17 and Liprin- β 2 promotes invasiveness of MDA-MB-231 cells	192
Figure 5-3 Knockdown of Rab17 and Liprin- β 2 increases persistence of MDA-MB-231 cells on CDM	193
Figure 5-4 Depletion of Rab17 and Liprin- β 2 promotes invasiveness of A2780-Rab25 and BE cells.....	195
Figure 5-5 Ectopic expression of Rab17 or Liprin- β 2 suppresses invasiveness MDA-MB-231 and A2780-Rab25 cells.....	197
Figure 5-6 Ectopic expression of Rab17 or Liprin- β 2 decreases the momentary velocity and increases cellular resting in MDA-MB-231 cells.....	198
Figure 5-7 siRNA of Rab17 or Liprin- β 2 restores the invasiveness of ERK2 knockdown cells.....	200
Figure 5-8 Suppression of Rab17 and Liprin- β 2 restores the migratory characteristics of ERK2 knockdown cells	201
Figure 5-9 RNAi of Rab17 and Liprin- β 2 does not restore motility defects of ERK2 knockdown cells on plastic	204
Figure 5-10 Rab17 associates with early and recycling endosomes	206
Figure 5-11 Rab17 associates with β 1 integrin-positive vesicles	208
Figure 5-12 Working paradigm.....	213
Figure 5-13 Expression profiles of Rab17 and Liprin- β 2 across various cancer types	215
Figure 6-1 Working model demonstrating how ERK2 drives invasive cell migration	218

Author's declaration

I am the sole author of the thesis and all the work presented is entirely my own unless stated otherwise.

Acknowledgements

Doing your PhD is by no means a one man job and there are many people I would like to acknowledge for supporting me throughout the last four years. First and foremost, I would like to express my sincerest gratitude to Prof. Jim Norman and Prof. Walter Kolch for their supervision, guidance and help throughout my PhD on both a personal and scientific level. Moreover, I owe a big thank you to Dr. Alexander von Kriegsheim for his continuing support, enthusiasm and encouraging words when things were tough. Special thanks to Dr. Marc Birtwistle, whose belief in success and pursuit of happiness have made me want to do better every day. I am also indebted to Dr. Gabriela Kalna for her invaluable help with the microarray analysis and Prof. Bob White for being an open, understanding and helpful advisor. A big thank you to all the members of R7 for easing me into life at the Beatson and to all the members of R20 (past and present) for “adopting” me half way through my PhD and supporting me in the final spurt of my thesis. I would also like to express my thanks to all the friendly, smiley scientists and the support staff for making the Beatson an enjoyable place to work at.

As always there are a few people that stand out from the crowd and deserve extra recognition. My time at the Beatson would not have been the same without the “coffee girls” who shared enthusiasm when things were good and welcomed me with open arms when things were tough. Many thanks also to all the lovely friends I made during my time in Scotland; especially Laura McKernan, Monika Heilmann and Dr. Xu Gu for their love, support and cheerfulness. They truly did brighten up my days! Last but by no means least I would like to thank my husband for his loving support throughout my PhD. I am so lucky to have him!

Finally, I would like to dedicate this thesis to all the supporters of Cancer Research UK, who have moved me so many times at charity events. It is their dedication and generous funding that made this work possible.

Abbreviations

aa	amino acids
AP-1	activating protein-1
ARE	adenylate and uridylate-rich element
ATP	adenosine triphosphate
BMK1	big MAP kinase 1
BOP	BH3-domain only protein
bp	base pair
CAM	cell adhesion molecule
CAT	collective-to-amoeboid transition
CBP	CREB-binding protein
CD domain	common docking domain
CDK	cyclin-dependent kinase
CDM	cell-derived matrix
cDNA	copy desoxyribonucleic acid
CLK	cyclin-dependent kinase (CDK)-like protein
CNK	connector enhancer of KSR
CR	conserved region
CRE	cAMP response element
CREB	CRE-binding protein
CRIC	conserved region in CNK
cRNA	copy ribonucleic acid
CRS	cytoplasmic retention sequence
D	aspartate
DED	death effector domain
DMBA	7,12-dimethylbenz(α)anthracene
DMSO	dimethyl sulfoxide
DNA	desoxyribonucleic acid
ds	double stranded
DUSP	dual specificity phosphatase
E	glutamate
ECM	extracellular matrix
ED site	ERK docking site
EEA1	early endosome antigen 1
EGF	epidermal growth factor
EGFR	EGF receptor
EGFR	epidermal growth factor receptor
EMT	epithelial-to-mesenchymal transition
ERK	extracellular signal-regulated kinase
FAK	focal adhesion kinase
FGF	fibroblast growth factor
FMI	forward migration index
GAP	GTPase-activating protein
GAPDH	glyceraldehyde 3-phosphate dehydrogenase
GDP	guanosine diphosphate

GEF	guanine nucleotide exchange factor
GFP	green fluorescent protein
GIT	G protein-coupled receptor kinase interacting ArfGAP1
GPCR	G-protein coupled receptor
GSK	glycogen synthase kinase
GST	glutathione <i>S</i> -transferase
GTP	guanosine triphosphate
H ₂ O ₂	hydrogen peroxide
HGF	hepatocyte growth factor
hrs	hours
IEG	immediate early gene
ING4	inhibitor of growth 4
JNK	c-Jun N-terminal kinases
kDa	kilo Dalton
KSR	kinase suppressor of Ras
L	lysine
LH domain	Liprin homology domain
mAb	monoclonal antibody
MAP2	microtubule-associated protein 2
MAPK	mitogen activated protein kinase
MAPKAP	MAPK-activated protein
MAPKAPK	MAPK-activated protein kinase
MAT	mesenchymal-to-amoeboid transition
MBP	myelin basic protein
MDR	multi-drug resistance
MEF2C	myocyte enhancer factor 2C
MEK	MAP/ERK kinase
MEKK	MEK kinase
min	minutes
miRNA	microRNA
MITF	microphthalmia-associated transcription factor
MK2	MAPKAP kinase-2
MKP	MAPK phosphatase
MLCK	myosin light chain kinase
MMP	matrix metalloproteinase
MORG1	mitogen-activated protein kinase organiser 1
MP1	MEK partner 1
mRNA	messenger RNA
MSK	mitogen- and stress-activated protein kinase
mTOR	mammalian target of rapamycin
NES	nuclear export signal
NGF	nerve growth factor
NLS	nuclear localisation signal
NPC	nuclear core complex
nPKC	novel protein kinase C
NT	non-targeting

NUP	nucleoporin
o/n	overnight
p	probability
PAK	p21-activated kinase
PCR	polymerase chain reaction
PDGF	platelet-derived growth factor
PEA-15	phosphoprotein enriched in astrocytes 15
PH	pleckstrin homology domain
PI3K	phosphoinositide 3-kinase
PIP ₃	phosphatidylinositol-3,4,5-phosphate
PKA	protein kinase A
PKB	protein kinase B
Pol I	polymerase I
PP	protein phosphatase
PP2A	protein phosphatase 2A
PTP	protein tyrosine phosphatase
qRT-PCR	quantitative real time polymerase chain reaction
R	arginine
Rab	Ras-related protein
Ras	Rat sarcoma protein
Rb	retinoblastoma protein
REP	Rab escort protein
RNA	ribonucleic acid
RNAi	RNA interference
ROCK	Rho-associated coiled-coil protein kinase
rRNA	ribosomal RNA
RSK	ribosomal S6 kinase
RT	room temperature
RTK	receptor tyrosine kinase
SAM	sterile α motif
Sef-1	similar expression to fgf 1
SELENBP1	selenium-binding protein 1
SEM	standard error of the mean
Ser	serine
SF-tag	streptavidin-flag tag
SH3	src homology domain
siRNA	short-interfering RNA
SL1	selectivity factor 1
SOS	son of sevenless
Src	sarcoma kinase
STEP	striatal-enriched protein tyrosine phosphatase
Sur-8	suppressor of Ras 8
TF	transcription factor
Thr	threonine
TPA	12- <i>O</i> -tetradecanoylphorbol-13-acetate
TXNIP	thioredoxin-interacting protein

Tyr	tyrosine
UBF	upstream binding factor
UTR	untranslated region
V	volt
WB	Western blot

1 Introduction

1.1 The nature of cancer

1.1.1 *Hallmarks of malignancy*

Cancer, a disease with more than 100 distinct types and subtypes, is driven by randomly occurring mutations and epigenetic changes [1]. These genetic alterations produce oncogenes with a dominant gain of function and ablate tumour suppressor genes, giving rise to a recessive loss of function [2]. Several lines of evidence have shown that tumourigenesis is a multistep process analogous to Darwinian evolution in which normal cells gradually evolve into malignant tumour cells through dynamic changes in the genome [3-5]. Depending on the degree of aggressiveness tumours are divided into two main categories. Those which grow at the site of origin without invading the surrounding tissue are classed as benign tumours, whereas tumours which have infiltrated the nearby tissue or spread to distant organs are classified as malignant. The term cancer refers to a malignant tumour [6].

Histological analysis of cancer tissues allows further subdivision into four main classes. The most common type, the carcinoma, arises from epithelial cells and accounts for more than 80% of cancer-related deaths. Sarcomas, which derive from a variety of mesenchymal cell types, constitute approximately 1% of clinically-treated cancers. The third class of cancers are termed hematopoietic cancers, which arise from blood-forming and immune cells. Lastly, neuroectodermal tumours form the fourth class and derive from cells of the central and peripheral nervous system. It is important to stress that some types of cancers, such as melanoma, do not neatly fit into this classification scheme [7].

Surprisingly, taking into account the vast variety of genomic changes identified as drivers of oncogenesis, only nine physiological hallmarks in tumour cell development have thus far been declared essential for malignant growth (Figure 1-1) [1, 8]. Firstly, tumour cells must acquire the ability to grow autonomously. Tumour cells reduce their dependency on extracellular stimuli either by generating their own growth signals, altering the ligand-dependency of the growth receptors or by modifying the cytoplasmic circuitry downstream of growth receptors. Secondly, tumour cells must become insensitive to

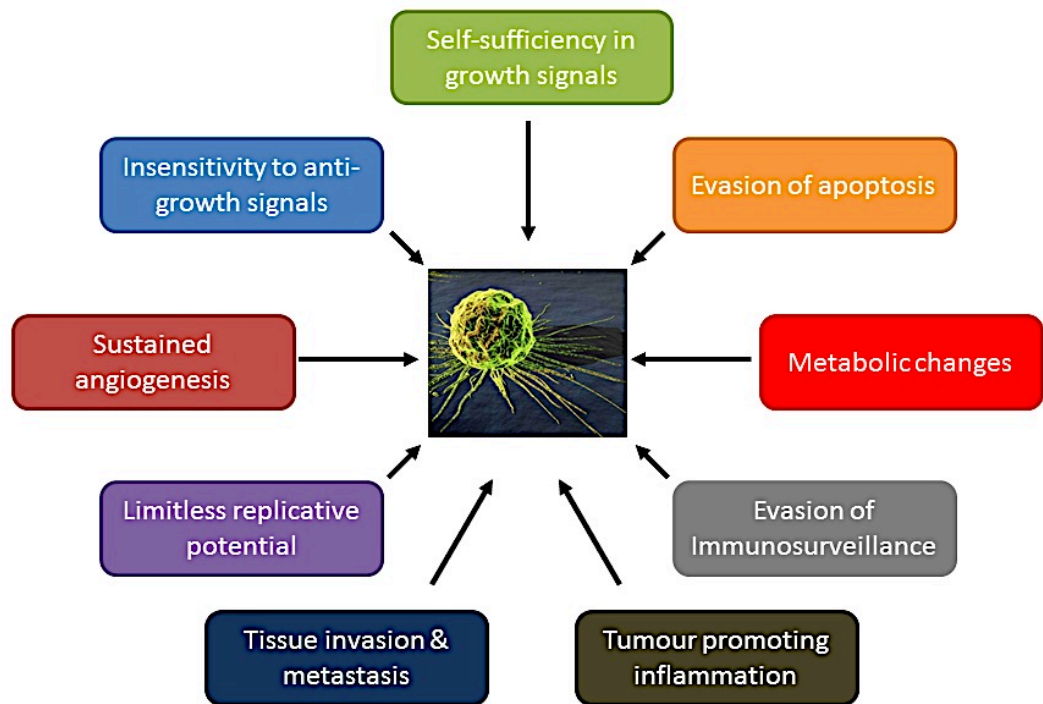


Figure 1-1 Nine hallmarks acquired by cancer
Adapted from [8].

anti-growth signals, which either induce cell differentiation or force proliferating cells into a quiescent G_0 state. Thirdly, tumour cells must find a way to evade programmed cell death, a process termed apoptosis. Abnormal signalling caused by oncogenes can be recognised by apoptotic sensors and trigger the onset of apoptosis, thereby providing a means by which transformed cells are removed from the tissue. Having gained the ability to grow and proliferate, tumour cells furthermore have to overcome the hurdle of a finite cellular lifespan of 60 to 70 doublings. Every DNA replication results in a shortening of the chromosome ends, called telomeres, due to the inability of the DNA polymerases to completely replicate the 3' ends of the chromosomes. In order to overcome this natural limit of replication, tumour cells acquire the trait to maintain and renew telomeres, thus becoming immortal.

The resulting uncontrolled proliferation, however, demands a good supply of oxygen and nutrients by the vasculature, which is ensured when a cell resides within 100 μm of a capillary blood vessel. As the tumour mass grows past a diameter of 0.1-0.2 mm, tumour cells must acquire the ability to induce, attract and sustain new blood vessel formation in a process termed angiogenesis. Moreover, the increase in proliferation requires rapid production of adenosine triphosphate (ATP), lipids, nucleotides and amino acids. Thus, a metabolic switch in tumour cells to meet the growing demand for energy and cellular building blocks has been proposed as a hallmark of tumour cells. Another important trait of tumour cells is the ability to evade immunosurveillance. Immune cells are an important player in tissue homeostasis and can eliminate transformed cells by triggering an innate immune response. However, as the disease progresses tumour cell variants, which are able to escape the immune attack, develop. Paradoxically, immune cells have also been shown to promote tumorigenesis, thus, inflammation has emerged as a new hallmark of cancer in the last decade. Immune cells contribute towards the development of cancer by supplying tumour cells with growth signals, promoting epithelial-to-mesenchymal (EMT) transition and by remodelling the extracellular matrix, which facilitates tumour cell migration, invasion and the process of angiogenesis [9]. Lastly, malignant tumour cells gain the ability to invade and metastasise at distant sites in the body [1, 10, 11].

1.1.2 Invasion-metastasis cascade

The metamorphosis of a normal cell to a malignant one requires many phenotypic and biochemical changes, which are acquired in a multi-step process called the invasion-metastasis cascade. The development of metastases has been subdivided into five crucial steps: primary invasion, intravasation, circulation, extravasation and homing (Figure 1-2) [12, 13].

In the first instance tumour cells need to detach from the primary tumour mass, which is achieved through the alteration of cell adhesion molecules (CAMs), mediating cell-cell and cell-matrix interactions. One of the most common changes in carcinomas allowing detachment is the functional loss of E-cadherin, a homotypic CAM, which is an important signalling molecule for conveying anti-growth signals to the intracellular signalling circuit of β -catenin and the Lef/Tcf transcription factor. E-cadherin function is lost by several mechanisms including mutational inactivation, transcriptional repression and proteolysis of the extracellular domain [14]. A loss in E-cadherin is often accompanied by increased N-cadherin expression. The display of N-cadherin molecules on the cell surface allows binding to stromal cells and eventually favours migration from the epithelium towards the connective tissue called stroma [15, 16]. Yet, epithelium and stroma are separated by the basement membrane, a dense meshwork of glycoproteins and proteoglycans consisting mainly of type IV collagen and laminin. The secretion of matrix-degrading proteases by tumour cells or recruited stromal cells disrupts this structural barrier and allows migration into the adjacent connective tissue. Under normal circumstances, protease activity is tightly regulated through both autoinhibition and secreted inhibitors. However, in tumours the expression of proteases is commonly augmented, while protease inhibitors are down-regulated [17]. The biochemical and phenotypical changes observed during the invasive process additionally facilitate intrusion of tumour cells into the lumen of lymphatic or blood vessels. During this step, which is termed intravasation, tumour cells penetrate into the lumen of either lymphatic or blood vessels and are then transported to distant tissue sites. This mode of travel, however, poses many risks for tumour cells. Firstly, they have to evade anoikis, a special form of programmed cell death activated upon loss of anchorage as normal (untransformed) cells cannot survive in conditions when cell-cell or cell-substratum interactions are lost. Tumour cells therefore

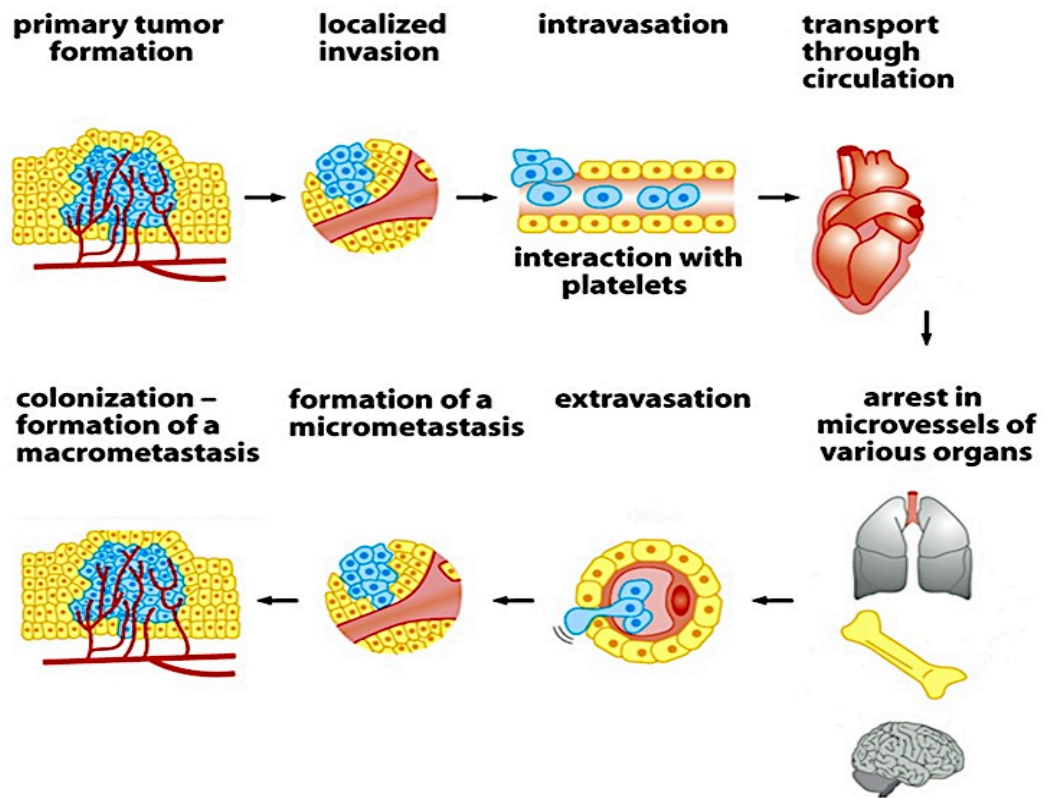


Figure 1-2 The invasion-metastasis cascade

Metastasis formation is a multistep process during which tumour cells invade the surrounding, enter blood vessels, adhere at distant sites, where the leave the blood stream to form new secondary lesions. Figure adapted from [7]

have to gain the ability to proliferate and survive in an anchorage-independent manner [18]. Secondly, high shear forces pose the risk of damaging the cells physically. As a way to oppose these non-viable conditions, tumour cells form so called micro-emboli, which are aggregations of tumour cells with thrombocytes and erythrocytes. This clumping is driven by a protein called tissue factor, which is highly expressed in malignant carcinomas cells [19, 20]. Mice deficient in micro-emboli formation show an over 90% decrease in metastasis formation, stressing the adverse conditions tumour cells face when in circulation [21].

Next, cancer cells need to lodge at a distant site before extravasating from the vasculature. Specific cell surface receptors, such as integrins and the CXCR4-receptor, have been demonstrated to facilitate lodging at the endothelium of blood vessels of specific organs [22, 23]. The process of extravasation is thought to occur in two different ways. Tumour cells either start to proliferate in the lumen of the vessel, thereby destroying the adjacent endothelium. Alternatively, they can penetrate a distant tissue in a process similar to intravasation by invading the endothelium and then degrading basement membrane with the help of proteases [12]. Yet, in order to colonise and proliferate successfully at ectopic sites, cancer cells need to adapt to the new micro-environment, where survival and growth signals differ from the original tumour site. Indeed, homing represents the most complex and challenging step of the invasion-metastasis cascade. Thus, most cells that have spread to ectopic sites do not develop into macroscopic lesions, but die rapidly or survive as dormant micro-metastases. In the early 1990s, genes, which inhibit colonisation, were identified. These so-called metastasis suppressor genes often alter fundamental signalling pathways regulating cellular growth and proliferation such as the MAPK/ERK (mitogen activated protein kinase/extracellular signal-regulated kinase) pathway. One example is the histidine kinase, nm23-H1, the first metastasis suppressor gene to be identified. Nm23-H1 phosphorylates the kinase suppressor of Ras (KSR) protein and thereby inhibits Ras-mediated activation of ERK [24-26].

The molecular principles of cancer invasion and metastasis are highly complex and therefore remain a major challenge in basic cancer research. Moreover, malignant tumours account for approximately 90% of all cancer-related deaths, thus new insight into the invasion-metastasis cascade may open up a novel therapeutic window.

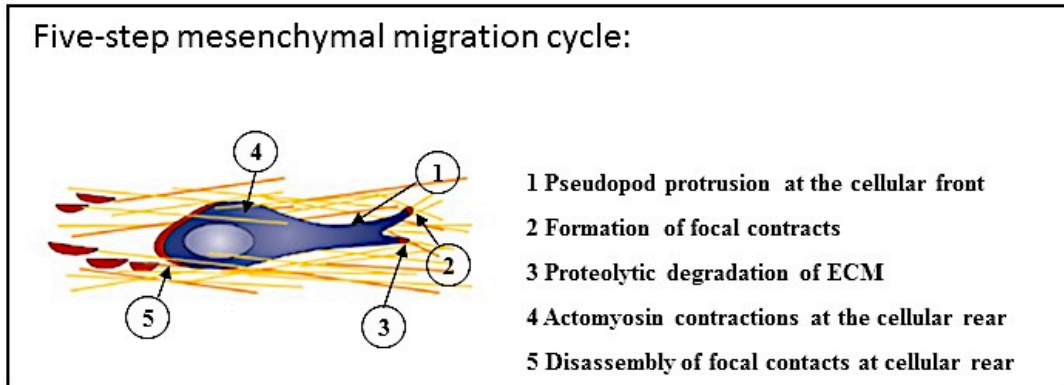
1.1.3 Modes of tumour cell migration

Cell migration is an essential characteristic during embryonic development, immune system function and tissue repair, but is also playing an important role in inflammatory diseases and tumourigenesis [27]. Cellular motility relies on the establishment of two physical forces. At the cellular front protrusive forces initiated by actin polymerisation and depolymerisation allow membrane extension, whereas at the cellular rear retraction forces generated by myosin-based motors initiate contraction [27]. Protrusion and retraction need to be tightly regulated in order to allow net translocation of the cellular body. This is achieved through an internal spatial asymmetry called cellular polarisation, which defines a cellular front and rear. Indeed, unpolarised cells, which simultaneously extend protrusions in opposite directions, have been shown to be immobile [28]. Thus, polarisation is a prerequisite for all modes of cellular migration, and the interplay of physical and molecular parameters of the cell and its surroundings determines how a cell migrates (Figure 1-3).

1.1.3.1 Amoeboid migration

Leukocytes [29] and hematopoietic stem cells [30] exhibit a crawling type of cell movement, which relies on rapid cycles of membrane extensions and contractions and is referred to as amoeboid migration. Amoeboid locomotion relies on cellular blebbing which is driven by cortical actin fibre contractions. Contractile forces initiate membrane blebbing by separating the plasma membrane from the cortex, thus allowing the inherent hydrostatic potential to cause bleb formation. A concentration of blebs at the cellular front creates a protrusive force necessary for cellular locomotion [31]. One of the features of amoeboid migration is the low and short-lived binding force towards the extracellular matrix (ECM). Thus, $\beta 1$ integrin mediated adhesions are completely or partially dispensable during amoeboid migration [32, 33]. The lack of stable focal contacts marks another feature of amoeboid migration, i.e. extraordinary deformability. Thus, cells overcome matrix barriers by means of shape adaptations rather than ECM remodelling. This shape-driven mode of cell movement is controlled by the small GTPase RhoA and its effector kinase ROCK (Rho-associated coiled-coil protein kinase) [34].

A



B

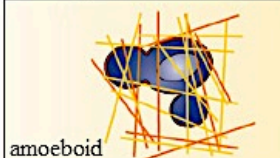
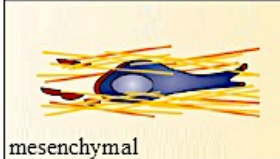
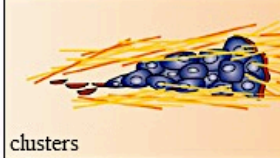
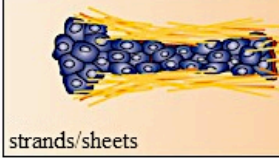
	Migration mode	Characteristics
individual	 amoeboid	<ul style="list-style-type: none"> • poorly adhesive • bleb-like protrusions • independent of proteolytic enzymes • high migration speed
	 mesenchymal	<ul style="list-style-type: none"> • moderately adhesive • pseudopodial protrusions • path generation through proteolytic enzymes • low migration speed
collective	 clusters	<ul style="list-style-type: none"> • intact and stable cell-cell adhesions • multicellular migratory unit • path generation through proteolytic enzymes • low migration speed
	 strands/sheets	<ul style="list-style-type: none"> • Intact and stable cell-cell adhesions • migrating unit still connected to primary tumor • path generation through proteolytic enzymes • infiltration of tissue surrounding primary tumour

Figure 1-3 Characteristics of different modes of migration

A. Depiction of the well-established five-step migration cycle characteristic of mesenchymal cells.

B. Comparison of individual migration modes, comprising amoeboid and mesenchymal migration, with collective cell migration in the form of cell clusters and strands. Adapted from [35]

Amoeboid tumour cells, commonly observed in lymphomas and small-cell lung carcinomas, express low levels of $\beta 1$ and $\beta 3$ integrins, which is thought to account for their highly metastatic and motile behaviour [36, 37].

1.1.3.2 Mesenchymal migration

In contrast to the path-finding motility described for amoeboid migration, mesenchymal cells follow a path-generating strategy which involves ECM degradation and remodelling. Mesenchymal cells are characterised by an elongated, spindle-shaped morphology which is brought about by stable integrin-mediated adhesions with the ECM [34]. This mode of motility follows a well-defined five-step migration cycle (Figure 1-3). Actin protrusions at the cellular front lead to pseudopod formation, where adhesion molecules, most notably integrin receptors, initiate binding to the matrix [35]. Enrichment of integrins at the cell front subsequently leads to formation of stable focal contacts. As different integrins bind to different ECM substrates, e.g. $\alpha 5\beta 1$ binds fibronectin [38] and $\alpha 2\beta 1$ binds fibrillar collagen [39], this mode of motility is highly dependent on the ECM composition. Engagement of surface receptors with the matrix triggers recruitment of surface proteases to focal contacts [40]. Subsequent degradation of ECM components in the proximity of the leading edge paves the way for the advancing cell body. In contrast, focal adhesions at the cellular back are disassembled and contractile forces propel the cellular body forward [35]. Mesenchymal migration is dependent on the coordination of three small GTPases, namely Rac, Cdc42 and RhoA. At the cellular front Rac and Cdc42 activity promote rapid turnover of focal contacts, whereas RhoA activity at the cellular back controls contractions forces, which propel the cell body forward [41, 42]. High turnover of focal adhesion results in low adhesiveness and increases the migratory speed, while strong integrin-substrate linkages impair cell motility. Given that cells employing an amoeboid mode of migration form very weak ECM interactions, it is not surprising that they move with velocities of up to 10-30 fold higher than mesenchymal cells [43].

1.1.3.3 Collective cell migration

Collective migration, as the name suggests, describes the locomotion of a multicellular contractile body, where cell-cell junctions are kept intact. This phenomenon occurs naturally during embryonic [44, 45] as well as mammary development [46]. In tumours, two types of collective migration have been described histologically, i.e. the invasion of

sheets and strands of tumour cells which retain contact with the primary tumour, and the invasion of detached cell clusters. Collective migration can only be achieved when contractile forces are coordinated. Therefore, the contractile body is divided into highly motile path-generating cells at the front, which engage with the ECM and remodel it with the help of proteolytic degradation, and cells in the inner or trailing regions which are thought to be dragged along passively. One characteristic of collective migration is the assembly of a specific form of cortical actin filaments along cell-cell junctions, which allow the concerted movement of the multicellular body [47].

Collective cell migration is predominantly found in highly differentiated tumours, such as oral squamous-cell carcinoma [48] and colon carcinoma [49], whereas single cell migration is believed to provide a means for the dissemination of haematological neoplasias. Travelling as a connective unit is thought to provide advantages during tumourigenesis. Firstly, the large cell mass can produce a higher concentration of pro-migratory as well as pro-survival signals than single cells, thereby increasing the overall chances of survival and invasion. Secondly, inner cells of the sheet or cluster are protected from immunosurveillance, irradiation and cytostatic drugs [50]. Thirdly, less motile cells, which may possess other advantageous biological abilities, can work together with highly mobile cells as one functional unit [35].

1.1.3.4 Plasticity in tumour cell migration

Although most cell types preferentially employ a particular type of migration, changes in the microenvironment (such as fluctuations in the ECM density) or cellular properties (such as loss-of-function mutations of adhesion receptors) can induce a switch from one migration mode to another, rather than inhibiting motility altogether (Figure 1-4) [51]. The most well-established example of tumour cell plasticity is called epithelial-to-mesenchymal transition (EMT) and is marked by the loss of cell-cell junctions while adhesive and proteolytic capacities are retained. EMT spontaneously occurs during the course of tumour progression and has been linked to an increased risk in metastatic spread and poor prognosis [52-54]. In contrast, the process of collective-to-amoeboid transition (CAT) is characterised by the dissemination of single cells displaying an amoeboid migration mode, which can dispense with $\beta 1$ integrin-mediated adhesion and ECM proteolysis. In addition, factors, including weakening of cell-matrix interactions

observed in loose interstitial tissues, inhibition of ECM remodelling or augmentation of RhoA/ROCK signalling, can trigger mesenchymal-to-amoeboid transition (MAT) [35, 51]. Notably, anti-invasive drugs, targeting one mode of migration only, can induce a switch in motile behaviour [34]. Therefore, it is believed that a successful anti-invasive therapeutic strategy must target multiple motility pathways.

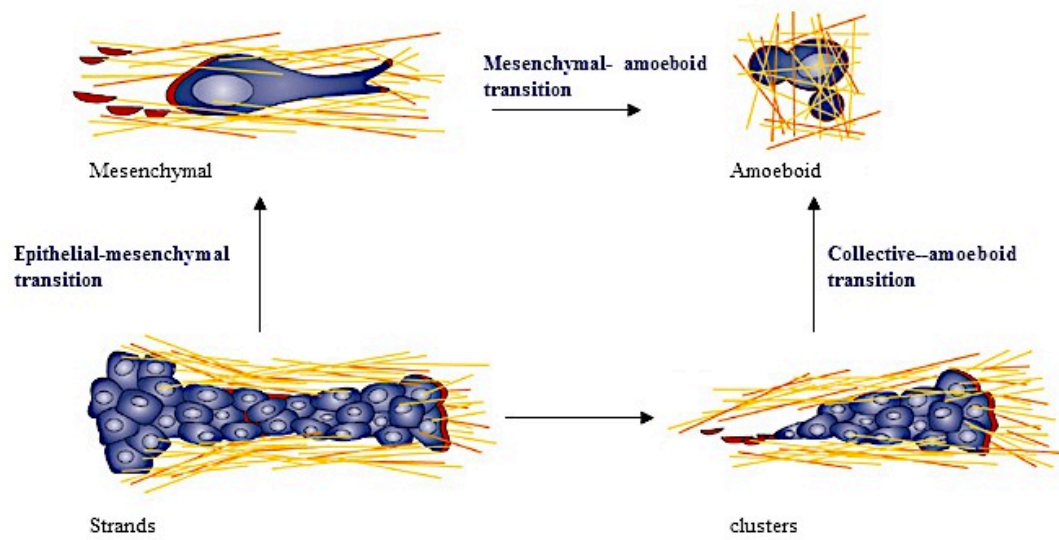


Figure 1-4 Plasticity of tumour cell migration

Changes in the microenvironment can induce a switch from one migration mode to another rather than inhibiting cell motility. Depicted are migration transitions monitored *in vivo*. Adapted from [35]

1.2 Mammalian MAPK pathways

1.2.1 *The history of the MAPK cascade*

The first mammalian mitogen-activated protein kinase (MAPK) was identified in 1990 in an attempt to isolate protein kinases activated by growth factors. The purified protein was phosphorylated following insulin treatment, 44 kDa in size and contained sequences reminiscent of serine/threonine protein kinases. With the help of degenerate primers based on these sequences, extracellular signal-regulated kinase 1 (ERK1) was cloned from rat fibroblasts [55]. ERK1 showed an over 50% sequence identity to the yeast protein kinases, Kss1 and Fus3, which had previously been shown to regulate the cell cycle in response to pheromones [56, 57]. Subsequent screening of a rat brain cDNA library with an ERK1 probe under low stringency led to the identification of ERK2 and ERK3, and this marked the birth of a new protein kinase family [58]. Traditionally, kinase activities of ERK1 and -2 were measured using the two substrates, myelin basic protein (MBP) and microtubule-associated protein-2 (MAP2), which gave rise to the historic nomenclature of MBP kinase and MAP2 kinase. In the following years the MAP acronym was retained with a novel denotation in order to acknowledge the activation of the kinases after mitogen stimulation, which originally led to its identification [59].

MAPK enzymes are activated via a phosphorylation (kinase) cascade, which is evolutionary conserved in plants, fungi and animals. Classically, the cascade is organised into a four-tier module comprising the MAP kinase kinase kinase (MAPKKK), MAP kinase kinase (MAPKK), MAP kinase (MAPK) and the MAP kinase-activated protein (MAPKAP) [59]. The sequential activation of kinases enables amplification of the input signal, feedback regulation as well as the integration of information from other signalling pathways. Thus, crosstalk of members of the MAPK pathway with other signalling circuits enables fine tuning (i.e. enhancement, suppression and localisation) of the transmitted signal.

1.2.2 *Overview of the six distinct mammalian MAPK pathways*

In mammals, nearly 20 MAPK have thus far been identified (Table 1-1). Based on their sequence similarity they are grouped into six distinct MAPK pathways, which regulate

	<i>NAME</i>	<i>Alternative names</i>	<i>Interesting features</i>	<i>Ref.</i>	
MAP kinase family members	MAPK1	ERK2, p42MAPK, MAPK2	85% identical to ERK1	[58]	
	MAPK3	ERK1, p44MAPK	First MAPK to be identified	[55]	
	MAPK4	ERK4, p63MAPK	Cloned in 1992 by virtue of its homology to ERK1	[60]	
	MAPK6	ERK3, p97MAPK	Suggested to have evolved recently through gene duplication	[59]	
	MAPK7	ERK5, BMK1	N-terminal domain exhibits a 66% sequence similarity to ERK1/2	[61]	
	MAPK8	JNK1, SAPK γ	Ubiquitously expressed with multiple splice variants	[62]	
	MAPK9	JNK2, SAPK α	Ubiquitously expressed with multiple splice variants	[62]	
	MAPK10	JNK3, SAPK β	Expression restricted to brain, heart and testis	[62]	
	MAPK11	p38 β	Phosphorylates MK2 and is sensitive to pyridinyl imidazole compounds	[63]	
	MAPK12	p38 γ , ERK6	Selectively activated by hypoxia in a Ca ²⁺ -dependent manner	[64]	
	MAPK13	p38 δ	Activated by novel PKC (nPKC) in response to TPA	[65]	
	MAPK14	p38 α	Phosphorylates MK2 and is sensitive to pyridinyl imidazole compounds	[63]	
	MAPK15	ERK7, ERK8	Breast cancer progression correlated with loss of ERK7 expression	[66]	
	Intermediates between the MAP kinase and cdk family	NLK	Nemo-like kinase	Regulates Wnt/ β -catenin signalling positively and negatively Phosphoacceptor site: TQY	[67, 68]
		MAK	Male germ cell associated kinase	Transcriptionally induced by androgen in prostate cancer Phosphoacceptor site: TDY	[69]
MRK		MAK-related kinase	87% identical to MAK, role in heart development Phosphoacceptor site: TDY	[70]	
MOK		MAPK/MAK/MRK overlapping kinase	Activated by okadaic acid and phorbol ester, Phosphoacceptor site: TEY	[71]	
KKIALRE		CDKL1	Related to cdc2 kinase, Phosphoacceptor site: TDY	[72]	
KKIAMRE		CDKL2	Phosphorylation of TDY motif not required for kinase activity Phosphoacceptor site: TDY	[73]	

Table 1-1 Overview of all Mammalian MAPK identified

diverse cellular functions such as embryogenesis, growth, proliferation, apoptosis, differentiation and migration [59, 62, 63]. Phylogenetically, MAPKs belong to the CMGC family of protein kinases (termed after its members, i.e. cyclin-dependent kinases (CDKs), MAPKs, glycogen synthase kinases (GSKs) and CDK-like kinases (CLK)) [74]. Members of the MAPK branch are further subdivided into conventional and atypical kinases (Table 1-2). Conventional MAPK include ERK1/2, ERK5, p38s and JNKs (c-Jun N-terminal kinases), which contain a Thr-Xaa-Tyr motif in the activation loop and are activated by MEKs (MAP/ERK kinases). Atypical kinases, including ERK3/4 and ERK7/8, either contain a single phosphoacceptor site in the activation loop or possess a novel activation mechanism dispensable of MEKs [75]. All MAPKs, however, display two common features. Firstly, they all preferentially phosphorylate serine or threonine residues followed by proline in their respective MAPKAP. Secondly, all MAPKs are activated by phosphorylation in the absence of a regulatory subunit [59].

The following subsections aim to highlight the main features of the different MAPK groups identified to date with the exception of ERK1/2, which will be covered in detail in section 1.3.

1.2.2.1 c-Jun N-terminal kinases (JNKs)/stress-activated protein kinases (SAPK)

The first JNK family member was purified from rat livers after cycloheximide treatment in 1990 [76]. Shortly afterwards, two further JNKs were purified in GST-pulldown assays using c-Jun as a bait [77]. The JNK family of MAPK is encoded by three genes (*jnk1*, *jnk2* and *jnk3*), which give rise to 13 splice variants. JNK1 and -2 are ubiquitously expressed, whereas JNK3's expression is restricted to the brain, heart and testis. Notably, JNKs are predominantly activated by stress signals such as cytokines, UV radiation, oxidative stress, growth factor deprivation and DNA-damaging agents. Hence, these kinases have also been described as the family of stress-activated protein kinases (SAPK) [59, 78]. MEK4 and -7 activate JNKs synergistically at the Thr-Pro-Tyr motif in the activation loop, with MEK4 preferentially phosphorylating the tyrosine residue and MEK7 phosphorylating the threonine residue. Following activation, JNKs translocate from the cytoplasm to the nucleus, where they phosphorylate and regulate transcription factors such as c-Jun, ATF2 and p53 [79, 80]. To date very little is known about JNKs' role in regulating cytoplasmic effectors. MEK4 and -7 themselves are activated by numerous

MAPKKs, including MEKK1-4, MLK2/3, YTpl-2, DLK, TAO1/2, TAK1 and ASK1/2 (Table 1-2) [62]. The role of JNK kinases in tumour development is highly controversial. Some reports have shown a pro-tumourigenic role [81-83], whereas others have demonstrated an anti-tumourigenic capacity for JNK signalling [84]. JNK activity enhances tumour development by decreasing the proliferation inhibitor p21^{CIP1}, increasing signalling of the growth promoter c-Myc, and allowing the formation of an inflammatory environment, which has recently been appreciated as a novel hallmark of cancer. In contrast, JNK signalling is also required for the induction of apoptosis, which might account for its putative tumour suppressive function [85]. Thus, the usefulness of JNK inhibitors in clinical settings is still in debate.

1.2.2.2 p38 kinases

The family of p38 kinases form another group of MAPKs activated by stress signals. In contrast to JNK enzymes, stress stimuli not only activate p38s, but also induce their gene expression. Four genes encode this group of enzymes comprising, i.e. p38 α , p38 β , p38 γ (which has also been termed ERK6), and p38 δ . Only the gene encoding the α -isoform gives rise to four splice variants. p38 α and β are ubiquitously expressed, whereas p38 γ and δ expression is tissue restricted [63]. Notably, p38 α and β activity is inhibited by pyridinyl imidazole, which originally led to its identification in 1994 [86], whereas p38 γ and δ are insensitive to the drug. Furthermore, p38 isoforms show differences in their substrate specificity. Whereas the α - and β -isoform phosphorylate MAPKAP kinase-2 (MK2), p38 γ and δ do not [63]. p38 enzymes are generally activated by MEK3 and MEK6, although MEK4 has also been shown to contribute to the phosphorylation of the distinct Thr-Gly-Tyr motif upon UV radiation *in vivo* [87]. MEK3 and -6 in turn are activated by MAPKKs similar to JNK enzymes such as MEKK1-4, TAO1/2, TAK1 and ASK1/2. To date little is known as to how stress stimuli can produce a distinct p38 or JNK signalling output with overlapping MAPKKs (Table 1-2).

Interestingly, disruption of the p38 pathway in mice leads to increased tumourigenesis due to defects in growth arrest [87]. Furthermore, a decrease in p38 activity has been observed in hepatocellular carcinomas in comparison to the adjacent normal tissue [88]. Taking these findings together, p38 signalling might have tumour suppressive functions by inducing cell cycle arrest, senescence and apoptosis [89].

Predominant Extracellular Stimulus ↓ MAPKKK ↓ MAPKK ↓ MAPK	Conventional MAPK				Atypical MAPK	
	Growth factors, Mitogens	Stress signals		Stress signals	Phorbol ester, Serum	Oxidative stress, mitogens
	RAF-1/A/B, c-MOS	MEKK1-4, MLK2/3, YTpl-2, DLK, TAO1/2, TAK1, ASK1/2		MEKK2/3	?	?
	MEK1/2	MKK4/7	MKK3/6	MEK5	?	?
	ERK1/2	JNK1/2/3	p38α/β/γ/δ	ERK5	ERK3/4	ERK7
Response	Proliferation Differentiation Apoptosis Migration	Cell cycle control Apoptosis Inflammation		Cardiovascular development, neural differentiation,	Putative role in cell cycle and/or apoptosis	
MAPK phosphoacceptor site	TEY	TPY	TGY	TEY	SEG	TEY
Predicted size (kDa)	41/43	46	38	98	97/63	60
Encoding genes	2	3	4	1	2	1
Transcript variants	3 (ERK1) 2 (ERK2)	4 (JNK1) 5 (JNK2) 4 (JNK3)	4 (p38α) 1 (p38β) 1 (p38γ) 1 (p38δ)	4	1 (ERK3) 1 (ERK4)	3
Isoforms	3 (ERK1) 1 (ERK2)	4 (JNK1) 5 (JNK2) 4 (JNK3)	4 (p38α) 1 (p38β) 1 (p38γ) 1 (p38δ)	2	1 (ERK3) 1 (ERK4)	3

Table 1-2 Overview of the common and divergent features of the 6 distinct mammalian MAPK pathways

1.2.2.3 ERK5

ERK5 was identified by two independent research groups in 1995 [90, 91] and is one of the largest MAPKs known to date (98 kDa). Therefore, it was originally termed the big MAP kinase 1 (BMK1) by Lee *et al.* [90]. Alternative splicing gives rise to 4 distinct transcript variants and 2 isoforms. The N-terminal half of the protein, comprising the kinase domain with a Thr-Glu-Tyr activation motif, exhibits a 66% sequence similarity to ERK1/2 [61]. ERK5's unique C-terminal domain, which contains a bipartite nuclear localisation signal (NLS) [92] and has transcriptional activation activity [93], sets this enzyme apart from other MAPKs [94]. In unstimulated cells, intramolecular interactions between the N- and C-terminal domain promote nuclear export. It is believed that the association between the two domains allows the formation of a region which itself might constitute a nuclear export signal (NES), or allow binding to a cytoplasmic anchor protein. Upon kinase activation a conformational change disrupts this association and promotes nuclear localisation of ERK5 [92], where its two functional domains allow either phosphorylation of target molecules (N-terminal region) or enhancement of transcription activity (C-terminal region) [93]. Despite the similarity to ERK1/2, this enzyme is activated by a unique MAPKK, namely MEK5, which itself is phosphorylated by MEKK2/3, also associated with p38 and JNK signalling [94]. ERK5 is activated in response to stress signals, such as oxidative stress and hyperosmolarity, and to a lesser extent by mitogenic signals, such as serum and nerve growth factor (NGF). Functional studies in cultured cells have demonstrated a role for ERK5 in cell proliferation [95], and migration [96]. *In vivo*, ERK5 was shown to play a role in blood vessel and heart development [97] as well as neural differentiation (Table 1-2) [98].

The first ERK5 substrate identified was myocyte enhancer factor 2C (MEF2C), which upon phosphorylation enhances *c-jun* gene expression in luciferase assays [99]. Moreover, ERK5 was shown to phosphorylate known ERK1/2 substrates such as Sap1a and c-Myc *in vitro* [100, 101]. However, to what extent ERK5 signalling regulates these transcription factors *in vivo* in comparison to ERK1/2 remains to be determined. The understanding of ERK5's involvement in tumourigenesis is still in its infancy. Recent work, however, showed MEK5 overexpression in metastatic prostate cancer biopsies [102] and increased ERK5 activity in a panel of human cancer cell lines [103]. This increased signalling is thought to drive tumour cell proliferation, motility and invasion.

1.2.2.4 ERK3/4

ERK3 was one of the first MAPKs to be identified alongside ERK2 in an attempt to clone ERK1-related serine/threonine protein kinases [58]. It is encoded by one gene and translates into a 97 kDa protein. In 1992 a shorter isoform (63 kDa), highly homologous to ERK3, was identified and termed ERK4 [60]. Comparative analysis highlighted a similar genomic arrangement of introns and exons as well as high sequence identity in the catalytic domain [104]. These observations, in conjunction with the lack of ERK3/4-encoding genes in yeast and *Caenorhabditis elegans* [105, 106], suggest a very recent evolutionary emergence via gene duplication. In contrast to conventional MAPK, ERK3 and -4 possess a single phosphoacceptor site (Ser-Glu-Gly). Moreover, both kinases are characterised by a Ser-Pro-Arg motif in the activation loop, which replaces the highly conserved Ala-Pro-Glu motif found in almost all protein kinases (Table 1-2) [61]. Although the glutamic acid residue has been linked to structural stabilisation and ultimately kinase activity [107], substitution of this residue has also been observed in casein protein kinases [108]. Therefore, an arginine replacement is still compatible with kinase activity.

Despite the absence of a NLS ERK4 is predominantly found in the nucleus [109]. In contrast, ERK3 is localised to nuclear and cytoplasmic compartments. Efforts to identify stimuli altering the subcellular localisation of ERK3 have proven unsuccessful [110]. Another difference between ERK3 and ERK4 is their respective half-lives, which argues for isoform-specific functions. ERK3 is highly unstable with a half-life of 30-40 min, whereas ERK4 is very stable [75]. ERK3/4 kinases are activated by phorbol ester and serum treatment, but not insulin or EGF [111]. No research group has yet identified upstream MAPKKs or MAPKKs for ERK3 and -4. Although Cheng *et al.* described an ERK3 kinase capable of specifically phosphorylating ERK3, they did not identify the enzyme [112]. Moreover, data on ERK3/4 substrates is limited and contradictory. Although Sauma *et al.* have demonstrated phosphorylation of MBP [113], Cheng *et al.* did not observe phosphorylation of traditional MAPK effectors such as MBP, MAP-2, c-Jun or Elk-1 *in vitro* [109]. ERK3 expression is markedly increased during early organogenesis in mice [104]. Moreover, cell culture studies have shown stabilisation of ERK3 upon cellular differentiation [114]. Thus, ERK3 might play a role in committing cells to acquire a quiescent differentiated state. Future studies, in particular ERK3^{-/-} and ERK4^{-/-}

phenotypes, will hopefully shed more light on the biological functions and regulation of this MAPK subfamily.

1.2.2.5 ERK7

ERK7 was cloned in 1999 from a neonatal rat brain cDNA library [115] and consists of an N-terminal kinase domain, which is 45% identical to ERK1. A further C-terminal extension, unique to ERK7, which contains a putative NLS and two alleged SH3-binding domains [75]. The ERK7 gene translates into a 60 kDa protein and is widely expressed [116]. Notably, this kinase, although found across many species, is less conserved throughout evolution than other MAPK [75]. To date work on the biological regulation and function of this MAPK is limited. Overexpressed ERK7 is predominantly localised to the nucleus, whereas the localisation of the endogenous protein is unknown [115]. The enzymatic regulation of this MAPK is unique in that the Thr-Glu-Tyr motif within the activation loop is subject to autophosphorylation and not to be phosphorylated by upstream MAPKKs (Table 1-2) [115]. This poses the question; how can ERK7 be regulated *in vivo*? So far, there is evidence that ERK7 activity and expression is regulated by protein turnover [117]. Although ERK7 can phosphorylate classical MAPK substrates such as MBP *in vitro*, physiological substrates remain unidentified. Notably, ERK7 can phosphorylate MBP on sites that are distinct from ERK1/2 phosphorylation. Thus, ERK7 exhibits distinct substrate specificity in comparison to ERK1/2 [115, 116]. Physiological functions of ERK7 also remain to be determined. So far, ERK7 has been proposed to play a role in proliferation [115], chloride transport [118] and nuclear receptor signalling [66]. Intriguingly, ERK7 displays functions dependent (degradation of estrogen receptor α) and independent (regulation of S-phase entry) of its catalytic activity.

Interestingly, ERK7 has also been implicated in tumourigenesis. A small study comparing ERK7 protein levels in normal and tumour tissues of the breast observed an ERK7 loss in the cancerous samples [66]. Yet, future work with larger patient cohorts and mice models will be necessary to further substantiate these observations.

1.2.3 MAPK docking sites

MAPK cascades regulate a variety of biological functions, such as cell proliferation, differentiation and stress responses. Moreover, aberrant MAPK signalling has been associated with numerous diseases such as cancer (ERK1/2), rheumatoid arthritis (p38 kinases) and Alzheimer's disease (JNKs) [119-121]. Besides the need for tight regulation, these cascades require high efficiency and fidelity in signal transduction, which is achieved through substrate binding motifs, also known as substrate docking sites. Conventional MAPKs and their substrate binding motifs have been studied extensively in search for putative drug inhibition sites. On the other hand, our understanding of atypical MAPKs is still in its infancy in regards to regulation and biological functions. Thus, no docking domains have yet been described for this MAPK subgroup.

1.2.3.1 Common docking site

As the name suggests, this docking site mediates binding of numerous proteins, such as MEKs, phosphatases and transcription factors [63]. It was originally identified in an attempt to abolish MEK binding to ERK2 through mutations and termed the cytoplasmic retention sequence (CRS) [122]. Later, however, this region was shown to facilitate interaction of ERK with a variety of proteins and therefore termed the common docking (CD) domain [123]. Moreover, this binding site, which is located C-terminal to the catalytic domain, is conserved among all conventional MAPKs (Figure 1-5) and comprises negatively-charged aspartate (D) and glutamate (E) residues [123]. Crystal structures of ERK2, p38 α and JNK3 have shown that the conserved amino acids are not only exposed on the surface of these enzymes, but also reside close to one another, thus forming a negatively charged interaction platform opposite to the catalytic centre [124-126]. Indeed, this region was shown to bind to a conserved sequence of basic amino acids in MAPK substrates, termed the D-motif [123, 127]. Notably, ERK1/2 substrates generally possess two consecutive basic amino acids in their D-motif, whereas substrates for JNK and p38 kinases display three or more consecutive lysines (L) and arginines (R) (Table 1-3). Thus, substrate specificity might be achieved through varying numbers of positively charged amino acids on the D-motif [124, 128].

<i>MAPK substrate</i>		<i>Proposed D-motif</i>	<i>MAPK specificity</i>
MAPKK	MEK1	MPKKKPTPIQLNPNP	ERK1/2
	MEK2	MLARRKPVLPALTINP	
	MKK3	KGKSKRKKDLRI	p38s
	MKK6	SKGKKRNPGLKIP	
	MKK4	QGKRKALKLNF	JNKs
	MKK7	EARRRIDLNLDISP	
	MEK5	LKKSSAELRKIL	ERK5
MAPKAPK	RSK1	SSILAQRVRKLPSTTL	ERK1/2
	RSK2	RSTLAQRGGIKKITSTAL	
	MAPKAPK2	NPLLLKRRKKARALEAAA	p38s
	MAPKAPK3	NRLLNKRRKKQAGSSSAS	
MKP	MKP-3 (DUSP6)	PGIMLRRLQKGNLPVR	ERK1/2
	MKP-5 (DUSP10)	CADKISRRLQQGKITV	p38, JNK

Table 1-3 Overview of proposed D-motifs of various MAPK substrates

The D-motif is characterised by a cluster of positively charged amino acids (coloured in grey). The number of consecutive arginines or lysines determines the MAPK-binding specificity.

A

ERK1	333	Y	Y	D	P	T	D	E	P	V	341
ERK2	316	Y	Y	D	P	S	D	E	P	I	324
ERK5	349	Y	H	D	P	D	D	E	P	D	357
p38 α	311	Y	H	D	P	D	D	E	P	V	319
p38 β	319	Y	H	D	P	E	D	E	P	E	327
p38 γ	314	L	H	D	T	E	D	E	P	Q	322
p38 δ	311	F	R	D	T	E	E	E	T	E	319
JNK1	324	W	Y	D	P	S	E	A	E	A	332
JNK2	324	W	Y	D	P	A	E	A	E	A	332
JNK3	362	W	Y	D	P	A	E	V	E	A	370

B

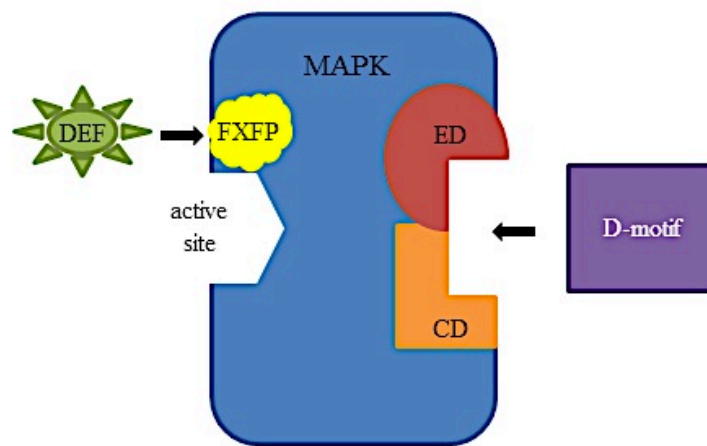


Figure 1-5 MAPK docking sites

A. Human amino acid sequences of the CD domains of various members of the MAPK family. Coloured characters represent negatively charged amino acids in the CD domain, which are supposed to be exposed at the surface and mediate substrate binding. Adapted from [124].

B. MAPKs comprise various docking domains, which mediate substrate binding. ED and CD domains mediate docking of D-motifs, whereas the FXFP-docking site allows binding of DEF-motifs.

1.2.3.2 ERK docking site

The ERK docking (ED) site is located close to the CD domain in the crystal structure and consists of hydrophobic residues from helices α D, α E and a reverse turn of β 7- β 8 [129]. This docking site is significantly different in ERK1/2, p38 kinases and JNKs and therefore provides a means for substrate specificity within the MAPK family [130]. Moreover, the CD and ED domains, which are close to one another in the folded protein, form a docking groove on the surface of the kinases (Figure 1-5). Thus, structural differences brought about by different hydrophobic residues can confer substrate specificity and alter substrate affinity [124]. Indeed, exchange of only two amino acids in the ED domain of p38 α and ERK2 (Glu160 and Asp161 in p38 with Thr157 and Thr158 in ERK2) is enough to alter substrate specificity [124]. It has to be noted, however, that amino acids close to the docking groove are likely to also be involved in docking interactions. Moreover, substrates might differentially recognise the ED and CD domain, thus providing another means of variability.

1.2.3.3 FXFP binding site

In addition to the hydrophobic groove, another interaction motif has been described for ERK1/2 and p38 α , which is called the FXFP binding site. This site was identified using hydrogen exchange mass spectrometry, and is marked by a cluster of hydrophobic amino acids distinct from the ED domain, which specifically interacts with a Phe-X-Phe (FXF) motif [131, 132]. The FXFP binding site is situated close to the active centre and is occluded in the inactive enzyme through intramolecular interactions (Figure 1-5). Many ERK1/2 substrates, including SAP-1 and Elk-1, have been shown to bind to the FXFP binding site with their corresponding DEF domain (docking site for ERK and FXFP) [132]. Notably, the hydrophobic residues important in ERK-DEF binding are conserved among various MAPK family members, yet DEF motif interactions have only been observed in ERK1/2 and p38 α , but not p38 β / γ / δ and JNK2 [131]. This suggests differences in the tertiary structure of these kinases which lead to the exposure of specific substrate recognition patterns.

1.2.3.4 Other MAPK-binding domains

Although many MAPK substrates and regulators contain one or more MAPK dockings sites described above, some interacting proteins lack these conserved domains, but still bind

to the enzymes efficiently. One such MAPK target is the well-known transcription factor Ets-1, which has been shown to bind to ERK2 via a unique pointed domain [133]. MITF (microphthalmia-associated transcription factor) also falls into this category, as its C-terminal sequence required for ERK2 binding does not resemble a D- or DEF-motif [134].

1.2.3.5 Kinase inhibitor binding sites

Due to the involvement of MAPKs in numerous diseases, significant effort has been made by the pharmaceutical industry to develop inhibitors that block specific MAPK pathways. This has led to the identification of two novel inhibitor binding sites, i.e. backside binding pocket and the “DFG-out”-site, where inhibitor interactions do not compete with ATP binding [135]. The backside binding pocket is a region in the vicinity of the CD domain in p38 α and binds inhibitors such as PD98056 [136]. In contrast, the “DFG-out”-site is a docking domain adjacent to the active site. Inhibitor binding to the conserved DFG sequence induces a conformational change in the activation loop of the enzyme and thereby blocks its activity [135, 137]. “DFG-out”-sites, however, are not unique for MAPK as they have also been described for MEK1/2 [138] and c-Abl [139].

1.3 The ERK-MAPK pathway

The ERK-MAPK pathway is one of the best studied mammalian kinase cascades and it has diverse cellular and physiological functions. ERK1/2 signalling modulates cellular processes such as cell cycle progression, proliferation, differentiation, migration, apoptosis and senescence [140]. Physiologically, this pathway is involved in cardiogenesis, immune system development and homeostasis, and plays a critical role in transducing responses to many hormones, growth factors and insulin. Thus, aberrant ERK1/2 signalling has been associated with equally diverse pathologies, including cancer [141-143], diabetes [144], and cardiovascular disease [145]. The cascade can be activated by a variety of extracellular stimuli, such as mitogens, growth factors, phorbol esters, cytokines, and insulin [63]. Moreover, ERK signalling can be induced by means of membrane depolarisation and Ca^{2+} influx [142].

The ERK-MAPK cascade is generally initiated through the activation of small GTPases, such as Ras or Rap1, which recruit Raf kinases to the plasma membrane [146]. To date three Raf kinase family members, namely A-Raf, B-Raf and c-Raf, have been identified. All isoforms contain three conserved regions, termed CR1, CR2 and CR3 [147]. The first two conserved regions have been implicated in regulating the catalytic domain, which is located in CR3. Activation of Raf kinases is a complex process, requiring protein-protein interaction, dimerization, as well as various phosphorylation and dephosphorylation events [147, 148]. In addition, Raf kinase activity can exist in multiple graded states, which are regulated by various kinases from other signalling pathways and allow signal modulation. For example, c-Raf phosphorylation at Ser338 and Tyr340/341 by PAK (p21-activated kinase) or Src, respectively, enhances the catalytic activity, whereas phosphorylation of Ser259 by AKT or PKA is inhibitory [149-151].

Activated Rafs subsequently phosphorylate and thereby activate MEK1/2 at two serine residues located in the Ser-Xaa-Ala-Xaa-Ser/Thr motif common to all MAPKKs [152]. During this step the incoming signal is amplified, as MEKs are more abundant than Raf kinases. MEK1/2 constitute an evolutionary conserved group of dual specificity kinases, which share an 85% sequence homology. Structurally, MEK isoforms are composed of a kinase domain, which is surrounded by an N-terminal regulatory and a short C-terminal domain [138]. The two genes encoding MEK1/2 give rise to three isoforms, which are

MEK1, its alternatively spliced form MEK1b, and MEK2 [153]. Although all kinases display catalytic activity, MEK1b does not phosphorylate the canonical ERK1/2 proteins, but stimulates activation of the splice variant ERK1c [154]. Once activated, MEK isoforms phosphorylate ERK1/2 at the conserved Thr-Glu-Tyr motif (human ERK1: aa 202-204, human ERK2: aa 185-187) in a two-collision, distributive manner rather than a single-collision, processive manner [155]. This allows the establishment of a threshold, where tyrosine-phosphorylated ERKs have to accumulate before phosphorylation of the threonine residue can occur. As singly phosphorylated ERK1/2 show very little kinase activity, this mode of activation allows signal propagation only when MEKs are activated for a prolonged period. Upon stimulation, ERK1/2 phosphorylate a multitude of substrates, including transcription factors, membrane proteins, cytoskeletal elements, phosphatases and kinases. So far more than 160 ERK substrates have been identified, yet the number is ever-growing [156]. ERKs are proline-directed kinases, which phosphorylate substrates on a Pro-Xaa-Ser/Thr-Pro consensus site. However, not all substrates contain this perfect consensus motif, but a shorter Ser/Thr-Pro sequence, which is still sufficient to direct ERK's phosphorylation [157].

1.3.1 ERK1/2 isoforms and splice variants

The two predominant ERK isoforms, namely ERK1 (44 kDa) and ERK2 (42 kDa), are evolutionary conserved enzymes, which show an overall sequence identity of nearly 85% [58]. Both kinases are ubiquitously expressed, albeit their relative abundance may vary across tissues. For example, ERK1 is highly expressed in intestines and placenta, whereas ERK2 expression predominates in muscle, thymus and heart tissues [58]. Notably, two genes, located on chromosomes 16 (*erk1*) and 22 (*erk2*), give rise to the canonical transcripts of ERK1, ERK2, and alternatively spliced forms [158, 159].

To date, two transcript variants have been described for ERK2, which encode the same protein, but differ in their 3' untranslated region (UTR). In contrast, alternative splicing of the ERK1 transcript results in three distinct isoforms (Figure 1-6 B). Isoform 1 represents the canonical ERK1 sequence, which translates into a 44 kDa protein [55, 58]. In comparison, isoform 3 lacks an in-frame exon in the 3' coding region, thus rendering a shorter transcript. So far, there is no evidence for expression of this variant at a protein level, thus questioning its physiological function. On the other hand, isoform 2 retains the

A

```

Human ERK1c  VGQSPAAVGLGAGEQGGTZ
              :   :::  :  :
Rat ERK1b    VSRPPAA-GRGISVPSVRPVPYCLCPQ

```

B



Figure 1-6 Structural differences between ERK1b and ERK1c

A. Sequence alignment of the intron 7 of human ERK1c and rat ERK1b. Identical amino acids are marked as (:). Introduced gaps to maximise the alignment are indicated by a dash.

B. Exon organisation of human ERK1, ERK1c and rat ERK1c. Adapted from [158].

intron 7, which, depending on its sequence, results in an ERK1 isoform of varying size. In the case of rodents, the 78 bp intron sequence is translated in frame and gives rise to a 46 kDa protein, called ERK1b [159]. In primates, however, the intron sequence (103 bp long) contains a premature stop codon, thus creating a shorter 40 kDa protein, termed ERK1c (Figure 1-6) [158]. Rodent ERK1b and primate ERK1c share many common features (Table 1-4). Firstly, both proteins are catalytically active, as demonstrated by *in vitro* kinase assays. Secondly, the inserted region sterically alters the CD-docking site, which leads to reduced interaction with D-motif containing proteins, such as MEK1 and ELK1 [156]. Thus, unlike ERK1/2, both splice variants fail to bind to the cytoplasmic retention signal in MEK and are constitutively localised to the nucleus [158, 159]. Moreover, reduced binding of protein tyrosine phosphatases (PTP), such as PTP-SL, results in a prolonged activation of these enzymes [158, 159]. Despite the latter similarities, ERK1b and ERK1c also possess distinct features (Table 1-4). For example, ERK1b is activated by MEK1/2 with comparable kinetics to those of ERK1 and ERK2, whereas ERK1c is activated primarily by the alternatively spliced isoform MEK1b [154, 159]. Moreover, mono-ubiquitination of ERK1c directs this enzyme to the Golgi apparatus, where it induces Golgi fragmentation [160]. Interestingly, ERK1c expression is increased in tumour tissues, suggesting a putative role for this enzyme in tumourigenesis [160]. In contrast, physiological functions for ERK1b are still unknown. It is assumed, however, that ERK1b is particularly important for signal transduction via the ERK-MAPK pathway in conditions, where the active pool of ERK1/2 is limited [159].

		<i>Rodent ERK1b</i>	<i>Primate ERK1c</i>
Common features	Derivation	Alternative splicing leads to incorporation of intron 7	
	Enzymatic activity	Catalytically active	
	Structure	Disrupted CD domain	
	Protein-protein interaction	Weak interaction with MEK and phosphatases	
	Subcellular localisation	Constitutive nuclear localisation in resting cells	
Distinct features	Predicted size	46 kDa	40 kDa
	Insert size	78 bp	103 bp with in-frame stop codon
	Activation by MEK	Activated by MEK1/2 with similar kinetics to ERK1/2	Activated by splice variant MEK1b
	Posttranslational modification	<ul style="list-style-type: none"> • Phosphorylation of TEY motif • No ubiquitination 	<ul style="list-style-type: none"> • Phosphorylation of TEY motif • Mono-ubiquitination leads to Golgi localisation
	Physiological function	Unknown	Involved in Golgi fragmentation necessary during mitosis

Table 1-4 Common and distinct features of the alternatively spliced ERK1 isoforms

1.3.2 ERK signalling specificity

One of the intriguing features of the ERK-MAPK pathway is its ability to stimulate different, and sometimes even opposing, cellular functions. This raises the question as to how different input signals can evoke distinct functional outcomes. Several mechanisms, determining signalling specificity, have been identified in recent years, including: (i) duration and strength of signals [161], (ii) interaction with scaffold and adaptor proteins [148], (iii) subcellular localisation [162, 163], (iv) crosstalk and interplay between the ERK-MAPK pathway and other signalling cascades [149-151, 164], (v) isoform specificity [59, 154], and (vi) cell-specific ERK substrates [156]. Notably, these mechanisms work cooperatively, rather than independently, to ensure proper downstream signalling. The following subsections focus on how ERK activity is regulated in a cellular context by means of protein phosphatases, scaffold proteins, subcellular localisation and feedback loops.

1.3.2.1 Regulation of ERK activity through protein phosphatases

Phosphorylation events are key regulators of the ERK-MAPK pathway. Not only are all members of the MAPK cascade activated by phosphorylation, the addition of phospho groups to MEKs and Rafs can also inhibit kinase activity. Thus, protein phosphates can impact both negatively and positively on ERK signalling. Full activation of ERK1/2 requires dual phosphorylation of the Thr-Glu-Tyr motif. Single phosphorylation of either threonine or tyrosine results in a marginally active kinase. Therefore, ERK activity can be inhibited through the removal of either one or two phospho groups. Generally, three groups of protein phosphatases act on ERK1/2 (Table 1-5), i.e. serine/threonine protein phosphatases (Ser/Thr-PPs), phosphotyrosine phosphatases (PTPs) and MAPK phosphatases (MKPs). MAPK phosphatases, as the name suggests, constitute a unique class of dual specificity phosphatases that act selectively on MAPKs and remove both phospho groups simultaneously (Figure 1-7).

Despite its broad substrate specificity, the Ser/Thr protein phosphatase, PP2A, is an important regulator of the ERK-MAPK pathway [165-167]. The holoenzyme consists of three subunits, i.e. a scaffolding subunit A, a regulatory subunit B, and a catalytic subunit C. Different combinations of A, B and C give rise to over 50 PP2A trimers [168, 169]. B subunits, which target PP2A to distinct subcellular localisations and are involved in

<i>NAME</i>	<i>Alternative name</i>	<i>Size (kDa)</i>	<i>Substrate specificity</i>	<i>Localisation</i>
A. Ser/Thr PP				
PP2A		37	ERK (when trimer with B \square subunit)	cytosolic
B. PTP				
He-PTP		38	ERK = p38	cytosolic
STEP		20-61	ERK	cytosolic
PTP-SL	PCPTP-1	42,65	ERK = p38	cytosolic
C. MKPs				
DUSP1*	MKP-1, CL100	39	P38 = JNK > ERK	nuclear
DUSP2*	PAC-1	34	ERK = p38 > JNK	nuclear
DUSP 4*	MKP-2	43	ERK = p38 > JNK	nuclear
DUSP5*	hVHR3	42	ERK	nuclear
DUSP6	MKP-3	43	ERK > JNK = p38	cytosolic
DUSP7	MKP-X	40	ERK > JNK = p38	cytosolic
DUSP8	hVH5	66	JNK = p38 > ERK	nuclear and cytosolic
DUSP9	MKP-4	42	ERK > p38 > JNK	nuclear and cytosolic
DUSP10*	MKP-5	53	P38 = JNK > ERK	nuclear and cytosolic
DUSP16	MKP-7	73	JNK = p38 > ERK	cytosolic

Table 1-5 Overview of the different groups of ERK phosphatases
Phosphatases marked with * are encoded by ERK1/2 inducible genes.

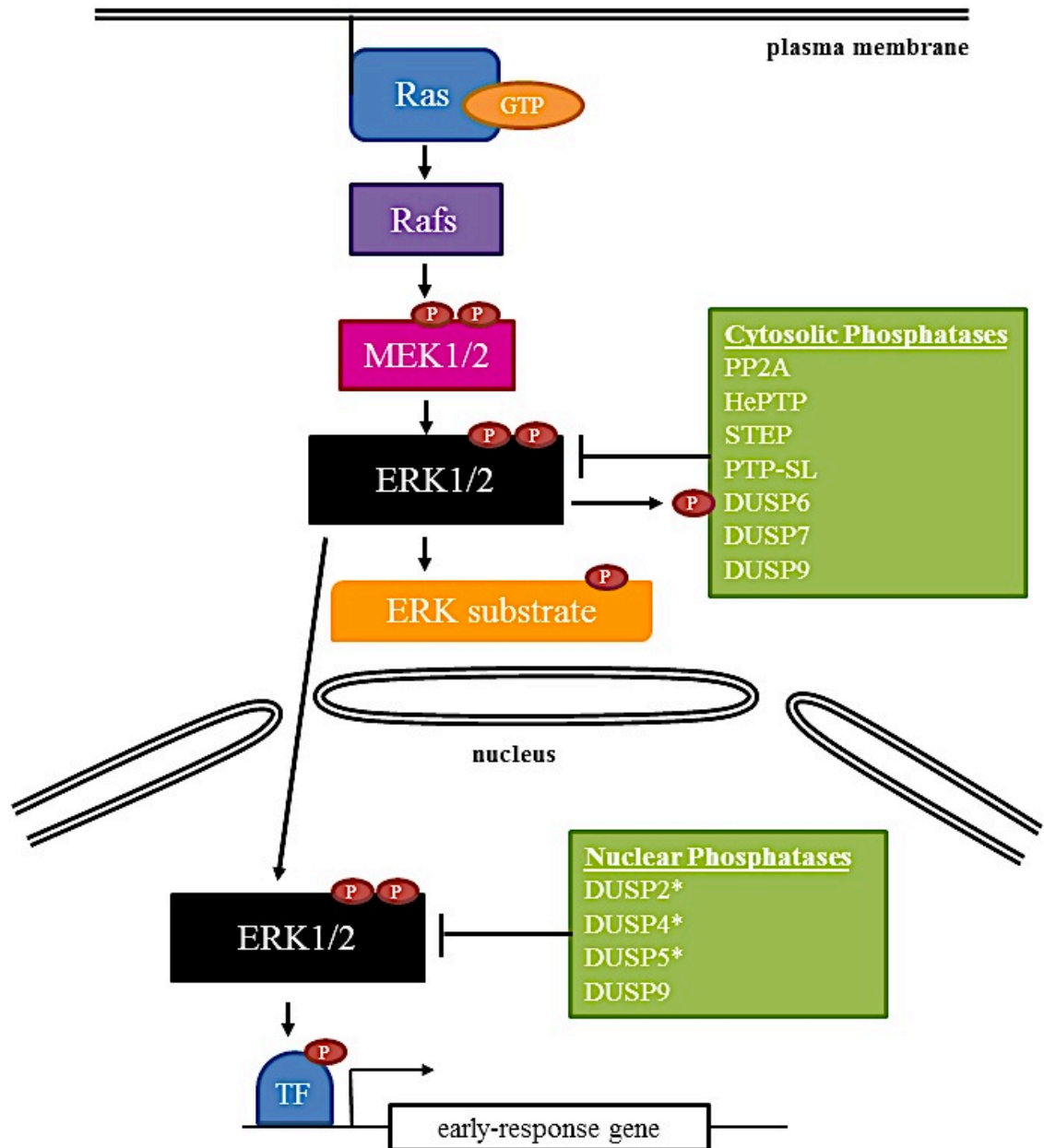


Figure 1-7 ERK signalling is regulated by cytoplasmic and nuclear phosphatases

ERK activity is regulated by three groups of phosphatases, namely Ser/Thr PPs, PTPs and DUSPs, which possess specific subcellular localisations. DUSP6 is subject to ERK phosphorylation, which targets the phosphatase for proteasomal degradation. Thus, ERK can prolong its own activity by inhibiting cytoplasmic inactivation. On the other hand, ERK can induce its inhibition, as the expression of multiple phosphatases marked here with (*) is induced by ERK signalling.

substrate recognition, have been divided into three gene families, named B (or PR55), B' (or B56) and B'' (PR72) [170]. Dephosphorylation of ERK1/2 is mediated by B' subunit containing enzymes in a process that is not yet fully understood. Interestingly, ERK1/2 itself can modulate PP2A activity by phosphorylating the B' subunits at a conserved serine residue. This process, however, requires expression of the immediate early gene IEX-1, which serves as an adaptor protein by positioning the B' subunit for ERK-mediated phosphorylation [171]. Thus, IEX-1 induction results in enhanced phosphorylation of B', subsequent inhibition of PP2A and prolonged ERK activation.

Phosphorylation represents a common mechanism for regulating phosphatase activity. For example, interaction of the hematopoietic protein tyrosine phosphatase (He-PTP) with ERK1/2 is inhibited by PKA-mediated phosphorylation of the D-motif [172]. Likewise, phosphorylation of the striatal-enriched protein tyrosine phosphatase (STEP) prevents ERK1/2 dephosphorylation [173]. Thus far, three PTPs with ERK1/2 activity have been identified: He-PTP, which is the only PTP expressed in hematopoietic cells, STEP, which is mainly expressed in the brain and PTP-SL, which is expressed in lung, heart and brain [174]. Interestingly, PTPs and PP2A sometimes form a complex with dual specificity, thus mimicking the activity of MKPs [174].

MKPs represent a well-characterised subgroup of dual specificity phosphatases (DUSP), which antagonize MAPK signalling. In general, MKPs are subdivided into two groups: (i) MKPs, which are encoded by growth factor or stress-inducible genes and are largely located in the nucleus, or (ii) MKPs, whose activity is not regulated by gene transcription and are primarily found in the cytoplasm [59]. All MKPs, however, are composed of an N-terminal regulatory and a C-terminal catalytic domain. Some MKPs, such as DUSP5 and DUSP6 demonstrate an increased specificity towards ERK1/2, whereas others, such as DUSP1, preferentially dephosphorylate p38s and JNKs [175]. The activity of MKPs can be regulated by means of protein-protein interaction, phosphorylation and oxidation. For example, DUSP6 interaction with ERK1/2 induces a conformational change, which results in the activation of the phosphatase. However, DUSP6 contains an ERK consensus site, which, when phosphorylated, targets the enzyme for proteasomal degradation without altering its catalytic activity [176]. In contrast, phosphorylation of DUSP1 by ERK1/2 results in the stabilisation of the phosphatase [177]. Additionally, reactive oxygen species, such as H₂O₂, oxidise MKPs, rendering the enzymes inactive [178].

1.3.2.2 Regulation of ERK activity through upstream and downstream scaffold proteins

One important determinant of ERK signalling strength and duration is the efficiency of its activation. When all components of the cascade are brought into close proximity, optimal pathway activation through sequential phosphorylation of Rafs, MEK1/2, and ERK1/2 can occur. One way of bringing these protein kinases into the vicinity of one another, is through direct interaction of pathway members. For example, MEK1/2 bind inactive ERK constitutively and thereby not only serve as cytoplasmic anchor proteins, but also allow the formation of a signalling module, which facilitates ERK activation [179]. The same is valid for RSK (ribosomal S6 kinase) proteins, which bind inactive ERK and thereby retain the kinase in the cytoplasm [180]. Alternatively, members of the ERK-MAPK pathway can be organised into multi-enzyme complexes through scaffold proteins. By definition, scaffolds serve as structural docking platforms, which bind two or more members of a signalling pathway and facilitate signal transduction. Besides this obvious function, however, scaffold proteins also influence pathway signalling by targeting multi-enzyme complexes to specific subcellular localisations (Figure 1-8 and Table 1-6). Moreover, scaffolds can prevent crosstalk with other signalling pathways by masking interaction or modification sites of its binding partners. Additionally, scaffolds can integrate signals from otherwise discrete signalling pathways, as their ability to bind signalling molecules can be regulated through post-translational modifications. Furthermore, adaptor proteins can link a signalling pathway to specific activating signals. Taken together, scaffolds can provide signalling specificity to the multi-functional ERK-MAPK pathway. An overview of the ERK-MAPK scaffolds known to date will be given in the following sections.

Kinase suppressor of Ras (KSR; binds Rafs, MEK1/2, ERK1/2 and 14-3-3)

Kinase suppressor of Ras (KSR) was originally identified as a suppressor of an activated Ras phenotype in genetic studies of *C. elegans* and *Drosophila* [181, 182]. To date, two KSR proteins (KSR1 and KSR2) have been discovered in mammals, both of which contain five conserved domains (CA1-5). The presence of a kinase-like domain and structural similarity to c-Raf sparked investigations into a putative catalytic activity. Whether or not the kinase domain is functionally active, however, remains an open issue [148, 183]. KSR proteins interact with all members of the ERK-MAPK cascade [184, 185]. Both MEK

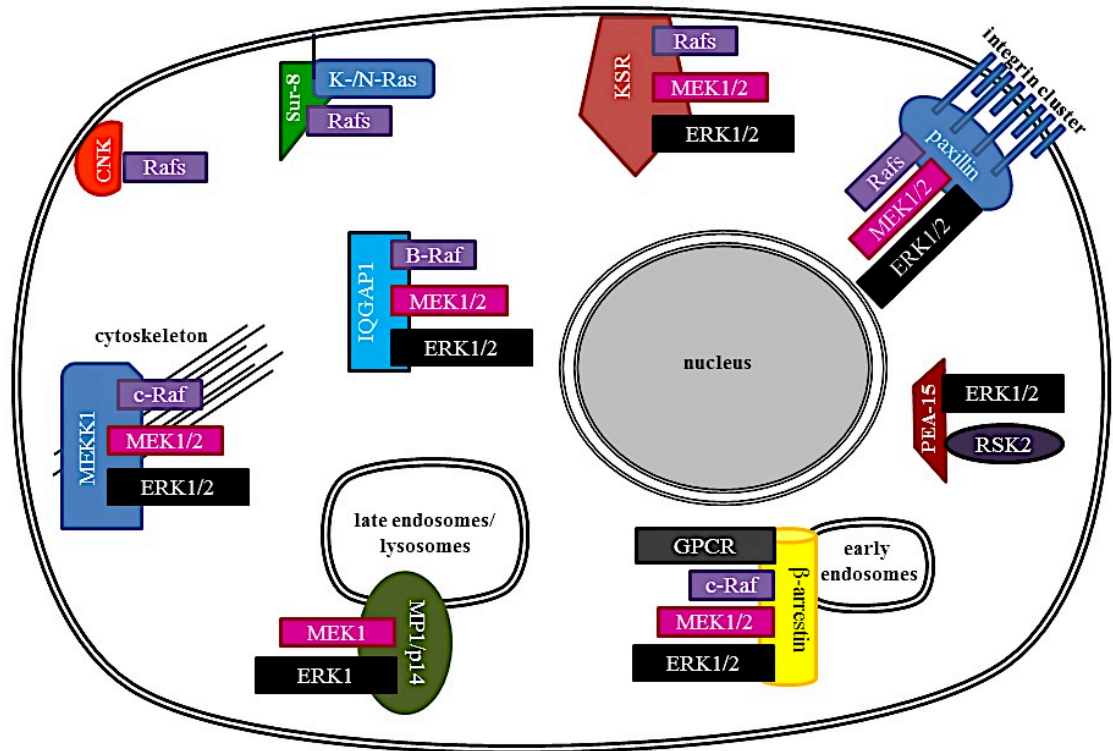


Figure 1-8 Subcellular localisation of ERK activity through scaffold proteins

Scaffold proteins facilitate ERK activation by assembling cascade components into functional modules. Moreover, scaffolds localise ERK activity at specific subcellular localisations and link the ERK activation to specific extracellular signals.

<i>Acronym</i>	<i>Name</i>	<i>Size (kDa)</i>	<i>Protein interactions</i>	<i>Subcellular target</i>
KSR	Kinase suppressor of Ras	~100	Raf, 14-3-3, MEK1/2, ERK1/2	plasma membrane
MP1	MEK partner 1	13.5	MEK1, ERK1	MP1/p14: late endosomes MP1/Morg-1: vesicular structures
β -arrestin		~46	c-Raf, MEK1/2, ERK1/2	early endosomes
MEKK1	MEK kinase 1	195	c-Raf, MEK1/2, ERK1/2	cytoskeleton
CNK	Connector enhancer of KSR	61-117	Rafs	plasma membrane
Sur-8	Suppressor of Ras 8	65	K-/N-Ras, Rafs	plasma membrane
IQGAP1		190	B-Raf, MEK1/2, ERK1/2	cytoplasm
Paxillin		68	Raf, MEK1/2, ERK1/2	focal adhesions
PEA-15	Phosphoprotein enriched in astrocytes	15	ERK1/2, RSK2	cytoplasm
RKIP	Raf kinase inhibitor protein	21	c-Raf, MEK1/2, ERK1/2	

Table 1-6 Mammalian scaffold proteins for the ERK-MAPK pathway

isoforms bind directly to the kinase-like domain, CA5, ERK1/2 interact with the DEF-motif found in CA4 and Raf association, at least in *Drosophila*, is mediated via the CA1 domain [183, 186]. KSR localisation is dynamic and regulated by phosphorylation and protein interactions. In quiescent cells, KSR, which is phosphorylated at Ser392, binds to 14-3-3 to localise the signalling complex to the cytoplasm. Upon Ras activation, this critical residue is dephosphorylated and 14-3-3 association is disrupted. Subsequently, the KSR signalling complex is translocated to the plasma membrane where the kinase cascade becomes activated. Upon activation, ERK is released from the KSR platform and accumulates e.g. in the nucleus to regulate gene transcription.

MEK partner 1 (MP1; binds MEK1 and ERK1)

MP1 was identified in a yeast two-hybrid screen for MEK1 interacting partners in 1998 [187]. Original work demonstrated a selective binding of MP1 to MEK1 and ERK1 and suggested specific activation of ERK1 over ERK2. Subsequent work, however, challenged this by showing that MP1 is required for activation of both ERK1 and ERK2 [188]. Thus, in contrast to the original data, MP1 might either represent a docking platform for MEK2 and ERK2, or activate ERK2 indirectly as part of the same signalling complex. Interaction with the adaptor protein, p14, localises the MP1 complex to late endosomes, where it enhances PAK1 phosphorylation and drives cellular spreading [189, 190]. Interestingly, the MP1/p14 complex is required for full ERK activation upon EGF stimulation, whereas another MP1 adaptor, namely Morg-1 (mitogen-activated protein kinase organiser 1) promotes ERK signalling in response to serum, lysophosphatidic acid, and phorbol ester [191]. Thus, MP1 links the ERK-MAPK cascade to EGF signalling through p14 interaction and to G-protein coupled receptor (GPCR) signalling through Morg-1 association. Like p14, Morg-1 targets MP1 to vesicular structures, the nature of which has not been determined yet [191].

β -Arrestins (bind c-Raf, MEK1/2 and ERK1/2)

It is well-established that β -arrestins terminate GPCR signalling by mediating receptor internalisation [192]. However, evidence is emerging that suggests an additional scaffolding function for β -arrestins [193]. In mammalian tissues, two β -arrestin proteins, named β -arrestin 1 and β -arrestin 2, are expressed. Following activation of GPCRs, β -arrestins translocate from the cytoplasm to the plasma membrane, which targets the

receptors for internalisation. During subsequent endocytosis, a multi-enzyme signalling complex encompassing the internalised GPCR, β -arrestin, c-Raf, MEK1/2 and ERK1/2 is formed and ERK signalling is activated [194, 195]. Interestingly, β -arrestins enhance cytosolic ERK activity and reduce transcriptional responses, thereby providing a counter to KSR-mediated ERK signalling [196].

MEK Kinase 1 (binds to c-Raf, MEK1/2 and ERK1/2)

MEK kinase 1 (MEKK1) is a multi-functional protein that is mainly appreciated as an upstream MAPKKK for JNK and p38 (Table 1-2) [62, 197]. In addition to its kinase activity, MEKK1 exhibits an E3 ubiquitin ligase activity [198] and can act as a scaffold for members of the ERK-MAPK cascade due to its large non-catalytic N-terminal domain, which serves as a docking platform [199]. MEKK1 binds c-Raf, MEK1/2, ERK1/2 constitutively [200] and is believed to regulate ERK activation. This is based on its ability to enhance ERK signalling when overexpressed [197] and because ERK activation is reduced in MEKK1-deficient cells [201]. Intriguingly, MEKK1 is tightly associated with the cytoskeleton, and this might therefore provide a means of targeting ERK signalling to cytoskeletal elements. In addition, MEKK1 can serve to reduce ERK activity by ubiquitinating ERK1/2 and thus targeting it for proteasomal degradation [198].

Connector enhancer of KSR (CNK; binds c-Raf and B-Raf)

In an attempt to identify functional binding partners of KSR, the connector enhancer of KSR (CNK) was identified in *Drosophila* in 1998. CNK is a large non-catalytic adaptor protein with multiple protein interaction domains. It contains a sterile α motif (SAM), a conserved region in CNK (CRIC), a PDZ domain, Src-homology-3 (SH3)-binding sites and a pleckstrin homology (PH) domain, which mediates membrane localisation [202]. In mammals, three CNK isoforms (CNK1, CNK2A and its truncated splice variant CNK2B) have been identified [203, 204], all of which associate with Raf but no other member of the ERK cascade and enhance its activation via Src and Ras [205, 206]. So far, it has been shown that CNK enhances ERK activation, but the exact mechanism through which this is achieved remains to be elucidated.

Suppressor of Ras 8 (Sur-8; binds Ras and c-Raf)

The Suppressor of Ras has been isolated in *C. elegans* as an adaptor protein, which increases Ras-mediated signal transduction [207]. Sur-8 is a conserved protein, which mainly consists of leucine repeats and forms a complex with mammalian Ras and c-Raf, thus coupling Raf to the plasma membrane in the vicinity of its upstream regulator [208]. Interestingly, Sur-8 may provide signalling specificity by binding to N-Ras and K-Ras, but not H-Ras *in vitro* [207].

IQGAP1 (binds B-Raf, MEK1/2 and ERK1/2)

IQGAPs form a conserved class of multidomain proteins, which mediate interactions with a variety of signalling molecules and regulate multiple cellular processes, such as cell-cell adhesion, transcription and cytoskeletal remodelling. To date, three IQGAP isoforms (IQGAP1, -2 and -3) have been identified in humans, with IQGAP1 being the most intensively studied. IQGAP1 has recently been identified as a novel MAPK scaffold, which binds directly to B-Raf, MEK1/2 and ERK1/2 [209-211]. This is particularly interesting as oncogenic Ras, prevalent in over 15% of all human cancers, primarily signals through B-Raf [212, 213]. Thus, IQGAP1's function as a MAPK scaffold might be an important contributor to tumorigenesis. Intriguingly, IQGAP1 binding to B-Raf enhances its activity *in vitro* and this may provide a novel mechanism for pathway regulation. Although EGF stimulation of ERK signalling requires IQGAP1, the exact mechanism of ERK activation remains to be elucidated [210].

Paxillin (binds Raf, MEK1/2 and ERK1/2)

Paxillin is a scaffold protein, which recruits both structural and signalling molecules to adhesion sites and regulates cell migration and gene transcription. It is essential for adhesion-mediated activation of ERK [214], and several mechanisms have been proposed to explain how this occurs. One mechanism suggests the assembly of a functional ERK module on paxillin itself, which exhibits distinct binding efficiencies for all members of the ERK cascade. It associates constitutively with MEK, but only interacts with activated Raf. ERK association with this scaffold is regulated by Src. During cell adhesion Src phosphorylates paxillin at Tyr118, which promotes binding of inactive ERK to the scaffold and initiates ERK activation [215]. ERK, in turn, phosphorylates paxillin, which enhances the binding of focal adhesion kinase (FAK) to the scaffold and activates Rac signalling

further downstream [216]. As a result, FAK promotes the turnover of focal adhesions, whereas Rac initiates lamellipodia formation. Thus, a functional ERK module on paxillin gives rise to a positive feedback loop that coordinates cell motility. Alternatively, the paxillin binding protein GIT1 may provide a docking platform for ERK signalling molecules at focal complexes [217]. GIT1 interacts with MEK and ERK1/2 to induce ERK signalling in response to EGF [218, 219]. Another mechanism for localising ERK at focal adhesions involves FAK. Indeed, FAK can recruit MEKK1, which itself is a docking platform for the ERK-MAPK cascade [220].

Phosphoprotein enriched in astrocytes 15 (PEA-15; binds ERK1/2 and RSK2)

The phosphoprotein PEA-15 was originally identified in astrocytes, where its expression is enriched [221]. It consists of a death effector domain (DED) and an unstructured C-terminal tail, which is involved in ERK binding [222]. PEA-15 is the only downstream ERK scaffold known to date and forms a complex with ERK1/2 and RSK2 (ribosomal S6 kinase) [223]. Furthermore, PEA-15 functions as a cytoplasmic anchor protein, although it is not completely understood how. The phosphoprotein contains a NES, which might represent one possibility for keeping ERK signalling in the cytoplasm [224]. Moreover, PEA-15 and nucleoporins compete for the same binding site on ERK. Thus, PEA-15 complex formations blocks nuclear import of ERK and might provide another means of cytoplasmic anchoring [225].

Raf kinase inhibitor protein (RKIP; binds c-Raf/B-Raf, MEK1/2 and ERK1/2)

The Raf kinase inhibitor protein is set apart from other known scaffolds in that it prevents efficient ERK activation rather than facilitating it. RKIP contains overlapping docking sites for MEK1/2 and Raf. Thus, binding of these two kinases is mutually exclusive and RKIP either forms a ternary complex with MEK and ERK, or interacts with Raf in a binary complex. Competitive binding of MEK and Raf prevents the assembly of a functional ERK module and thereby suppresses ERK activation [226].

1.3.2.3 Localising ERK activity to specific subcellular compartments

The localisation of ERK to specific subcellular compartments provides an important means of controlling downstream substrates and biological outcomes. Neuronal differentiation of PC12 cells, for example, requires nuclear ERK signalling. Thus, blocking ERK's translocation to the nucleus through cytoplasmic anchoring proteins inhibits the formation of neurite extensions [227]. As the previous section (1.3.2.2) has highlighted how docking platforms can act to localise ERK to distinct subcellular locations, the following paragraphs aim to describe how ERK-specific anchoring proteins other than scaffolds can function to recruit ERKs to specific cellular locales.

The cellular distribution of ERK changes upon its activation. Whereas, in quiescent cells the enzyme is mainly cytoplasmic, ERK activation triggers its redistribution to different cellular loci. Thus, active enzyme then accumulates in the nucleus, where it drives or inhibits transcriptional events. This dynamic shuttling of ERK is controlled by various anchoring proteins, including MEK, which was the first cytoplasmic retainer to be identified [179]. ERK activation by MEK1/2 triggers a conformational change, which disrupts the interaction between the two kinases [130]. Thus, MEK-mediated retention of ERK is stimulus-dependent and reversible. In contrast, PEA-15 association with ERK is non-reversible and therefore independent of ERK's phosphorylation status [224].

Although the biggest portion of active ERK is either localised in the cytoplasm or nucleus, about 10% of the enzyme translocates to the surface of organelles. Sef-1 (similar expression to *fgf 1* [228]) is an example of an organelle recruiter, that targets ERK specifically to membrane ruffles and the Golgi. Interestingly, Ras has also been found to reside at the Golgi, where it is activated by the RasGRP1, rather than SOS. Thus, localising ERK at the Golgi might specifically induce kinase activity through mechanisms other than the canonical stimuli [229]. Moreover, Sef-1 inhibits nuclear ERK translocation without altering phosphorylation of cytoplasmic targets. It acts as a cytoplasmic retainer by binding to activated MEK and inhibiting stimulus-dependent dissociation of ERK from MEK [230]. In contrast, a protein called Mxi2 has recently been shown to promote stimulus-independent translocation of ERK to the nucleus [231]. Two features of this p38 α splice isoform [232] aid to accumulate ERK molecules in the nucleus. Firstly, Mxi2 binds directly to ERK1/2 and thereby disrupts pre-existing PEA-15/ERK complexes [140].

Secondly, Mxi2 interacts with nucleoporins, thus localising ERK in the vicinity of nuclear transporters and in doing so increasing its nuclear import [231]. Moreover, Mxi2 has been shown to prolong nuclear ERK activity [233]. One possible explanation for this observation is that Mxi2 masks phosphatase binding sites on ERK. Future work, including competition binding assays and crystal structures of the Mxi2/ERK complex, will shed light on how Mxi2 extends nuclear ERK signalling.

DUSPs (described in 1.3.2.1) may also serve as nuclear or cytoplasmic anchoring proteins. DUSP6, for example, anchors ERK molecules in the cytoplasm via its NES [234]. In contrast, DUSP5 comprises a NLS adjacent to its D-motif and this sequesters ERK in the nucleus [235]. In addition, DUSP2 and -4 have also been shown to retain ERK in the nucleus through direct binding [236]. Given the significant role of ERK signalling in regulating transcriptional events, more nuclear anchoring proteins are expected to be identified.

1.3.2.4 Regulating ERK activity through feedback loops

ERK plays a central role in regulating many biological processes. Previous sections have described how targeting ERK activity to subcellular loci can achieve signalling specificity. Studies in PC12 cells, however, provide evidence that signal duration can also be a determining factor in biological outcomes; as sustained activation of ERK by NGF induces differentiation in this cell system, whereas transient signalling results in proliferation [237]. Therefore, ERK substrates that either feedback to increase or decrease signal duration are of particular interest in understanding the MAPK cascade.

Several points of negative feedback have been described for the ERK-MAPK pathway (Figure 1-9). Firstly, ERK regulates its own activation by phosphorylating MEK at Thr292. The added phospho group prevents further enhancement of MEK activity and diminishes ERK signalling [238]. Another example of a negative feedback loop involves PAK1 phosphorylation. Generally, PAK1 influences the ERK-MAPK pathway by priming MEK for c-Raf activation. By phosphorylating Thr212, ERK inhibits priming of MEK and therefore limits its own signalling [239, 240]. Additionally, multiple ERK phosphorylation sites on Raf have been described. Hyperphosphorylation of these residues inhibits membrane recruitment of Raf and promotes its inactivation by PP2A [241]. Intriguingly, a positive feedback loop to Raf has also been reported. Thus, Raf phosphorylation by ERK

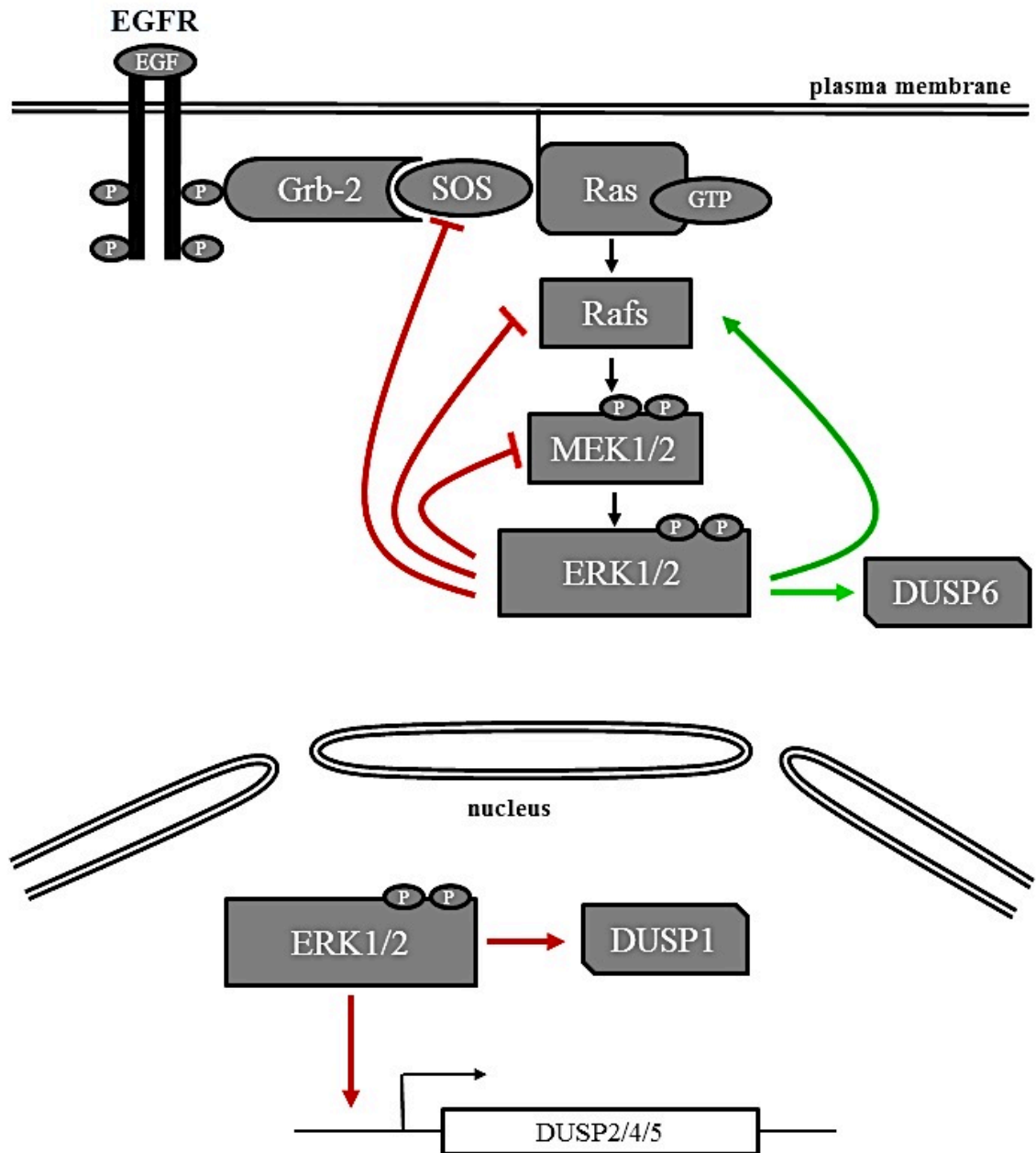


Figure 1-9 ERK pathway regulation by feedback loops

Canonical activation of the ERK-MAPK pathway is depicted in its simplest form. EGF molecules bind to EGFR receptors and initiate receptor dimerisation followed by transphosphorylation. Next, Grb-2 binds to phosphotyrosine residues in the cytoplasmic receptor tail and recruits the guanine nucleotide exchange factor SOS. Subsequent activation of Ras leads to the recruitment of Raf to the plasma membrane, where the kinase is activated and sequential phosphorylation of MEK and ERK finalise the activation of the pathway. Active ERK can increase its activity through positive feedback loops (depicted in green) or diminish its signalling capacity through negative feedback loops (depicted in red). Negative feedback loops display a mechanisms by which ERK signalling can be shut down to basal levels following pathway activation. Adapted from [140].

can either increase or reduce its activity [242]. Phosphoacceptor sites identified to increase Raf signalling are also involved in inhibiting the kinase, and it is unclear what determines a positive or negative feedback loop to Raf.

The guanine nucleotide exchange factor SOS (son of sevenless) is subject to ERK phosphorylation. SOS activates Ras by promoting a GTP-bound state and is usually localised in the cytoplasm. Upon activation of transmembrane receptor tyrosine kinases (RTK), SOS is recruited to the plasma membrane to activate Ras. Phosphorylation by ERK prevents this recruitment and blocks pathway activation [243]. Furthermore, sustained ERK activation induces the transcription of MKPs, such as DUSP2 and -5, which turn off ERK signalling by dephosphorylating the enzyme [244]. In addition, DUSPs may also be subject to ERK phosphorylation, although this can initiate a positive or negative feedback loop depending on the phosphatase. Phosphorylation of DUSP1 stabilises the phosphatase and ultimately decreases ERK activity in the nucleus [177]. On the other hand, DUSP6 phosphorylation marks the phosphatase for proteasomal degradation without altering its activity [176]. Moreover, direct interaction of ERK and DUSPs (e.g. DUSP5) may stabilise the phosphatases and reinforce their enzymatic activity [245]. Taken together, feedback loops play an important role in regulating ERK activity. They enable fine-tuning signalling strength and duration, which ultimately governs biological processes.

1.4 The ERK-MAPK pathway in cancer

It has long been appreciated that the ERK-MAPK pathway has a key role in regulating fundamental cellular processes such as proliferation, differentiation and cell motility. Cellular homeostasis, therefore, requires tight regulation of the cascade and aberrant ERK signalling contributes to multiple diseases, including cancer. Indeed, hyperactivation of the ERK-MAPK pathway is prevalent in one third of all human tumours and is implicated in many hallmarks of cancer [246]. Subsequent sections will describe how ERK signalling promotes tumourigenesis and discuss therapeutic strategies targeting the pathway.

1.4.1 *Activating mutations of the ERK-MAPK pathway*

Aberrant ERK signalling is triggered by activating mutations and/or overexpression of upstream components of the cascade. Canonically, ERK is stimulated by growth factors, which bind to transmembrane receptor tyrosine kinases (RTK), such as PDGFR, EGFR, ErbB2 and c-Met. Ligand binding activates the receptor by initiating receptor dimerisation (or in some cases oligomerisation) and subsequent transphosphorylation. In cancer, several mechanisms can stimulate inappropriate receptor activation. Firstly, tumour cells often synthesize their own growth factors, which trigger constitutive receptor activation in an autocrine manner. Clinical examples include PDGF and TGF α (a ligand for EGFR) secretion in glioblastomas and sarcomas, respectively [1]. Moreover, cell surface receptors themselves can be subject to deregulation. In many tumours genes, encoding RTKs, are amplified and lead to receptor overexpression. Examples include *egfr* amplification in brain and breast tumours [247, 248] or Her2 overexpression in mammary and ovarian carcinomas [249, 250]. Increasing the concentration of one particular receptor changes the overall composition of surface receptors in the plasma membrane and switches growth factor responsiveness of the tumour cell to previously non-stimulating ligands. Intriguingly, gross overexpression of surface receptors can trigger receptor dimerization and subsequent activation in the absence of extracellular ligands [251]. Moreover, activating truncations and mutations of RTKs have been observed in human tumours [252].

Further downstream, Ras proteins, of which there are four isoforms (N-Ras, H-Ras, K-Ras a and b), may be subject to deregulation. Indeed, Ras mutations occur very frequently in human tumours and are found in 90% of pancreatic lesions, 50% of colon carcinomas and

40% of lung carcinomas [213]. Ras proteins belong to the protein family of small GTPases, which have been characterised as molecular switches, because they cycle between an inactive GDP-bound and an active GTP-bound state. GTP exchange factors (GEFs) can turn these molecular switches on by promoting GDP dissociation and subsequent GTP binding. In contrast, GTPase activating proteins (GAPs) act to accelerate GTP hydrolysis, thus turning Ras signalling off. In human cancers, single amino acid substitutions impair the intrinsic hydrolase activity, thus rendering Ras constitutively GTP-bound and activated. Single point mutations have been identified for codon 12, 61 and less frequently 13 [253, 254].

Raf oncogenes comprise another group of deregulated signalling molecules in human cancers. Among the three Raf kinases, B-Raf is frequently mutated in many cancer subtypes, such as melanomas (70%), thyroid cancer (53%), colorectal cancer (22%) and ovarian carcinoma (30%) [255, 256]. Interestingly, c-Raf mutations are rare and very little evidence exists for A-Raf mutations. A screen of colorectal adenocarcinomas identified one silent exogenic mutation in the *A-raf* gene and no exogenic mutation for c-Raf [257]. In contrast, over 30 mutations have been detected for the *B-raf* gene, with the V600E mutation being the most frequent one (>90%). It is not entirely clear, why A-Raf and c-Raf mutations are underrepresented in human tumours. One possible explanation is based on the activation mechanism of the three kinases, which requires a negative charge in the N-region. In A-Raf and c-Raf, this is achieved through activating phosphorylation of two residues. In B-Raf however, the N-region is constitutively phosphorylated and thereby primed for activation. Consequently, activation of B-Raf can be accomplished in a single mutation event, whereas constitutive activation of either A-Raf or C-Raf requires at least two genetic alterations [258]. In general, B-Raf mutations are subdivided into two groups: (i) those which give rise to a constitutively active kinases and (ii) mutations, which entail an impaired or unaltered kinase activity [259]. The V600E mutation constitutively activates B-Raf and triggers continuous phosphorylation of MEK in the absence of extracellular stimuli and active Ras. In contrast, some B-Raf mutations are compromised in their ability to activate MEK, but rather elevate ERK signalling indirectly by activating wildtype c-Raf in an uncontrolled manner [259].

Notably, no activating MEK or ERK mutations have been identified in human cancers. This is no surprise, as both kinases require dual phosphorylation for full enzymatic activity.

Thus, two genetic alterations would be required for constitutive activation of these enzymes.

1.4.2 The role of ERK in growth and proliferation

Enhanced biosynthesis of macromolecules, membranes and organelles, increases the cellular volume and represents a prerequisite for cell division. Thus, it is no surprise that cell growth and cell cycle entry are tightly coordinated to maintain a constant cell size. ERK signalling stimulates protein synthesis through various mechanisms (see Table 1-7). Firstly, ERK1/2 phosphorylate and thereby activate MAPKAPKs, MNK1 and MNK2, which subsequently phosphorylate the translation initiation factor eIF4E at Ser209 [260, 261]. Although eIF4E is a general translation initiation factor, the phosphorylated protein preferentially augments translation of mRNAs with extensive 5'UTRs, including ribosomal, growth-related and anti-apoptotic mRNAs [262]. Moreover, the ERK-MAPK cascade impinges on the mTOR (mammalian target of rapamycin) pathway, which is regarded as the master regulator of growth, because it modulates ribosome biogenesis and translation initiation. The mTOR kinase is sterically activated by a small GTPase called Rheb [263]. The heterodimer of the tuberous sclerosis complex 1 and 2 (TSC1/TSC2) acts as a GAP for Rheb and thus antagonises mTOR stimulation. Direct phosphorylation of TSC2 by ERK1/2 disrupts heterodimer formation and consequently enhances mTOR signalling [264]. Moreover, RSK1, a downstream ERK substrate, has also been shown to inactivate the TSC1/TSC2 complex through phosphorylation of Ser1798 [265]. Additionally, RNA polymerase I (Pol I)-mediated transcription of ribosomal genes is subject to ERK regulation. Initiation of Pol I transcription requires the sequential binding of two transcription factors, i.e. UBF and SL1, at the transcription initiation site. First, the upstream binding factor (UBF) binds to the promoter element and the upstream control element, thus bringing them together and creating a platform for SL1 (selectivity factor 1) binding. Subsequently, Pol I is recruited to the promoter site and an initiation complex is formed. Interestingly, UBF is subject to direct phosphorylation by ERK1/2 and only modified UBF can recognise rRNA promoter sites. Thus, the initiation of Pol I transcription directly depends on ERK1/2 signalling [266]. In addition, ERK1/2 phosphorylate the transcription initiation factor-1A (TIF1A) at Ser633 to promote RNA Pol I transcription [267]. Interestingly, transcriptional events of Pol II and III are also modulated through ERK-mediated phosphorylation events. Thus, TFII-I promotes transcriptional

<i>Cellular function</i>	<i>Protein</i>	<i>Name</i>	<i>Phosphorylation site(s)</i>	<i>Ref</i>
Cellular growth	TSC2	tuberous sclerosis complex 2	Ser664	[264]
	TFII-I	transcription factor II-I	Ser627, Ser633	[268]
	Brf1	subunit of transcription factor III B	unknown	[269]
	TIF1A	transcription factor 1A	Ser633	[267]
	UBF	upstream binding factor	Thr117	[266]
	RNA Pol II	RNA polymerase II	multiple sites	[270]
Proliferation	Tob1	transducer of Erbb2	Ser152, Ser154, Ser164	[271]
	c-Myc	myelocytomatosis oncogene	Ser62	[272]
Survival	FOXO3A	forkhead box O3	Ser294, Ser344, Ser425	[273]
	Bim _{EL}	Bcl-2 like 11	Ser109, Thr110	[274]
	Caspase 9		Thr125	[275]
Cell migration	FAK	focal adhesion kinase	Ser910	[276]
	MLCK	myosin light chain kinase	Ser13	[277]
	Cortactin		Ser405, Ser418	[278]
	Paxillin		unknown, Ser83 (mouse)	[216]
	Stathmin		Ser16, Ser25, Ser38	[279]
	Vinexin β		Ser189	[280]
	Calpain		Ser50	[281]

Table 1-7 *Bona fide* ERK substrates grouped according to their biological functions

activity on the c-Fos promoter as a result of direct phosphorylation by ERK [268]. Moreover, the transcriptional activity of RNA Pol II is induced through direct phosphorylation of ERK at multiple sites [270]. Likewise, RNA Pol III transcription is induced as a result of direct phosphorylation of the TFIIB subunit, Brf1 [269].

In addition to an increased demand for proteins, growing cells require *de novo* synthesis of RNA, DNA, lipids and glycogen. Pyrimidine nucleotides are precursors for the production of all these molecules and its biosynthesis is carried out by a multi-enzyme complex called CAD. ERK1/2 phosphorylates CAD on Thr456 and thereby promotes pyrimidine synthesis [282].

The process of cell division is governed by three regulatory molecules, namely cyclins, cyclin-dependent kinases (CDKs) and cyclin-dependent kinase inhibitors (CDKI). During the first step of the cell cycle, which marks the progression from G₀/G₁ to S phase, cyclin D expression is initiated and accumulates in the nucleus. The regulatory subunit interacts with CDK4 and CDK6, to form a catalytic complex, which phosphorylates the retinoblastoma (Rb) protein. In quiescent cells, Rb inhibits members of the E2F family of transcription factors through direct interaction. Phosphorylation of Rb, however, disrupts the association with E2F and promotes expression of E2F target genes, such as *cyclin E*. Subsequent accumulation of cyclin E induces an active E/CDK2 complex, which phosphorylates Rb further and stimulates S phase entry [283]. Interestingly, *cyclin D* expression is under the control of sustained ERK activation. Thus, active ERK induces transcription of the immediate early genes (including *fos*, *jun* and *egr*) first, then stabilises the resulting AP1 transcription factors through direct phosphorylation, which then promotes transcription of the delayed early genes, one of which is *cyclin D* [284]. Moreover, ERK1/2 decreases expression of anti-proliferative genes, such as *tob1*. Tob1 is a transcriptional co-repressor, which inhibits cyclin D expression by recruiting histone deacetylases to the *cyclin D* promoter [285]. Moreover, existing Tob1 proteins are inhibited by ERK1/2-dependent phosphorylation, although it is unclear how the phospho transfer renders the TF inactive [271]. In addition, Rb/E2F association can be disrupted by direct phosphorylation of Rb by ERK1/2, thus relieving the inhibitory function of Rb [286].

The transcription factor c-Myc is another critical regulator of the cell cycle. Its expression is induced upon mitogen stimulation as part of the immediate early genes [287]. c-Myc

heterodimerises with other members of the Myc family of transcription factors, including Max and Miz-1. The Myc/Max transcription factor complex induces *cyclin D2* and *CDK4* expression [288, 289], while the Myc/Miz-1 complex represses the expression of the CDK inhibitors p15^{INK4} and p21^{Cip1} [290-292]. Additionally, c-Myc impacts profoundly on cellular growth by activating gene transcription of ribosomal proteins and translation factors [293]. However, c-Myc has an extremely short half-life (less than 30 minutes in growing cells) [294]. Thus, in order to induce cell cycle progression, the protein must be stabilised. Active ERK1/2 markedly enhance c-Myc stability as a result of direct phosphorylation of Ser62 [287, 295]. Thus, ERK signalling promotes both the expression of c-Myc and subsequently increases the protein's half-life.

Moreover, stimulation of the ERK-MAPK pathway induces the transcription of the CDK inhibitors, p21^{Cip1}, which paradoxically promotes cell cycle progression. The inhibitor has conflicting functions: While it inhibits the activity of cyclin E/CDK2 and cyclin A/CDK2, p21^{Cip1} stimulates cyclin D/CDK4/6 complexes upon binding. Thus, an ERK-dependent expression of the protein promotes G₁ progression to S phase [296].

It has to be noted that signal duration as well as signal strength of the ERK-MAPK cascade are key in determining whether or not a cell commits to mitosis, as strong activation of ERK cause cell cycle arrest [297]. Mutational activation of other signalling molecules, e.g. Rb, however, can override this halt and drive proliferation despite strong ERK signalling.

1.4.3 The role of ERK in cell survival

A dual signal model, proposed by Harrington *et al.*, suggests a direct link between cell proliferation and cell death. It argues that proliferative signals prime the cell death machinery, which, unless overruled by survival signals, will promote apoptosis [298]. Consequently, proliferative autonomy conveyed by oncogenes can trigger apoptosis unless cell survival signals countermand the death programme [299]. It is therefore not surprising that the ERK pathway cooperatively enhances cellular growth, proliferation and survival (see Table 1-7).

The mitochondrial (or intrinsic) apoptotic pathway is regulated by the Bcl-2 family of proteins, which are generally subdivided into pro-apoptotic factors (e.g. Bax and Bak), pro-survival factors (e.g. Bcl-2, Bcl-x_L and Mcl-1) and apoptotic sensors (e.g. Bid, Bim and

Puma). All Bcl-2 proteins comprise multiple Bcl-homology (BH) domains (BH1-4) with the exception of the apoptotic sensors, which only contain the BH3 domain. Therefore, they are termed BH3-only proteins (BOPs). In general, cell death is inhibited when the pro-apoptotic proteins like Bax and Bak are kept in a complex with pro-survival Bcl-2 proteins. Cellular stress stimulates the expression or activation of BOPs, which subsequently form a complex with pro-survival proteins to release Bax and Bak at the mitochondria and induce cytochrome C release [300, 301].

ERK1/2 stimulates cell survival by modulating multiple components of the apoptotic programme. Firstly, it represses Bim expression by phosphorylating the regulatory transcription factor FOXO3A and targeting it for proteasomal degradation [273]. Moreover, the most abundant splice isoform of Bim, Bim_{EL}, is subject to ERK phosphorylation, which promotes dissociation from pro-survival factors [302] and subsequent degradation [303, 304]. The apoptotic sensor Bad contains three inhibitory phosphorylation sites. Ser112 is phosphorylated by the ERK substrate RSK [305], Ser136 phosphorylation is catalysed by AKT [306] and Ser155 is phosphorylated by PKA [307]. ERK-dependent phosphorylation of Ser112 might facilitate phospho transfer onto Ser155 by PKA, which ultimately blocks association with pro-survival proteins [308]. Moreover, phosphorylation at Ser112 targets Bad for ubiquitination followed by proteasomal degradation [309]. ERK, furthermore, mediates the phosphorylation of caspase 9 and inhibits subsequent caspase 3 cleavage, thus preventing the onset of the caspase cascade [275].

There is evidence that signalling of the ERK-MAPK pathway stimulates the transcription of pro-survival factors, Bcl-2, Bcl-x_L and Mcl-1 [310]. Notably, the 5' regulatory elements of all three genes contain a CREB-binding site and the transcription factor CREB (cAMP responsive element binding protein) is activated as a result of RSK or MSK (mitogen- and stress-activated protein kinase) phosphorylation at Ser133 [311, 312]. Additionally, direct phosphorylation of Mcl-1 at Thr163 by ERK1/2 stabilises this pro-survival factor which otherwise has a very short half-life [313].

1.4.4 The role of ERK in cell migration

Over the past decade, more and more evidence supporting a critical role for the ERK-MAPK pathway in the acquisition of an invasive phenotype has been revealed. Most importantly, an invasive response requires ERK activity in the nucleus as well as in the cytoplasm [314]. However, the underlying mechanisms by which ERK signalling is connected to migratory processes are still being unravelled. Thus, the following paragraphs will try to give an overview of ERK-mediated responses linked to cell migration and invasion and discuss how *bona fide* targets of the kinases may be linked to these processes (see Table 1-7 also).

Cell migration is a complex and highly regulated process, which requires the continuous assembly and disassembly of adhesion complexes. There is evidence that ERK regulates both of these processes by modulating the signalling of the RHO family of small GTPases, including Rho, Rac and Cdc42, although the precise mechanism by which it does so is still unknown. Together, these three GTPases are central regulators of cell motility and require tight spatial and temporal regulation. At the leading edge Rac and Cdc42 promote actin polymerisation and branching through WAVE and WASP, respectively. In contrast, RhoA activity can oppose Rac and Cdc42 function by promoting stress fibre formation and initiating cellular contraction [315].

At the cell front ERK signalling has been shown to drive lamellipodium and pseudopod formation by enhancing actin protrusions. One important player in this process is cortactin, a cytoskeletal scaffold protein that can be directly phosphorylated by ERK at Ser405 and Ser418. This post-translational modification enhances cortactin-mediated N-WASP activation and promotes actin polymerisation at the leading edge [278].

Interestingly, ERK signalling is proposed to spatially restrict Rac, Cdc42 and RhoA activation by regulating GEF localisation and this may be achieved by controlling microtubule dynamics. ERK has been shown to phosphorylate stathmin, also known as oncoprotein 18 at Ser25 which inhibits sequestration of tubulin and frees the molecular building block for microtubule assembly at the cellular front [279, 316]. Moreover, kinesin motors are implicated in transporting GEFs along polarised microtubules [315]. Given that small GTPases of the Rab family, which interact with motor proteins, were shown to be

subject to ERK phosphorylation [315, 317], it is conceivable that ERK might also regulate microtubule-directed transport of GEFs to the cell front.

Stress fibres are important to the contractility of migrating cells, and it is known that they contribute to the retraction of the cell rear to enable effective forward movement. Stress fibres are composed of actin filaments associated with myosin filaments. In non-muscle cells myosin activity is known to be controlled by phosphorylation and the interplay of three regulatory proteins; namely the myosin kinases ROCK (Rho kinase) and MLCK (myosin light chain kinase), and the myosin light chain phosphatase, which dictate the phosphorylation state of myosin and thus control cellular contractility. Intriguingly, ERK can enhance MLCK activity by phosphorylating the myosin kinase at Ser13 and possibly Ser19 [156, 277, 314]. Moreover, ERK indirectly controls ROCK signalling by altering the activity of RhoA as mentioned above [315].

There are several lines of evidence that suggest an important role for the ERK-MAPK pathway in driving focal adhesion disassembly (Figure 1-10). Firstly, the scaffolding protein paxillin has been identified as a *bona fide* ERK target, which regulates integrin signalling at focal complexes. Phosphorylation of paxillin by ERK promotes the recruitment and activation of FAK, which ultimately induces adhesion disassembly [156]. Paradoxically, FAK itself is subject to ERK phosphorylation, which renders the kinase inactive, thereby impairing focal adhesion turnover [276]. Thus, ERK localisation with respect to paxillin and FAK can be a determining factor in the stability of focal adhesions. Vinexin- β poses another interesting ERK substrate, which is enriched at the leading edge of migrating cells. Indeed, phosphorylation of vinexin- β at Ser189 is implicated in promoting adhesion turnover and thus inhibiting cellular spreading [280, 318]. Lastly, the protease calpain 2 is subject to ERK phosphorylation at Ser50 which increases its proteolytic activity and promotes its association with FAK at focal complexes, where calpain cleaves cytoskeletal proteins [281, 319]. Depending on the downstream effector, calpain-induced cleavage can have opposing effects on adhesion stability. For example, paxillin cleavage stabilises focal adhesions [320], whereas severing of talin was shown to promote adhesion turnover [321]. Moreover, proteolysis of the protein tyrosine phosphatase PTP1B enhances Src activity, which in turn promotes adhesion disassembly [322].

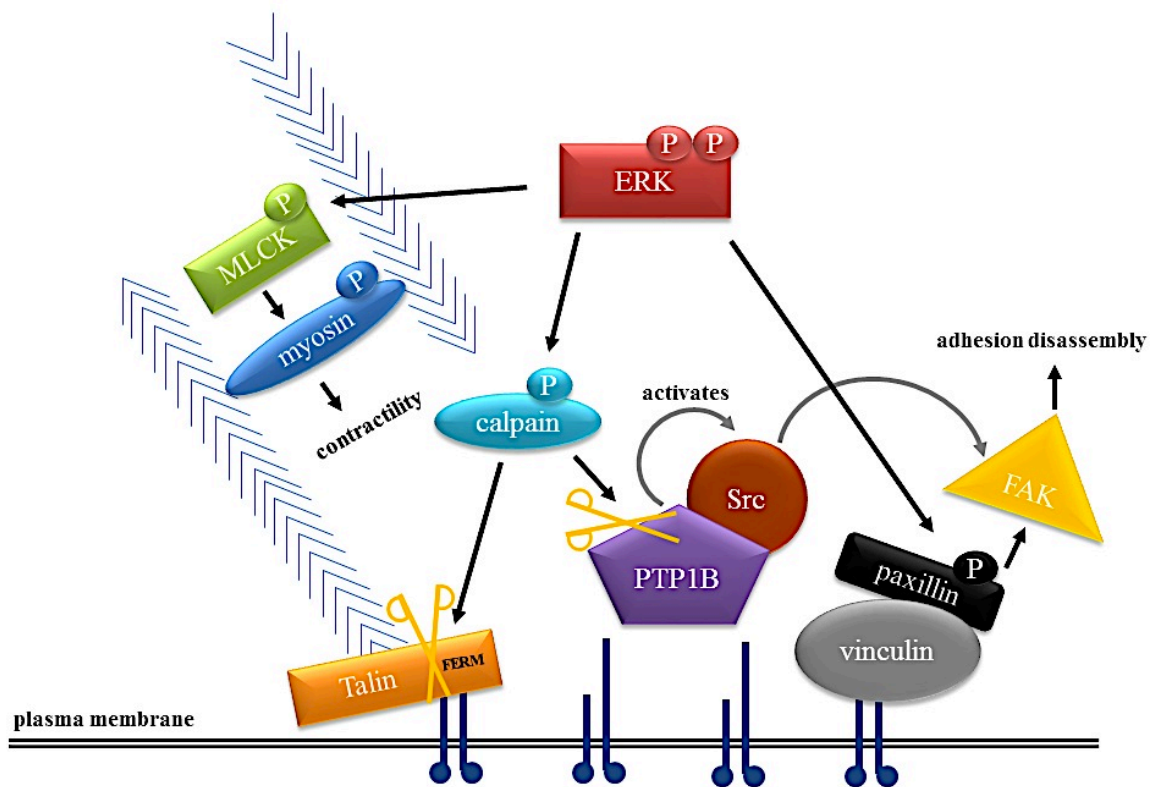


Figure 1-10 Role of ERK in cell contractility and focal adhesion disassembly

Multiple ERK substrates are involved in focal adhesion turnover. Firstly, myosin light chain kinase (MLCK) regulates cell contractility which promotes forward migration and is activated by phosphorylation. Secondly, ERK-mediated phosphorylation of calpain enhances its proteolytic activity and subsequent cleavage of talin and protein tyrosine phosphatase (PTP1B) stimulate focal adhesion turnover. Moreover, phosphorylation of the adaptor protein paxillin promotes the recruitment of focal adhesion kinase (FAK), a central regulator of adhesion disassembly.

Besides many cytoplasmic effectors, nuclear ERK targets also play a pivotal role in stimulating cell migration. One of the best-studied nuclear targets is Elk-1 [323, 324]. Phosphorylation enhances DNA-binding and increases the transcriptional activity of Elk-1, which drives the transcription of *c-fos* [156, 325]. c-Fos is a basic leucine zipper transcription factor that, together with Jun or ATF proteins, forms the AP-1 transcription factor. Sustained nuclear ERK signalling provokes phosphorylation of the newly synthesised c-Fos protein by ERK, which stabilises the transcription factor and allows the formation of a functional AP-1 complex [326]. Subsequently, AP-1 drives the transcription of many proteolytic enzymes such as matrix metalloproteinase-1 (MMP-1), MMP-3, MMP-7, MMP-9, urokinase-type plasminogen activator (uPA) [314]. These proteases in turn regulate matrix degradation – an important parameter of tumour invasion and metastasis [1, 327].

1.4.5 The role of ERK in angiogenesis

Highly proliferating tumour cells display an increased demand for oxygen and nutrients. Yet, when tumour islets grow past a diameter of 0.2 mm, this demand cannot be met and tumour cells become hypoxic. This, in turn, triggers the onset of apoptosis and provides a natural constraint to grow past a critical volume. However, tumour cells eventually overcome this limitation by activating angiogenesis. In normal tissues vascular sprouting is suppressed by angiogenic inhibitors, such as thrombospondin, endostatin and angiostatin. During tumourigenesis, however, an enhanced expression of pro-angiogenic factors, such as VEGF (vascular endothelial growth factor), PDGF and TGF- β , with a concomitant decrease of angiogenic inhibitors and stromal remodelling, triggers the onset of vascular sprouting [328].

Oncogenic Ras signalling increases angiogenesis in a process, which mainly relies on AKT activation [329]. However, inhibition of MEK1/2 markedly reduces the expression of VEGF in response to hypoxia and suggests at least some role for the ERK-MAPK pathway in regulating vascular sprouting [330]. Although it is still unclear how ERK signalling contributes to VEGF expression, all evidence points towards AP-1 (activating protein-1). VEGF expression is dependent on AP-1 activity and the *vegf* promoter contains an AP-1 consensus site [331]. ERK's role in regulating AP-1 is well-established and thus ERK may induce transcription of *vegf* by activating AP-1. Moreover, ERK signalling has recently

been shown to mediate the downregulation of thrombospondin-1 [332]. The underlying mechanism, however, remains to be elucidated.

The extracellular matrix (ECM) functions as a natural barrier during the process of angiogenesis, because it efficiently sequesters angiogenic factors and physically obstructs infiltration of newly forming vessels. With the help of proteolytic enzymes, which liberate angiogenic factors and create space for newly forming vessels, this barrier can be overcome [333, 334]. Interestingly, the promoters of many proteinases contain an AP-1 consensus site, thus linking ERK signalling to the proteolytic induction of angiogenesis.

Moreover, the ERK-MAPK pathway stimulates the expression of tissue factor, an important regulator of angiogenesis, which triggers stromal remodelling and promotes VEGF expression [335, 336].

1.4.6 ERK-MAPK pathway and multi-drug resistance

Tumour cells are marked by highly instable genomes which give rise to continuous generation of novel genetic configurations. Thus, a cancer cell has scope to adapt to changes in the microenvironment and modify signalling circuits to promote survival and proliferation. This hallmark, however, complicates therapeutic intervention and ultimately decreases clinical success rates, when tumour cells acquire the ability to withstand cytotoxic drugs or become resistance in response to ionisation. The ERK-MAPK pathway has been linked to acquired resistance during e.g. radiation therapy [337] or doxorubicin treatment [338]. As described in section 1.4.3, ERK signalling promotes cell survival by stimulating the expression pro-survival factors and inhibiting BH3-only proteins (BOPs). This mechanism may also provide a means by which cancer cells can be protected from drug-induced apoptosis. Moreover, increased ERK signalling has been shown to either stimulate or enhance the expression of multi-drug resistance (MDR) genes, which encode transmembrane drug efflux pumps [339, 340]. The MDR transporter belongs to the superfamily of ATP-binding cassette (ABC) transporters which enable cancer cells to actively expel various chemical compounds from the cytoplasm, thereby decreasing the intracellular concentration of the drugs to sub-toxic levels. Drug resistance represents a general challenge in cancer treatment and has led to the introduction of

combination therapies, which are thought to minimise tumour cell adaptations and provide a promising strategy to curing cancer.

1.4.7 Inhibiting ERK signalling as a therapeutic strategy

Owing to the fact that the ERK-MAPK pathway is commonly deregulated in cancer and plays an important role in the acquisition of a malignant phenotype, the cascade and its upstream activators are attractive targets for the development of anticancer drugs. Overexpression of EGFR is commonly observed in cancer [341] and this triggers activation of the ERK cascade. Two strategies have been employed to inhibit EGFR signalling, and they include the development of monoclonal antibodies (mAbs) directed against the extracellular domain of EGFR, and small-molecule tyrosine kinase inhibitors which block the intracellular kinase domain. Cetuximab was the first FDA-approved chimeric antibody directed against EGFR [342]. Although the drug has proven successful in the clinic, the patient response did not correlate with the degree of EGFR overexpression. Moreover, the risk for anaphylactic reactions led to the development of humanised (e.g. matuzumab) and fully human (e.g. panitumumab) mAbs [343, 344]. Panitumumab has shown a significant improvement on progression-free survival and demonstrated no antibody-dependent cell-mediated cytotoxicity, thus proving promising candidate for future therapies [345].

Ras is mutationally activated in approximately one third of all human cancers [213] and therefore huge efforts have been made to target the small GTPase in therapeutic strategies. As mutational activation of the Ras molecules inhibits GTP hydrolysis, original work attempted to reactivate the intrinsic GTPase or antagonise GTP binding to Ras molecules. However, these efforts were not successful. As Ras requires correct subcellular localisation for downstream signalling, researchers then attempted to block membrane localisation of Ras by inhibiting farnesylation of its C-terminus [346]. Farnesyltransferase inhibitors, however, did not prove very effective in blocking membrane targeting, as N- and K-Ras can undergo alternative prenylation in the absence of farnesyltransferase. Current work focuses on the development of inhibitors against Rce1 (Ras converting enzyme 1) and ICMT (isoprenylcysteine-*O*-carboxyl methyltransferase), which prime the C-terminus of Ras for farnesylation or prenylation [341].

Considerable efforts have also been made to develop chemical inhibitors targeting Raf kinases. One of the most successful Raf inhibitors is sorafenib, which binds to the ATP-binding pocket and prevents kinase activation [259]. Although phase III clinical trials

showed improved survival, it is difficult to determine whether sorafenib's success can be attributed to Raf inhibition, as it also potently inhibits VEGFR, PDGFR, FGFR and c-Kit signalling [347]. Other inhibitors, which selectively target mutant B-Raf have been developed. One such example is PLX4032 also known as vemurafenib, which proved very successful in phase III clinical trials and is currently awaiting FDA-approval [348]. Yet, sorafenib's success has sparked the debate on whether multi-kinase inhibitors due to their resemblance to combination therapy are more potent in cancer therapy.

In contrast to sorafenib, MEK inhibitors, which prevent MEK activation in a non-ATP competitive manner, are highly specific. The first two inhibitors developed against MEK were PD98059 and U0126 and proved not suitable as clinical candidates [349]. However, due to their potent inhibition, they have been invaluable tools in academic research. The first MEK inhibitor to enter clinical trials was PD184352. Despite the fact that poor pharmacokinetic properties rendered the compound unsuitable in phase II clinical trials [350], derivatives of PD184352 with better pharmacokinetic features have been developed and are currently undergoing clinical trials in phase I.

So far, no ERK inhibitors have entered clinical trials although, in principle, ERK represents a putative drug target in cancer therapy. Potential inhibitors can be designed to block ERK activity by competing with ATP binding or inhibiting specific substrate binding. As the two primary docking domains on ERK are sterically separated, small molecular weight compounds could be designed to interfere with the interactions of DEF-motif or D-motif containing substrates. In this way, a subset of ERK targets may specifically be inhibited while other ERK functions are unaltered. Future studies expanding our knowledge on how ERK substrates are involved in acquiring malignant phenotypes and a better understanding of ERK docking platforms, will facilitate the design of such ERK-specific inhibitors.

1.5 Project Aims

Upregulation of the ERK/MAPK pathway occurs in approximately one third of all human cancers and was shown to promote tumour cell invasion and progression [314]. To date, however, it is unclear whether or not the two predominant ERK isoforms have distinct functions in these processes. Therefore, this project set out to address the question in dispute by studying the role of ERK1 and ERK2 in tumour cell migration in 2D and 3D microenvironments. Moreover, we aimed to investigate whether true isoform-specific functions with regard to cell migration do exist or whether gene dosage effects are accountable.

Although some cytoplasmic and nuclear ERK targets involved in migratory processes have recently been identified, the underlying mechanisms by which invasive cell migration is linked to ERK signalling are at present poorly understood. To shine light on this understudied area, we set out to identify novel ERK effectors by carrying out a comparative gene expression analysis in a 3D-like microenvironment. Putative ERK mediators were subsequently studied in cell migration assays.

2 Materials and methods

2.1 Materials

2.1.1 Reagents

<i>Reagent</i>	<i>Details</i>	<i>Supplier</i>
2% gelatine	diluted in PBS	Sigma
2-Propanol		Merck
Agarose (High Gel Strength)		Melford Laboratories Ltd
Ascorbic acid		Sigma
Blue/Orange Loading Dye	6X	Fermentas
Calcein-AM		Invitrogen
Calf intestine alkaline phosphatase		New England Biolabs
Cryo-SFM		PromoCell
DB3.1 Competent Cells		Invitrogen
DNase1		Roche
dNTP	100 mM	Invitrogen
Dulbecco's Modified Eagle Medium (DMEM)		Gibco
ECL Western blotting substrate		Pierce
EGF		Peprotech
Ethidium bromide	10 mg/ml	Sigma
Foetal Calf Serum		Autogen Bioclear

Reagent	Details	Supplier
Fungizone	250 µg of amphotericin B and 205 µg of sodium deoxycholate per ml of distilled water	Invitrogen
Gateway® BP CLONASE™ II Enzyme Mix		Invitrogen
Gateway® LR CLONASE™ II Enzyme Mix		Invitrogen
GeneRuler™	1kb DNA Ladder	Fermentas
Glutaraldehyde	25%	Sigma
HiPerFect		Qiagen
Hybond-P PVDF membrane		GE Healthcare
Illumina HumanHT-12 v4 Expression BeadChips		Illumina
ImProm-IITM Reverse Transcription System		Promega
L-glutamine	200 mM	Invitrogen
Matrigel™ Basement Membrane Matrix		Becton Dickinson
NuPAGE MOPS SDS Running Buffer	20x	Invitrogen
NuPAGE pre-cast gels		Invitrogen
NuPAGE Sample Buffer	4x	Invitrogen
NuPAGE Transfer Buffer	20x	Invitrogen
Orange G		Sigma
Parafilm Wrap		Fisher
PBS containing Calcium and Magnesium		Sigma
PCRX Enhancer Solution	10X	Invitrogen

Reagent	Details	Supplier
pDONR™ 201		Invitrogen
Penicillin/Streptomycin	5,000 units of penicillin (base) and 5,000 µg of streptomycin (base)/ml	Invitrogen
PLATINUM® Taq DNA Polymerase High Fidelity		Invitrogen
Precision Plus Protein All Blue standard		Biorad
Rapid Ligation Buffer	2X	Promega
RMPI-1640 medium		Gibco
SOC media		Invitrogen
soluble fibronectin	1 mg/ml	Sigma
Super RX Blue medical X-ray film		Fuji
SURE2 Super Competent Cells		Stratagene
T4 DNA Ligase		Promega
TOP10 OneShot Cells		Invitrogen
Transwell Permeable Support	pore size of 8 µm diameter	Fisher
Trypsin		Invitrogen
U0126 MEK inhibitor	used at 10 µM	Sigma
Vectashield mounting medium with DAPI		Vector laboratories

Table 2-1 List of all reagents

2.1.2 Solutions

Solution	Recipe
DNA loading dye	30% (w/v) sucrose, 0.35% Orange G
HEPES lysis buffer	20 mM HEPES pH 7.5, 150 mM NaCl, 2 mM EDTA pH 7.4, 1 % NP-40 (v/v), 1 mM Na ₃ VO ₄ , 10 mM NaF, 1 mM PMSF, 5 µg/ml leupeptin
LB-agar:	85 mM NaCl, 1% (w/v) bacto-trypton, 0.5% (w/v) yeast extract, 1.5% (w/v) agarose addition of either: 100 µg/ml Ampicillin, 50 µg/ml Kanamycin, or 30 µg/ml Chloramphenicol
LB-broth	85 mM NaCl, 1% (w/v) bacto-trypton, 0.5% (w/v) yeast extract addition of either: 100 µg/ml Ampicillin, 50 µg/ml Kanamycin, or 30 µg/ml Chloramphenicol
Lysis buffer:	20 mM HEPES pH 7.5, 150 mM NaCl, 2 mM EDTA pH 7.4, 1 %NP-40, 1 mM Na ₃ VO ₄ , 2 mM NaF, 1 mM PMSF, 5 µg/m l mM leupeptin
NDLB lysis buffer	50 mM Tris HCl (pH 7.0), 150 mM NaCl, 10 mM NaF, 1 mM Na ₃ VO ₃ , 5 mM EDTA, 5 mM EGTA, 1% Triton X 100 (v/v), 0.5% NP 40 (v/v), 5 µg/ml leupeptin, 1 mM PMSF
PBS (phosphate buffered saline)	170 mM NaCl, 3.3 mM KCl, 1.8 mM Na ₂ HPO ₄ , 10.6 mM H ₂ PO ₄
PBST	PBS, 0.1% Triton X-100
PE	PBS, 1 mM EDTA
Penicillin/Streptomycin	5,000 units of penicillin (base) and 5,000 µg of streptomycin (base)/ml
RIPA lysis buffer	50 mM Tris HCl (pH 7.0), 150 mM NaCl, 0.5% sodium deoxycholate, 1% NP 40 (v/v), 1 mM PMSF, 1 mM Na ₃ VO ₄ , 10 mM NaF, 5 µg/ml leupeptin
TBE 10x:	890 mM Tris-base, 890 mM boric acid, 25 mM EDTA, pH = 8.3
TBS (Tris-buffered saline)	10 mM Tris-HCl (pH 7.4), 150 mM NaCl
TE	10.0 mM Tris:HCl, 1.0 mM EDTA, pH 8.0

Table 2-2 List of all solutions

2.1.3 Antibodies and dyes

Antigen	Species	Dilutions	WB Incubation	Supplier
Total ERK1/2	Rabbit	WB: 1/5K, 5% BSA (w/v)	1 hour at RT	Sigma
pERK1/2	Mouse	WB: 1/5K, 5% BSA (w/v)	1 hour at RT	Sigma
β -tubulin	Mouse	WB: 1/5K, 5% BSA (w/v)	1 hour at RT	Insight
Fra-1	Rabbit	WB: 1/1K, 5% BSA (w/v)	o/n at 4°C	Abcam
PARP	mouse	WB: 1/1K, 5% BSA (w/v)	o/n at 4°C	BD
EEA-1	Mouse	IF: 1/100		Transduction Labs
β 1 integrin	Mouse	WB: 1/2K, 5% BSA (w/v) IF: 1/200	o/n at 4°C	Chemicon
EGFR	Mouse	WB: 1/2K, 5% BSA (w/v)	o/n at 4°C	BD
GFP	Mouse	IP: 1.5 μ l per 10 cm dish		Abcam
GFP	Rabbit	WB: 1/10K, 5% milk in TBST(w/v)	1 hour at RT	Abcam
FITC	Mouse	IF: 1/200		Southern Biotech
Alexa 488	Rabbit	IF: 1/200		Invitrogen

Table 2-3 Antibodies and dyes

2.1.4 Enzymes and kits

Kit	Supplier
QIAquick® Gel Extraction Kit	Qiagen
Cell Line Nucleofactor® Kit T	Amaxa
Cell Line Nucleofactor® Kit V	Amaxa
F-410 DyNAmo™ SYBR® Green qPCR kit	Thermo Scientific
Illumina® TotalPrep™ RNA Labelling Kit	Ambion
Nuclear Extract Kit	Active Motif
Pierce® BCA Protein Assay Kit	Thermo Scientific
QIAGEN Plasmid Maxi Kit	QIAGEN
QIAprep® Spin Miniprep Kit	Qiagen
QIAquick® PCR Purification Kit	Qiagen
Quick Change® Site-Directed Mutagenesis Kit	Stratagene

Table 2-4 List of kits

2.1.5 Primers for qPCR

Gene name	Assay name	Catalogue Number
ERK1	Hs_MAPK3_1S_SG	QT00000532
ERK2	Hs_MAPK1_1_SG	QT00065933
Rab17	Hs_RAB17_1_SG	QT00009590
Liprin- β 2	Hs_PPFIBP2_1_SG	QT00005012
Liprin- β 1	Hs_PPFIBP1_2_SG	QT01666378
Liprin- α 2	Hs_PPFIA2_1_SG	QT00072296
Liprin- α 4	Hs_PPFIA4_1_SG	QT00027251
Rab20	Hs_RAB20_1_SG	QT00229495
GAPDH	Hs_GAPDH_2_SG	QT01192646
CSF2	Hs_CSF2_1_SG	QT00000896

Table 2-5 List of Qiagen Quantitect primers

2.1.6 Tissue culture plastic ware

<i>Plastic ware</i>	<i>Supplier</i>
Falcon tissue culture dishes (6 cm, 10 cm, 15 cm)	BD Biosciences
Falcon multi-well plates	BD Biosciences
IWAKI-3cm glass bottom dishes	Appleton Woods
Nunc tissue culture flasks and dishes	TCS Biologicals
Nunc cryotubes	TCS Biologicals

Table 2-6 List of plastic ware and supplier

2.2 Methods

2.2.1 Molecular biology

2.2.1.1 Polymerase chain reaction (PCR)

PCR was performed using the following set-up:

<i>Reagent</i>	<i>Sample (μl)</i>
10x High Fidelity PCR Buffer	2
10x PCR _x Enhancer Solution	2
50 mM MgSO ₄ (0-4 mM)	0-1.6
Template (10 ng/μl):	1
Primer fwd: (5 μM)	1
Primer rev: (5 μM)	1
2.5 mM dNTPs	2
autoclaved ddH ₂ O	9.2-10.8
Platinum [®] High-Fidelity Polymerase	0.2
total volume	20

Temperature cycling was performed in a DNA Engine Thermal Cycler (Biorad) using the following conditions:

Initial denaturation	95°C	2 min
25-35 cycles:		
Denaturation	95°C	45 s
Annealing	50-60°C	45 s
Extension	72°C	60 s
Final extension	72°C	7 min
Final hold	4°C	∞

Primers used during this project were synthesised by Invitrogen and are listed below:

ERK1 5'-GGGGACAAGTTTGTACAAAAAAGCAGGCTTCGCGGCGGCGGCGGCTCAGGG-3'
attB1

ERK1 5'-GGGGACCACTTTGTACAAGAAAGCTGGGTTTTACTAGGGGGCCTCCAGCACTCC-3'
attB2

ERK2 5'-GGGGACAAGTTTGTACAAAAAAGCAGGCTTCGCGGCGGCGGCGGCGGCGG-3'
attB1

ERK2 5'-GGGGACCACTTTGTACAAGAAAGCTGGGTTTTATTAAGATCTGTATCCTGGCTG-3'
attB2

The integrity of generated DNA fragments was tested by agarose gel electrophoresis.

2.2.1.2 Agarose gel electrophoresis

Depending on the expected length of the DNA fragment, gels containing between 0.8% to 2% agarose were prepared. For this, the agarose was suspended in 1x TBE and boiled in the microwave oven until the agarose was completely dissolved. After the solution had cooled down to approximately 55°C, ethidium bromide from the stock solution (0.2 mg/ml) was added at a dilution of 1:1000. As soon as the gel completely solidified, it was put into a gel chamber containing 1x TBE as running buffer. DNA loading buffer was added to the respective nucleic acid samples and the gel was loaded. Gels were run at 75 V for approximately one hour. DNA was visualised using UV transillumination. If DNA fragments were required in subsequent cloning steps, gel slices containing the DNA were excised from the gel and purified using the QIAquick Gel Extraction Kit according to the manufacturer's protocol.

2.2.1.3 Restriction digestion

Digestion of DNA with restriction endonucleases was performed for 2 hours (plasmid DNA, DNA fragments) with a two-fold excess (2 U/ μ g DNA) of restriction enzyme. Temperature and buffer for the respective digestion were used according to the manufacturer's protocol. In order to separate digested DNA fragments and confirm the enzymatic reaction, the digested DNA was subjected to agarose gel electrophoresis. DNA of interest was then purified from the gel slice using the QIAquick Gel extraction Kit according to the manufacturer's protocol.

2.2.1.4 Ligation of DNA

To inhibit self-ligation, the digested vector was dephosphorylated before ligation. To do this, the DNA was diluted in NEBuffer 3 to a final concentration of 0.05 μ g/ μ l and 1 unit of CIP was added to the solution. After 15 minutes at 37°C an additional unit of CIP was added and incubation continued for another 15 minutes. Afterwards the DNA was purified with the QIAquick PCR purification kit according to the manufacturer's instruction. For the actual ligation process, 50 ng of dephosphorylated vector and 150 ng of DNA insert were added to 5 μ l of 2x Rapid ligation buffer and 1 μ l ligase (4 U/ μ l) to give a total volume of 10 μ l. Ligation was performed for 2 hours at room temperature.

2.2.1.5 Recombination

For the BP clonase reaction TE buffer (pH 8.0), *attB*-PCR product (15-150ng) and Donor vector (150ng/ μ l) were mixed together at room temperature in a microcentrifuge tube (Figure 2-1 A). For the LR clonase reaction TE buffer, entry vector and destination vector were mixed together in a microcentrifuge tube (Figure 2-1 B). The respective Clonase™ II enzyme mix (stored at -80°C) was briefly thawed on ice, vortexed twice for 2 sec and spun down, before it was added to the reaction mix, which was set up as follows:

<i>BP clonase reaction</i>	<i>Sample (μl)</i>
<i>attB</i> -PCR product	150 ng
Donor vector (pDONR™ 201)	150 ng
TE Buffer	To 8
BP Clonase Enzyme Mix	2
total volume	10

<i>LR clonase reaction</i>	<i>Sample (μl)</i>
<i>attB</i> -PCR product	150 ng
Donor vector (pDONR™ 201)	150 ng
TE Buffer	To 8
LR Clonase Enzyme Mix	2
total volume	10

The reaction was incubated at 25°C for 1 hour. Then, 1 μ l Proteinase K solution was added and the solution briefly vortexed. A 10 minute incubation at 37°C stopped the reaction. 1.5 μ l of this solution was subsequently used for bacterial transformation.

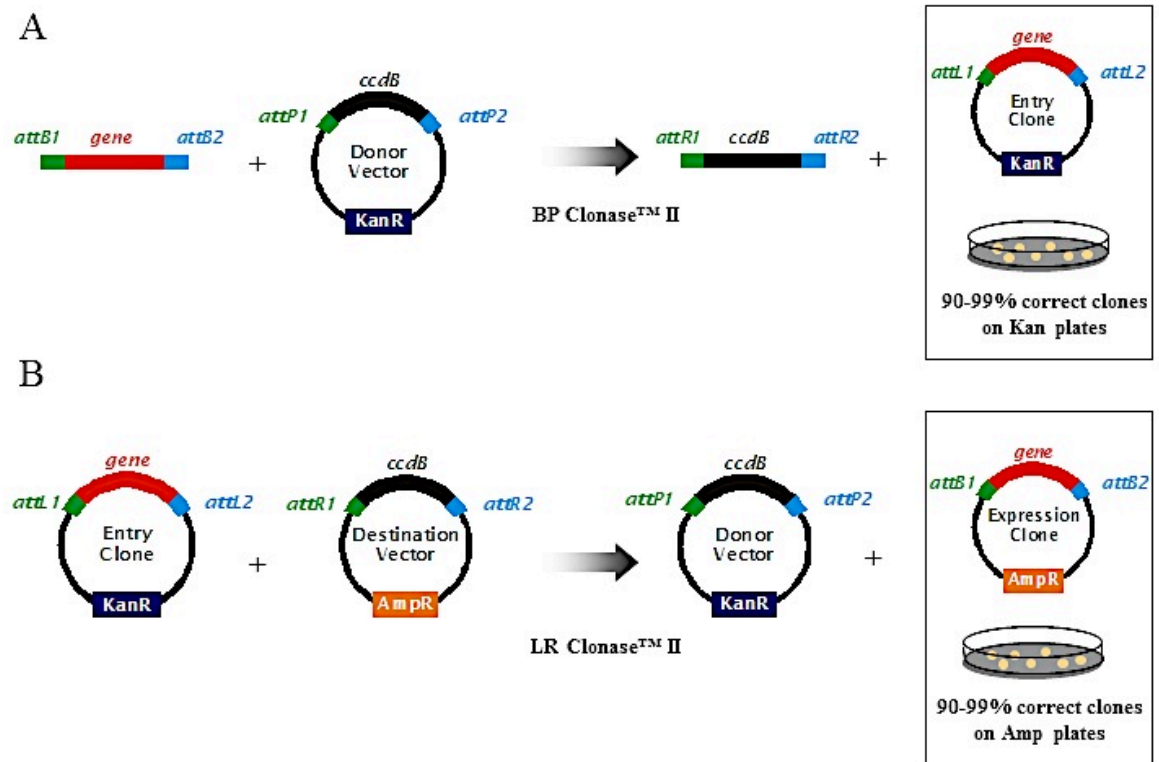


Figure 2-1 Schematic outline of the Gateway®-system

A. Preparation of the Entry clone containing the gene of interest. B. Construction of an expression vector via recombination of any destination vector with any entry vector. Images adapted from <http://www.invitrogen.com/etc/medialib/en/filelibrary/html.Par.74823.File.tmp/gateway-entry-options-seminar.html>.

2.2.1.6 Site-directed mutagenesis

Site-directed mutagenesis was performed using the following set-up:

Reagent	Sample (μl)
10x Reaction Buffer	5
dsDNA template	0.5-1 μ g
Primer fwd: (5 μ M)	125 ng-0.5 μ g
Primer rev: (5 μ M)	125 ng-0.5 μ g
dNTPs (30 μ M)	1
autoclaved ddH ₂ O	up to 50
Pfu turbo DNA polymerase	1
total volume	50

Temperature cycling was performed in a DNA Engine Thermal Cycler (Biorad) using the following conditions:

Initial denaturation	95°C	2 min
20 cycles:		
Denaturation	95°C	30 s
Annealing	50-60°C	60 s
Extension	72°C	60 s
Final extension	72°C	7 min
Final hold	4°C	∞

Primers used during this project were synthesised by Invitrogen and are listed below:

ERK2 forward 5'-GCCTACGGCATGGTGTGTAGTGCTTATGATAATGTCAACAAAGTTCG-3'

ERK2 reverse 5'-CGAACTTTGTTGACATTATCATAAGCACTACACACCATGCCGTAGGC-3'

2.2.1.7 Bacterial strains

E. coli DH5 α or TOP10 OneShot cells were utilised for most cloning procedures. Where plasmids contained the *ccdB* gene, DB3.1 cells were used instead.

2.2.1.8 Heat-shock transformation of competent bacteria

A vial of frozen competent bacteria was thawed on ice. Subsequently 1.5 μ l of the respective ligation reaction mix was added to 50 μ l of competent cells and incubated on ice for 30 minutes. The bacteria were then heat-shocked for 45 seconds in a water bath at

42°C and put on ice for 2 minutes. After adding 250 µl of SOC medium (at room temperature), the vials were shaken horizontally at 37°C for 1 hour at 225 rpm in a rotary-shaking incubator. 150 µl of each transformation was then spread on LB agar plates containing the antibiotic of choice (100 µg/ml Ampicillin / 50 µg/ml Kanamycin / 30 µg/ml Chloramphenicol). In the case of a retransformation 5 ng of vector DNA were used and only 50 µl were plated. After the liquid was totally absorbed, the plates were inverted and placed in a 37°C incubator for at least 18 hours. Later they were wrapped in parafilm and stored at 4°C.

2.2.1.9 Plasmid preparation (Miniprep)

4 ml of LB media containing the appropriate antibiotic were inoculated with individual colonies and incubated at 37°C overnight. The following morning, glycerol stocks were prepared for long term storage by mixing 500 µl of bacterial culture with equal volumes of glycerol and stored at -80°C. The remainder of the overnight bacterial culture was pelleted by centrifugation at 3,000 rpm for 10 minutes in a Beckham Coulter centrifuge. DNA was isolated from the pellets using the QIAprep® Spin Miniprep Kit according to the manufacturer's instructions. Next, the DNA was sequenced by the Beatson Molecular Technology Services on an Applied Biosystems 3130xl sequencer. The resulting data was analysed using VectorNTI (Invitrogen).

2.2.1.10 Plasmid preparation (Maxiprep)

Large scale (200-500 ml) overnight bacterial cultures were set up in LB media containing the appropriate antibiotic and 20 µl of a starting culture were used for inoculation. The following morning cultures were pelleted at 3,000 rpm for 30 minutes. The DNA was then isolated using the QIAprep® Spin Maxiprep Kit according to the manufacturer's protocol. The DNA concentration of the resulting plasmid solution was measured using an Eppendorf Biophotometer with an absorbance of 260 nm.

2.2.2 Tissue Culture

2.2.2.1 Cell origin

Stable clones of A2780-DNA3 and A2780-Rab25 were generated as previously described by Cheng *et al.* [351] and generously provided by Gordon Mills. MDA-MB-231 cells were

purchased from the American Type Culture Collection cell bank. Various other cell lines used in this project were obtained from research groups within the Beatson Institute for Cancer Research, including Telomerase-immortalised human fibroblasts (TIFs) and colon carcinoma BE cells.

2.2.2.2 Cultivation of cells

A2780 cells were cultured in RPMI-1640 medium supplemented with 10% (v/v) foetal calf serum and 2 mM L-glutamine at 37°C in a humidified atmosphere containing 5% CO₂. All other cell lines were cultured in DMEM containing 10% (v/v) foetal calf serum and 2 mM L-glutamine under the same conditions as described above. When cells reached 80% confluence, they were sub-cultured. To do this, the culture medium was removed, the cellular monolayer then rinsed with PBS and a 10% Trypsin/PE solution was added. After a brief incubation, the detached cells were re-suspended in the appropriate cell culture medium and centrifuged for 2 minute at 900 rpm. Next, the cell pellet was resuspended in fresh medium and an aliquot was seeded into an appropriate tissue culture dish or flask.

2.2.2.3 Freezing and thawing of cells

At least 1×10^6 cells in excellent condition were trypsinised and centrifuged for 2 minutes at 900 rpm. Once the supernatant was completely removed, the cell pellet was resuspended in 1 ml Cryo-SFM medium and transferred into a labelled cryo vial and placed in a freezing container (NALGENE™ 1°C Cryo Freezing Container) at -80°C. When cells were to be stored longer than 6 months they were transferred into liquid nitrogen the following day.

According to the rule of “freeze slowly, thaw fast”, frozen cells were put immediately into a 37°C water bath. When only a small lump of ice was left, the vial was opened and the cells were immediately transferred into 5 ml of pre-warmed medium. After centrifugation for 2 minutes at 900 rpm, the supernatant was removed and cells were resuspended in their specified growth medium and plated onto a cell culture dish. The following morning, the medium was replaced.

2.2.2.4 Transfection using the Amaxa™ Nucleofector™

Amaxa nucleofection provides an efficient way to introduce DNA plasmids or siRNA oligos. Hence, this method was used for A2780-Rab25 and MDA-MB-231 cells, which were grown to 70-85% confluency, trypsinised and resuspended in growth medium. Depending on the cell line between $1-5 \times 10^6$ cells were used for one transfection reaction. The appropriate number of cells were centrifuged at 900 rpm for 2 min. The supernatant was aspirated off and 100-200 pmol of siRNA or appropriate amounts of DNA were added on top of the cell pellet. Afterwards, 100 μ l of solution T (A2780-Rab25) or V (MDA-MB-231) were added and mixed thoroughly by pipetting up and down. The mixture was then transferred into a Nucleofector cuvette and inserted into the Amaxa™ Nucleofector™. Transfections were carried out using the appropriate programme (see table below). Subsequently, transfected cells were taken up in 500 μ l pre-warmed growth medium and seeded onto tissue culture dishes. Transfected cells were allowed to recover and settle for at least 12 hours prior to any experiments.

<i>Cell line</i>	<i>Nucleofection programme</i>
A2780	A-023
MDA-MB-231	X-013

Typically, 3 μ g of DNA plasmid were transfected unless otherwise stated in the table below:

<i>Plasmid</i>	<i>Transfected amount (μg)</i>
GFP	1
Destination vector	1
SF-ERK1	0.4
SF-ERK2	1.5

2.2.2.5 Transfection using HiPerFect

For RNA interference experiments, MDA-MB-231 and BE cells were transfected using HiPerFect, because this increased cellular viability. When cells reached 80% confluence, a

solution of 500 μ l of DMEM supplemented with L-glutamine only, 7.5 μ l HiPerFect and 1.5 μ l siRNA (from 20 μ M stock) was prepared and left at room temperature for 10 minutes to allow transfection complex formation. Next, the mixture was added onto the cells and the plates were gently swirled to ensure a uniform distribution. Transfected cells were then incubated under normal growth conditions. Two days later, the cells were passaged at a ratio of one in three and transfected immediately after sub-culturing following the above protocol. After the second round of transfection gene silencing was monitored by Western blotting or qRT-PCR.

2.2.2.6 Cell proliferation assays

10.000 cells were seeded per 6-well dish and left to settle overnight. The following morning cells were counted for the first time. For each measurement, cells were thoroughly trypsinised in 200 μ l of Trypsin/PE solution. Next, the trypsin was inactivated with 200 μ l of medium. The cell number was determined by adding 20 ml of PBS to the 0.4 ml of cell suspension and measuring the cell number with a Casy[®] 1 cell counter. Cell proliferation was assayed over the course of 5-6 days. Relative cell numbers were determined by using day one as a reference point. Every condition was set up in triplicate and the experiments were repeated twice. Moreover, Casy[®] 1 cell counter measurements were checked manually using a haemocytometer.

2.2.2.7 Inverted invasion assay

Inverted invasion assays, previously described by Hennigan et al. were modified as follows [352]. An aliquot of Matrigel was slowly thawed on ice and then diluted 1:1 in ice-cold PBS supplemented with 25 μ g/ml fibronectin. Subsequently, 100 μ l of this solution was carefully pipetted into a Transwell (pore size of 8 μ m), which had been inserted into a well of a 24-well tissue culture plate. In order for the Matrigel to polymerize, the plate was incubated for at least 30 minutes at 37°C. Meanwhile, cell suspensions between 1×10^5 and 4×10^5 cells per ml were prepared in the appropriate growth medium. After the Matrigel set, the Transwells were inverted and 100 μ l of the cell suspension were pipetted onto the underside of the filter. The Transwells were then carefully covered with the base of the 24-well tissue culture plate so that it contacted the droplet of cell suspension. Next, the inverted plate was incubated at 37°C, 5% CO₂ for 4 hours to allow cells to attach to the filter. Afterwards, the Transwells were turned

right-side-up, washed by sequential dipping in 1 ml of the appropriate serum-free growth medium twice and finally placed into 1 ml of the serum-free medium. Then, 100 μ l of growth medium containing 10% serum and the chemoattractant EGF (25ng/ml) was gently pipetted on top of the Matrigel. Cells were allowed to invade into the Matrigel over a course of 2-3 days at 37°C and 5% CO₂.

In order to visualize the migrated cells, the Transwells were transferred into a new 24-well tissue plate and covered drop-wise with 1 ml of calcein acetomethyl ester diluted to 4 μ M in serum free medium. After one hour at 37°C samples were assayed using a LEICA SP2 confocal microscope with a 20x objective. The fluorescent dye was excited with a wavelength of 488 nm and emitted at 515 nm. Optical sections were captured at 15 μ m intervals starting from the underside of the Transwell filter and moving upwards in the direction of cell invasion. The resulting images were quantified using the area calculator tool from the ImageJ software. The threshold fluorescence intensity was set so that background intensities were erased and only cells within the optical slice were visualised. The sum of fluorescence of the sections from 45 μ m and above was divided by the total fluorescence of all the optical sections, thus giving an invasion index of ≥ 45 μ m. Mean values were generated from three individual experiments. Within one experiment each condition was set up in duplicate and optical sections for three areas were taken for each Transwell.

2.2.2.8 Generation of cell-derived matrix

Cell-derived matrix was generated as previously described [38, 353]. Briefly, tissue culture plates were coated with 0.2% sterile gelatine for one hour at 37°C. Next, the gelatine solution was aspirated off and plates were washed twice with PBS. In order to crosslink the layer of gelatine, 1% sterile glutaraldehyde was added for 30 minutes at room temperature. Following two washes with PBS, the crosslinking reaction was quenched with 1 M sterile glycine in PBS (pH ~7) for 20 minutes at room temperature. After another 2 washes, the tissue culture dishes were equilibrated with DMEM containing 10% foetal calf serum and 2 mM L-glutamine. Then, human telomerase-immortalised fibroblasts were plated at near confluence ($\sim 2 \times 10^4$ /cm²). The following day, collagen production was stimulated through supplementation of the medium with 50 μ g/ml ascorbic acid. Fibroblasts were cultured for 10-14 days and the medium (supplemented with ascorbic

acid) was exchanged every other day. Matrices were then denuded of living fibroblasts by incubating the dishes with PBS containing 20 mM NH_4OH and 0.5% Triton X-100 for 2 minutes, after which cell lysis was examined using a phase light microscope. Next, the extraction buffer was aspirated off and matrices were washed twice in PHS containing calcium and magnesium. Residual DNA was digested with PBS containing calcium, magnesium and 10 $\mu\text{g/ml}$ DNase1 at 37°C for 30 minutes. Following another two washes with PBS containing magnesium and calcium, matrices were stored at 4°C in the same solution supplemented with pen/strep and fungizone. Before use, the matrix condition was examined by phase light microscopy. Prior to seeding the cell line of interest, matrices were washed twice with PBS and equilibrated with complete medium for 20 minutes at 37°C.

2.2.2.9 Migration on cell-derived matrix

Respective cells (50,000 cells for A2780-Rab25 cells, 100,000 cells in the case of MDA-MB-231 cells) were seeded into a well of a 6-well dish coated with cell-derived matrix and allowed to adhere for 4 hours prior to imaging. Migration was monitored using a Nikon time-lapse microscope and migration characteristics were analysed using the Manual Tracking and Chemotaxis tool of ImageJ and a customised MATLAB script written by Dr. Marc Birtwistle.

2.2.2.10 Scratch wound assays

Cells were seeded into a 6-well dish, so that they reached confluence 48 hours post transfection. Next, a wound was introduced by scratching the plastic dish with a 200 μl pipette tip. Following three washes in fully-supplemented medium wound closure was monitored at 10 minute intervals using a time-lapse microscope. Images for each condition were taken from five distinct fields along the wound and a minimum of five cells were tracked for each field. Migration characteristics from three independent experiments were analysed using the ImageJ cell tracking software.

2.2.2.11 Immunofluorescence

Cells were cultured on sterile coverslips placed in a 6-well tissue culture dish. Where indicated, coverslips were coated with fibronectin (20 $\mu\text{g/ml}$ in PBS) for 20 minutes at 37°C. Medium was removed and the cells were washed twice with PBS and fixed in a 4%

paraformaldehyde solution. After 15 minutes, the crosslinking reaction was quenched by adding an equal volume of a 2M glycine solution. Next, the coverslips were washed twice with PBS, after which cells were permeabilised with 0.05% Triton X-100 in PBS for 2 minutes, which was followed by 3 washes in PBS. In order to block non-specific antibody binding, cells were incubated in PBS containing 1% BSA for one hour. Then, primary antibodies diluted in blocking solution were applied for one hour. Following another three washes, secondary antibodies in blocking solution were applied for 45 minutes. Coverslips were washed another two times with PBS before being mounted onto glass slides using Vectashield containing DAPI. Slides were dried overnight at 4°C. Colocalisation studies were performed on a Zeiss 710 upright confocal microscope with a 64x objective. Different fluorescent channels were recorded sequentially to prevent bleed-through.

2.2.3 Protein biology

2.2.3.1 Cell lysis

After cells were grown to 80% confluence, the cell culture dishes were placed on ice, the medium was aspirated off and the cells were washed twice with ice-cold PBS. Depending on the experiment different lysis buffers were used (Table 2-7). Subsequently, protein extracts were generated by adding lysis buffer to the dishes (0.4 ml per 10 cm dish, 1 ml per 15 cm dish) and scrapping the cells off the plate. The lysates were then transferred into 1.5 ml microcentrifuge tubes and incubated on ice for 10 minutes with occasional vortexing. Afterwards, lysates were cleared by centrifugation at 14,000 rpm in a pre-cooled benchtop centrifuge for 10 minutes. Cleared lysates were collected in new tubes and either processed further or stored at -20°C.

<i>Lysis buffer</i>	<i>Composition</i>	<i>Application</i>
HEPES lysis buffer	20 mM HEPES pH 7.5 150 mM NaCl 2 mM EDTA pH 7.4 1 % NP-40 (v/v) 1 mM Na ₃ VO ₄ 10 mM NaF 1 mM PMSF 5 µg/ml leupeptin	Western blot
NDLB lysis buffer	50 mM Tris-HCl (pH 7.0) 150 mM NaCl 10 mM NaF 1 mM Na ₃ VO ₃ 5 mM EDTA 5 mM EGTA 1% Triton X-100 (v/v) 0.5% NP-40 (v/v) 5 µg/ml leupeptin 1 mM PMSF	Immunoprecipitation
RIPA lysis buffer	50 mM Tris-HCl (pH 7.0) 150 mM NaCl 0.5% sodium deoxycholate 1% NP-40 (v/v) 1 mM PMSF 1 mM Na ₃ VO ₄ 10 mM NaF 5 µg/ml leupeptin	Western blot, when interested in membrane proteins

Table 2-7 Comparison of different lysis buffers: Composition and Application

2.2.3.2 Protein quantification

Protein concentrations were measured using the Pierce® BCA Protein Assay Kit according to the manufacturer's instructions. In brief, diluted albumin standards were prepared (0.08, 0.1, 0.2, 0.4, 1, 2 mg/ml) and the appropriate lysis buffer was used as a blank. A standard curve was determined by adding 20 µl of blank and standards to the bottom of a 96-well plate. Protein lysates were also added in duplicate. 200 µl of the constituted protein assay reagent (50:1, reagent A:B) were added to all wells and incubated at 37°C for 15 minutes. Next, absorbance values were measured using a Dynatech MR7000 plate reader at 595 nm and plotted to generate a standard curve. Lastly, protein concentrations were determined from the curve and lysates diluted if necessary.

2.2.3.3 Co-immunoprecipitation

Prior to co-immunoprecipitation experiments, the GFP antibody was coupled to beads. To do this, 1.5 µl of antibody per lysate were incubated with 25 µl of magnetic beads in 100 µl of PBS containing 0.1% BSA for 1 hour at 4°C. After 2 washes with PBS containing 0.1% BSA, the lysate was applied (containing approximately 400 µg of protein) and incubated at 4°C for 2 hours. Then, beads were washed 3 times with lysis buffer and boiled in lysis buffer supplemented with reducing sample buffer at 95°C for 5 minutes. Protein interactions were examined by Western blot.

2.2.3.4 SDS-PAGE and Coomassie staining

SDS-polyacrylamide gels were used to resolve protein samples according to their molecular weight. Firstly, the protein lysate was mixed with 4x reducing sample buffer and heated to 95°C for 5 minutes on a thermomixer to denature the proteins. After a brief centrifugation, 5 µg of protein were resolved on a denaturing, pre-cast NuPAGE polyacrylamide gel (4-12% gradient or 10%). Molecular weight markers were loaded onto the gel next to lysate samples. In general, gels were run in tanks containing 1x MOPS running buffer at 150 V for approximately 1.5 hours. Afterwards, the gel was either stained with Coomassie reagent to visualize the resolved proteins in the gel or transferred onto a PVDF membrane by Western blotting.

For Coomassie staining, the gel was transferred into a clean bacterial cell culture dish and washed 3 times for 5 minutes with distilled water. Afterwards, the gel was incubated with

SimplyBlue SafesStain[®] Coomassie reagent for 45 minutes. Next, background staining was removed by several washes with water over the course of 3 hours. All washing and staining steps were carried out under gentle agitation.

2.2.3.5 Western Blotting

Proteins previously separated by SDS-PAGE were transferred onto a PVDF membrane in 1x NuPAGE Blotting buffer for one hour at 30 V. The membrane was then blocked for 30 minutes with 5% (w/v) milk powder in TBST. After thorough washing with TBST, the primary antibody of choice was added at a suitable dilution in 5% (w/v) BSA containing 0.02% (w/v) of sodium azide. Incubation times varied depending on the primary antibody employed (Table 2-3). Membranes were then washed 3 times in TBST for 5 minutes each. The blots were then incubated with the appropriate secondary antibody conjugated to horseradish peroxidase for one hour at room temperature. Proteins were visualised by chemiluminescence using the Pierce ECL Western Blotting Substrate and subsequent autoradiography with Fuji Super RX medical X-ray films using a Kodak X-Omat 480 RA X-Ray processor.

2.2.4 Microarray screen and validation

2.2.4.1 RNA extraction and quality control

Total cellular RNA was extracted from respective cells grown on cell-derived matrix (see 2.2.2.8) or plastic surfaces for 16 hours following transfection. RNA isolation was carried out using the RNeasy kit according to the manufacturer's protocol. Briefly, cells were washed twice with ice-cold PBS (pH 7.4), and lysed in RLT buffer supplemented with β -mercaptoethanol. Next, cell lysates were homogenised using QIAshredder columns and RNA was extracted and purified. Residual genomic DNA was removed through an on-column DNase1 digest. Following elution of the purified RNA, samples were snap-frozen on dry ice and stored at -80°C until further use.

2.2.4.2 RNA labelling for the microarray screen

Isolated RNA was labelled using the Illumina[®] TotalPrep[™] RNA Labelling Kit according to the manufacturer's instructions. In brief, 0.5 μ g of isolated RNA were placed into a PCR plate for first strand cDNA synthesis and brought up to a volume of 11 μ l before 9 μ l of

the reverse transcription master mix were added. After mixing the solution was incubated at 42°C for 2 hours using a thermal cycler. For second strand cDNA synthesis, 80 µl of master mix were added to each sample and incubated at 16°C for two hours. The synthesised cDNA was purified and labelled cRNA was transcribed *in vitro* over 14 hours at 37°C. The resulting cRNA was purified and the yield evaluated by measuring the absorbance at 260 nm on a NanoVue spectrophotometer. The RNA integrity was examined on a bioanalyser prior to comparative whole-genome expression profiling, which was performed using two Illumina HumanHT-12 v4 Expression BeadChips.

2.2.4.3 Microarray data analysis

Gene signal profiles of 24 samples were normalised and analysed in Partek® Genomics Suite Software (version 6.5). Quantile normalisation and log₂ transformation of the data was followed by removal of batch effects between three groups of replicates. Outliers were removed and remaining 19 samples re-normalised. Differentiated genes were identified by ANOVA and post-hoc linear contrasts performed between all pairs of experimental conditions. Multiple test corrections were performed for all calculated p-values. Genes, which showed significant changes in expression level when comparing ERK2 knockdown versus control (step-up p-value <0.05) and inverse changes when comparing ERK2 knockdown versus re-expression of ERK2 (step-up p-value <0.05, fold change >±1.3) were identified. ERK2-specific genes also had to meet the criteria of a step-up p-values greater than 0.5 when comparing ERK2 knockdown cells to ERK1 re-expression.

2.2.4.4 First strand cDNA synthesis

The following components were added to a nuclease-free microcentrifuge tube:

Reagent	Sample (µl)
oligo (dT) ₁₅	1
purified RNA	1 µg
RNase/DNase-free ddH ₂ O	up to 10
total volume	10

The mixture was heated to 70°C for 10 minutes and incubated on ice for at least 1 minute. Afterwards, 10 µl of a master mix, prepared as follows, was added:

Reagent	Sample (μl)
ImProm-II™ 5X Reaction Buffer	4
MgCl ₂	3
dNTPs Mix	1
RNasin	0.5
IMProm-II™ Reverse Transcriptase	1
total volume	10

The solution was gently mixed by pipetting up and down. The sample was then incubated at 25°C for 5 minutes to allow initial annealing of the oligos. Following the annealing, the sample was incubated at 42°C for 1 hour for cDNA extension. Afterwards, the reaction was heat-inactivated at 70°C for 10 minutes and cooled to 4°C before sample was frozen at -20°C until further use.

2.2.4.5 qPCR

The DyNAmo™ SYBR® Green qPCR kit was used to perform quantitative PCR on a BioRAD DNA Engine thermal cycler fitted with a Chromo4 Engine and coupled to Opticon Monitor3 software. The following reagents were pipetted together:

Reagent	Sample (μl)
2x MasterMix	10
Quantitect primer	2
cDNA template	1
RNase/DNase-free H ₂ O	7
total volume	20

PCR reactions were performed according to the following protocol:

Initial denaturation	95°C	10 min
40 cycles:		
Denaturation	95°C	30 s
Annealing	50-60°C	30 s
Extension	72°C	30 s
Plate read		
Final extension	72°C	5 min
Dissociation curve	70°C-90°C in 0.3°C increments	
Final hold	4°C	∞

Extracted data was used to determine changes in gene expression according to the $\Delta\Delta C_t$ method previously described [354]. GAPDH was used as a reference. Control transfected transcript levels were assigned the arbitrary value of 1. Each experiment was performed in triplicate and replicas incorporated three technical repeats.

2.2.4.6 Statistical analysis

All experiments were done in triplicates. Statistical significance of differences was determined by nonparametric Mann-Whitney *U* tests using GraphPad Prism 5. *P* values of less than 0.05 were considered significant.

3 ERK2 but not ERK1 contributes to invasive cell migration

3.1 Introduction

3.1.1 Common features of ERK1 and ERK2

The two major ERK isoforms, ERK1 and ERK2, demonstrate an overall sequence identity of nearly 85% and are encoded by separate genes located on chromosome 16 and 22, respectively (Figure 3-1). In humans, both isoforms are ubiquitously expressed, albeit their relative abundance varies [58]. With the exception of a few studies demonstrating a preferential activation of a single ERK isoform [355, 356], most reports have demonstrated that ERK1 and -2 are co-activated in response to extracellular stimuli. Moreover, both enzymes rely on the same upstream kinase module, which does not discriminate between them. Additionally, ERK1 and ERK2 display indistinguishable kinase activities *in vitro* [357] and phosphorylate common substrates such as MBP kinase and MAP2 kinase at the same phosphoacceptor sites [55, 58].

Owing to the fact that ERK1 and -2 are highly homologous, both proteins share common features in their tertiary structure and are composed of two domains (N-terminal and C-terminal), which are connected by a flexible linker. The N-terminal domain predominantly consists of β -sheets, whereas the C-terminal domain mainly comprises α -helices [358]. Most substrates bind to ERK via two docking sites, the hydrophobic groove formed by the CD and ED domain, or the FXFP-motif [123, 129, 131-133]. Co-crystallisation studies of ERK with a D-motif peptide elucidated which ERK amino acids are involved in substrate binding. Out of the 11 residues determined, ERK1 and ERK2 only differ in one amino acid, with ERK1 displaying an isoleucine instead of a leucine [130]. Moreover, DEF-motif interacting residues are fully conserved between ERK1 and ERK2 [131]. Taken together, the structural data points towards similar substrate specificities for the two kinases and argues for functional redundancy.

ERK1 and ERK2 emerged early during vertebrate evolution with fish expressing both isoforms [357]. Moreover, both enzymes are evolutionary conserved, although it has to be noted that *Xenopus laevis* only expresses ERK2 and has lost the *erk1* orthologue [359]. Thus, the question arises whether or not both enzymes are functionally redundant and

ERK1 vs ERK2 (human)

```

ERK1      MAAAAAQGGGGEPRTTEGVGPGVPEVEMVKGQPFVDVGPRTYQLQYIGE 50
ERK2      MAAAAAG-----AGP-----EMVRGQVFDVGPRTNLSYIGE 33
          *****+*          .**          ***: **+*****: * : *****

ERK1      GAYGMVSSAYDHVRKTRVAIKKISPFQHYTCQRTLREIQILLRFRHENV 100
ERK2      GAYGMVCSAYDNVKNKRVVAIKKISPFQHYTCQRTLREIKILLRFRHENI 83
          *****: *****: * : * : *****: *****: *****:

ERK1      IGIRDILRASTLEAMRDVYIVQDLMETDLYKLLKSQQLSNDHICYFLYQI 150
ERK2      IGINDIIRAPTIEQMKDVYIVQDLMETDLYKLLKTQHLSDHICYFLYQI 133
          ***: ** : ** : * : * : * : *****: *****: *****:

ERK1      LRGLKYIHSANVLRDLKPSNLLINTTCDLKICDFGLARIADPEHDHTGF 200
ERK2      LRGLKYIHSANVLRDLKPSNLLINTTCDLKICDFGLARVADPDHDHTGF 183
          *****: *****: *****: *****: *****:

ERK1      LTEYVATRWRAPPEIMLNSKGYTKSIDIWSVGCILAEMLSNRPIFPQKHY 250
ERK2      LTEYVATRWRAPPEIMLNSKGYTKSIDIWSVGCILAEMLSNRPIFPQKHY 233
          *****: *****: *****: *****: *****:

ERK1      LDQLNHILGILGSPSQEDLNCCIINMKARNYLQSLPSKTKVAVAKLFPKSD 300
ERK2      LDQLNHILGILGSPSQEDLNCCIINLKARNYLLSLPHKNKVPWNRLFPNAD 283
          *****: *****: *****+*** : ** : * : ** : : ** : : ** :

ERK1      SKALDLLDRMLTFNPNKRITVEEALAHFPYLEQYDPTDEPVAEEPFTFAM 350
ERK2      SKALDLLDKMLTFNPKRIEVEQALAHFPYLEQYDPSDEPIAEAPFKFDM 333
          *****: *****: *** ** : *****: *** : **+** : **+

ERK1      ELDDLPERLKLKELIFQETARFQPGVLEAP 379
ERK2      ELDDLPERLKLKELIFEETARFQPGYRS-- 360
          *****: *****: *****++ .

```

Figure 3-1 Sequence comparison of human ERK1 and ERK2

interchangeable and if so, why both proteins have been conserved evolutionarily. Lefloch *et al.* proposed that the expression of two isoforms with functional redundancy allows the fine-tuning of ERK protein levels depending on the cellular needs and thereby represents an evolutionary advantage to higher organisms [359].

3.1.2 ERK isoforms in whole animal studies

In recent years, however, more and more evidence, suggesting non-redundant functions for the two ERK kinases, has been reported. In particular, the marked discrepancy between the phenotypes of ERK1^{-/-} and ERK2^{-/-} mice indicates clear functional differences *in vivo*. ERK1^{-/-} mice are viable, fertile and of normal size [360], whereas ERK2^{-/-} mice die early in embryonic development [361-363]. Moreover, ERK1^{-/-} mice display enhanced behavioural responses in avoidance tasks and are hypersensitive to drug abuse [364]. In contrast, ERK2^{+/-} mice, which display a 40% reduction in ERK2 protein levels, show a deficit in long-term memory [365]. Likewise, humans with only one ERK2 allele show learning disabilities and developmental delays, thus arguing for ERK-specific function in cognition and memory [366]. In addition, ERK1-deficient mice are impaired in thymocyte maturation and adipogenesis [360, 367]. Interestingly, adipocyte differentiation in isolated ERK1^{-/-} pre-adipocytes was not reduced further, when ERK2 activation was inhibited chemically, thus arguing for an isoform-specific role of ERK1 in this process. This view is furthermore supported by the fact that, in contrast to most tissues, ERK1 and ERK2 are expressed and activated to similar levels in adipocytes. Thus, equal expression levels may indicate an important role for ERK1 in fat tissue. Furthermore, ERK1-deficient mice exhibit an increased metabolic rate, and are protected from insulin resistance and obesity [367].

Studies in zebrafish provide further evidence of ERK isoform-specific functions. First, ERK1 and -2 display differential spatio-temporal expression patterns during zebrafish development. Second, ERK1 and -2 morphants show distinct phenotypes during embryogenesis [368]. In agreement with mice studies, ERK2 morphants are 70% lethal and portray severe developmental defects. On the contrary, ERK1 ablation during zebrafish development also gives rise to a distinct phenotype with 10% lethality. Remarkably, *erk2* mRNA is able to cross-rescue the ERK1 morphant phenotype, whereas *erk1* mRNA fails to cross-rescue developmental defects brought about by ERK2

knockdown. Thus, in zebrafish ERK2 can compensate for ERK1, while exhibiting isoform-specific functions that are distinct from ERK1 [369].

3.1.3 ERK isoforms in cell culture studies

In vitro studies employing RNA interference (RNAi) have also suggested distinct biological functions for ERK1 and ERK2. For example, silencing ERK2 in C2C12 myoblasts inhibits myogenin expression and blocks myoblast fusion, while ERK1 ablation has no effect [370]. Owing to the fact that ERK signalling plays a critical role in proliferation, multiple studies investigated whether ERK1 and ERK2 have distinct functions in this cellular process. Intriguingly, Vantaggiato *et al.* observed enhanced cell proliferation in mouse fibroblasts upon ablation of ERK1 by either gene targeting or RNA interference (RNAi), while silencing of ERK2 reduced the proliferative response to mitogenic stimuli [371]. The authors, therefore, suggested an antagonistic role for ERK1 and ERK2 in proliferation. However, this observation was challenged by multiple studies showing no changes [357, 372] or a reduced proliferative response upon ERK1 ablation [373-375]. In an attempt to resolve these discrepant observations, Lefloch *et al.* turned their attention towards the expression ratio of ERK1 and ERK2 and proposed a threshold-dependency for ERK signalling, i.e. a requirement for a certain pool of active ERK for the execution of physiological functions [357]. Thus, as ERK1 and ERK2 are mostly expressed at different levels, with ERK2 being the predominant kinase, silencing ERK2 may decrease total ERK levels below a threshold and result in functional defects, whereas ERK1 knockdown may not markedly decrease the pool of active ERK, therefore resulting in no or mild phenotypic changes. Thus, apparent biological differences may be attributed to differences in the expression levels rather than distinct biological features. Indeed, redundant functions of ERK1 and -2 in proliferation were subsequently confirmed in experiments, where conditional invalidation of ERK2 in the developing cortex of mice significantly reduced cell proliferation, but could be rescued when ERK1 was overactivated [366]. Moreover, Voisin *et al.* demonstrated that loss of either ERK1 or ERK2 reduced proliferation in fibroblasts, which reflected their expression level [376]. Taken together, the data shows that both ERKs are positive regulators of proliferation and differences in their expression levels may give the impression of distinct biological functions. Thus, studies investigating isoform-specific features have to address this issue in order to draw meaningful conclusions from the data.

3.1.4 *ERK isoforms and tumourigenesis*

ERK's role in tumourigenesis is well-established with the kinases impinging on many hallmarks of cancer. In 2002, Adeyinka *et al.* demonstrated a direct correlation between pERK1/2 levels and tumour progression in breast cancer. Thus, a role for active ERK in the metastatic process was proposed [377]. Moreover, high levels of active ERK are associated with enhanced cell motility [378].

In experiments examining the role of ERK1 in skin homeostasis and tumourigenesis, ERK1-deficient mice developed fewer papillomas than wild type mice after tumour induction with DMBA and promotion with TPA. Additionally, tumour onset was delayed and the burden decreased. Moreover, studies of isolated ERK1^{-/-} keratinocytes showed an impairment of cellular growth, a resistance to apoptotic signals as well as a diminished expression of *fra1* [373]. Thus, Bourcier *et al.* concluded an important role of ERK1 in skin tumour development by contributing to cellular growth and proliferation and postulated a role of this isoform in tumour cell invasion.

In 2007, Bessard *et al.* investigated the role of ERK signalling in cell motility in human hepatocarcinoma cells. The authors observed a reduction in cell motility in wound healing assays after treatment with the MEK inhibitor, U0126. Moreover, silencing of ERK2 but not ERK1 with short hairpin duplexes impaired wound closure, reduced uPAR expression and S6K phosphorylation at Thr389 [379]. Although the data strongly suggest a role for ERK signalling in cell migration, the study did not address whether or not the observations can truly be attributed to an ERK2-specific function or differences in the expression levels of the two kinases [379]. Thus, whether or not the major ERK isoforms have distinct functions in cell migration remains an open issue.

This present study set out to address the question in dispute by studying the role of ERK1 and ERK2 in tumour cell motility in 2D and 3D microenvironments and investigating whether isoform-specific differences observed in cell migration experiments are true functional disparities or the result of different expression levels.

3.2 Results

3.2.1 *The invasive phenotype of A2780-Rab25 cells is dependent on ERK signalling*

To study the contribution made by ERK1 and ERK2 to invasive tumour cell migration, we required a suitable cancer cell line with an ERK-dependent invasive phenotype. To this end, we chose the well-characterised invasive ovarian carcinoma cell line A2780-Rab25 which, through stable overexpression of ectopic HA-Rab25, show enhanced invasiveness into *bona fide* 3D matrices such as collagen or Matrigel [380] and increased aggressiveness in xenograft studies of ovarian and breast tumours in nude mice [351]. We postulated that the invasive phenotype of A2780-Rab25 cells requires ERK signalling and performed inverted invasion assays (previously described by Hennigan *et al.* [352] and adapted by Caswell *et al.* [380]), where tumour cells were plated onto the underside of a Matrigel plug supplemented with 25 µg/ml fibronectin. (N.B. The addition of fibronectin was shown to be necessary for Rab25-driven invasion [380]). A2780-Rab25 cells were allowed to migrate through the porous membrane of the Transwell insert into the Matrigel. Subsequently, a chemotactic gradient was established by adding full medium containing 25 ng/ml EGF into the upper chamber and serum-free medium into the lower chamber (see Figure 3-2 A for experimental set-up). After 36 hours, living cells were stained using Calcein-AM and imaged on a confocal microscope. Optical sections were gathered every 15 µm, starting at the bottom of the Matrigel plug and moving upwards in the direction of cell invasion. To test whether ERK signalling was required for the invasion of A2780-Rab25 cells, the MEK inhibitor, U0126 was added to the lower and upper chamber at a concentration of 10 µM. Figure 3-2 B shows representative strips, which were assembled from individual images obtained during optical sectioning of the Matrigel plug. Cells are stained green and their migration from left to right indicated by the arrow, corresponds to their upward migration. Quantification of three independent experiments, within which each experimental condition was represented by two Matrigel plugs and three regions (corresponding to x,y positions) of each plug, was performed using the ImageJ. Invasive migration was expressed as a percentage of cells that migrated beyond 45 µm relative to the control condition. When ERK activation was inhibited by U0126 treatment, we observed a significant decrease in invasion by approximately 50% ($p < 0.0001$) (Figure 3-2 C). Furthermore, ERK inhibition was validated by Western blotting to be completely abolished 24 hours, and marginally recovered 48 hours after U0126

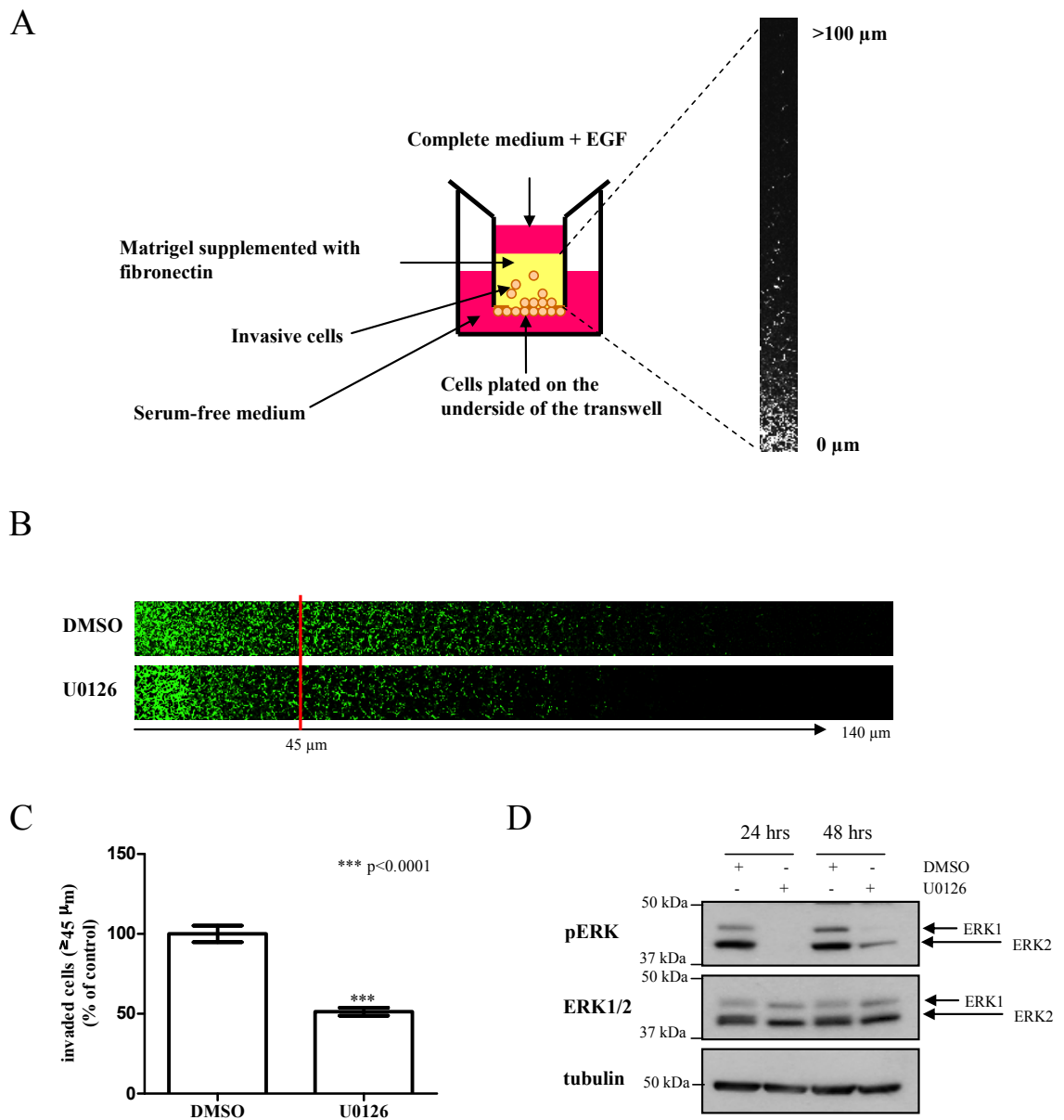


Figure 3-2 The invasive phenotype of A2780-Rab27 cells is dependent on ERK signalling

A. Schematic diagram on how inverse invasion assays are set up and quantified.

B. Matrigel plugs were enriched with $25 \mu\text{g/ml}$ fibronectin and 4×10^4 A2780-Rab25 cells were plated onto the underside of each Transwell. The MEK inhibitor, U0126 ($10 \mu\text{M}$), or DMSO was added to the media. After 36 hrs invading cells were visualized by Calcein-AM staining. Serial optical sections were captured every $15 \mu\text{m}$ and are presented as a sequence in which the depth increases from left to right.

C. Invasive migration was quantified by measuring the fluorescence intensity of cells penetrating the Matrigel plug to depths of $\geq 45 \mu\text{m}$ and expressed relative to cells treated with DMSO. Values are means \pm standard error of the mean (SEM) of 18 replicates from three independent experiments. Statistical significance of difference was determined by Mann-Whitney U test analysis.

D. ERK inhibition by U0126 was assessed by Western blotting at 24 hrs and 48 hrs.

treatment (Figure 3-2 D). Taken together the data indicates that invasion of A2780-Rab25 cells is dependent on ERK signalling, thus proving as a suitable cell line to study the isoform-specific contributions towards invasive tumour cell migration.

3.2.2 Silencing of ERK2 impairs invasion into Matrigel

Next, we wanted to investigate the respective roles of ERK1 and ERK2 in invasive migration. Therefore, A2780-Rab25 cells were transfected with non-targeting (NT) siRNA oligos or SMARTpools targeting either ERK1 or ERK2. Knockdown of ERK was validated by Western blotting 48 and 72 hours post transfection (Figure 3-3 A). Surprisingly, silencing of ERK1 resulted in enhanced invasion ($p < 0.05$), whereas knockdown of ERK2 significantly decreased migration into the Matrigel plug by approximately 40% ($p < 0.0001$). When both ERK isoforms were knocked down simultaneously, a 30% decrease in invasion was observed ($p < 0.01$) (Figure 3-3).

RNA interference is a commonly used method to study gene function in biological processes, such as apoptosis, differentiation and cell migration. However, short-interfering RNAs (siRNAs) have been reported to silence unintended transcripts, which are only partially complementary in sequence [465]. Moreover, siRNAs can affect mRNA translation [466] and induce an unspecific interferon response [467]. Therefore, caution is warranted when interpreting functional and phenotypical changes following RNAi. The validity of biological changes observed following siRNA of a given target gene is generally assessed by using multiple independent siRNA duplexes. Thus, while all duplexes employed display the same on-target activity, their non-specific effects will differ and functional changes observed with at least two siRNA duplexes are likely to be attributed to silencing of the target gene rather than overlapping off-target effects.

In order to control for any off-target effects caused by the siRNA oligos of the SMARTpool, invasion assays were repeated with two independent oligos targeting either ERK1 or ERK2. Silencing of the respective isoform was confirmed 72 and 96 hours post transfection by Western blotting (Figure 3-4 A). Knockdown of ERK1 with oligo #1 or #2 showed no significant effect on invasion when compared to NT controls. In contrast, silencing of ERK2 with oligos #1 or #2 significantly reduced invasion into Matrigel by approximately 50% ($p < 0.0001$) (Figure 3-4 B/C).

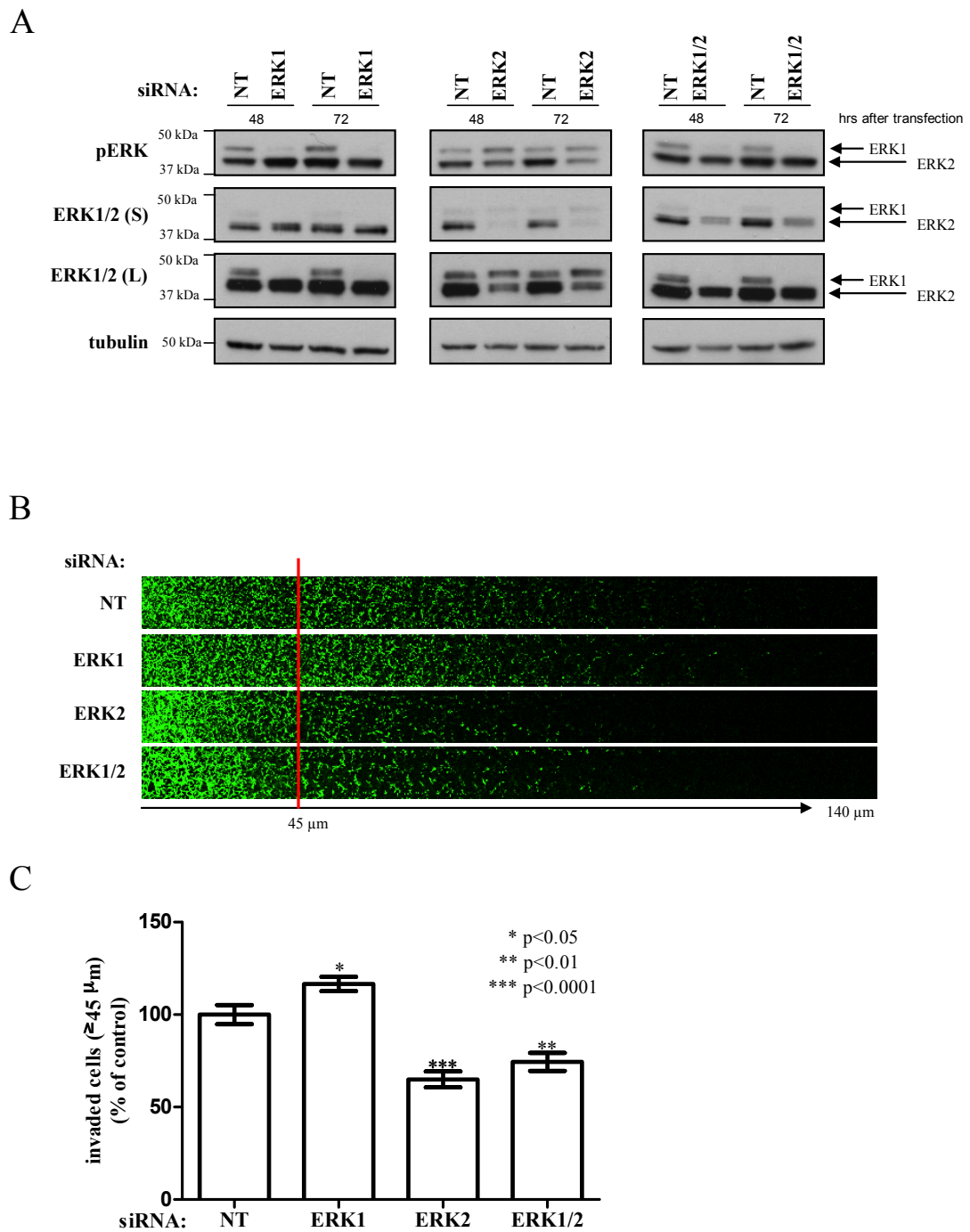


Figure 3-3 Suppression of ERK2 levels reduces invasiveness of A2780-Rab25 cells

A. A2780-Rab25 cells were transfected with non-targeting siRNAs (NT), or SMARTpools targeting ERK1 or ERK2. The effectiveness of the ERK knockdown was assessed by Western blot 48 hrs and 72 hrs after transfection. (S) and (L) refer to a short and long exposure times, respectively.

B. Matrigel plugs were enriched with 25 $\mu\text{g}/\text{ml}$ fibronectin and 4×10^4 cells were plated onto the underside of each Transwell 24 hrs post transfection. 36 hrs following this, invading cells were visualized by Calcein-AM staining. Serial optical sections were captured every 15 μm and are presented as a sequence in which the depth increases from left to right.

C. Invasive migration was quantified by measuring the fluorescence intensity of cells penetrating the Matrigel plug to depths of $\geq 45 \mu\text{m}$ and expressed relative to cells transfected with non-targeting (NT) siRNA. Values are means \pm standard error of the mean (SEM) of 18 replicates from three independent experiments. Statistical significance of differences was determined by Mann-Whitney U test analysis.

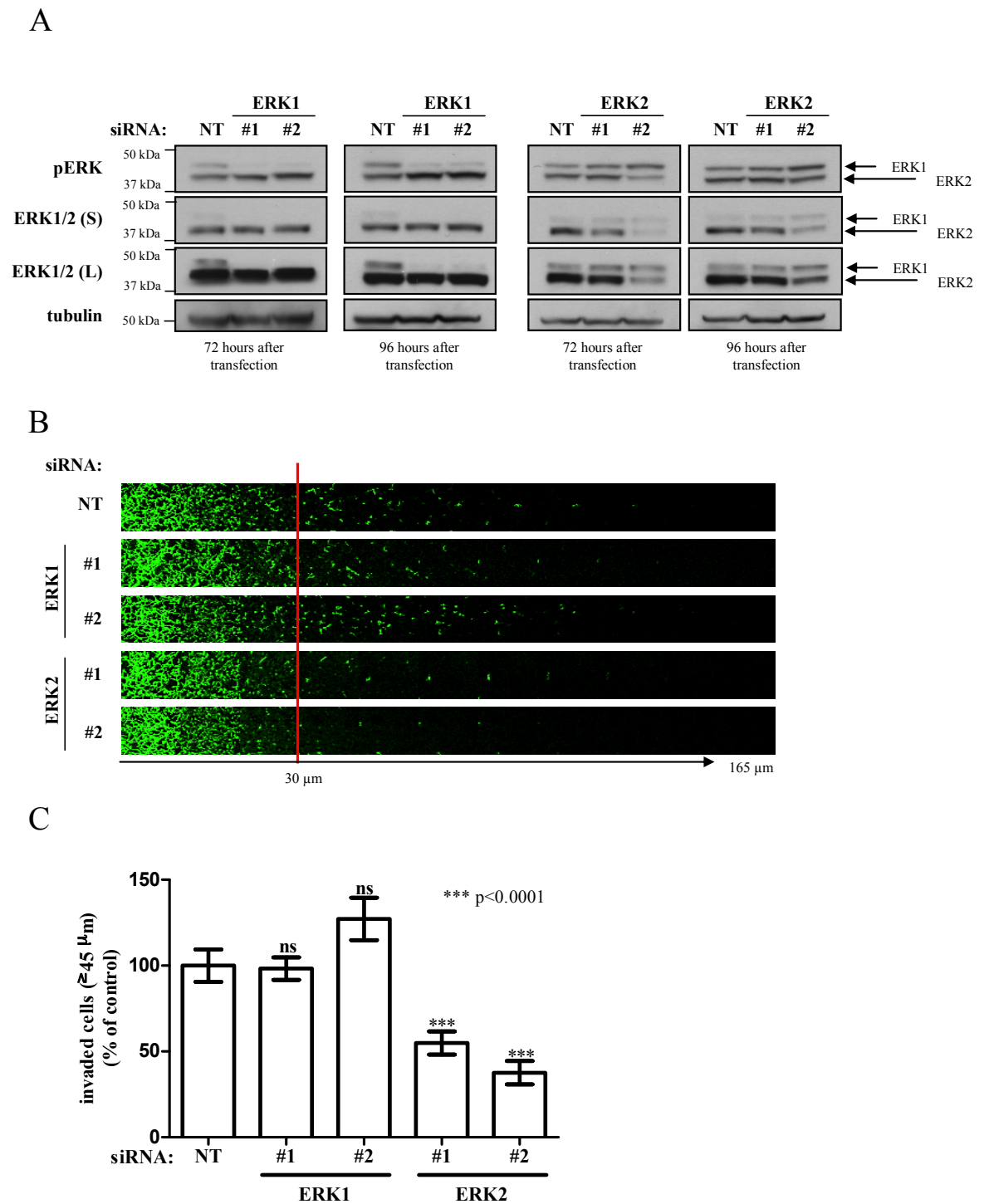


Figure 3-4 siRNA of ERK2 opposes invasion into Matrigel

A. A2780-Rab25 cells were transfected with non-targeting siRNAs (NT), or single oligos targeting ERK1 or ERK2. The effectiveness of the ERK knockdown was assessed by Western blot 72 hrs and 96 hrs after transfection. (S) and (L) refer to a short and long exposure times, respectively.

B. Matrigel plugs were enriched with 25 $\mu\text{g/ml}$ fibronectin and 4×10^4 cells were plated onto the underside of each Transwell 24 hrs post transfection. 36 hrs following this, invading cells were visualized by Calcein-AM staining. Serial optical sections were captured every 15 μm and are presented as a sequence in which the depth increases from left to right.

C. Invasive migration was quantified by measuring the fluorescence intensity of cells penetrating the Matrigel plug to depths of $\geq 45 \mu\text{m}$ and expressed relative to cells transfected with non-targeting (NT) siRNA. Values are means \pm standard error of the mean (SEM) of 18 replicates from three independent experiments. Statistical significance of differences was determined by Mann-Whitney *U* test analysis.

3.2.3 Transient knockdown of ERK does not induce apoptosis or alter proliferation in A2780-Rab25 cells

ERK signalling cooperatively enhances cellular growth, proliferation and cell survival. Thus, diminishing ERK signalling through transient knockdown may affect cell viability and thereby alter the invasive phenotype of A2780-Rab25 cells. Given that ERK2 is the predominant kinase in these cells (Figure 3-2 D), silencing ERK2 may greatly reduce the amount of active ERK, whereas knockdown of ERK1 might result in a marginal reduction of pERK levels. Our data, however, demonstrates a compensatory increase in pERK1 levels upon ERK2 knockdown and vice versa. Thus, transient knockdown of either ERK1 or ERK2 does not alter the pool of active ERK dramatically.

In order to test, whether knockdown of either ERK isoform induces apoptosis, A2780-Rab25 cells were transfected with NT siRNA and oligos targeting ERK1 and ERK2. As a positive control the extrinsic apoptotic pathway was induced in non-transfected cells by treatment with Fas-ligand (50 nM) and 5 µg/ml cycloheximide for 24 hours. Fas-ligand binding to the death receptor, FasR, activates the caspase cascade, while cycloheximide inhibits protein synthesis by blocking the translational elongation step [381]. Caspase activation will ultimately promotes the cleavage of poly ADP ribose polymerase (PARP), which is involved in DNA repair of single-stranded nicks [382]. PARP cleavage gives rise to two fragments of 24 kDa and 89 kDa, which can be visualised by Western blotting. When examining cells treated with Fas-ligand and cycloheximide using a phase-contrast light microscope, A2780-Rab25 cells were round, largely unattached and fragmented. In order to harvest any apoptotic cells, we collected the media of each experimental condition and centrifuged at 10,000 rpm for five minutes at 4°C. The supernatant was discarded and the pellet kept on ice. PBS from subsequent wash steps and the trypsinised cell suspension were also spun down in the same tube. The final pellet, containing both apoptotic and non-apoptotic cells, was lysed in HEPES lysis buffer and PARP-1 cleavage was determined by Western blotting. Interestingly, the 89 kDa PARP-1 fragment was clearly visible in apoptosis-induced A2780-Rab25 cells, whereas control-transfected and ERK knockdown cells showed no PARP-1 cleavage (Figure 3-5 A). We, therefore, concluded that apoptosis was not triggered as a result of transient ERK knockdown.

With the exception of Vantaggiato et al. [371], multiple reports studying the role of ERK1 and ERK2 in proliferation have demonstrated that both isoforms positively contribute

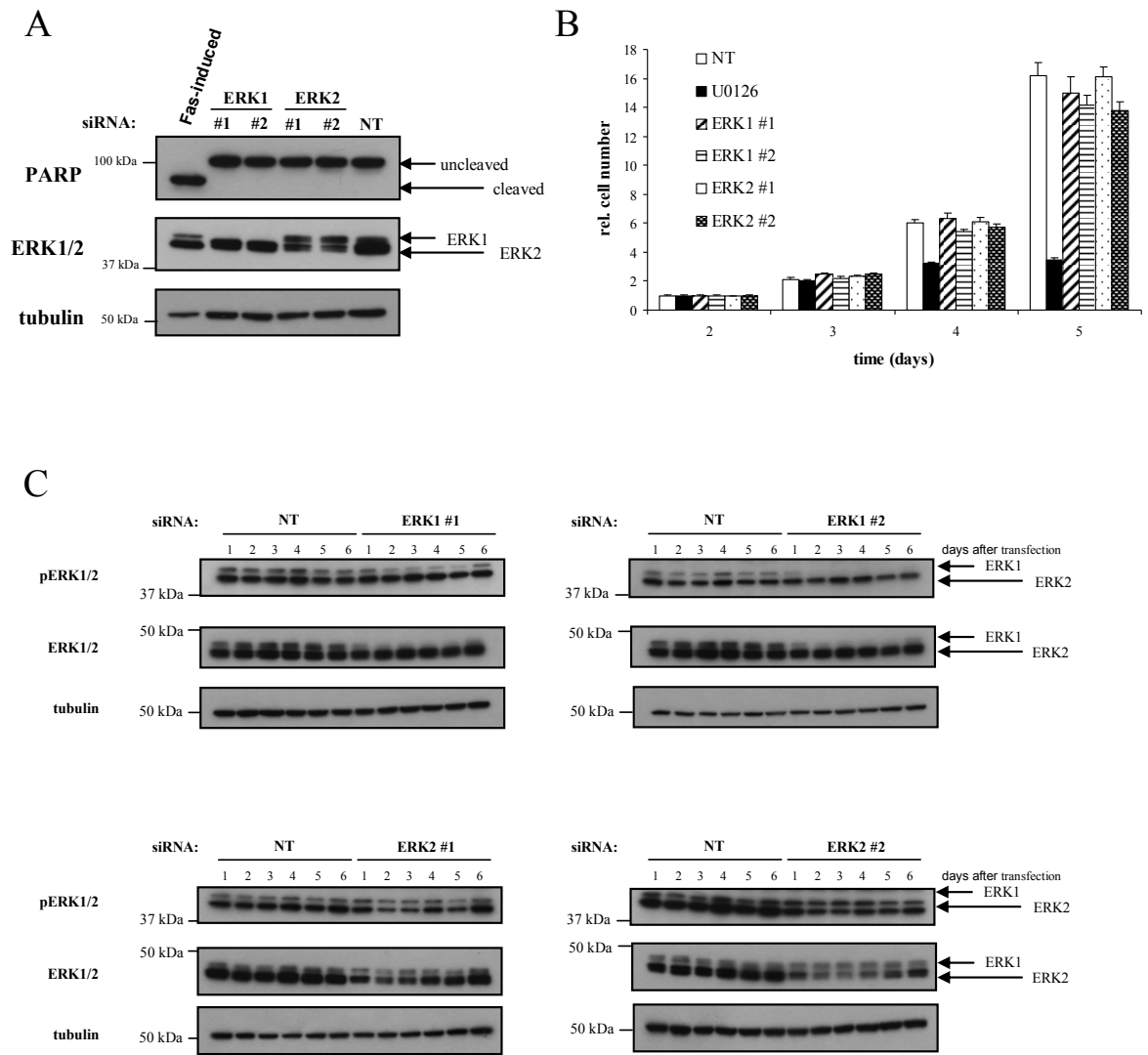


Figure 3-5 siRNA of ERK1 or ERK2 does not induce apoptosis or inhibit proliferation

A2780-Rab25 cells were transfected with non-targeting siRNAs (NT), or those targeting ERK1 or ERK2. A. Apoptosis was induced in control transfected cells by Fas-ligand (50nM) and cycloheximide (5 μ g/ml) treatment. PARP-cleavage was determined 24 hours after induction.

B. The proliferation assay was set up 24 hrs after transfection by seeding 20,000 cells into a 6-well dish. The following 4 days, cells were counted using a Casy counter. Relative cell number was plotted against time. Values are means \pm standard error of the mean (SEM) of 9 replicates from three independent experiments.

C. The effectiveness of the ERK knockdown was assessed over the course of 6 days by Western blot.

towards cellular growth [357, 359, 366, 376] and therefore reducing the pool of active ERK by silencing either isoform may result in proliferative changes. To test this, we transfected A2780-Rab25 cells with NT siRNA, or those targeting ERK1, or ERK2 and seeded 40,000 cells into a 6-well dish one day after transfection. As a negative control, one set of control-transfected cells were treated with the MEK inhibitor, U0126, which has previously been shown to inhibit proliferation *in vitro* and *in vivo* [383-385]. Cellular growth was monitored by cell counting using a Casy cell counter and a haemocytometer. The cell number of each experimental condition was measured over the course of four days and is represented as a relative cell number in Figure 3-5 B. Three independent experiments were performed, in which each experimental condition was set up in triplicate. As expected, we observed a proliferative inhibition two days after U0126 treatment. In contrast, transient knockdown of either ERK1 or ERK2 did not affect cellular growth, although an efficient knockdown was achieved during the course of the experiment (Figure 3-5 C).

In summary, we found that knocking down either ERK isoform had no effect on proliferation or apoptosis indicating that effects of ERK signalling on cell viability did not influence our invasion and motility results.

3.2.4 Both ERK isoforms contribute to migration on plastic surfaces

Rab25, which was shown to be a component of an invasive gene signature in breast cancer cells [386], alters the way in which A2780 cells migrate on extracellular matrices, but not on 2D plastic surfaces [380]. Given that changes in invasiveness do not necessarily reflect on plastic, we set out to investigate whether ERK2 altered cell migration in 2D. Thus, we transiently transfected A2780-Rab25 cells with non-targeting siRNAs (NT), or single oligos targeting ERK1 or ERK2. Subsequently, cells were seeded into a 6-well dish, so that they were confluent 48 hours post transfection. After introducing a wound by scratching the plastic dish with a 200 μ l pipette tip, wound closure was monitored at 10 minute intervals using a time-lapse microscope. The movement of individual cells was followed using the ImageJ cell tracking software. Images were taken from five distinct fields along the wound in every well and a minimum of five cells were tracked in each field. The migratory speed, persistence and FMI were extracted from the trackplots from three independent experiments and are represented in Figure 3-6. Persistence is a measurement on how direct a cell moves from A to B and is calculated by dividing the vectorial cell path by the accumulated distance. The forward migration index (FMI) is commonly extracted from wound healing assays, as it is a measurement of wound sensing. The FMI represents the ratio of the perpendicular distance and the accumulated path (Figure 3-6 B). The migration speed of ERK1 or ERK2 knockdown cells was expressed relative to the migration velocity of cells transfected with NT siRNA to account for differences in the absolute migration speed between different experiments.

Treatment of A2780-Rab25 cells with the MEK inhibitor, U0126, significantly impaired wound closure and severely reduced the migratory speed to approximately 50% of NT-transfected cells. Interestingly, silencing of ERK1 or ERK2 with two independent oligos significantly delayed wound closure and resulted in a 25% decrease in migratory speed ($p < 0.0001$) (Figure 3-6 A/C). In contrast, persistence and FMI did not change upon inhibition of ERK signalling with U0126 or knockdown of either ERK isoform (Figure 3-6 D/E). Thus, whereas invasion into Matrigel is specifically regulated by ERK2 in A2780-Rab25 cells, migration on 2D plastic surfaces appears to be regulated by both ERK isoforms and may depend on the total ERK activity present in the cell.

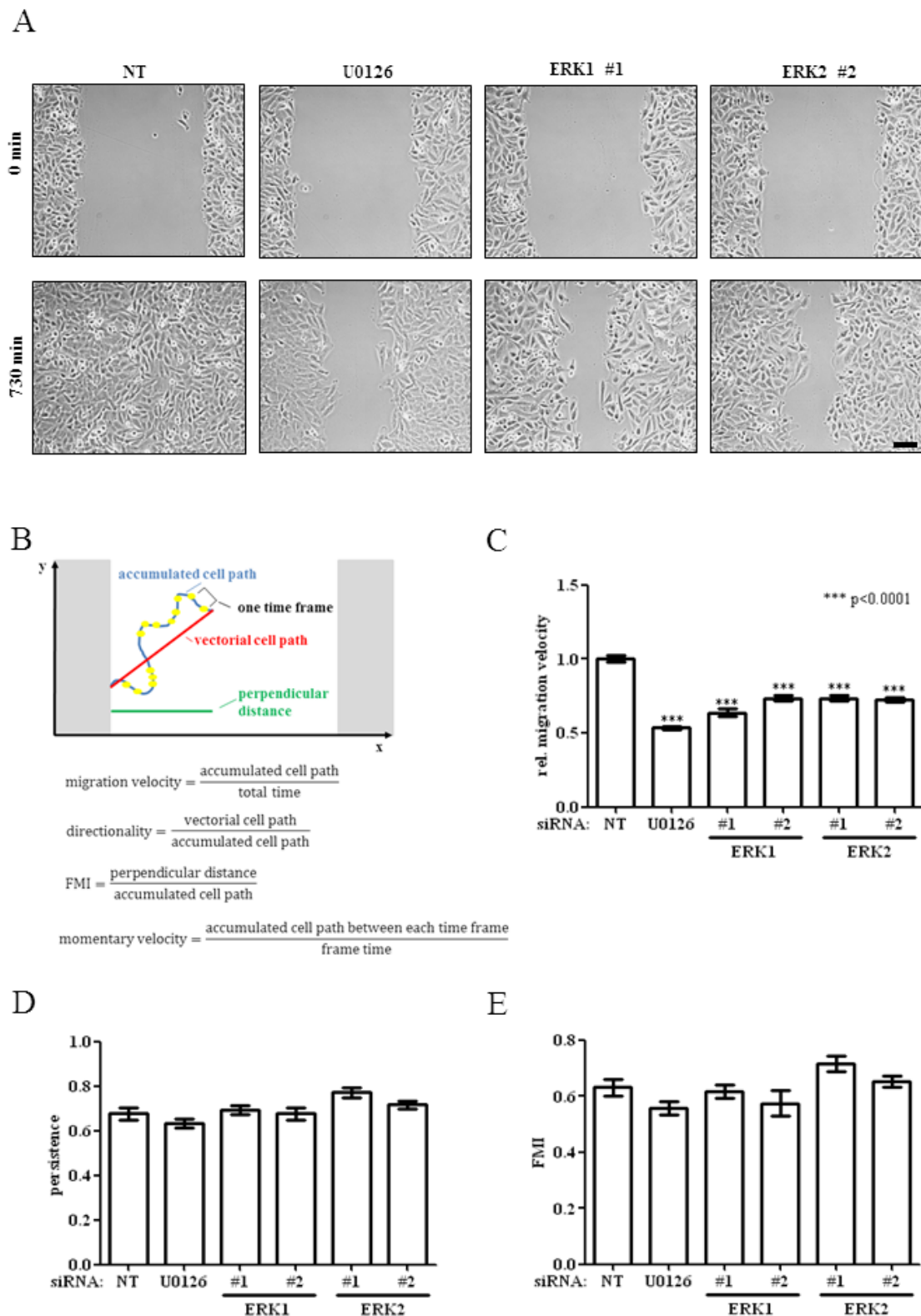


Figure 3-6 Both ERK isoforms contribute towards migration on plastic in A2780-Rab25 cells

A. A2780-Rab25 cells were transfected with non-targeting siRNAs (NT), or single oligos targeting ERK1 or ERK2. Subsequently, cells were seeded into a 6-well dish, so that they were confluent 48 hrs post transfection. After scratching wound closure was monitored and representative time frames are shown. Scale bar, 100 μm .

B. Schematic outline of the cell tracking analysis. The overall migration velocity is defined as the ratio of accumulated path length and time. Persistence is defined as the ratio of the vectorial distance a cell travelled and the accumulated path length. The forward migration index (FMI) is a measure for wound sensing and is determined by dividing the distance travelled into the wound by the accumulated path length. The momentary velocity represents a frame-to-frame migration speed. (see next page also)

C-E. The movement of individual cells into the wound was followed using ImageJ cell tracking software. The overall migration velocity (C), persistence (D) and forward migration index (FMI) (E) were extracted from the trackplots. Values are means \pm SEM of >75 trackplots from three independent experiments. Statistical significance of differences was determined by Mann-Whitney U test analysis.

3.2.5 Knockdown of ERK2 impairs migration on cell-derived matrices

To get a better understanding of how ERK2 silencing controls invasive cell migration, we decided to use cell-derived matrix (CDM), which was previously described by Cukierman *et al.*, and which represents a good physiological model of the ECM [38]. CDMs are generated by human telomerase-immortalised fibroblasts, which naturally produce extracellular matrix-like fibres around themselves and thereby create a relatively thick (10 μm), pliable matrix composed mainly of fibrillar collagen and fibronectin, which recapitulates key aspects of the type of matrix found in connective tissues [38, 353]. After growing these fibroblasts as a confluent monolayer for 10-14 days, during which ECM fibers are synthesized, the cells were removed from the surrounding ECM by treatment with a non-ionic detergent. Cancer cells may then be plated onto the remaining fibrillar CDM to study their migratory and morphological characteristics in this quasi-3D environment. As expected, there is a striking difference in morphology and mode of migration of A2780-Rab25 between plastic surfaces and CDM (Figure 3-7). During migration on plastic and other rigid substrates many cell types migrate by forming lamellipodia and stress fibers [387, 388]. Moreover, adhesion structures on 2D surfaces, which are divided into focal and fibrillar adhesions, are rich in $\alpha_v\beta_3$ integrin, paxillin, vinculin and FAK, or $\alpha_5\beta_1$ integrin and tensin, respectively [389]. In 3D, however, cells either acquire an elongated, mesenchymal-like morphology, which is marked by pseudopod formation at the cellular front and requires matrix remodeling, or an amoeboid, rounded shape, which is characterized by high Rho/ROCK activity and the formation of bleb-like protrusions [34]. In addition, cells, cultured in 3D, lose the dorsal-ventral asymmetry and form 3D matrix adhesions, which are composed mainly of paxillin and $\alpha_5\beta_1$ integrin [38].

We transfected cells with either NT siRNA, or single oligos targeting ERK1 or ERK2. 50,000 cells were seeded onto a 6-well cell culture dish coated with CDM 48 hours post transfection and allowed to adhere to the 3D substratum for approximately four hours. Cell migration was monitored on a time-lapse microscope over the course of 16 hours and images were acquired every 10 minutes. Stills of representative movies are shown in Figure 3-8 A. Notably, no morphological differences between NT siRNA-transfected, U0126-treated and ERK knockdown cells were observed. However, when cell movement was analysed using the ImageJ cell tracking software, we detected a significant decrease

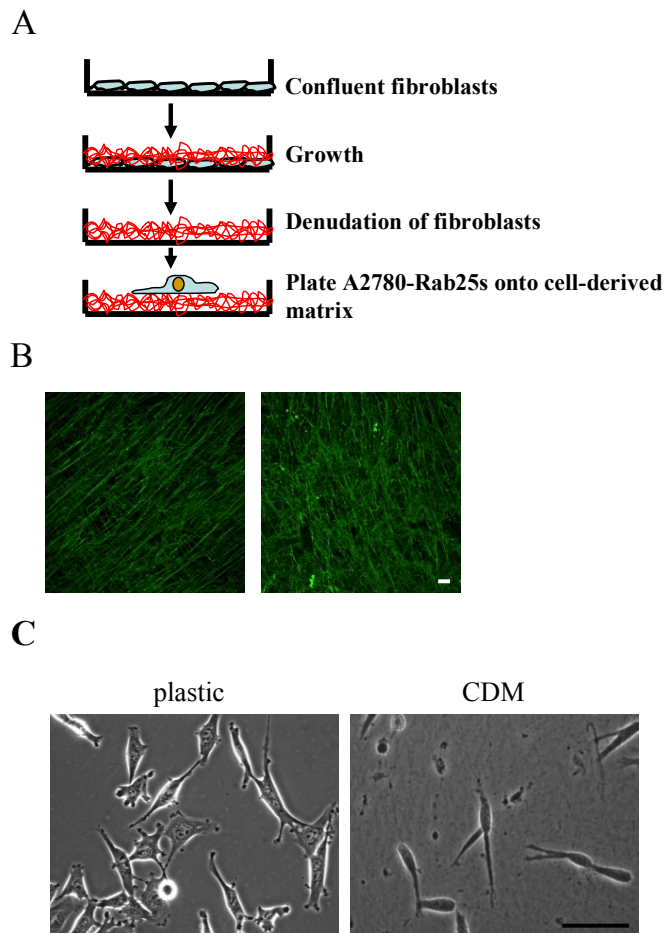


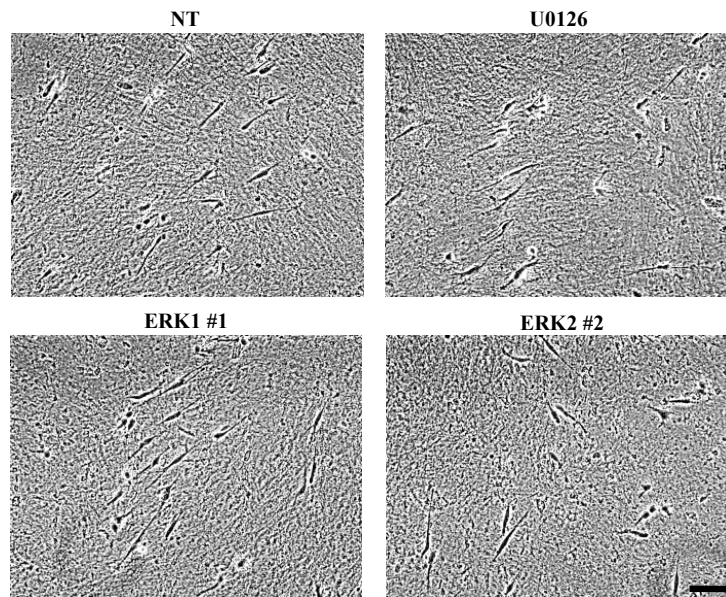
Figure 3-7 Cell-derived matrices (CDM) represent a 3D-like environment

A. Schematic diagram illustrating the protocol for generating CDM.

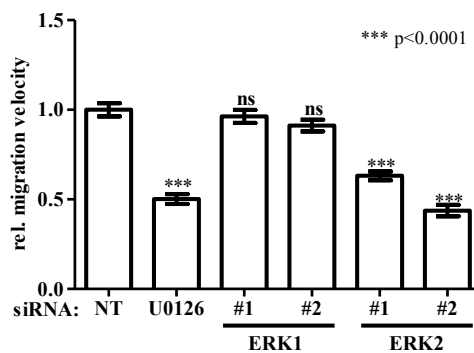
B. Confocal sections of CDM displaying either parallel (left) or intersecting (right) fibronectin fibres. Fibronectin was visualised by indirect immunofluorescence using a Cy2-conjugated secondary antibody (green). Scale bar, 10 μm

C. A2780-Rab25 cells were seeded onto plastic and CDM-coated dishes. After 16 hours cells were visualised using a bright field microscope. Scale bar, 100 μm .

A



B



C

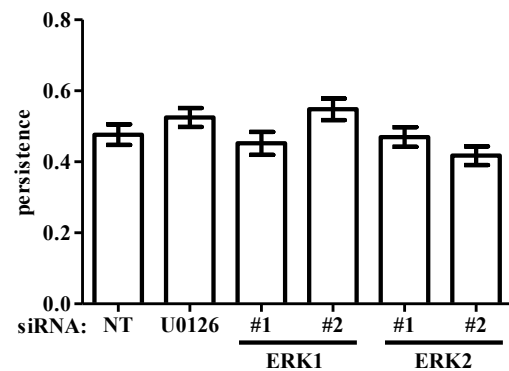


Figure 3-8 siRNA of ERK2 reduces migration of A2780-Rab25 cells on CDM

A. A2780-Rab25 cells were transfected with non-targeting siRNAs (NT), or those targeting ERK1 or ERK2 and plated onto cell-derived matrix. Images were captured every 10 minutes over a 16 hrs period using a Nikon time-lapse microscope. Still images from a representative movie are displayed. Scale bar, 100 μ m. B-C. The movement of individual cells was followed using the ImageJ cell tracking software. The overall migration velocity (B) and persistence (C) were extracted from the trackplots. Values are means \pm SEM of >75 trackplots from three independent experiments. Statistical significance of differences was determined by Mann-Whitney *U* test analysis.

in the migration velocity on CDM, when cells were treated with the U0126 inhibitor or ERK2 was silenced with two independent oligos ($p < 0.0001$). In contrast, knockdown of ERK1 did not alter the migration speed when compared to control (Figure 3-8 B).

Moreover, we determined the persistence of cell migration and found no significant difference between NT siRNA, U0126 treatment and ERK knockdown cells (Figure 3-8 C).

During our cell tracking analysis, we noticed that ERK2 knockdown cells had a tendency to remain stationary for extended periods of time. Thus, the previously observed difference in the relative migration speed may be attributed to the stationary phases, which we term 'cellular resting' (Figure 3-9 B). To quantify this we defined a cell that moved less than 2 μm within 90 minutes as one that was engaged in 'cellular resting'. ERK2 knockdown or addition of U0126 markedly increased the proportion of cells that were resting, whereas siRNA of ERK1 was ineffective in this regard (Figure 3-9 C). Moreover, we compared the average duration of each rest (resting time) and found no significant difference among our various experimental conditions (Figure 3-9 C). Next, we determined whether silencing of ERK2 influenced cell movement during the period in which cells were not resting. To do this, we calculated frame-to-frame displacement of cells whilst they were not resting and termed the 'momentary velocity'. We found the momentary velocity to be significantly reduced following ERK2 knockdown or addition of U0126, but it was unaffected by siRNA of ERK1 (Figure 3-9 B). To represent this pictorially, we generated trackplots of cells in which the migration speed is denoted by a colour code, the scale of which is indicated on the left side of the panels, and the points at which cells moved less than 2 μm in 90 min (cellular resting) are indicated by white dots. These trackplots indicate that knockdown of ERK2 increases cellular resting and decreases momentary velocity whilst siRNA of ERK1 is ineffective in both these regards (Figure 3-9 D)

Taken together these data indicate that knockdown of ERK2 decreases cell invasiveness, and that this corresponds to a combination of reduced momentary velocity and an increased tendency of ERK2 knockdown cells to remain immobile or rest for extended periods on CDM.

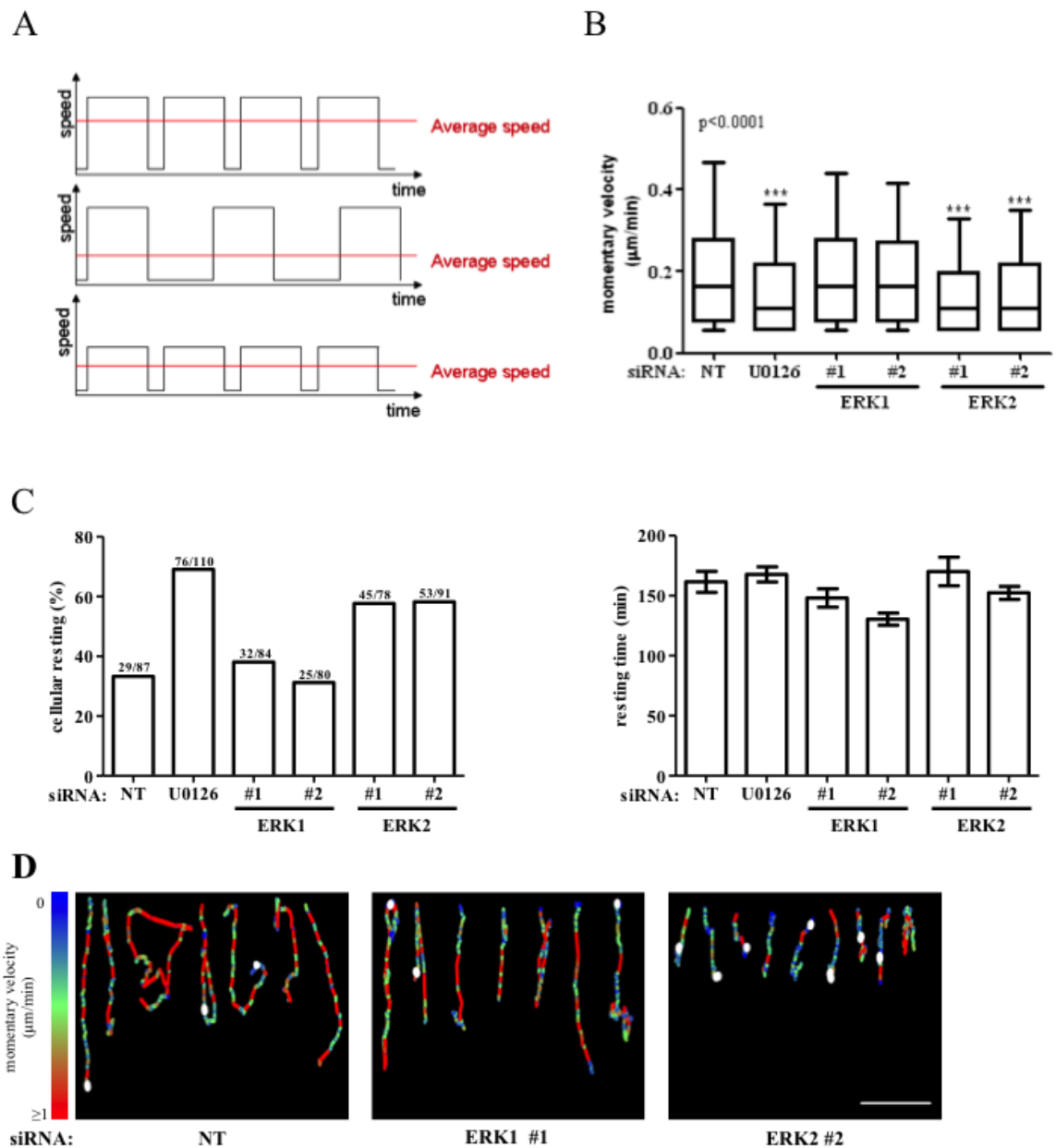


Figure 3-9 Knockdown of ERK2 decreases the momentary velocity and increases cellular resting

A2780-Rab25 cells were transfected with non-targeting siRNAs (NT), or those targeting ERK1 or ERK2 and plated onto cell-derived matrix. Images were captured every 10 min over a 16 hrs period. Cell movement was followed using cell-tracking software.

A. Schematic illustration on how the overall migration velocity can be affected by cellular resting and momentary velocity.

B. Momentary migration velocities were calculated for each timeframe of the time-lapse experiment giving rise to over 7,000 values for each condition. Values are represented as box and whisker plots (whiskers: 10-90 percentile) and represent three independent experiments. Statistical significance of differences was determined by Mann-Whitney U test analysis.

C. Percentage of resting cells is displayed with absolute numbers for each condition above the column. The resting time was extracted from the trackplots and represents means \pm SEM of three independent experiments.

D. Representative migration trackplots are displayed. The migration speed is denoted by a colour code, the scale of which is indicated on the left side of the panels. The points at which cells moved less than 2 μ m in 90 min (cellular resting) are indicated by white dots. Scale bar 100 μ m.

3.2.6 ERK2 promotes invasion in the breast cancer cell line MDA-MB-231

To assess whether the results obtained with A2780-Rab25 cells were more generally applicable, we decided to repeat the invasion and migration assays in a second cell line and chose the well-characterised mammary adenocarcinoma cells, MDA-MB-231, which were derived from a pleural effusion.

Having confirmed an efficient and prolonged knockdown of either ERK1 or ERK2 with two independent oligos in MDA-MB-231 cells (Figure 3-10 A), we then performed inverted invasion assays to test the role of these homologous kinases in invasive cell migration. As a negative control, we inhibited ERK activation by treating NT siRNA-transfected cells with U0126. This drug prevents MEK activation and blocks ERK signalling within 30 minutes of application. Indeed, the Western blot in Figure 3-10 B shows a strong inhibition of ERK signalling even after 48 hours of U0126 treatment and therefore suggests an efficient impediment in ERK activation during the assay. We analysed the relative contribution of ERK1 and ERK2 during invasive cell migration using inverted invasion assays. ERK1 knockdown with either oligo had no significant effect on invasive migration into fibronectin-containing Matrigel, whereas invasion was clearly reduced by approximately 50% when ERK2 was silenced (Figure 3-10 C/D). Moreover, in the presence of U0126 invasive migration into the Matrigel plug was significantly impaired ($p < 0.0001$) when compared to control. Thus, like A2780-Rab25, the invasive phenotype of MDA-MB-231 cells requires active ERK2, but not ERK1, signalling.

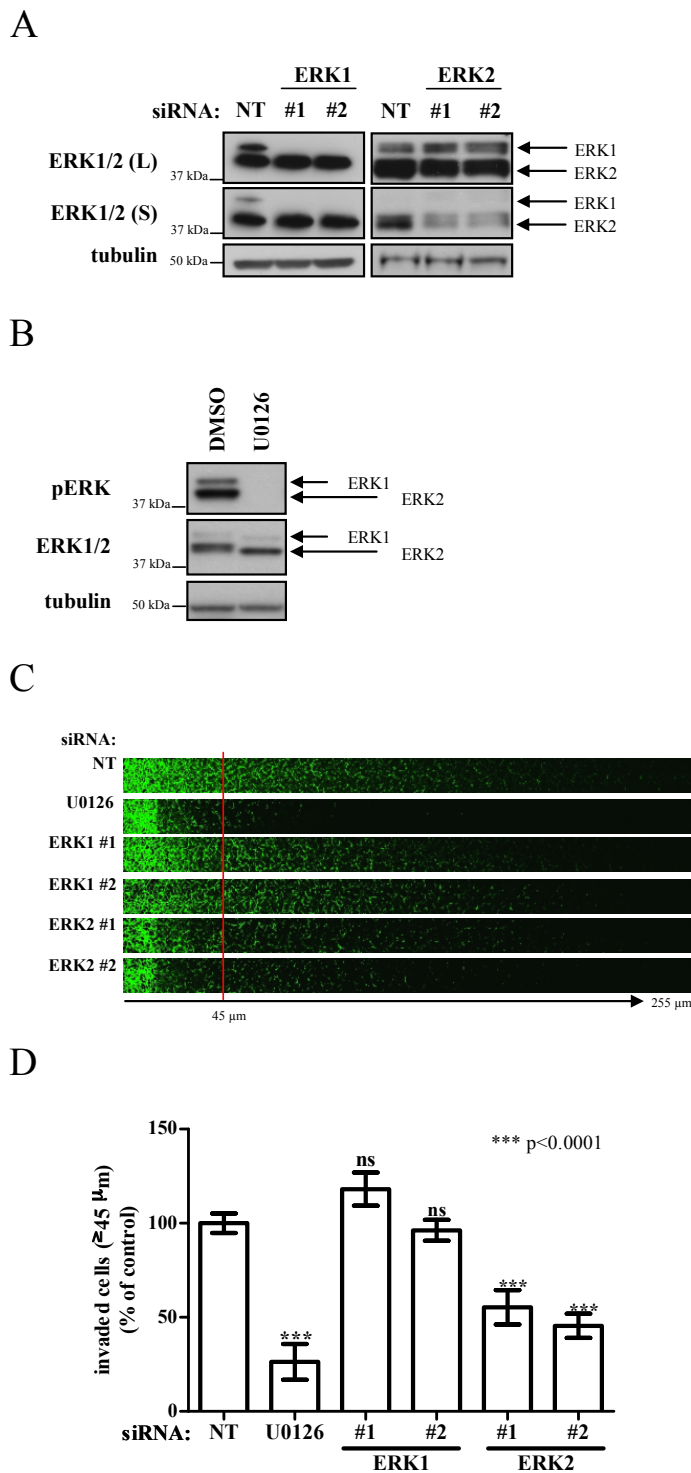


Figure 3-10 ERK2 opposes invasion in MDA-MB-231 cells

A. MDA-MB-231 cells were transfected with non-targeting siRNAs (NT), or those targeting ERK1 or ERK2. The effectiveness of the ERK knockdown was assessed by Western blot 48 hrs after transfection.

B. ERK inhibition by U0126 (10 μ M) was assessed by Western blotting 48 hrs after treatment.

C. MDA-MB-231 cells were transfected with non-targeting siRNAs (NT), or those targeting ERK1 or ERK2 and plated onto plugs of Matrigel supplemented with fibronectin. The MEK inhibitor, U0126 (10 μ M) was included as indicated. 36 hrs following this, invading cells were visualized by Calcein-AM staining. Serial optical sections were captured every 15 μ m and are presented as a sequence in which the depth increases from left to right.

D. Invasive migration was quantified by measuring the fluorescence intensity of cells penetrating the Matrigel plug to depths of $\geq 45 \mu$ m and expressed relative to cells transfected with non-targeting (NT) siRNA. Values are means \pm standard error of the mean (SEM) of 18 replicates from three independent experiments. Statistical significance of differences was determined by Mann-Whitney *U* test analysis.

3.2.7 Transient ERK silencing in MDA-MB-231 cells has no effect on apoptosis or proliferation

As impaired cell viability may adversely affect cellular invasion and migration, we investigated, whether ERK knockdown influenced apoptosis and cellular growth in MDA-MB-231 cells. To this end we transiently transfected MDA-MB-231 cells with NT siRNA or oligos targeting ERK1 and ERK2. As a positive control, we induced the extrinsic apoptotic pathway through treatment with the Fas-ligand (50 nM) and 5 µg/ml cycloheximide for 24 hours. Similar to A2780-Rab25 cells, induction of the cell death pathway induced cell rounding, detachment and fragmentation, which was visible with the help of a phase-contrast light microscope. When we assessed PARP-1 cleavage by Western blotting, we detected an intense band of the 89 kDa fragment in Fas-induced cells, whereas full-length PARP-1 was hardly visible. In contrast, MDA-MB-231 cells transfected with NT siRNA or oligos targeting ERK1 and ERK2, predominantly exhibit the uncleaved PARP-1 protein with a very faint band for the 89 kDa fragment (Figure 3-11 A). Although the 89 kDa fragment band is more intense in ERK2 knockdown cells when compared to the NT siRNA control, we conclude that cell viability is largely unaffected and therefore does not account for the differences seen in the inverted invasion assays.

Next, we examined how ERK knockdown affected cellular growth in MDA-MB-231 cells. To this end, we transfected cells with NT siRNA, or those targeting ERK1, or ERK2 and seeded 40,000 cells into a 6-well dish one day after transfection. As a negative control, NT siRNA-transfected cells were treated with U0126. As expected, we observed a proliferative inhibition two days after U0126 treatment (Figure 3-11 B). In contrast, transient knockdown of either ERK1 or ERK2 did not affect cellular growth (Figure 3-11 B), even though an efficient knockdown was achieved during the course of the experiment as was determined by Western blotting (Figure 3-11 C). It is worth pointing out, that ERK1 activation increased in the absence of ERK2 and resulted in a compensatory up-regulation of pERK1. Thus, the total amount of active ERK hardly changes, when the predominant kinase ERK2 is silenced.

To conclude, our 3D migration experiments are not impaired due to changes in cellular viability, indicating that true migratory defects exist when ERK2 is silenced.

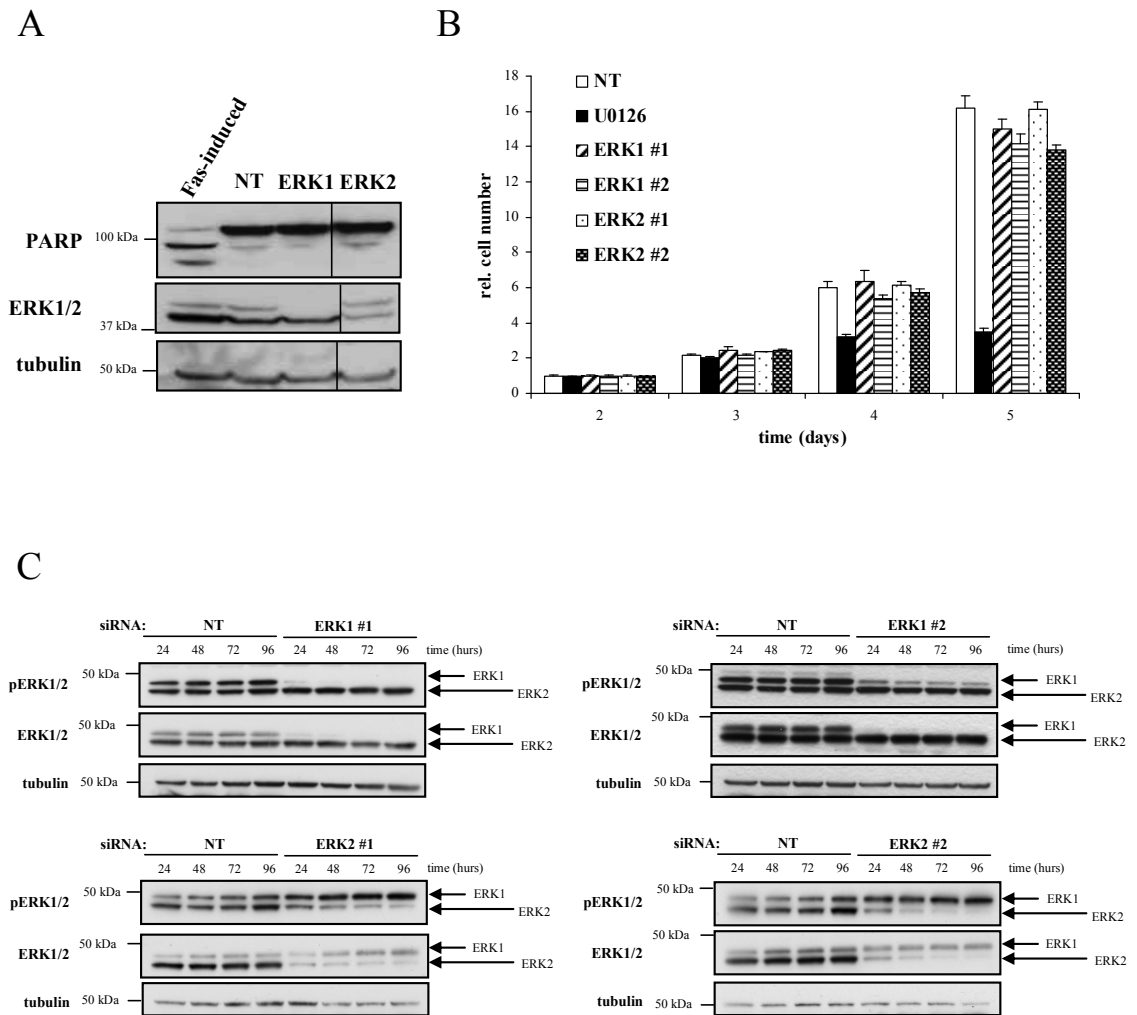


Figure 3-11 siRNA of ERK1 or ERK2 does not induce apoptosis or inhibit proliferation

MDA-MB-231 cells were transfected with non-targeting siRNAs (NT), or those targeting ERK1 or ERK2. A. Apoptosis was induced in control transfected cells by Fas-ligand (50nM) and cycloheximide (5 μ g/ml) treatment. PARP-cleavage was determined 24 hours after induction by Western blot.

B. The proliferation assay was set up 24 hrs after transfection by seeding 40,000 cells into a 6-well dish. The following 4 days, cells were counted using a Casy counter. Relative cell number was plotted against time. Values are means \pm standard error of the mean (SEM) of 9 replicates from three independent experiments.

C. The effectiveness of the ERK knockdown was assessed over the course of 4 days by Western blot.

3.2.8 Migration of MDA-MB-231 cells on plastic surfaces is impaired following knockdown of ERK2

In A2780-Rab25 cells we demonstrated that silencing of ERK2 impairs invasion into Matrigel plugs and migration on cell-derived matrix. This phenomenon, however, was not mirrored in 2D wound healing assays, where both ERK isoforms contributed to wound closure. Having observed this discrepancy between 2D and 3D migration in A2780-Rab25 cells, we set out to investigate, how knockdown of ERK1 and ERK2 affects migration on 2D surfaces in MDA-MB-231 cells. To test this, we transiently knocked down either ERK1 or ERK2 with two independent siRNA oligos for each isoform and plated cells, so that they were confluent 48 hours post transfection. As a negative control, we opposed ERK signalling by blocking MEK activation with U0126 (10 μ M). After introducing a wound by scratching the plastic dish with a 200 μ l pipette tip, wound closure was monitored at 10 minute intervals using a time-lapse microscope. We found that U0126 treatment and knockdown of ERK2 delayed wound closure. Using the manual tracking plugin in ImageJ, we followed individual cells and extracted the migration velocity, persistence and forward migration index (FMI) from the trackplots. Analysis of U0126-treated cells showed a significant decrease in the migration speed when compared to NT siRNA-transfected cells ($p < 0.0001$) (Figure 3-12 B), while persistence and the FMI were unaffected (Figure 3-12 C/D). Likewise, knockdown of ERK2 with two independent oligos significantly diminished the migration velocity ($p < 0.0001$), while persistence and FMI were not altered. In contrast, all of these indices of cell migration were unaffected, when ERK1 was silenced.

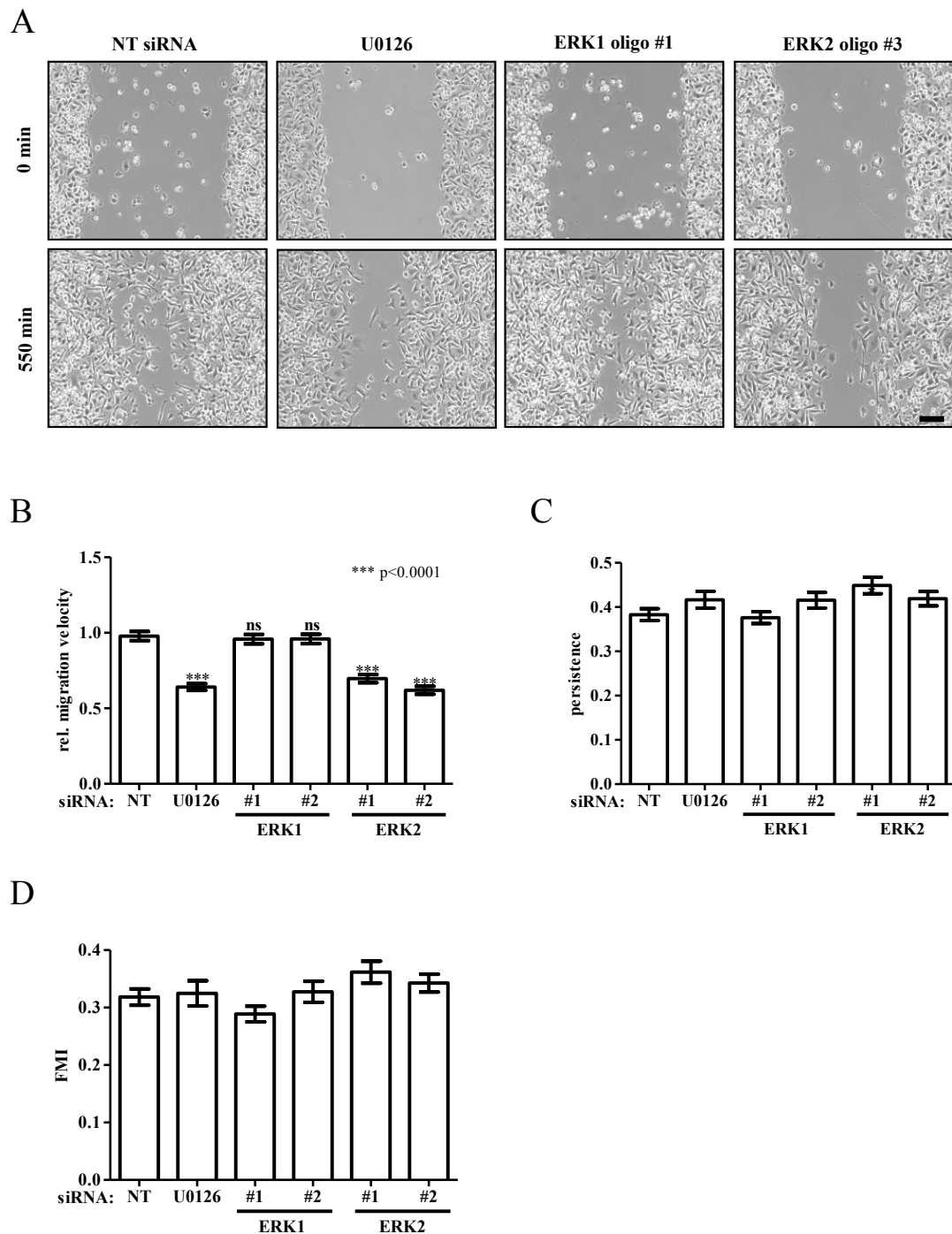


Figure 3-12 ERK2 silencing inhibits migration of MDA-MB-231 cells on plastic

A. MDA-MB-231 cells were transfected with non-targeting siRNAs (NT), or single oligos targeting ERK1 or ERK2. Subsequently, cells were seeded into a 6-well dish, so that they were confluent 48 hrs post transfection. After scratching, wound closure was monitored and representative time frames are shown. Scale bar, 100 μ m.

B-D. The movement of individual cells was followed using ImageJ cell tracking software. The overall migration velocity (C), persistence (D) and forward migration index (FMI) (E) were extracted from the trackplots. Values are means \pm SEM of >75 trackplots from three independent experiments. Statistical significance of differences was determined by Mann-Whitney *U* test analysis.

3.2.9 Silencing of ERK2 impairs migration on CDM in MDA-MB-231 cells

We set out to investigate the respective roles of ERK1 and ERK2 in MDA-MB-231 cell migration, when plated onto CDM. To do this, we transiently knocked down either ERK1 or ERK2 with two independent oligos for each isoform and seeded 100,000 cells onto CDM-coated 6-well dishes, where cell motility was monitored in five-minute intervals using a time-lapse microscope. In general, it is worth mentioning that MDA-MB-231 cells are smaller than A2780-Rab25 cells and adopt a spindle-like shape with small pseudopods, while migrating on CDM.

When ERK signalling was impaired by means of U0126 treatment or knockdown of ERK, we observed no morphological changes when compared to control-transfected cells (Figure 3-13 A). However, the overall migration velocity was significantly decreased, when MEK activation was inhibited or ERK2 was silenced with either oligo #1 or #2 ($p < 0.0001$). On the other hand, silencing of ERK1 had no effect on the overall migratory speed (Figure 3-13 B). Moreover, the persistence of migration was not significantly affected by knockdown of either ERK or by addition of U0126 (Figure 3-13 C).

During our cell tracking analysis, it was apparent that MDA-MB-231 cells silenced for ERK2, like A2780-Rab25, had a tendency to remain stationary for extended periods of time. Thus, we quantified the momentary velocity and cellular resting, as defined for A2780-Rab25 cells, and found a reduced momentary velocity and increased cellular resting when cells were treated with U0126 or silenced for ERK2. In contrast, ERK1 knockdown cells exhibited similar momentary velocities and resting incidences when compared to control (Figure 3-14 A-C). Because only three resting incidences occurred in control-transfected cells, we were unable to carry out a meaningful statistical comparison of resting times between our experimental conditions. Thus, the right panel of Figure 3-14 B may only be interpreted as a range of resting times, from which no conclusions about differences in the stationary periods can be deduced.

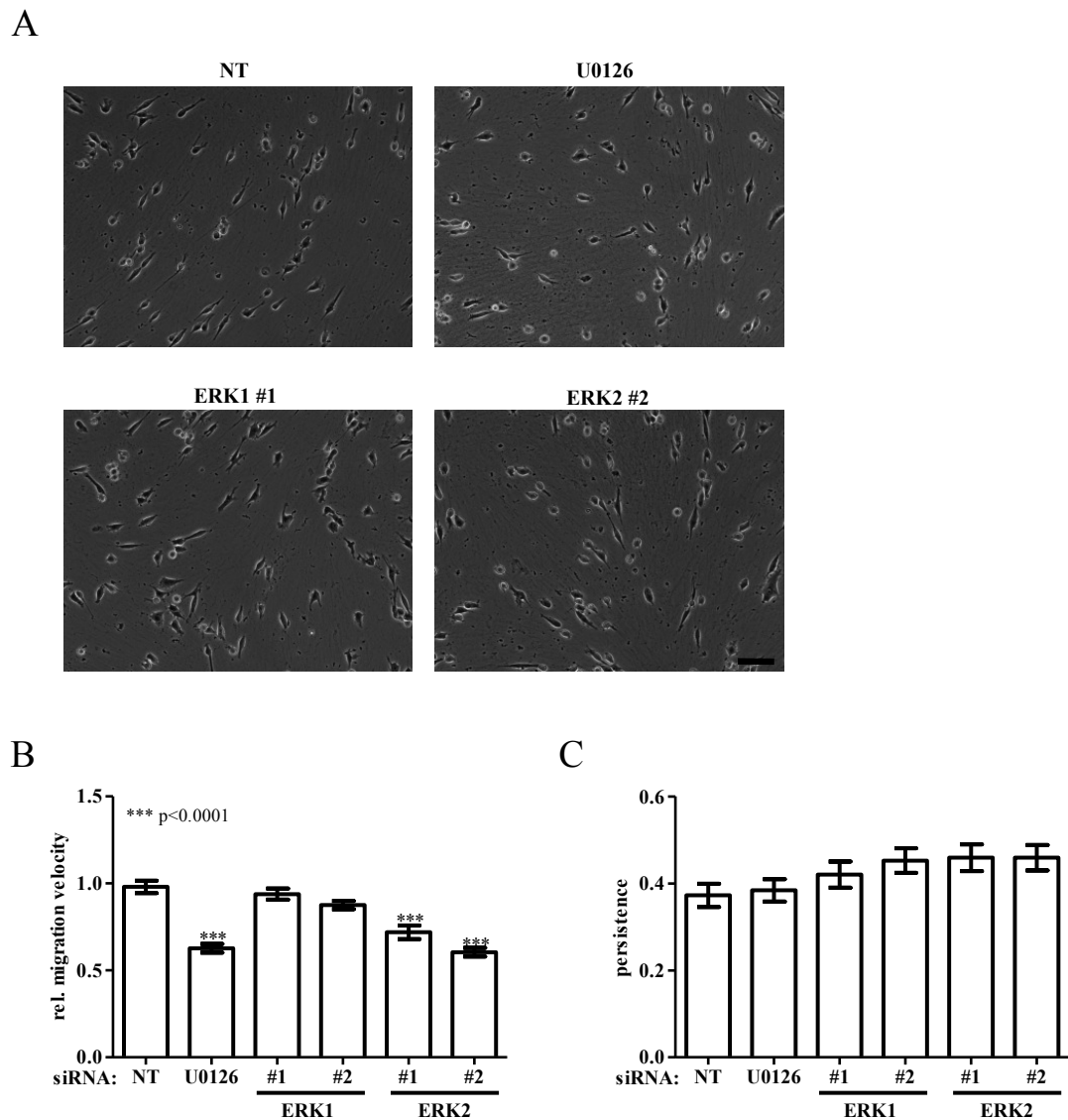


Figure 3-13 siRNA of ERK2 reduces migration of MDA-MB-231 cells on CDM

A. MDA-MB-231 cells were transfected with non-targeting siRNAs (NT), or those targeting ERK1 or ERK2 and plated onto cell-derived matrix. Images were captured every 5 minutes over a 16 hrs period using a Nikon time-lapse microscope. Still images from a representative movie are displayed. Scale bar, 100 μ m. B-C. The movement of individual cells was followed using the ImageJ cell tracking software. The overall migration velocity (B) and persistence (C) were extracted from the trackplots. Values are means \pm SEM of >75 trackplots from three independent experiments. Statistical significance of differences was determined by Mann-Whitney *U* test analysis.

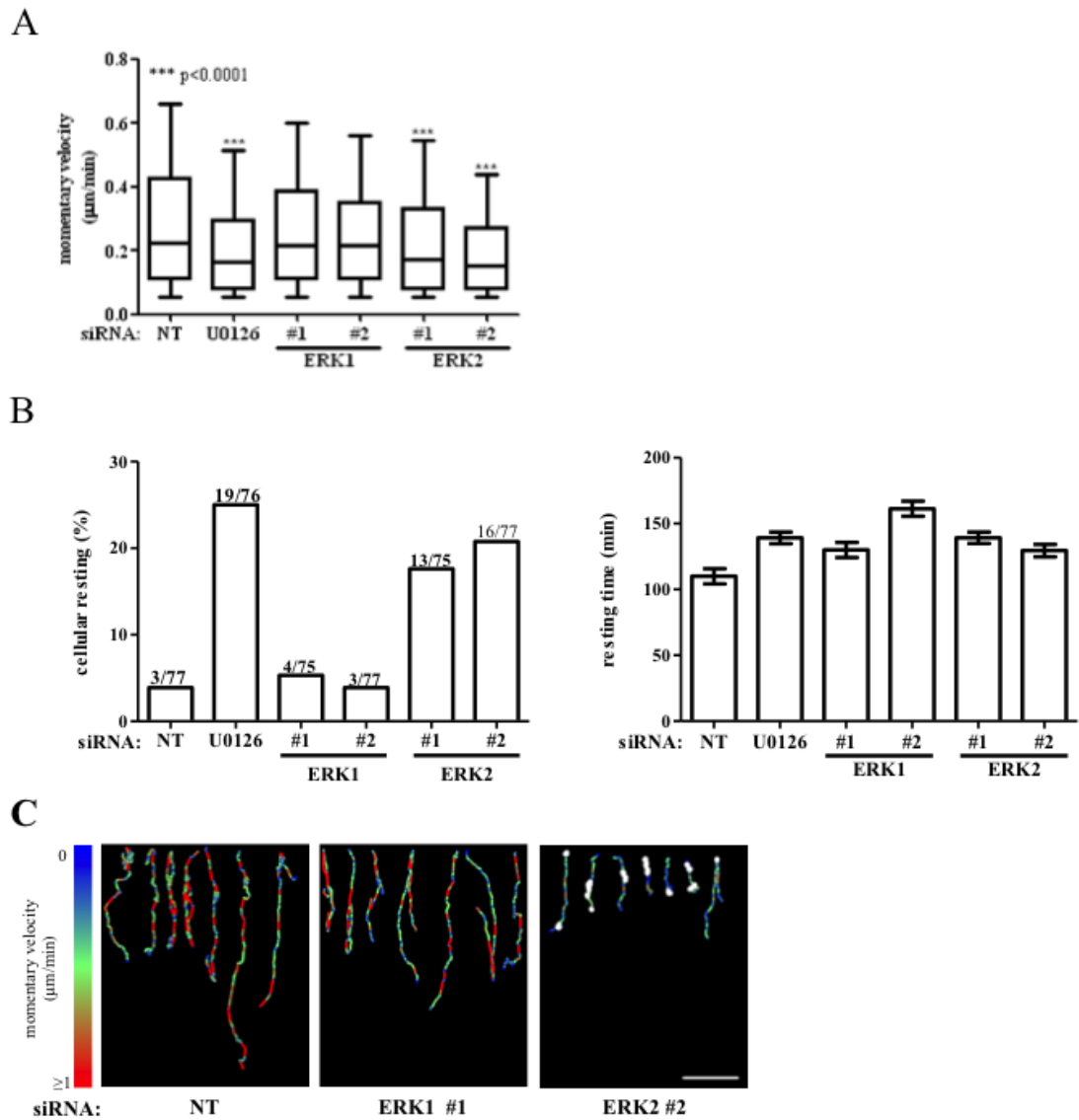
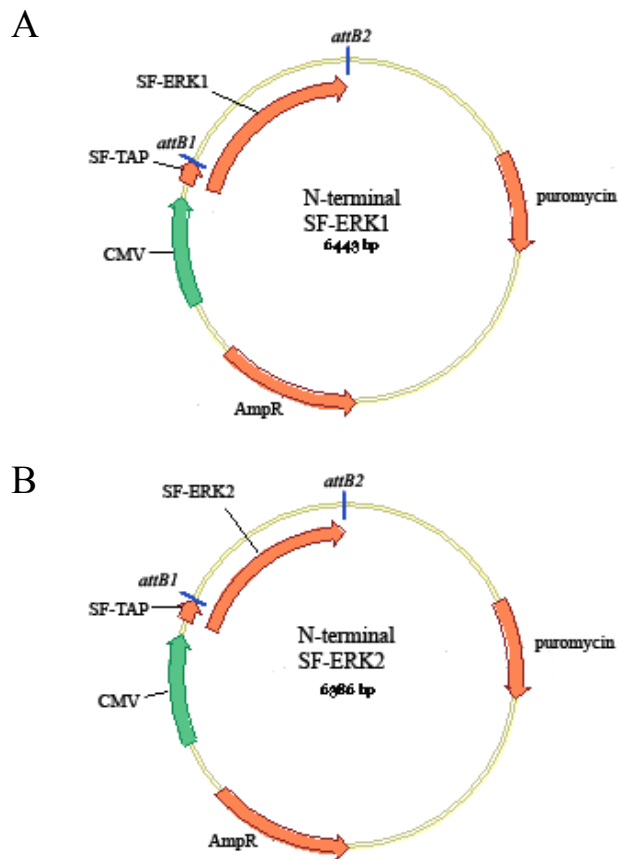


Figure 3-14 Knockdown of ERK2 decreases the momentary velocity and increases cellular resting
 MDA-MB-231 cells were transfected with non-targeting siRNAs (NT), or those targeting ERK1 or ERK2 and plated onto cell-derived matrix. Images were captured every 10 min over a 16 hrs period. Cell movement was followed using cell-tracking software.
 A. Momentary migration velocities were calculated for each timeframe of the time-lapse experiment giving rise to over 7,000 values for each condition. Values are represented as box and whisker plots (whiskers: 10-90 percentile) and represent three independent experiments. Statistical significance of differences was determined by Mann-Whitney U test analysis.
 B. Percentage of resting cells is displayed with absolute numbers for each condition above the column. The resting time was extracted from the trackplots and represents means \pm SEM of three independent experiments.
 C. Representative migration trackplots are displayed. The migration speed is denoted by a colour code, the scale of which is indicated on the left side of the panels. The points at which cells moved less than $2 \mu\text{m}$ in 90 min (cellular resting) are indicated by white dots. Scale bar $100 \mu\text{m}$.

3.2.10 Expression of recombinant ERK2 (but not ERK1) restores the migratory characteristics of MDA-MB-231 cells after ERK2 knockdown

Although our data obtained in A2780-Rab25 and MDA-MB-231 cells strongly suggests an ERK2-specific function in invasive cell migration, our experimental design does not consider the fact that ERK2 is much more abundant than ERK1 in these cells. Therefore, observations that knockdown of ERK2 affects invasion (whereas siRNA of ERK1 does not) do not necessarily reflect functional differences between the two kinases, but may be attributable to differences in their expression level as demonstrated by Lefloch and colleagues [357]. To address this, we cloned expression plasmids of both ERK1 and ERK2 and tagged the kinases N-terminally with a Streptavidin-Flag (SF) tag (Figure 3-15) [390]. Using these constructs, we were able to express recombinant ERK1 or siRNA-resistant ERK2 to equal levels after knocking down ERK2 with oligo #2. The ectopically-expressed ERK1 and ERK2 isoforms were phosphorylated at the Thr-Glu-Tyr motif to the same extent as one another, indicating that both of these recombinant ERKs were equally activated by MEK in MDA-MB-231 cells (Figure 3-16 A). Moreover, the pool of activated ERK was comparable between all conditions despite opposite ratios of activated ERK1 and ERK2, thus allowing us to test whether there is a true functional difference between the two isoforms in cell migration.

Next, we monitored invasive cell migration by means of inverted invasion assays and studied cell movement on CDM using the siRNA-rescue paradigm. We found that ectopic expression of ERK1 did not reverse the inhibitory effect of ERK2 knockdown on invasion, whereas siRNA-resistant ERK2 expression completely rescued the invasive phenotype of MDA-MB-231 cells (Figure 3-16 B/C). Moreover, when cell migration on CDM was analysed, re-expression of siRNA-resistant ERK2 increased the momentary velocity and reduced the tendency of cells to pause (cellular resting) relative to that of control cells, whereas re-expression of ERK1 did not rescue the migratory defects of ERK2 knockdown cells (Figure 3-17).



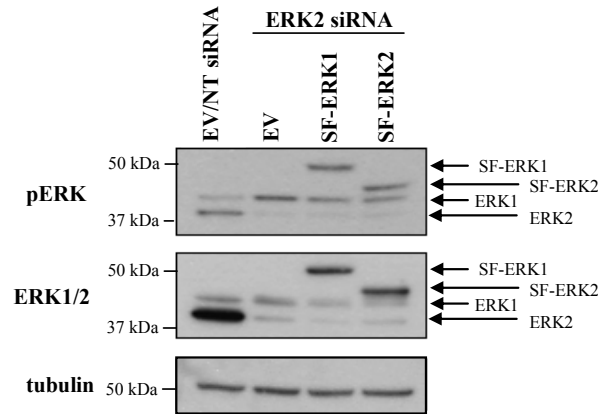
C

SF-TAP (sequence): mdykdddddksaaswshpqfekgggsgggsgggswshpqfegars

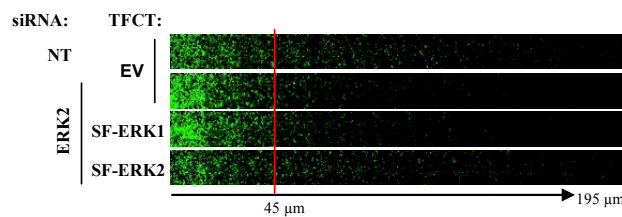
Figure 3-15 ERK expression vectors

ERK1 (NM_002746) and ERK2 (NM_002745) genes were amplified from a cDNA library using primers with an *attB1* and *attB2* site and cloned into the N-terminal SF-TAP destination vector [390] via homologous recombination, giving rise to N-terminal SF-ERK1 (A) and N-terminal SF-ERK2 (B). Amino acid sequence of the SF-TAP tag is displayed. Residues marking the streptavidin (S) tag are coloured purple, while amino acids constituting the FLAG tag are coloured blue.

A



B



C

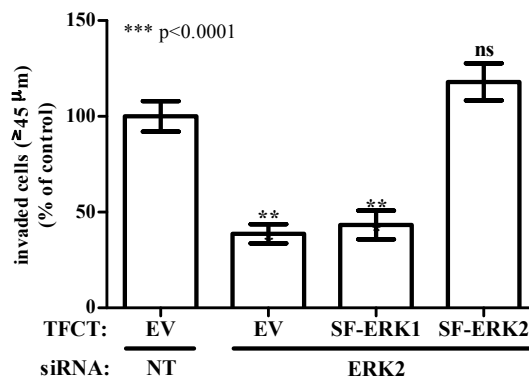


Figure 3-16 Ectopic expression of ERK2 but not ERK1 restores invasion of ERK2 knockdown cells

A. MDA-MB-231 cells were transfected with non-targeting siRNAs (NT), or siRNA targeting ERK2 in combination with expression plasmids for SF-ERK1, SF-ERK2 or an empty vector control (EV). Cells were harvested two days after transfection and ERK expression levels were determined by western blotting.

B. MDA-MB-231 cells were transfected with non-targeting siRNAs (NT), or siRNA targeting ERK2 in combination with expression plasmids for SF-ERK1, SF-ERK2 or an empty vector control (EV). Cells were plated onto plugs of fibronectin-supplemented Matrigel. 36 hrs following this, invading cells were visualized by Calcein-AM staining. Serial optical sections were captured every 15 μm and are presented as a sequence in which the depth increases from left to right.

C. Invasive migration was quantified by measuring the fluorescence intensity of cells penetrating the Matrigel plug to depths of ≥ 45 μm and expressed relative to cells transfected with non-targeting (NT) siRNA. Values are means ± standard error of the mean (SEM) of 18 replicates from three independent experiments. Statistical significance of differences was determined by Mann-Whitney *U* test analysis.

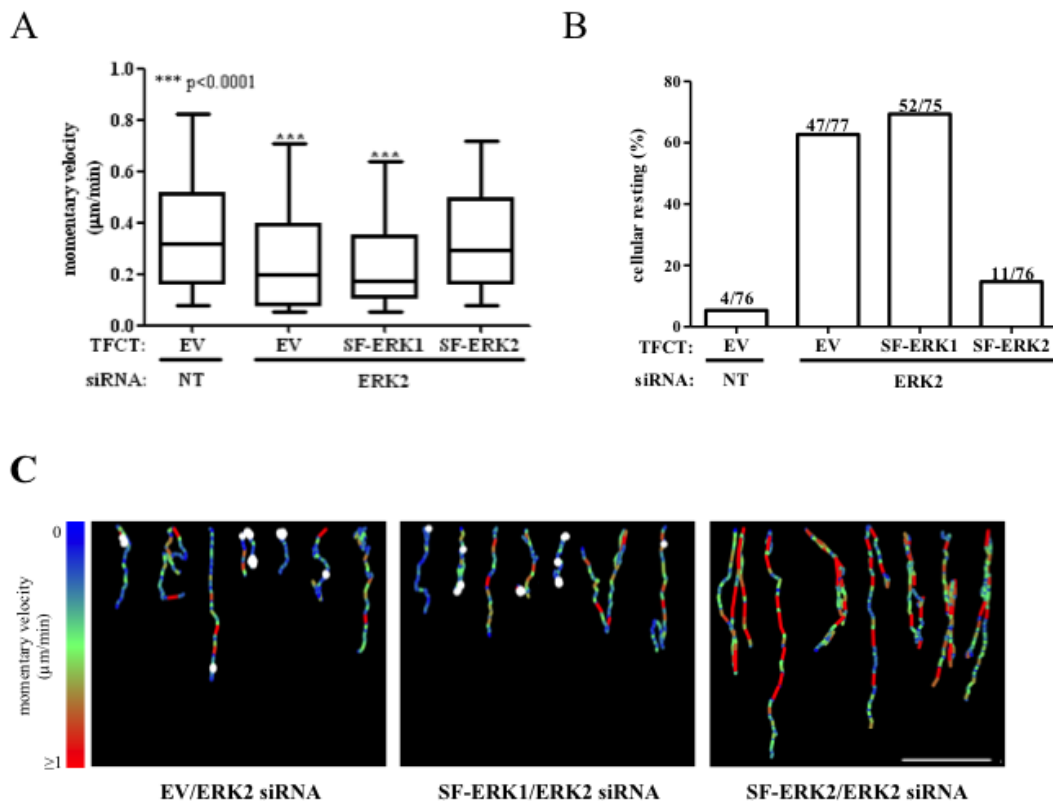


Figure 3-17 Ectopic expression of ERK2 but not ERK1 restores invasion of ERK2 knockdown cells

MDA-MB-231 cells were transfected with non-targeting siRNAs (NT), or siRNA targeting ERK2 in combination with expression plasmids for SF-ERK1, SF-ERK2 or an empty vector control (EV). Cells were plated onto cell-derived matrix. Images were captured every 10 min over a 16 hrs period. Cell movement was followed using cell-tracking software.

A. Momentary migration velocities were calculated for each timeframe of the time-lapse experiment giving rise to over 7,000 values for each condition. Values are represented as box and whisker plots (whiskers: 10-90 percentile) and represent three independent experiments. Statistical significance of differences was determined by Mann-Whitney *U* test analysis.

B. Percentage of resting cells is displayed with absolute numbers for each condition above the column. The resting time was extracted from the trackplots and represents means \pm SEM of three independent experiments.

C. Representative migration trackplots are displayed. The migration speed is denoted by a colour code, the scale of which is indicated on the left side of the panels. The points at which cells moved less than 2 μ m in 90 min (cellular resting) are indicated by white dots. Scale bar 100 μ m.

3.3 Discussion

3.3.1 Summary

Although some research scientists believe that ERK1 and ERK2 are functionally redundant and interchangeable, our data supports the view that these two kinases have different roles in cell migration. Indeed, ERK2 but not ERK1 knockdown significantly inhibits invasive cell migration of two independent cancer cell lines. Moreover, a detailed quantitative analysis of cell movement on 3D matrices indicates that ERK2 (but not ERK1) knockdown impairs cellular motility by decreasing the migration velocity as well as increasing the time that cells remain stationary. Furthermore, we show that all these migratory defects can be rescued by re-expression of ERK2 but not ERK1. Taken together, our data provides evidence that ERK2 is particularly important in the invasiveness of cancer cells and that true functional disparities between ERK1 and ERK2 exist with regard to cell migration.

3.3.2 Discrepancy between migration in 2D and 3D in A2780-Rab25 cells

In 2001, it was shown that inhibition of ERK signalling with U0126 clearly compromised cell motility of A375 melanoma cells in invasion assays [391]. Moreover, Bessard and colleagues have carried out wound healing assays with hepatocarcinoma cells and showed that knockdown of ERK2 (but not ERK1) compromised motility in 2D [379]. In our studies, we have shown that A2780-Rab25 cells rely on both ERK1 and ERK2 signalling during scratch wound assays, while in MDA-MB-231 cells silencing of ERK2 but not ERK1 decreased wound closure. In 3D experiments, however, ERK2 was the main driver of cell migration in both cell lines. What may account for the differences in 2D and 3D migration? Firstly, wound scratch assays examine the ability of a cell culture to recolonize the wound, which is dependent on both migration and cellular growth. Although this method is well adapted for studying tissue injury, it has limitations when assessing tumour cell motility. Firstly, tumour cells are asked to migrate across a rigid and planar substrate, which hardly resembles an *in vivo* situation, where cancer cells migrate into the extracellular matrix [387]. Secondly, scratching the cell monolayer induces morphological changes and physically stresses the cells at the edge of the wound, which changes intracellular signalling events [392, 393]. Thirdly, cells cultured in 2D exhibit completely different gene expression signatures, portray differences in proliferation, morphology,

and migration, when compared to 3D [38, 394, 395]. Moreover, cell movement in 2D is characterized by stress fibre formation and membrane ruffling at the cell front, which have been linked to p38, JNK as well as ERK signalling [315, 396, 397]. In 3D, cells migrate by extending a pseudopod at the cellular front, which attaches to the extracellular matrix while the cell's rear detaches and retracts. We believe that signalling differences are the cause of these distinct modes of motility and therefore believe that it is plausible that ERK's role in 2D migration might be different from 3D and that these differences might be cell-type specific.

3.3.3 Roles of ERK in tumour cell migration

Our data clearly shows that ERK2 signalling orchestrates the cell migration machinery as the momentary velocity of migrating cells was compromised in ERK2 knockdown cells. Moreover, we observed an increase in cellular resting, where A2780-Rab25 cells, in particular, developed two opposing pseudopods and struggled to form a single dominant pseudopod required for migration. Persistent cellular movement during chemotactic experiments, such as inverted invasion assays, requires the establishment of a front to tail polarity towards the chemotactic gradient, which is achieved by the interplay of three central signalling events. Firstly, developing pseudopods display high Cdc42 and Rac1 activity, which are linked to cellular polarisation and F-actin formation respectively. Moreover, increased phosphoinositide 3-kinase (PI3K) activity at the cellular front elevates phosphatidylinositol-3,4,5-phosphate (PIP₃) levels, which allows the recruitment of PH-domain containing signalling proteins and ensures further pseudopod extension. In order to allow forward migration the formation of lateral or opposing pseudopods at the cellular rear must be suppressed [398]. This is achieved through the establishment of a contractile myosin cortex, where active RhoA binds to its downstream effector protein, Rho-associated kinase (ROCK), which generates a contractile force by phosphorylating and inactivating the myosin binding subunit of myosin phosphate (MYPT1), and phosphorylating myosin light chain (MLC) directly [399]. As our data clearly demonstrates a migratory defect in ERK2 knockdown cells, we believe that ERK2 may partly regulate some of the aforementioned signalling events. Indeed, a link between ERK signalling and the small GTPases central to cell migration has been well-established, albeit the exact mechanism of regulation is still unknown. It is thought that ERK signalling may control Rac1 and Cdc42 activity by regulating GEF localisation and/or activity. Thus, chemotactic

extracellular stimuli may activate ERK signalling, which in turn induce Rac1 and Cdc42 activation and thereby promote pseudopod formation towards the chemotactic gradient [190, 398]. However, Rac1 and Cdc42 have also been shown to induce ERK activation via PAK [400-402]. Thus, rather than ERK activating Rac1 and Cdc42 at the leading edge, these small GTPases might be responsible for activating ERK signalling in the forming pseudopod, where the kinase regulates extracellular matrix (ECM) adhesions [216, 276, 403], which are crucial in stabilising the developing pseudopod. Moreover, ERK activity induces myosin light chain phosphorylation by activating MLCK (myosin light chain kinase) [277] and thereby controls the generation of a contractile force required to translocate the cell body following pseudopodial extension [404]. When comparing the pseudopod length of ERK2 knockdown cells with control, however, we do not observe significant changes (data not shown), which argues that inhibition of ERK2 does not influence pseudopod extension or retraction at the leading edge. Our data rather suggests a defect in the suppression of lateral or opposing pseudopods at the cellular back, when ERK2 is silenced. Thus, ERK2 might be important in regulating RhoA signalling at the cellular rear. Indeed, ERK was shown activate GEF-H1, a RhoA GEF, through direct phosphorylation [405] and might thus provide a means by which ERK promotes cellular retraction. Moreover, ERK is involved in focal adhesion disassembly [276], which is required for effective forward migration. Defects in adhesion turnover or RhoA activation brought about by ERK2 silencing may allow lateral pseudopod formation, prevent the acquisition of a dominant pseudopod and may ultimately decrease cellular motility. Moreover, failure or delay in Golgi and centrosome orientation may slow down cell migration or induce cellular resting as seen in our experiments. Notably, ERK has been shown to regulate Golgi and centrosome orientation towards the leading edge of migrating cells [406]. Thus, an ERK2-specific function in this process is also possible.

3.3.4 Isoform-specific functions for ERK1 and ERK2

In recent years, much evidence supporting ERK isoform-specific functions has accumulated (see 3.1.2 and 3.1.3). First and foremost, striking discrepancies between the ERK1^{-/-} and ERK2^{-/-} phenotypes in mice argue for distinct roles for these kinases in embryogenesis [360-364, 367]. Moreover, ERK2 may play specific roles in learning and memory as well as differentiation [365, 370]. However, this data was challenged by

Lefloch *et al.* in 2008, who proposed *erk* gene dosage as the reason for the differences in the ERK^{-/-} phenotypes [357]. They showed that ERK1 and ERK2 kinase activities were indistinguishable *in vitro* and suggested that both isoforms contribute towards signalling outcomes according to their expression ratio [357]. However, experimental limitations did not allow Lefloch and colleagues to show that an increase in ERK1 expression in the absence of ERK2 could indeed rescue the proliferation defects observed [357]. However, subsequent work by Samuels and colleagues showed that proliferative defects in the developing cortex of mice with conditional ERK2 knockout could be rescued by ERK1 overactivation, thus showing that ERK's role in regulating proliferation is indeed dependent on *erk* gene dosage [366]. Here, we show that ERK2 is crucial for invasive migration, as knockdown of ERK2 severely compromised invasion into Matrigel plugs and migration on CDM. The fact that we observed a compensatory increase in pERK1 upon ERK2 knockdown and vice versa in either A2780-Rab25 or MDA-MB-231 cells contradict assumptions that total ERK signalling, regardless of the isoform, regulates cell invasion. Moreover, by developing a system, in which we can knockdown ERK2 and then ectopically express either ERK1 or ERK2 to similar levels, we have shown that ERK2 is the main driver of cell migration and invasion in 3D microenvironments in a way that is not influenced by gene dosage.

The role of the ERKs in cell migration has been studied extensively and it is established that these kinases play a key role in tumour progression by regulating cell invasiveness [277, 314, 407-409]. However little is known about the respective contributions of ERK1 and ERK2 to cell migration. Our finding that it is ERK2, and not ERK1, that contributes to cell migration in 3D microenvironments is certainly in agreement with observations *in vivo*, where ERK2^{+/-} mice show a delay in wound healing after partial-thickness burn in comparison to ERK2^{+/+} mice [410]. Satoh and colleagues hypothesized that differences observed in wound healing were due to defects in proliferation as well as migration. Studies in Zebrafish further support this view as ERK2 but not ERK1 morphants showed defects in cytoskeletal reorganisation processes, which led to anterior-to-posterior migration retardations [411]. More recently, by using a retroviral system to express ERK 1 and -2 to similar levels, a study has demonstrated a specific role for ERK2 in cell migration in MCF-10A cells, which was due to the participation of this ERK isoform in Ras-induced epithelial-to-mesenchymal transformation (EMT) [412].

The ERK pathway has been a favourable target in anti-cancer drug development since a study of breast cancer carcinomas in 2001 showed a correlation between high pERK levels and low survival from the initiation of therapy [413]. Our data suggests that specific targeting of ERK2 rather than blocking both ERKs might prove to be a more selective anti-invasive strategy. This hypothesis is strongly supported by data from Milde-Langosch and colleagues who showed that high pERK1 expression in tumours correlated with low frequencies of relapses and higher survival. Moreover, patients with weak pERK1 levels showed an increased number of recurrences and deaths of disease. The same trend was seen when high levels of pERK2 were detected in the patients' tumours [414]. Consistent with this, ERK1 has been hypothesized as a negative modulator of ERK signalling in recent years, as ectopic expression of this kinase attenuates colony formation of Ras-transformed cells as well as Ras-dependent tumour growth in nude mice [371]. Hence, the data suggest that a therapy aiming at decreasing pERK2 and increasing pERK1 levels might be most beneficial. Our work with the MDA-MB-231 and A2780-Rab25 cells showed a clear compensatory increase of pERK1 levels after ERK2 knockdown. The compensatory increase in pERK1 levels after ERK2 silencing has been observed in other cell lines, such as NIH 3T3 [371] as well as rat and mouse hepatocytes [372]. Furthermore, a compensation in pERK has also been observed in ERK2^{+/-} mice compared to ERK2^{+/+} [415]. As MEK1 and -2 do not discriminate between the ERKs, we speculate that silencing of ERK2 might not only compromise invasive migration, but also result in a beneficial increase in pERK1 levels. Thus, changing the ratio of ERK1 and ERK2 should result in enhanced activation of the remaining kinase.

Our findings have shown a clear ERK2-dependent role in 3D migration. How can this isoform-specificity be achieved on a cellular level, if both kinases show indistinguishable kinase activities *in vitro*? Marchi *et al.* have shown isoform-specific nuclear shuttling rates caused by differences in the N-terminal amino acid sequence, suggesting that ERK1 and ERK2 may perform different roles within the nucleus [416]. As ERK isoforms are dephosphorylated and therefore inactivated in the nucleus [175], high shuttling rates are required to maintain an active pool of ERK. Therefore, lower ERK1 shuttling rates make ERK2 a better candidate for the activation of nuclear targets [416]. ERK1/2 have been shown to drive transcription of numerous proteins involved in migration, such as MMP-9, MMP-1 and uPA [391, 417, 418]. It is, therefore, possible, that ERK2 is the main driver of transcription of these pro-invasive proteins. However, it is unlikely that ERK2's role in

invasive tumour cell migration can solely be triggered by higher nuclear activity, as ERK signalling has also been linked cytosolic effectors involved in migration, such as vimentin- β , stathmin and myosin light chain kinase (MLCK) [316, 403, 419].

Isoform specificity within the cytoplasm may be achieved via distinct subcellular localisation of the two enzymes. However, there are currently no ERK isoform-specific antibodies, which allow this hypothesis to be tested using immunofluorescence microscopy. Moreover, isoform-specific scaffolds, as well as uncharacterized isoform-specific substrate binding domains, may exist. Indeed, Shin *et al.* demonstrated an ERK2 specificity in Fra1 phosphorylation, which was dependent on ERK2's FXFP motif [412]. Intriguingly, previous work by Lee and colleagues showed that the residues constituting the FXFP-motif are fully conserved between ERK1 and ERK2 [131]. To explain this discrepancy, we speculate that the Tyr261Ala mutation in the FXFP-motif may sterically distort an unknown isoform-specific substrate binding domain in ERK2 and therefore abrogate Fra1 stabilisation.

To conclude, this study is the first to show a pivotal role of ERK2 in invasive tumour cell migration and suggests that ERK1 and -2 do have distinct functions. Our data challenges the belief that both ERK isoforms are interchangeable and redundant, and propose a new level of complexity of the Raf-MEK-ERK pathway.

4 ERK2 regulates expression of CSF2, Rab17 and Liprin- β 2 in 3D microenvironments

4.1 Introduction

4.1.1 Regulation of gene expression through ERK1/2

Growth factors and mitogens induce synthesis of new proteins required for cellular responses. Changes in protein expression can be detected within minutes following growth factor addition, and genes encoding these proteins are known as immediate early genes (IEGs). This rapid burst in mRNA synthesis requires a switch-like activation of transcription factors in the nucleus, which can be achieved through post-translational modifications. Indeed, activation of the ERK-MAPK pathway promotes translocation of ERK1/2 to the nucleus, where the kinases phosphorylate transcription factors such as Elk1 and c-Fos to drive expression of IEGs [420]. Phosphorylation can affect transcription factor function in various ways. Whereas phosphorylation of Elk1 enhances DNA binding and may induce the recruitment of transcriptional co-activators, such as p300 or CREB-binding protein (CBP) [323], phosphorylation of c-Fos by ERK itself or its downstream target, RSK, prevents proteasomal degradation and thus stabilises the transcription factor [326]. In contrast, nuclear ERK may also inhibit transcriptional events through direct or indirect phosphorylation. For example, phosphorylation of Ser307 of heat shock factor-1 (HSF1) by ERK1/2 represses its transcriptional activity during growth and development [421]. Furthermore, ERK-mediated phosphorylation of inducible cAMP early repressor (ICER) targets the transcription factor for ubiquitin-mediated degradation [422].

In addition to direct or indirect phosphorylation of transcription factors, the ERK-MAPK pathway has been implicated in altering the chromatin structure of actively transcribed genes [423-425]. Nucleosomal proteins, such as histone H3 and high mobility group protein (HMG)-14, are phosphorylated by ERK effectors (i.e. MSK1, MSK2, and RSK2) on Ser10 and Ser6, respectively [426-428]. Phosphorylated histone H3 and HMG-14 are primarily found at actively transcribed genes, e.g. IEGs, and are thought to provide a docking domain for the recruitment of histone acetyltransferases, such as p300 and CBP [427]. Indeed, phosphorylation and acetylation can coexist on the same histone H3 tail, as was recently shown for the *c-fos* gene [429]. Thus, a function of histone H3 and

HMG-14 phosphorylation may be to prime the histone tail for acetylation. However, the precise role of this ERK-mediated modification in regulating gene transcription remains to be elucidated.

The ERK-MAPK pathway has been shown to regulate pre-mRNA processing and alternative splicing [430, 431]. The heterogeneous nuclear ribonucleoprotein (hnRNP)-K is a *bona-fide* ERK target protein and phosphorylation at Ser284 and Ser353 stimulates its nuclear export [431]. In the cytoplasm hnRNP-K's function are diverse. It can inhibit mRNA translation by binding to the differentiation-control element in the 3' untranslated region (UTR) of target mRNAs [431], stabilise mRNA transcripts and thereby increase the expression of certain proteins, such as thymidine phosphorylase [432], or promote splicing of mRNA precursors, such as EGR1 [433]. Thus, ERK signalling indirectly impinges on pre-mRNA processing by regulating hnRNP-K localisation and thus affects gene expression both transcriptionally and post-transcriptionally.

Additionally, ERK signalling has recently been shown to regulate gene expression by altering microRNA (miRNA) biogenesis [434]. MicroRNAs are small ribonucleic acid molecules with an average length of 21 nucleotides. They bind to specific sequences of their target mRNAs and inhibit gene expression by promoting mRNA degradation, sequestration, or translational suppression [435]. In mammals, miRNA biogenesis follows a well-defined maturation process. Firstly, the transcribed precursor molecules called pri-miRNAs fold into a double stranded hairpin-like structure, which is processed into mature miRNA molecules in two consecutive cleavage processes involving RNase III type endonucleases. In the nucleus the pri-miRNA is converted into a 70 nucleotides long pre-miRNA by a complex containing Drosha and DGCR8 (DiGeorge syndrome critical region gene 8). Following export from the nucleus, a further maturation process driven by the miRNA-generating complex, consisting of DICER and phospho-TRBP (TAR RNA-binding protein), yields a mature miRNA, which is subsequently assembled into functionally active ribonucleoprotein complexes [435]. ERK1/2 have been shown to interact with TRBP *in vivo* and phosphorylate this component of the miRNA-generating complex *in vitro*. Moreover, phosphorylation of TRBP enhances the stability of the miRNA-generating complex, resulting in an increase in miRNA biogenesis and miRNA-mediated gene silencing [434].

4.1.2 Nuclear translocation of ERK1/2

The nuclear envelope separates the nucleus from the cytoplasm and ensures selective transport between the two cellular compartments. Although small molecules can passively enter and exit the nucleus, transport of larger entities, such as proteins or RNAs, is tightly controlled by transport channels called nuclear pore complexes (NPCs). A family of proteins called nucleoporins (NUPs) assemble to form these channels, which are also known as nuclear pores [436]. In general, proteins, which are designated for nuclear transport, carry a nuclear localisation signal (NLS), which is recognised and bound by importins. Once importins are loaded with cargo proteins, they interact with the NPC and travel through the transport channels. In the nucleus, the small GTPase RAN binds to the importin-cargo complex and induces a conformational change, which promotes dissociation of the cargo from importins and renders RAN inactive. Subsequently, RAN-GDP and importin are exported to the cytoplasm, where RAN can be activated by GTP loading and importins can bind new cargo proteins [437].

Neither ERK1/2 nor MEK1/2 contain conventional [438] or non-conventional [439] NLSs, which suggests that the kinases must depend on alternative mechanisms driving their nuclear import. It is possible that ERK1/2 interact with proteins containing NLS, and thus, hitch a ride into the nucleus. However, no direct interaction partner comprising a NLS has so far been identified, suggesting that other mechanisms drive ERK translocation into the nucleus. In 1999, ERK1/2 were shown to penetrate the NPC by means of passive diffusion as a monomer or active transport as a dimer [440]. Whether active import really involves ERK dimerization, however, is controversial, as mutants impaired in dimerization were still translocated using an energy-dependent mechanism [441]. Moreover, Casar *et al.* demonstrated that ERKs accumulate in the nucleus as monomers, and that phosphorylation of transcription factors by ERK1/2 does not require protein dimerization [442]. Yet, Lidke *et al.* showed that inhibition of ERK dimerization resulted in delayed nuclear ERK accumulation, suggesting that ERK dimers and monomers are transported across nuclear pores with different kinetics [443]. Intriguingly, Marchi *et al.* demonstrated clear differences in the nuclear shuttling frequencies between ERK1 and ERK2, with ERK1 being imported and exported at a much slower rate than ERK2 [416]. Moreover, domain swapping inverted the shuttling frequencies of ERK1 and ERK2 and attributed the discrepancy in nuclear trafficking to differences in the N-terminal amino

acid sequence. Owing to the fact that ERKs are predominantly inactivated in the nucleus, continuous cytoplasmic-nuclear shuttling ensures a constant level of active ERK. Thus, lower shuttling rates for ERK1 may make the kinase more susceptible for nuclear inactivation and ERK2 the predominant kinase driving gene expression [416].

Yet, how are ERK proteins targeted for nuclear translocation? Three residues on ERK, i.e. Ser²⁴⁶-Pro²⁴⁷-Ser²⁴⁸ (for ERK2), have been shown to be important in regulating nuclear translocation. This motif resides in the kinase insert domain (KID) of ERK and both serine residues undergo phosphorylation following TEY motif activation by MEK1/2 [444]. Synergistic phosphorylation of the Ser-Pro-Ser motif induces binding to importin7, which is believed to escort ERK1/2 through nuclear pores. Moreover, ERK1/2 may promote nuclear entry through energy-independent and energy-dependent mechanisms by phosphorylating NUPs (NUP50, NUP153 and NUP214) directly [445, 446].

Another important regulator of nuclear ERK shuttling is Mxi2, which promotes translocation of ERK1/2 in a stimulus-independent manner by acting as an adapter molecule. Mxi2 interacts with both ERKs and NUPs directly, and thereby promotes nuclear import [231]. More work is required to deduce how ERK1/2 are shuttled into the nucleus and whether ERK-mediated phosphorylation of NUPs promotes nuclear entry. Moreover, future research will have to address the isoform-specific shuttling frequencies of ERK1 and ERK2 questioning how these are provoked mechanistically.

4.1.3 The role of extracellular matrix adhesions on nuclear ERK signalling

The ERK-MAPK pathway serves to convert extracellular stimuli into physiological responses by transducing input signals to subcellular compartments and thereby regulating fundamental cellular processes, such as proliferation, differentiation and cell migration. This role in signal transduction, however, demands a link between pathway activation and the extracellular environment to ensure adequate signalling responses. Interestingly, a body of work has shown that cell adhesion via integrin engagement is frequently required for efficient ERK activation, as growth factors fail to induce ERK signalling, when cells were kept in suspension [447-450]. Moreover, anchorage dependency has also been demonstrated for ERK's role in regulating gene expression, as phosphorylation of the transcription factor ELK at Ser385 is reduced in the absence of

integrin-mediated adhesions [451]. This suggests that extracellular matrix adhesions play an important role in activating the ERK-MAPK cascade as well as localising ERK1/2 to subcellular localisations. Integrins are cell surface receptors, which contribute to the tethering of the actin cytoskeleton to the membrane at adhesion sites, and can also recruit a variety of structural and signalling molecules. It is well-established that ERK signalling is enhanced at focal adhesions sites [214], but it has yet to be determined how integrin engagement controls ERK trafficking. It is possible, however, that integrin-mediated organisation of the cytoskeleton facilitates transport and/or nuclear entry of activated ERK molecules.

4.1.4 Experimental paradigm

In the previous chapter we showed that ERK2 but not ERK1 drives tumour cell invasion and migration on 3D matrices by increasing the momentary migration velocity and decreasing cellular resting. Although we were able to demonstrate clear functional disparities between the two kinases with regards to cell motility, the underlying mechanism remained unresolved. Given that Marchi *et al.* demonstrated differential nuclear shuttling frequencies for ERK1 and ERK2, and proposed ERK2 to be the predominant kinase driving gene expression [416], we decided to perform a mRNA microarray screen to search for genes that are expressed in an ERK2-specific manner. As cells cultured in 3D exhibit completely different gene expression signatures when compared to 2D [395] and nuclear translocation of ERK is altered by matrix adhesions [451], we chose to perform our comparative gene expression analysis in a 3D microenvironment. A diagram illustrating the experimental set-up and our data filtering strategy is presented in Figure 4-1. ERK2-regulated genes are expected to show an increase (or decrease) in mRNA levels upon ERK2 silencing. Re-expression of ectopic ERK2 (but not ERK1) should be able to revert the induction (or inhibition) of mRNA levels to control.

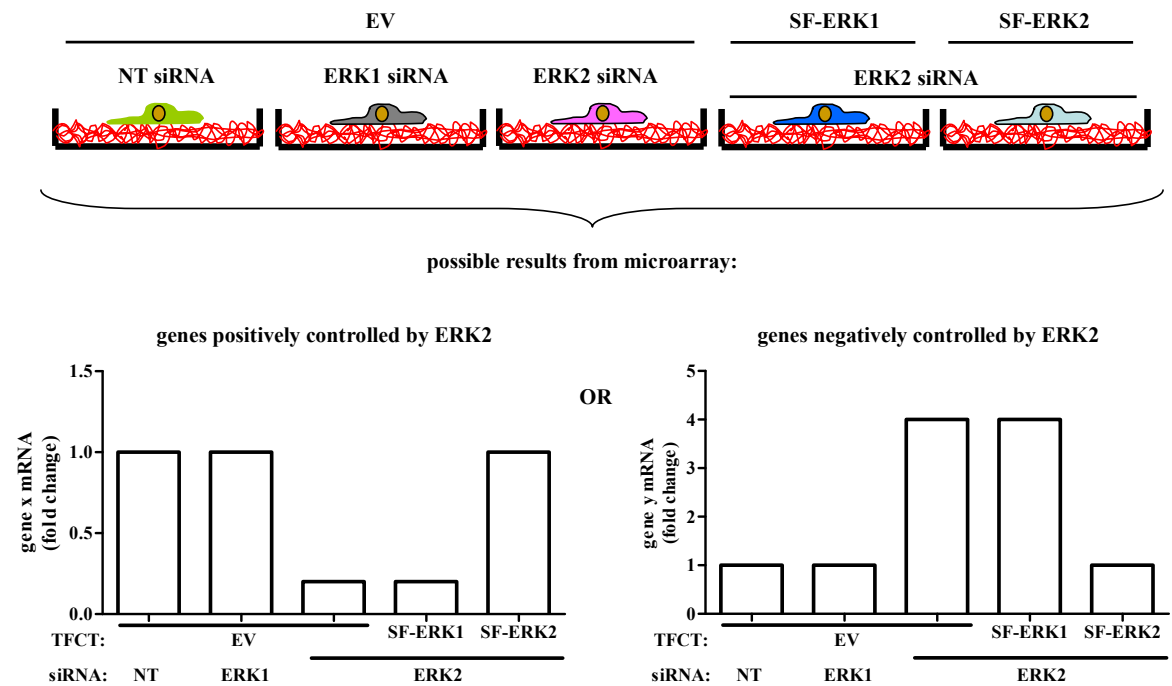


Figure 4-1 Experimental paradigm

Diagram illustrating the experimental approach for the identification of an ERK2-dependent gene expression signature in a 3D microenvironment. In brief, MDA-MB-231 cells are transfected with NT siRNA, single oligos targeting ERK1 or ERK2 in combination with expression plasmids for SF-ERK1, siRNA-resistant SF-ERK2 or an empty vector control (EV) and plated onto cell-derived matrix. Bar graphs show possible mRNA expression levels for genes, which are induced or suppressed in an ERK2-dependent manner.

4.2 Results

4.2.1 *Microarray analysis identified an ERK2-specific gene expression signature*

4.2.1.1 Quality control of microarray samples

To determine whether isoform-specific regulation of gene expression was responsible for ERK2's influence over cell migration and invasion, MDA-MB-231 cells were transfected with non-targeting siRNAs (NT), or single oligos targeting ERK1 or ERK2 in combination with expression plasmids for SF-ERK1, siRNA-resistant SF-ERK2 or an empty vector control (EV) and plated onto cell-derived matrix. 16 hours following plating, the cells were lysed. The efficacy of ERK knockdown and expression of SF-ERKs were determined by Western blotting (Figure 4-2 A), and this showed that both ERK isoforms were efficiently silenced by their respective siRNAs. Furthermore, SF-ERK1 and siRNA-resistant SF-ERK2 were expressed to equal levels after knocking down ERK2, thus ensuring that disparities in the expression levels of these kinases were not responsible for any results obtained from the microarray.

Total RNA was harvested from MDA-MB-231 cells using the RNeasy Kit (Qiagen) and traces of genomic DNA were removed by mechanical shear and DNase1. The concentration and purity of the isolated RNA were determined by measuring the absorbance at 260 nm and 280 nm using a NanoVue spectrophotometer. All samples exhibited $A_{260\text{nm}}/A_{280\text{nm}}$ absorbance ratios greater than 1.8, indicating that contamination with protein was negligible. We then labelled the isolated RNA using the Illumina® TotalPrep™ RNA labelling Kit (Ambion). In brief, the mRNA of each sample was converted into cDNA, which was then used as a template for *in vitro* transcription with biotin-16-UTP to produce labelled cRNA molecules. The yield of the cRNA amplification step was assessed by measuring the absorbance at 260 nm. After adjusting the cRNA concentrations to 0.2 µg/µl, the samples were sent to the Wellcome Trust Clinical Research Facility in Edinburgh, where the integrity of the biotinylated cRNA was assessed using an Agilent Bioanalyser. The electropherograms for each sample displayed a distribution of RNA molecules of varying sizes ranging from 250 to 5500 nucleotides with most of the cRNAs at 1000 to 1500 nucleotides. This suggests that no mRNA or cRNA degradation occurred during sample preparation (Figure 4-2 B). Subsequently, the

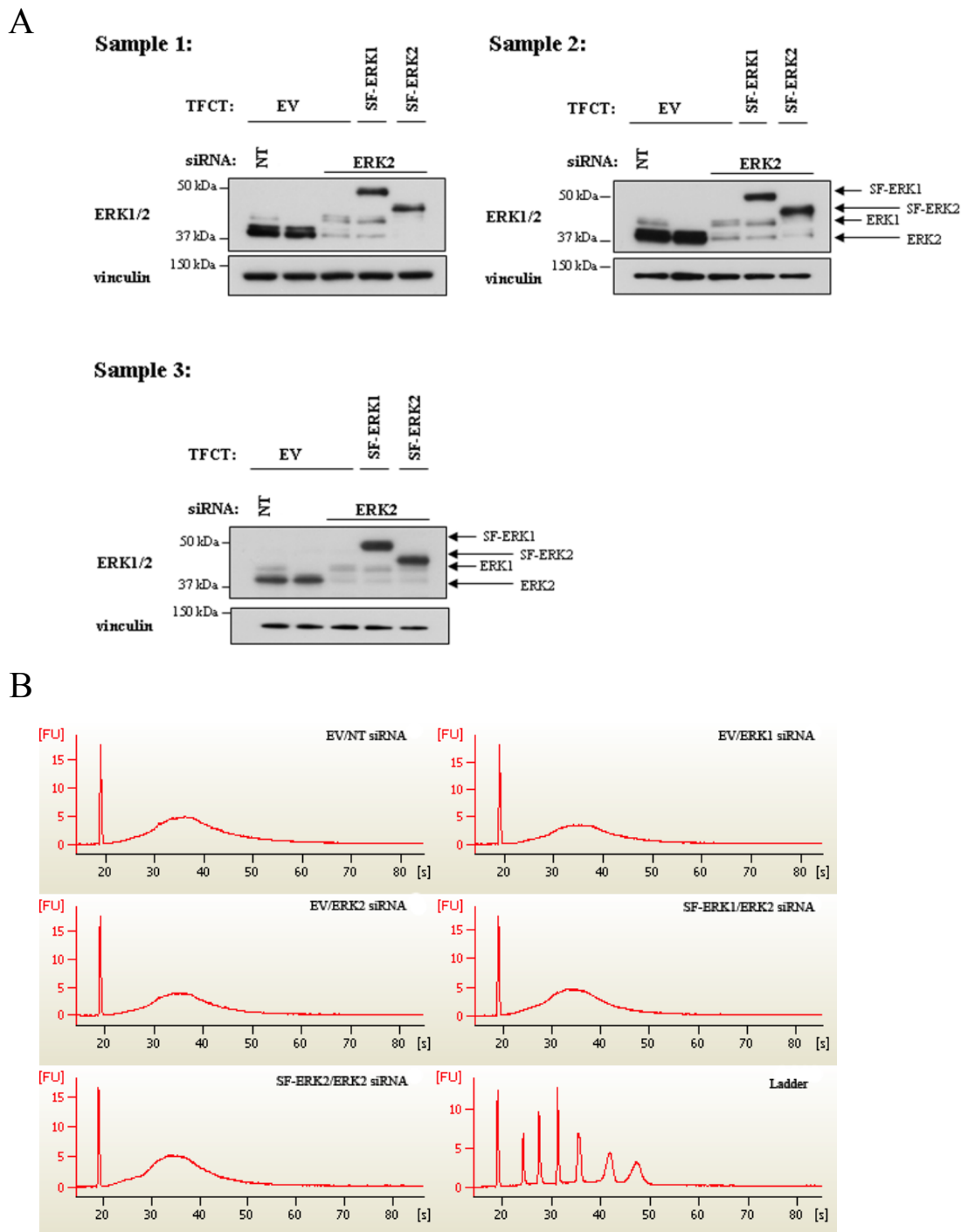


Figure 4-2 Quality control of the microarray samples

MDA-MB-231 cells were transfected with non-targeting siRNAs (NT), or single oligos targeting ERK1 or ERK2 in combination with expression plasmids for SF-ERK1, siRNA-resistant SF-ERK2 or an empty vector control (EV) and plated onto cell-derived matrix.

A. The efficacy of RNAi and ectopic ERK expression was assessed by Western blot 16 hours post nucleofection for all three microarray samples.

B. Total RNA was isolated using the RNeasy kit (Qiagen) and subsequently converted into labelled cRNA using the TotalPrep RNA Labeling Kit (Ambion). The integrity and concentration of the cRNA samples were assessed with the help of an Agilent Bioanalyser. Representative electropherogram scans for all conditions of one biological replicate are shown.

Genetic Core Facility performed whole genome expression analysis on HumanHT-12 v4 Expression BeadChips, which allows comparative expression analysis of over 47,000 transcripts.

4.2.1.2 Normalisation of microarray data yields good clustering of experimental replicas

As non-biological variations between bead chips (such as technical variations during bead chip generation, sample labelling and hybridisation) may obscure changes in gene alterations, it is imperative to normalise raw data obtained from the BeadArray Reader [452]. We acquired 24 gene signal profiles after direct hybridisation of the HumanHT-12 v4 Expression BeadChips, which were normalised and analysed with the help of the Partek® Genomics Suite Software, version 6.5 by Dr. Gabriela Kalna. All values were adjusted by quantile normalisation and log₂ transformation, which was previously shown to give the best results for Illumina gene expression data [453]. Subsequent principle component analysis gave rise to scatter plots, which showed a good overlap of sample replicates from two chips (Figure 4-3 A) but also an undesirable experimental replica clustering (Figure 4-3 B). To remove this batch-dependent effect a mixed model ANOVA (analysis of variances) was performed, which adjusts the data in such a way that batches are comparable to one another (Figure 4-3 C) [454]. Finally, outliers of samples were removed according to standard protocol and the remaining 19 samples renormalized as described above, which resulted in good clustering of the experimental microarray replicas (Figure 4-3 D). Differentially expressed genes were identified by ANOVA (analysis of variances) and post-hoc linear contrasts performed between all pairs of experimental conditions. Multiple test corrections (Bonferroni and step up Benjamini-Hochberg) were performed for all calculated p-values.

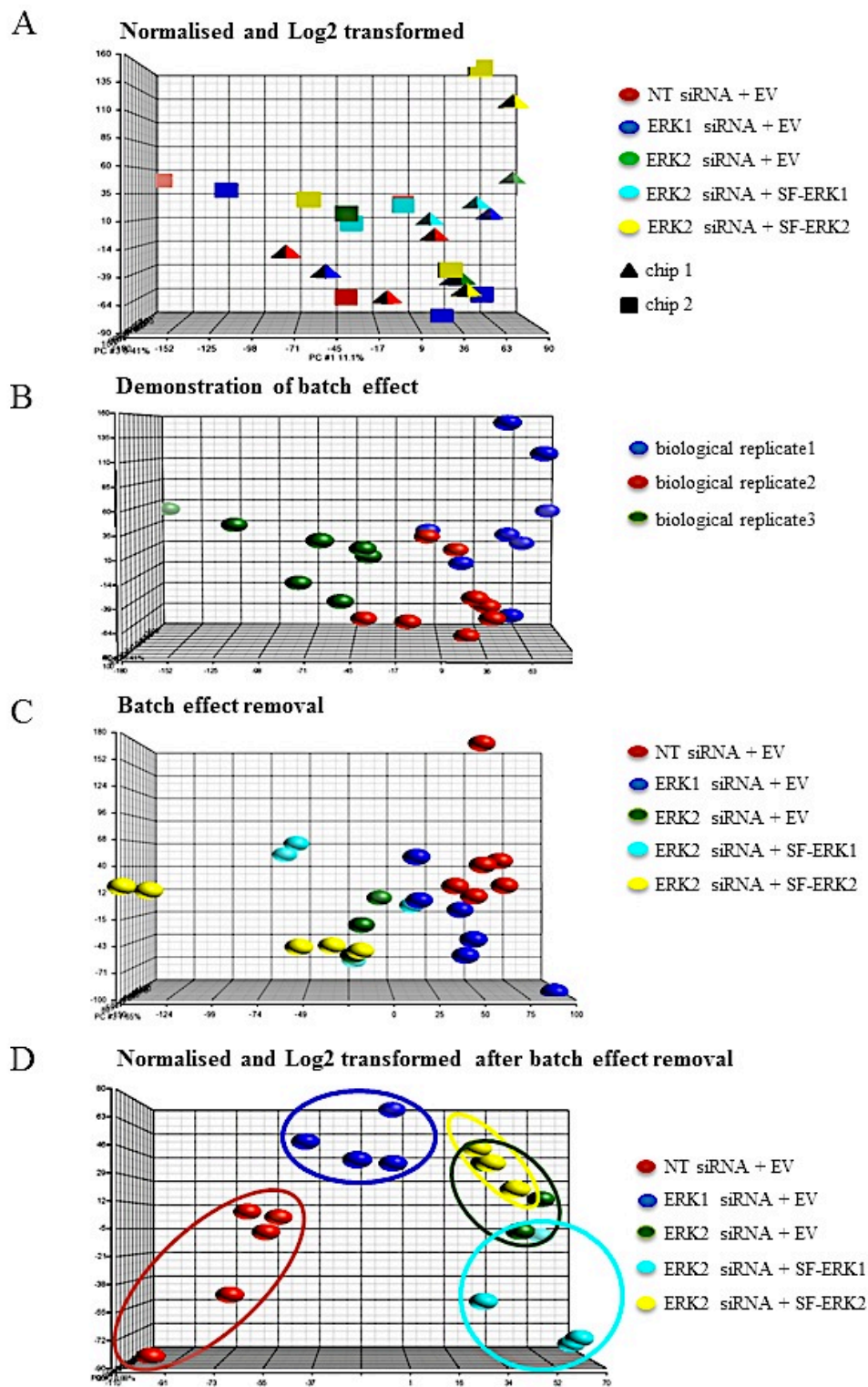


Figure 4-3 Normalisation results in good clustering of experimental replicas

Microarray raw data was normalised and analysed in PARTEK[®] Genomics Suite Software. Demonstrated are:

- Clustering patterns of all 24 samples after normalisation and Log2 transformation.
- Scatter plots of batch effects from different biological replicas.
- Clustering patterns after batch effect removal through mixed model ANOVA.
- Data clustering after the removal of outliers, renormalisation and Log2 transformation.

4.2.1.3 Microarray analysis identifies genes whose expression is down-regulated following ERK2 knockdown

Following normalisation, batch effect removal and log transformation, Multiway ANOVA (analysis of variances) was used to identify genes whose expression was down-regulated following ERK2 silencing. Multiple filtering steps were performed to generate a list of ERK2-regulated genes. Thus, genes had to show (i) a significant decrease in expression when ERK2 depleted cells were compared to NT siRNA (step-up p-value ≤ 0.05) and (ii) inverse changes with respect to fold changes and p-value when siRNA-resistant SF-ERK2 was re-expressed (step-up p-value ≤ 0.05 , fold change ≥ 1.3). After applying these filtering criteria, we obtained a set of 47 genes, whose expression was decreased following ERK2 depletion (Figure 4-4). These genes were then ranked according to fold changes obtained when ERK2 knockdown was compared to ERK2 re-expression.

To further refine the list of genes whose expression was regulated in an ERK2-dependent manner, we introduced two additional filter criteria. Thus, when comparing overexpression of SF-ERK1 versus ERK2 depletion, no significant changes in gene expression were expected with respect to fold changes and p-value (fold changes of ≤ 1.1 , step-up p-values of ≥ 0.35). Indeed, these criteria allowed the identification of 13 genes, whose expression was regulated in an isoform-specific manner (Figure 4-4). ERK2 itself fell into this group of genes, validating our experimental set-up and filtering strategy. Moreover, our data suggest that the *egr1* gene is regulated by both ERK isoforms, as ectopic expression of either ERK1 or ERK2 restored gene expression to control levels. This observation is in agreement with data published by Lefloch *et al.*, who demonstrated that re-expression of either ERK isoform in ERK2 depleted cells is sufficient to restore *egr1* mRNA levels [357].

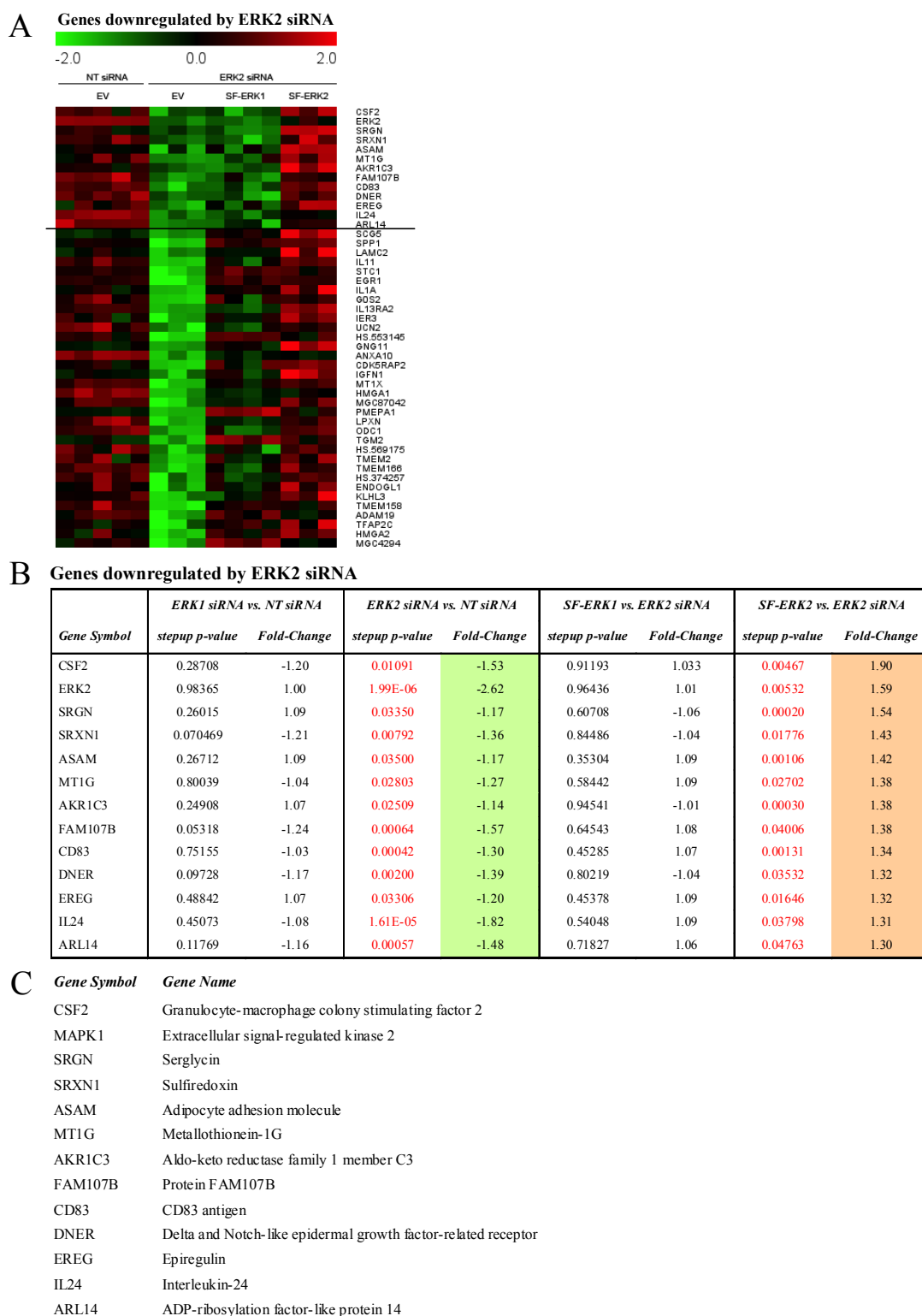


Figure 4-4 List of genes down-regulated upon ERK2 silencing

MDA-MB-231 cells were transfected with non-targeting siRNAs (NT), or siRNAs targeting ERK1 or ERK2 in combination with expression plasmids for SF-ERK1, SF-ERK2 or empty vector control (EV) and plated onto CDM. Total RNA was extracted, labelled, and comparative whole-genome expression profiling was performed using Illumina HT-12 v4 expression chips. (see next page also)

A. The heat map displays genes, which are down-regulated in an ERK2-dependent manner. Genes, which showed significant changes in expression level when comparing ERK2 knockdown versus NT siRNA (step-up p-value < 0.05) and inverse changes when comparing ERK2 knockdown versus re-expression of siRNA resistant SF-ERK2 (step-up p-value < 0.05, fold change ≥ 1.3) were identified and ranked according to fold changes. The expression of the first 13 genes is regulated in an ERK2-dependent manner (step-up p-values > 0.35, fold change ≤ 1.1 when comparing ERK2 knockdown cells to SF-ERK1 overexpression). The colour and intensity of the boxes allocated to each data point represent fold changes in expression level: low expression (green), high expression (red).

B. Table of genes, whose expression is down-regulated in an ERK2-dependent manner. Listed are: gene symbols, step-up p-values (significant p-values are in red), and fold changes for experimental comparisons. A significant decrease in fold change following ERK2 knockdown is marked by a green background colour, while inverse changes upon re-expression of ERK2 are marked by a red background colour.

C. List of gene names for ERK2-regulated genes from (B).

4.2.1.4 Microarray analysis identifies genes whose expression is up-regulated following ERK2 knockdown

Having identified genes, whose expression is induced by ERK2, we asked whether this kinase may also act to suppress gene expression. Thus, we set out to identify a set of genes, whose expression is up-regulated in cells lacking ERK2. We normalised and processed the data as for Figure 4-1. Subsequent filtering steps generated a list of ERK2-regulated genes, which met the following criteria: genes showed (i) a significant increase in gene expression when ERK2 knockdown was compared to NT siRNA (step-up p-value ≤ 0.05) and (ii) inverse changes with respect to fold changes and p-value, when siRNA resistant SF-ERK2 was re-expressed (step-up p-value ≤ 0.05 , fold change ≥ 1.3). This produced a set of 36 genes, whose expression was decreased following ERK2 depletion (Figure 4-5) which were then ranked according to fold changes as before.

To further refine this list we introduced an additional filter criterion by predefining that genes had to exhibit no significant changes in gene expression when ERK1 was overexpressed (fold changes of ≥ -1.1 , step-up p-values of ≥ 0.4). This allowed the identification of 14 genes whose expression was suppressed in an ERK2-specific fashion (Figure 4-5). Interestingly, ERK1 depletion significantly induced gene expression of C10ORF10 (fold change=1.40, step-up p-value=0.0061), SELENBP1 (fold change=1.36, step-up p-value=0.0047), and GPR64 (fold change=1.44, step-up p-value=0.0002), suggesting that both ERK isoforms suppress their expression (Figure 4-5). Yet, overexpression of ERK1 in cells depleted for ERK2 was not sufficient to restore mRNA levels to control, which indicates that these mRNA transcripts are regulated post-transcriptionally in an ERK2-dependent manner.

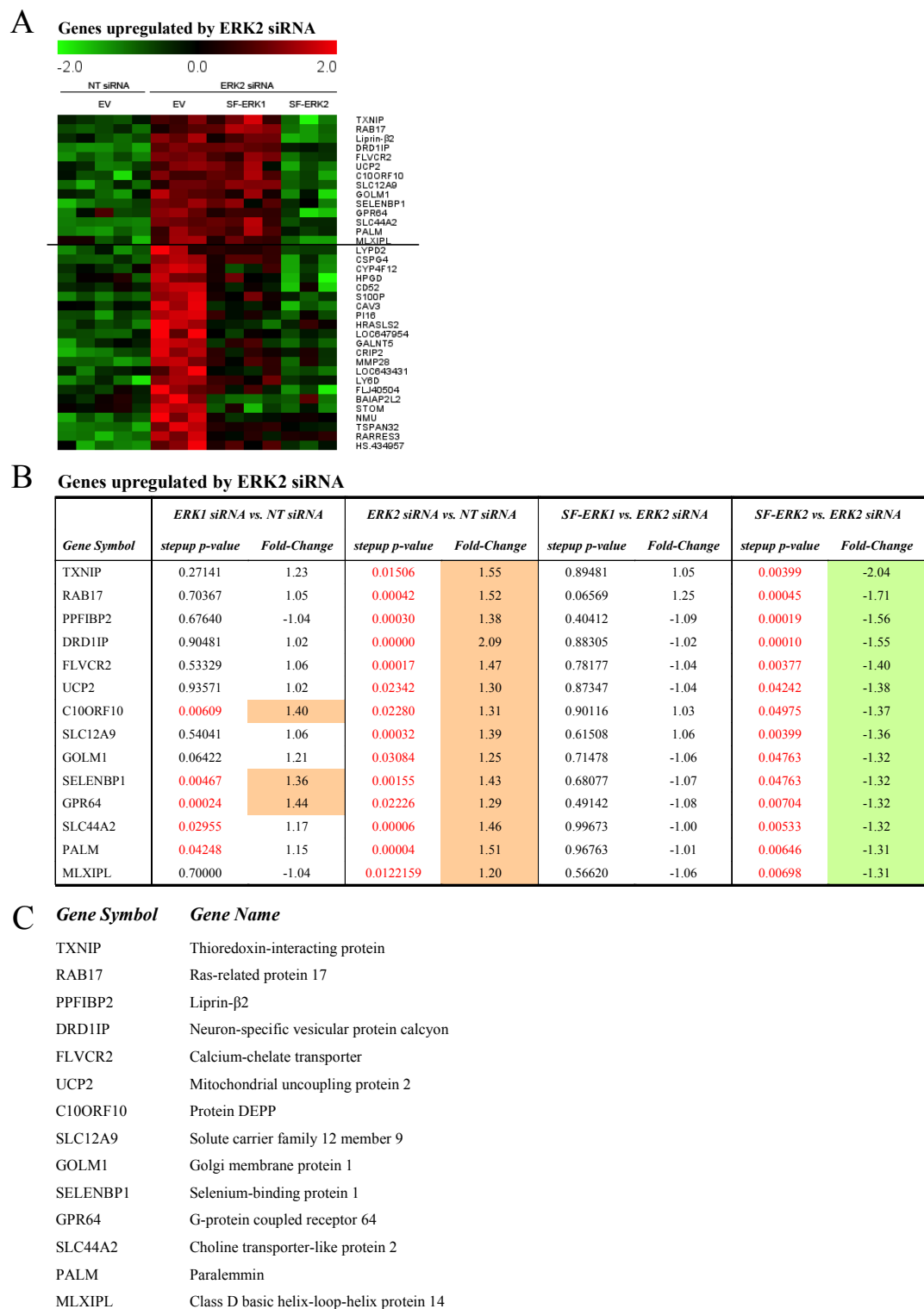


Figure 4-5 List of genes up-regulated upon ERK2 silencing

MDA-MB-231 cells were transfected with non-targeting siRNAs (NT), or siRNAs targeting ERK1 or ERK2 in combination with expression plasmids for SF-ERK1, SF-ERK2 or an empty vector control (EV) and plated onto CDM. Total RNA was extracted, labelled, and comparative whole-genome expression profiling was performed using Illumina HT-12 v4 expression chips. (see next page also)

A. The heat map displays genes, which are up-regulated in an ERK2-dependent manner. Genes, which showed significant changes in expression level when comparing ERK2 knockdown versus NT siRNA (step-up p-value < 0.05) and inverse changes when comparing ERK2 knockdown versus re-expression of siRNA resistant SF-ERK2 (step-up p-value < 0.05, fold change ≥ -1.3) were identified and ranked according to fold changes. The expression of the first 14 genes is regulated in an ERK2-dependent manner (step-up p-values > 0.4, fold change ≥ -1.1 when comparing ERK2 knockdown cells to SF-ERK1 overexpression). The colour and intensity of the boxes allocated to each data point represent fold changes in expression level: low expression (green), high expression (red).

B. Table of genes, whose expression is up-regulated in an ERK2-dependent manner. Listed are: gene symbols, step-up p-values (significant p-values are in red), and fold changes for experimental comparisons. A significant increase in fold change following ERK1 or ERK2 knockdown is marked by a green background colour, while inverse changes upon re-expression of ERK2 are marked by a red background colour.

C. List of gene names for ERK2-regulated genes from (B).

4.2.2 Validation of ERK2-dependent gene expression using qRT-PCR

4.2.2.1 qRT-PCR primer pairs amplify a single product in a linear manner over a range of cDNA concentrations

Quantitative real-time polymerase chain reaction (qRT-PCR) is methodically based on the polymerase chain reaction, but allows simultaneous quantification of the amplified template. Moreover, when qRT-PCR is combined with reverse transcription, mRNA levels of different tissues or experimental conditions can be compared. To this end the quantity of mRNA for an experimental condition is typically expressed relative to its control sample. This, however, requires equal mRNA loading for both samples, which is ensured by adjusting the concentration of RNA input for each reverse transcription and normalising obtained values for genes of interest against a housekeeping gene, such as glyceraldehyde 3-phosphate dehydrogenase (GAPDH). Amplicon accumulation during qRT-PCR is monitored with the help of a fluorescent dye (such as SYBR Green), which intercalates with dsDNA product.

The qRT-PCR consists of four stages, which are characterised by different reaction kinetics. Initially, product amplification does not yield a measurable read-out, because the generated fluorescence is below the detection threshold. This stage is called the lag phase and is followed by the exponential phase, in which the copy number of the template doubles with each amplification cycle and the fluorescent signal increases linearly. This stage allows the determination of the threshold cycle (C_t), which marks the cycle in which the fluorescent signal crosses the threshold. The C_t value is inversely proportional to the log of the initial template, which means that more initial mRNA transcripts give rise to lower C_t values. The exponential phase is followed by a retardation phase, where reaction components become limiting and thus, the reaction rate decreases. Finally, amplification reaches a plateau, when all reaction constituents are used up and if left long enough, the PCR products will begin to degrade [455].

It is important to stress that SYBR Green will intercalate with any dsDNA molecules present in the reaction mixture. Therefore, primer dimers as well as non-specific PCR products will alter your overall fluorescent signal and ultimately your quantitation results. In order to ensure an accurate amplicon measurement, the choice of suitable primers is a crucial step in setting up a successful qRT-PCR. Thus, prior to any comparative qRT-PCR

analysis, the suitability for every primer used must be determined. To assess whether the primer pairs amplify a single product, qRT-PCR reaction mixes were resolved on agarose gels and visualised with ethidium bromide (data not shown). Moreover, dissociation (melting) curves for each amplification product were generated by the Opticon Monitor Software. The melting curve analysis of each amplicon of interest confirmed the presence of a single spike, indicative of a single amplification product (see following sections for some representative images).

Having ensured that the primer pairs give rise to a single amplicon during PCR, we next assessed whether primer pairs were amplifying in a linear manner over a range of different input concentrations. We, therefore, performed qRT-PCR on serial dilutions of cDNA templates and plotted C_t values against the logarithmic values of standard cDNA amounts, which were expressed as dilution factors (i.e. 1.75x, 1.5x, 1.25x, 1x, 0.75x, 0.5x). The correlation coefficient (R^2) values were greater than 0.98 for all primers tested, suggesting a near perfect linear relationship between C_t value and cDNA concentration (Figure 4-6). Moreover, these results indicate that the fluorescence measured during our qRT-PCR was proportional to the template input. Next, we assessed the amplification efficiencies for each amplicon using this formula $E = 10^{\frac{-1}{a}} - 1$, where 'a' represents the gradient of linear fit as defined by Arezi *et al.* [456]. We obtained amplification efficiencies of 0.78, 0.83, 0.73, 0.8, 0.75 and 0.73 for GAPDH, CSF2, Rab17, Liprin-β2, ERK1 and ERK2, respectively.

Changes in mRNA levels between two experimental conditions can be expressed as absolute or relative values. Absolute quantification of input concentrations requires the generation of standard curves from known concentrations of mRNA species and is commonly used when amplification efficiencies for target and reference gene differ greatly. Relative quantification can be obtained by expressing target gene expression of one sample relative to another. One commonly used method for relative quantification is the $\Delta\Delta C_t$ method [354], which takes loading variations into account by normalising target gene expression to a reference gene. However, this quantification method assumes near equal amplification efficiencies for target and reference gene. As we obtained similar amplification efficiencies for our genes of interest, we were confident in using the $\Delta\Delta C_t$ method to compare expression levels for CSF2, Rab17 and Liprin-β2 in different experimental conditions. Yet, we also calculated relative expression ratios for each of the

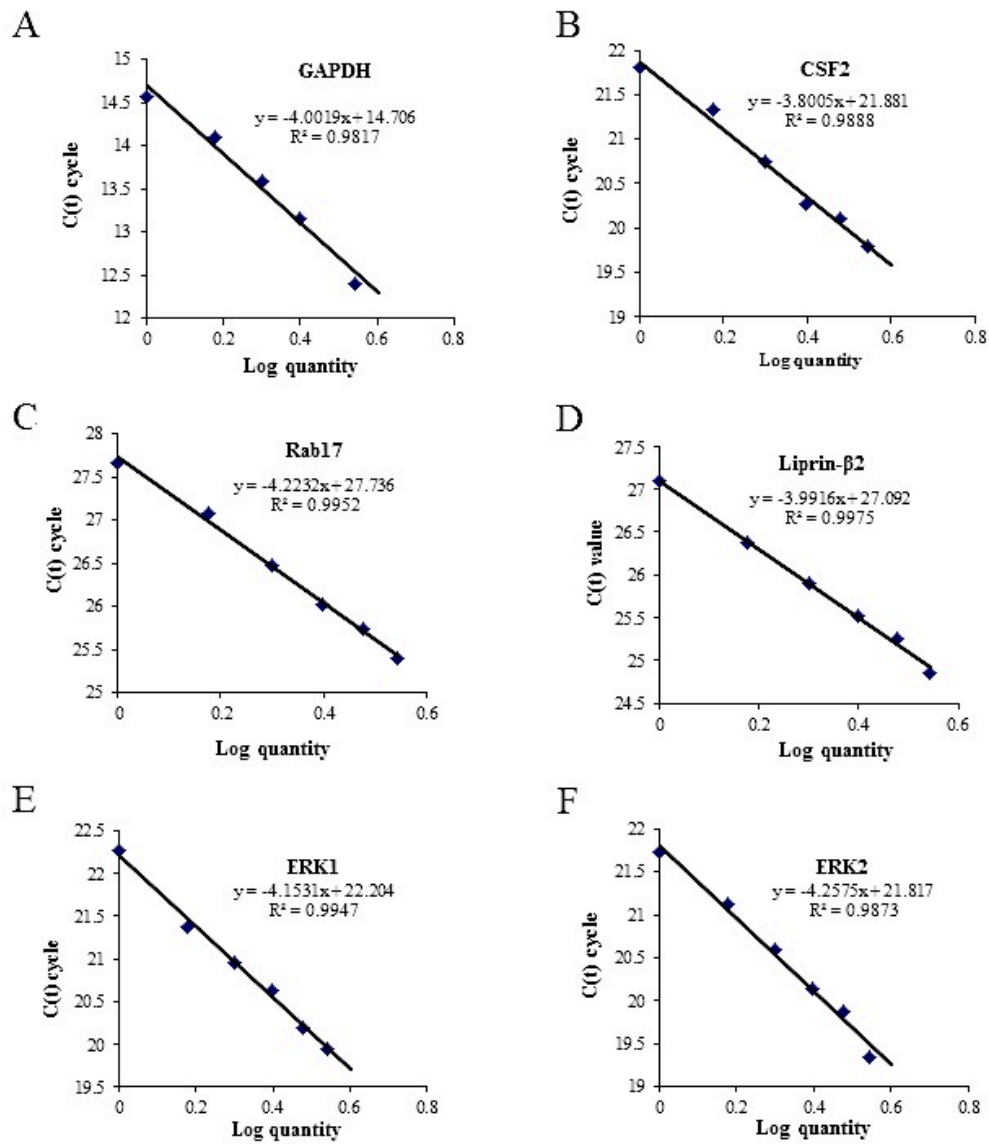


Figure 4-6 qRT-PCR primer pairs amplify in a linear manner over a range of cDNA concentrations
 cDNA was synthesised from RNA isolated from MDA-MB-231 cells grown on plastic. Serial dilutions of cDNA were used in a qRT-PCR reaction to test the efficiency of amplification of the respective primer sets. Standard curves representing a plot of C(t) against the initial log₂ quantity of the template and corresponding R² values are shown for GAPDH (A), CSF2 (B), Rab17 (C), Liprin-β2 (D), ERK1 (E), ERK2 (F).

latter genes using a method which does not assume equal amplification efficiencies using the following formula: $ratio = \frac{E^{\Delta CP_{target}(control-sample)}}{E^{\Delta CP_{reference}(control-sample)}}$, where 'E' represents the efficiency and 'ΔCP' the absolute deviation [457]. Both quantification methods yielded near identical expression ratios (data not shown), thus verifying the suitability of the $\Delta\Delta C_t$ method for relative quantification.

4.2.2.2 ERK2 (but not ERK1) regulates the expression of CSF2, Rab17 and Liprin-β2 in cells attached to CDM

Our Illumina gene expression array allowed the identification of 27 genes, whose expression was either increased or decreased in an ERK2-dependent manner. Prominent amongst these were colony-stimulating factor 2 (CSF2), Ras-related protein 17 (Rab17) and Liprin-β2, whose mRNA levels were strongly altered by knockdown of ERK2, and normalised by re-expression of siRNA-resistant ERK2 (but not ERK1). CSF2 is known to regulate haematopoiesis, but recent evidence suggests a role for this cytokine in tumour cell invasion and disease progression [458-461]. Rab17 is a small GTPase, which has been shown to regulate intracellular transport of proteins and lipids [462]. Moreover, there are indications that this GTPase is involved in the maintenance of epithelial polarity [463]. Liprin-β2 belongs to the family of LAR-interacting proteins (Liprins) and has been shown predominantly to localise to membrane structures [464]. To verify these ERK2-dependent gene expression signatures we transfected MDA-MB-231 cells with non-targeting siRNAs (NT), or siRNAs targeting ERK1 or ERK2 in combination with expression plasmids for SF-ERK1, SF-ERK2 or empty vector control (EV) and plated cells onto CDM for 16 hours. After harvesting the total RNA for each experimental condition, we performed qRT-PCR combined with reverse transcription and normalised our data to the housekeeping gene, GAPDH.

Firstly, we assessed the expression of CSF2 in our different experimental settings. It is important to stress that melting curve analysis gave rise to a single peak, which is indicative of a single amplification product for CSF2 (Figure 4-7 A). Moreover, when the input cDNA was replaced by RNase/DNase-free water, no fluorescent signal was detected during qRT-PCR within 40 reaction cycles (Figure 4-7 B). This suggests that qRT-PCR components were not contaminated with DNA or RNA, which might obscure our data analysis. Interestingly, qRT-PCR of six independent experiments demonstrated that silencing of either ERK1 or ERK2 significantly decreased CSF2 mRNA levels (Figure 4-7 C). This is in direct contrast to the numerical values obtained from the HumanHT-12 Expression BeadChip scanning and suggests that both ERK1 and ERK2 drive CSF2 expression. Moreover, consistent with the microarray data the reduction in CSF2 transcript levels observed upon ERK2 depletion could only be restored to control levels, when siRNA-resistant ERK2 (but not ERK1) was re-expressed (Figure 4-7 C).

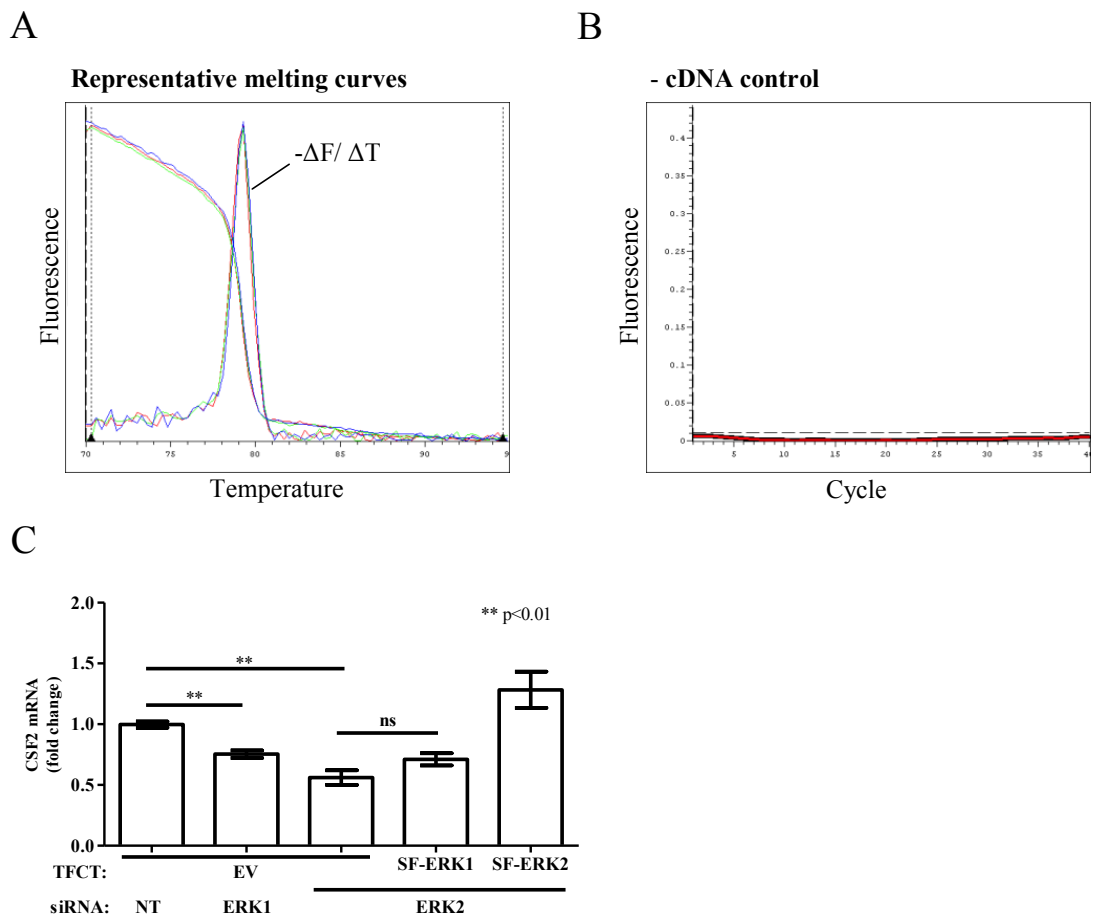


Figure 4-7 CSF2 expression is reduced upon ERK2 silencing

A. Primer pairs targeting CSF2 amplify a single product as shown by representative melting curves, which were generated using Opticon Monitor software.

B. qRT-PCR reactions run with the omission of cDNA yield no amplicon as shown on the plot derived from Opticon Monitor software.

C. MDA-MB-231 cells were transfected with non-targeting siRNAs (NT), or siRNAs targeting ERK2 in combination with expression plasmids for SF-ERK1, SF-ERK2 or an empty vector control (EV) and plated onto CDM. RNA was extracted, converted into cDNA and qRT-PCR was performed to validate the differential regulation of CSF2. Data was normalised to GAPDH and values relative to the control transfected are expressed as means \pm standard error of the mean (SEM) of 18 replicates from 6 independent experiments. Statistical significance of differences was determined by Mann-Whitney *U* test analysis.

Next, we used qRT-PCR to confirm that ERK2 was able to suppress Rab17 and Liprin- β 2 expression in MDA-MB-231 cells. qRT-PCR of either Rab17 or Liprin- β 2 gave rise to melting curves with one distinct peak (Figure 4-8 and Figure 4-9 A), indicating that the primer pairs were specific. Moreover, when reactions were set up without cDNA as a template, no amplicon was detected by the Opticon Monitor Software within 40 reaction cycles, suggesting that reaction components were not contaminated with DNA or RNA molecules, which would obscure our results (Figure 4-8 and Figure 4-9 B). Importantly, qRT-PCR of six independent experiments showed that transcript levels of either Rab17 or Liprin- β 2 were significantly increased following knockdown of ERK2, while ERK1 depletion did not elevate mRNA levels. Furthermore, re-expression of siRNA-resistant ERK2 but not ERK1 restored expression of Rab17 and Liprin- β 2 to levels displayed by control cells (Figure 4-8 and Figure 4-9 C).

Next, we determined whether mRNA levels of related members of the Rab or Liprin family were regulated by ERK2. Expression of Rab20, a Rab GTPase that exhibits close homology to Rab17, was minimally, but significantly, affected by manipulation of ERK2 expression (Figure 4-8 D). In contrast, transcript levels of other Liprin family members expressed in MDA-MB-231 cells (i.e. Liprin- β 1, - α 2, and - α 4) were not affected in the same manner as Liprin- β 2 when ERK2 levels were manipulated (Figure 4-9 D). Expression of Liprin- α 2 and - α 4 was decreased only when siRNA-resistant ERK2 was re-expressed following ERK2 depletion, whereas Liprin- β 1 expression was reduced when ERK2 levels were manipulated by means of gene silencing or ectopic expression.

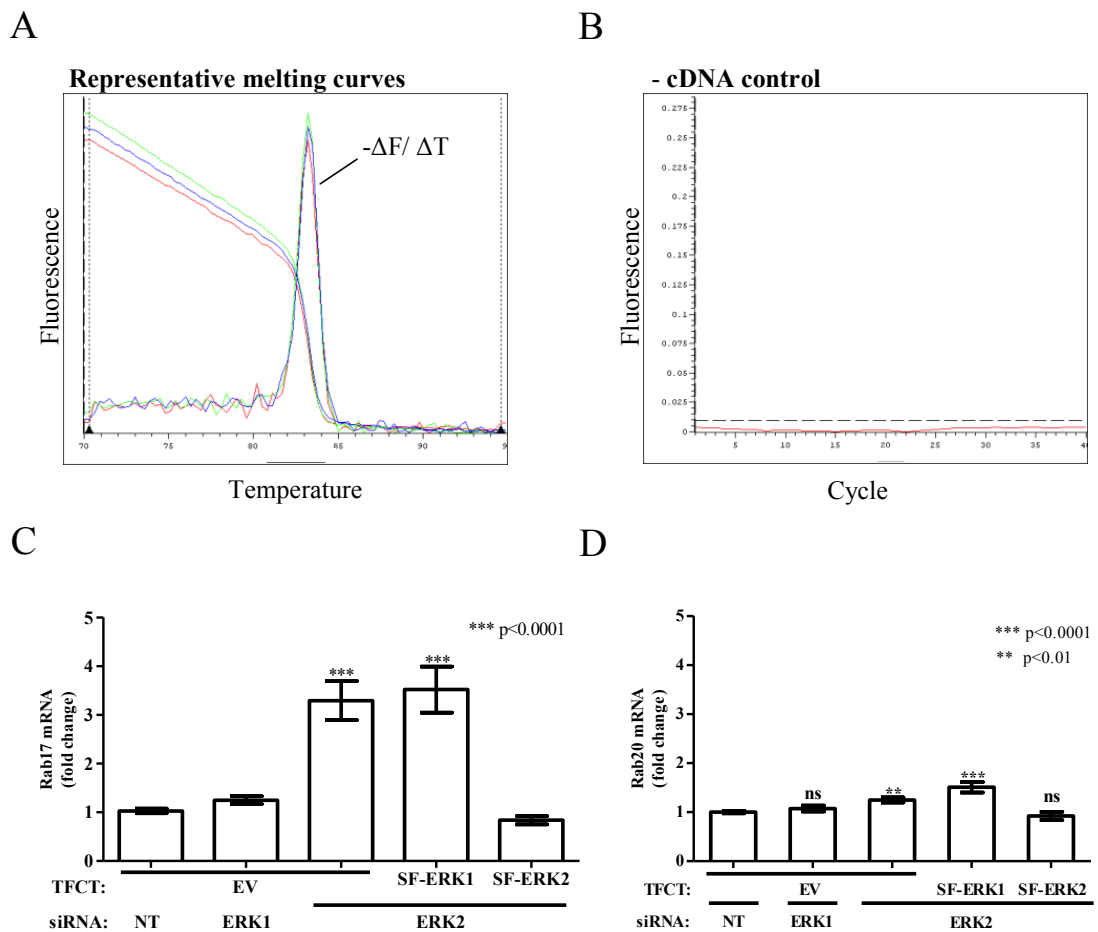


Figure 4-8 Rab17 expression is induced upon ERK2 silencing

A. Primer pairs targeting Rab17 amplify a single product as shown by representative melting curves, which were generated using Opticon Monitor software.

B. qRT-PCR reactions run with the omission of cDNA yield no amplicon as shown on the plot derived from the Opticon Monitor software.

C-D. MDA-MB-231 cells were transfected with non-targeting siRNAs (NT), or siRNAs targeting ERK2 in combination with expression plasmids for SF-ERK1, SF-ERK2 or an empty vector control (EV) and plated onto CDM. RNA was extracted, converted into cDNA and qRT-PCR was performed to validate the differential regulation of Rab17 (C) and Rab20 (D). Data was normalised to GAPDH and values relative to the control transfected are expressed as means \pm standard error of the mean (SEM) of 18 replicates from 6 independent experiments. Statistical significance of differences was determined by Mann-Whitney *U* test analysis.

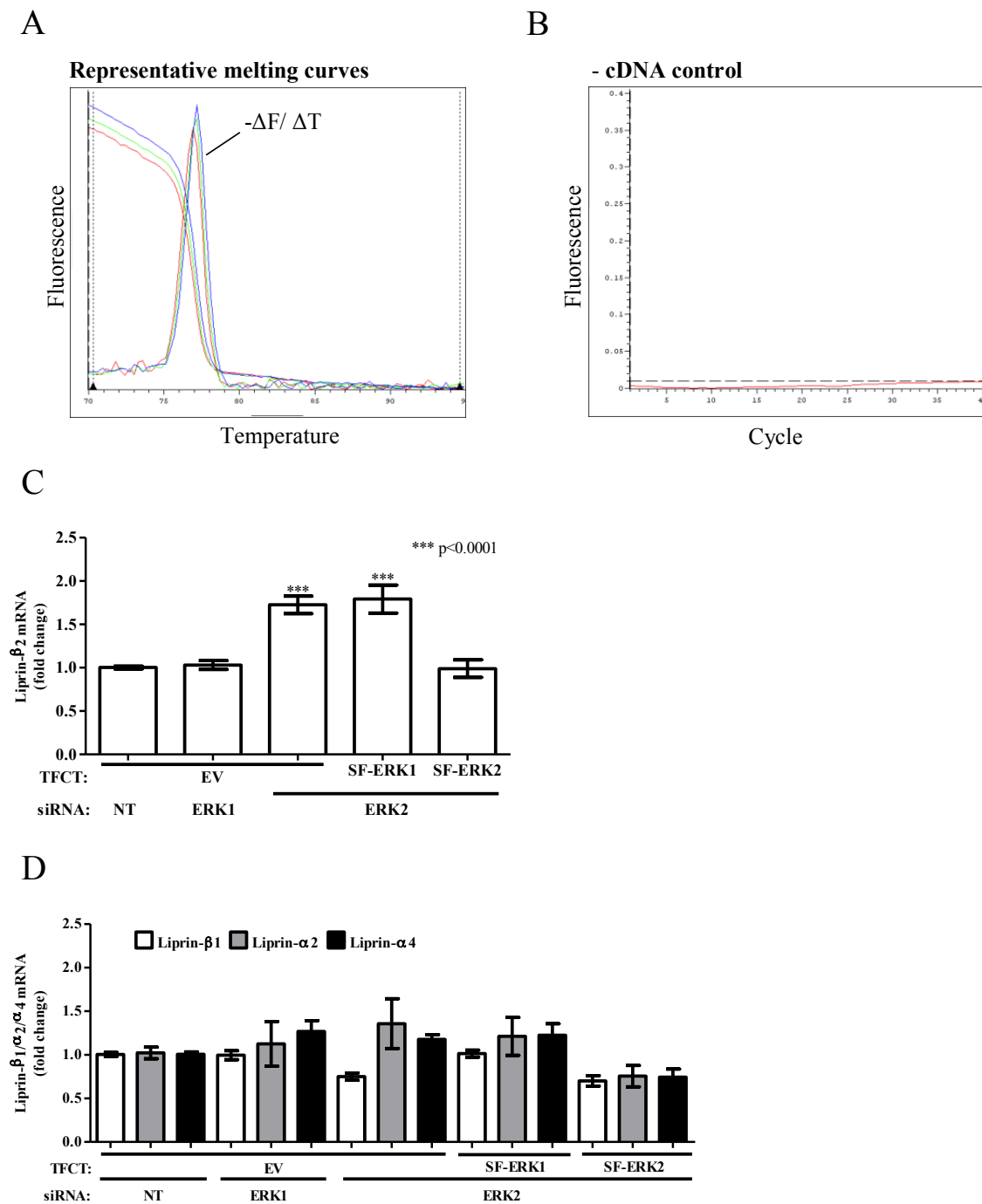


Figure 4-9 Liprin-β2 expression is induced upon ERK2 silencing

A. Primer pairs targeting Liprin-β2 amplify a single product as shown by representative melting curves, which were generated using Opticon Monitor software.

B. qRT-PCR reactions run with the omission of cDNA yield no amplicon as shown on the plot derived from Opticon Monitor software.

C-D. MDA-MB-231 cells were transfected with non-targeting siRNAs (NT), or siRNAs targeting ERK2 in combination with expression plasmids for SF-ERK1, SF-ERK2 or an empty vector control (EV) and plated onto CDM. RNA was extracted, converted into cDNA and qRT-PCR was performed to validate the differential regulation of Liprin-β2 (C) and Liprin-β1/α2/α4 (D). Data was normalised to GAPDH and values relative to the control transfected are expressed as means ± standard error of the mean (SEM) of 18 replicates from 6 independent experiments. Statistical significance of differences was determined by Mann-Whitney *U* test analysis.

4.2.2.3 Single siRNA oligos confirm an induction of Rab17 and Liprin- β 2 expression following ERK2 depletion

To determine whether altered expression of CSF2, Rab17 and/or Liprin- β 2 were the result of off-target siRNA effects, we silenced ERK1 and ERK2 with two independent siRNA duplexes, plated the cells on CDM and assessed respective transcript levels by RT-PCR. This indicated that knockdown of either ERK1 or ERK2 with two independent oligos diminished CSF2 transcript levels (Figure 4-10 A). Furthermore, levels of Rab17 and Liprin- β 2 mRNA were significantly increased following knockdown of ERK2, whereas ERK1 silencing was ineffective in this regard (Figure 4-10 B/C). We also confirmed the knockdown of ERK1 and ERK2 by means of qRT-PCR (Figure 4-10 D and E). Taken together these data indicate that ERK2 (but not ERK1) suppresses expression of Rab17 and Liprin- β 2, while both ERK isoforms are involved in maintaining the levels of CSF2 mRNA.

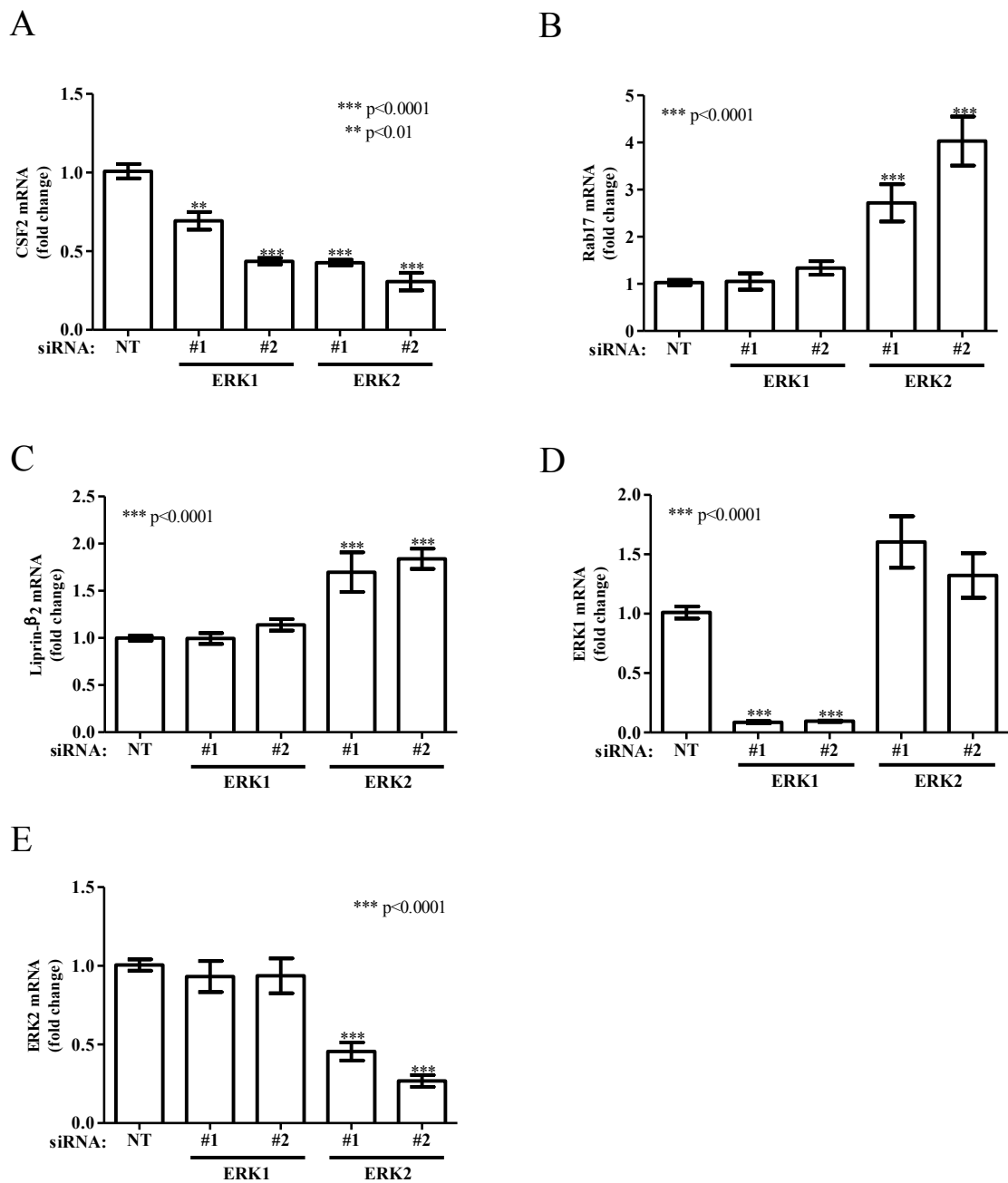


Figure 4-10 Validation of ERK2-dependent gene expression using single siRNA oligos for ERK1 and ERK2

MDA-MB-231 cells were transfected with non-targeting siRNAs (NT), or single siRNA oligos targeting ERK1 or ERK2 and plated onto CDM. Total RNA was isolated and converted into cDNA. A-C. qRT-PCR was performed to assess mRNA expression levels after ERK1 or ERK2 knockdown. Data was normalised to GAPDH and values relative to the control transfected are expressed as means \pm standard error of the mean (SEM) of 9 replicates from 3 independent experiments. Statistical significance of differences was determined by Mann-Whitney U test analysis. D-E. ERK knockdown was validated for each experiment using qRT-PCR. Data was analysed as in (A).

4.2.2.4 ERK2 also acts to suppress Rab17 and Liprin-β2 when cells are grown on plastic

Given that cells cultured in 3D exhibit completely different gene expression signatures when compared to 2D [395], and that activation as well as localisation of ERK1/2 are altered depending on the substratum [449, 451], we aimed to investigate whether suppression of Rab17 and Liprin-β2 by ERK2 was specific to 3D microenvironments. To this end, MDA-MB-231 cells were transfected with non-targeting siRNAs (NT), or siRNAs targeting ERK1 or ERK2 and plated onto plastic dishes (instead of CDM) and determined the expression levels of Rab17 and Liprin-β2.

Clearly, siRNA of ERK2 increased expression of Rab17 and Liprin-β2 when cells were plated onto plastic surfaces, and knockdown of ERK1 also drove Rab17 and Liprin-β2 expression, but to a lesser extent (Figure 4-11). These data indicate that the presence of a 3D microenvironment is not a prerequisite for ERK2's ability to suppress Rab17 and Liprin-β2 expression, but that ERK1 may also acquire some capacity to control these genes when cells are plated onto plastic.

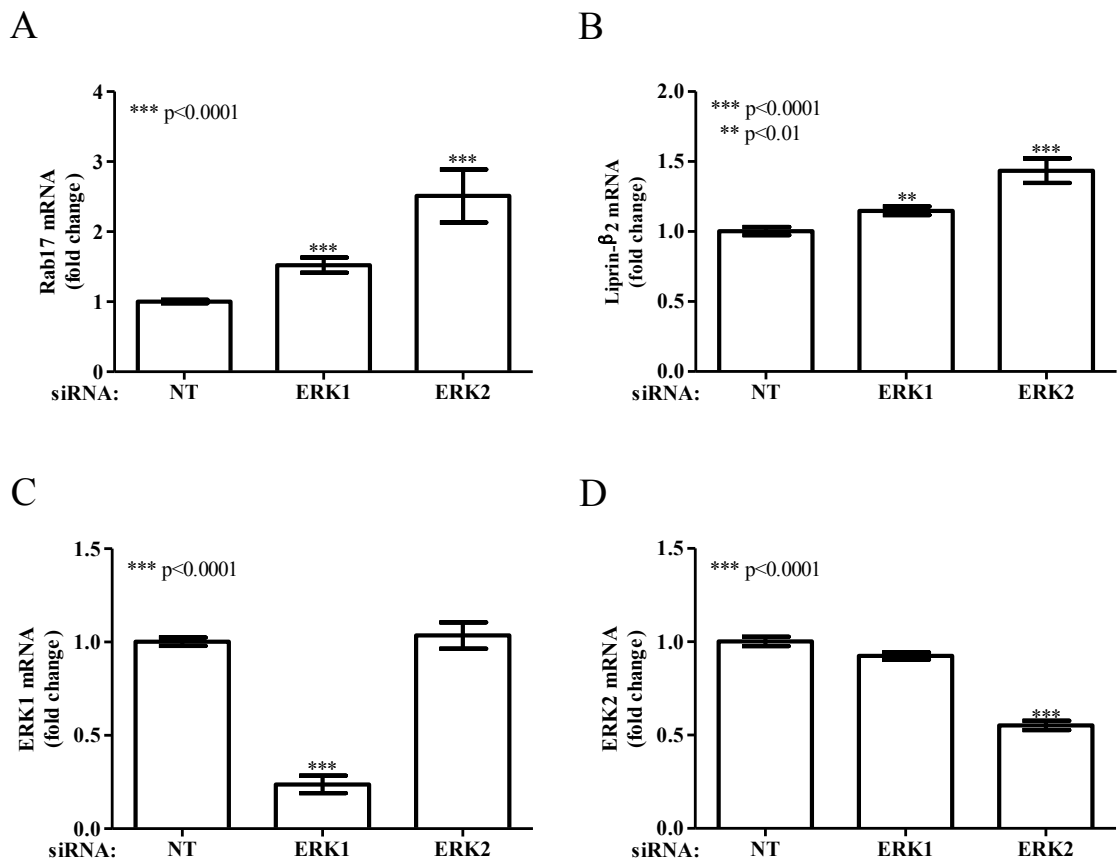


Figure 4-11 Knockdown of ERK2 induces Rab17 and Liprin-β2 expression in 2D

MDA-MB-231 cells were transfected with non-targeting siRNAs (NT), or siRNAs targeting ERK1 or ERK2 and plated onto plastic. Total RNA was isolated and converted into cDNA.

A-B. qRT-PCR was performed to assess mRNA expression levels after ERK silencing. Data was normalised to GAPDH and values relative to the control transfected are expressed as means \pm standard error of the mean (SEM) of 9 replicates from 3 independent experiments. Statistical significance of differences was determined by Mann-Whitney *U* test analysis.

C-D. ERK knockdown was validated for each experiment using qRT-PCR. Data was analysed as in (A).

4.2.2.5 Regulation of CSF2, Rab17 and Liprin- β 2 is dependent on MEK activity

In an attempt to characterise the human protein-DNA interactome, ERK2 was identified as an unconventional DNA-binding protein, which can bind directly to a G/CAAAG/C consensus motif and thereby repress transcription as shown by electrophoretic mobility shift assays and cell-based luciferase analysis. Intriguingly, this role as a transcriptional repressor is independent of its kinase activity and can be attributed to a cluster of positively charged residues on the C-terminus of the protein, with Lys259 and Arg261 being the key residues required for DNA binding [468]. Having identified an ERK2-specific gene expression signature, we wanted to investigate whether this novel role as a DNA-binding protein was responsible for regulating mRNA levels of CSF2, Rab17 and Liprin- β 2.

To determine whether phosphorylation of ERK by MEK was necessary for its role in regulating Rab17, Liprin- β 2 and CSF2 expression, we seeded 300,000 cells onto CDM and treated them with DMSO (dimethyl sulfoxide) as mock or the MEK inhibitor, U0126. We harvested cells at different time points following treatment (5 minutes, 1 hour, 2 hours and 24 hours), extracted total RNA and performed qRT-PCR combined with reverse transcription. Intriguingly, levels of CSF2 mRNA were maximally inhibited one hour after U0126 treatment, indicating that ERK is directly involved in driving CSF2 expression, and that this is depending on its kinase activity (Figure 4-12 A). In contrast, transcription of Rab17 and Liprin- β 2 were only induced 24 hours following MEK inhibition, which suggests that ERK2 suppresses these two genes less directly than it affects CSF2 expression (Figure 4-12 B/C).

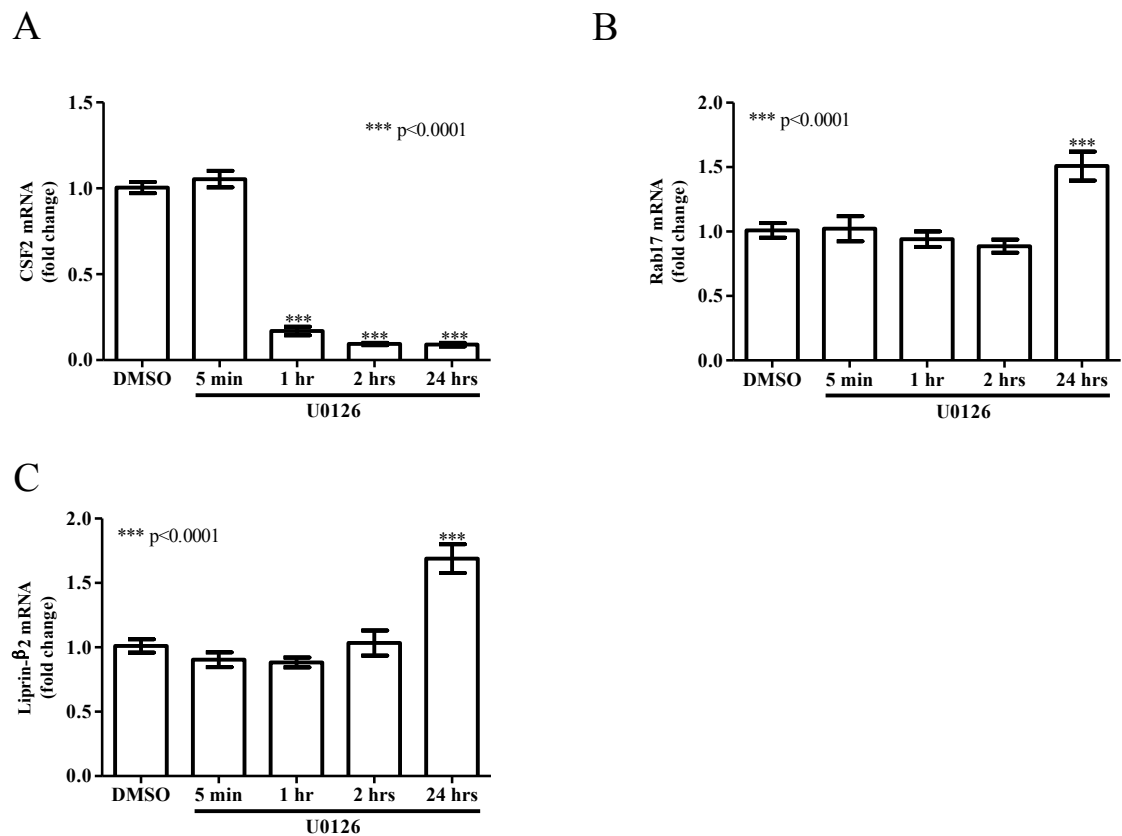


Figure 4-12 Expression of CSF2, Rab17 and Liprin-β2 is dependent on ERK2's kinase activity

MDA-MB-231 cells were treated with DMSO or the MEK inhibitor, U0126. Subsequently, cells were lysed, total RNA isolated, and converted into cDNA. qRT-PCR was performed to assess mRNA expression levels of CSF2 (A), Rab17 (B), and Liprin-β2 (C) following MEK inhibition. Data was normalised to GAPDH and values relative to the control transfected are expressed as means \pm standard error of the mean (SEM) of 9 replicates from 3 independent experiments. Statistical significance of differences was determined by Mann-Whitney *U* test analysis.

4.2.2.6 Rab17 and Liprin- β 2 transcription is suppressed by CSF2

Given that expression of CSF2 is maximally reduced after one hour of U0126 treatment, but Rab17 and Liprin- β 2's mRNA levels are only altered after 24 hours, we wanted to investigate the possibility that Rab17 and Liprin- β 2 are downstream effectors of CSF2, which might explain the late induction in gene expression. To test this interdependency, MDA-MB-231 cells were transfected with NT siRNAs, or oligos targeting CSF2, Rab17, or Liprin- β 2 and plated onto cell-derived matrix. We found that siRNA of Liprin- β 2 did not alter levels of Rab17 mRNA, and neither did Rab17 knockdown affect Liprin- β 2 expression. However, silencing of CSF2 significantly induced both Rab17 and Liprin- β 2 expression (Figure 4-13 A/B), indicating that transcription of these two genes is regulated by CSF2. Next, we wanted to investigate whether expression of CSF2 itself is regulated by Rab17 or Liprin- β 2 through a positive or negative feedback loop. However, we observed no significant changes in CSF2 mRNA levels, when either Rab17 or Liprin- β 2 were silenced (Figure 4-13 C).

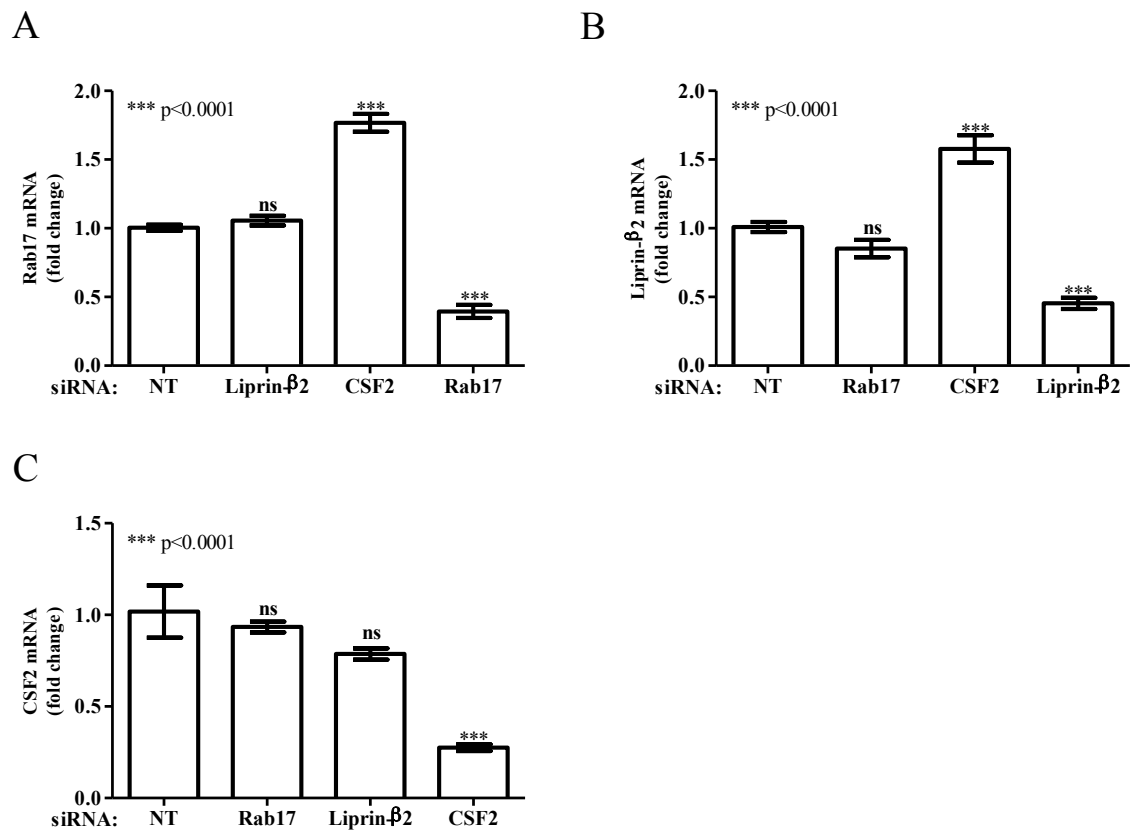


Figure 4-13 Rab17 and Liprin-β2 expression is suppressed by CSF2

MDA-MB-231 cells were transfected with non-targeting siRNAs (NT), or siRNAs targeting CSF2, Rab17, or Liprin-β2 and plated onto cell-derived matrix. Total RNA was isolated and converted into cDNA. qRT-PCR was performed to assess mRNA expression levels of CSF2 (A), Rab17 (B), and Liprin-β2 (C) following respective knockdowns. Data was normalised to GAPDH and values relative to the control transfected are expressed as means \pm standard error of the mean (SEM) of 9 replicates from 3 independent experiments. Statistical significance of differences was determined by Mann-Whitney *U* test analysis.

4.3 Discussion

4.3.1 Summary

Chapter 3 presented data demonstrating that the invasiveness of MDA-MB-231 cells depends specifically on ERK2 and not ERK1. Here, we performed a gene expression array to identify genes whose expression is regulated by ERK2 but not ERK1. We found 27 genes whose expression was altered after knockdown of ERK2 and restored to normal levels following re-expression of ERK2 (but not ERK1). Among these, we confirmed the ERK2-dependency for *csf2*, *rab17* and *liprin-β2* on CDM by qRT-PCR. Moreover, siRNA of ERK2 clearly increased expression of Rab17 and Liprin-β2 when cells are grown on plastic surfaces, indicating that the presence of a 3D microenvironment is not a prerequisite for ERK2's ability to suppress these genes.

4.3.2 ERK2 as a regulator of transcriptional initiation

In this chapter we provide clear evidence for an isoform-specific, ERK2-dependent gene expression signature from which we validated three genes, i.e. *csf2*, *rab17* and *liprin-β2*. Interestingly, we observed very distinct kinetics of changes in transcript levels following U0126 treatment, which implicates that ERK2 can regulate gene expression both directly and indirectly. Although we chose not to investigate how ERK2 promotes or suppresses transcriptional events in an isoform-specific manner, we would still like to discuss various tiers of gene expression that might be influenced by this isoform.

Active ERK signalling has been implicated in chromatin remodelling processes giving rise to both open [427] and closed chromatin structures [469]. The downstream ERK targets involved in these processes still remain to be elucidated, although phosphorylation of histone H3 and HMG-14 by the ERK effectors MSK1/2 and RSK2 are thought to promote loosening of chromatin by recruiting histone acetyltransferases [426-428]. Moreover, active ERK has been shown to stimulate topoisomerase IIα in a mechanism that is independent of its enzymatic activity [470]. Thus, ERK2 might promote or suppress DNA accessibility of a subset of genes by regulating the phosphorylation or activity of chromatin remodelling factors, such as topoisomerase IIα.

Once the chromatin is loosened, transcription factors bind to the exposed DNA sequence and thereby enhance or suppress the formation of the transcription initiation complex. As transcriptional activators and repressors generally compete for the same binding site on the DNA, alterations in DNA binding affinities through post-translational modifications can promote or inhibit gene transcription [471]. Indeed, phosphorylation of c-Jun and N-Myc by ERK1/2 was shown to enhance the transactivation and transcriptional repression activity, respectively [472, 473]. Thus, ERK2 might regulate gene transcription by altering the DNA-binding affinity of transcription factors through direct or indirect phosphorylation. In addition, ERK2 has recently been identified as an unconventional DNA-binding protein [468], which represses interferon gamma signalling. Although not reported so far, DNA-binding by ERK2 may also promote gene transcription. Notably, both ERK isoforms contain the critical residues involved in DNA binding [468], which argues against an ERK2-specific function in transcription. However, amino acids flanking the critical arginine and lysine are only partially conserved between the two kinases (Figure 4-14 A) and this may give rise to differing DNA binding grooves. Whether or not both kinases recognise different DNA consensus motifs remains to be elucidated.

Interestingly, the *csf2* promoter region contains 2 G/CAAAG/C motifs and this suggests that ERK2 might bind to its 5' UTR. Although DNA-binding is independent of ERK kinase activity [468], it is possible that active ERK bound to the promoter region may phosphorylate neighbouring transcription factors and thereby alter their ability to transactivate or repress. Moreover, active ERK might be recruited to specific genes through its DNA-binding ability. Intriguingly, CSF2 mRNA levels are reduced by knockdown of either ERK1 or ERK2, indicating that both kinases are involved in driving CSF2 expression. Yet, CSF2 transcript levels are only restored to control levels when ectopic ERK2 is re-expressed, indicating that ERK regulates both the initial transcription as well as mRNA stability. Indeed, the *csf2* promoter region contains an AP-1-binding site, which is critical for CSF2 transcription (personal communication with Dr. Gareth Inman). The AP-1 transcription factor is regulated both transcriptionally and post-transcriptionally by both ERK1 and ERK2. Thus, it is not surprising that silencing of either gene significantly reduces CSF2 mRNA levels. Yet, the MEK inhibitor U0126 maximally reduces *csf2* mRNA levels within one hour of treatment, although Fra and Jun levels only decrease after a prolonged inhibition of MEK [378]. This indicates that there are AP-1 independent mechanisms, which are also important in the initial stages of *csf2* transcription.

A

ERK2: 251 dlnciinlka rnyllslphk nkvpwnrlfp 280

ERK1: 268 dlnciinmka rnylqslpsk tkvawaklfp 299

B

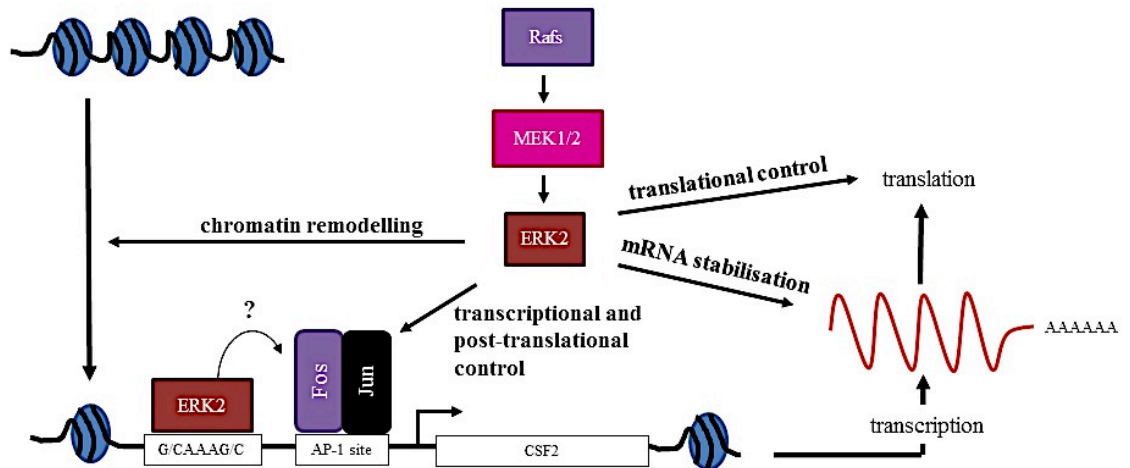


Figure 4-14 ERK2 as a regulator of gene expression

A. Comparison of ERK2's sequence shown to be involved in direct DNA-binding. Crucial basic amino acids are coloured in red. Diverging amino acids in the flanking sequences are coloured grey.
 B. Schematic illustration of how ERK2 drives expression of CSF2.

4.3.3 *Post-transcriptional regulation of gene expression*

Messenger RNA levels are influenced by changes in nuclear transcription rates, mRNA processing and cytoplasmic decay. Interestingly, mRNA degradation is thought to be a major regulator of gene expression and deregulated mRNA stability has been linked to diseases, such as Alzheimer's disease and thalassaemia [474]. Eukaryotic mRNAs are subject to co-transcriptional processing, which protects the transcripts from phosphatases and ribonucleases, and entails 5' capping, 3' polyadenylation and splicing [475]. Moreover, mRNA stability can be regulated through sequence-specific elements located in the 5' or 3' UTR. For example, A+U-rich elements (ARE) are potent destabilising features of mRNAs, which promote degradation by recruiting RNA-binding proteins, such as tristetraprolin [474]. The ERK-MAPK pathway stimulates the phosphorylation of tristetraprolin and subsequent binding to 14-3-3 proteins, which sequesters the RNA-binding protein in the cytoplasm and is linked to an enhanced stability of ARE-containing mRNAs [476, 477].

Intriguingly, tristetraprolin was shown to enhance CSF2 mRNA stability by promoting mRNA deadenylation [478]. Given that ERK promotes phosphorylation of tristetraprolin, this may represent another level, by which ERK signalling can impinge on CSF2 expression. Indeed, our data are consistent with a mechanism in which ERK2 but not ERK1 is important in stabilising CSF2 mRNA, as overexpression of ectopic ERK1 was not sufficient to restore normal transcript levels after knockdown of ERK2. Taken together, our results suggest a mechanism in which the ERK-MAPK pathway controls *csf2* expression at various stages (Figure 4-14 B). Firstly, both ERK isoforms may promote gene transcription by stabilising the AP-1 transcription factor and potentially inducing an open-chromatin structure. Secondly, CSF2 transcripts may be stabilised via an isoform-specific mechanism, which might involve phosphorylation of tristetraprolin. Thirdly, ERK signalling could stimulate initiation of the translation machinery by activating MNK1 (MAPK interacting kinase 1), which in turn phosphorylates and activates the translational initiation factor eIF4E [479].

Notably, our Illumina gene expression array also identified genes, whose expression was induced by knockdown of either ERK1 or ERK2, but could only be restored to control levels, when ectopic ERK2 (but not ERK1) was re-expressed and suggested an

isoform-specific role in mRNA decay. Among those genes were the Selenium-binding protein (SELENBP1), the protein DEPP (C100RF10) and the G-protein coupled receptor 64 (GPR64). Thus, a possible future avenue for investigation may be to determine how ERK2 signalling can selectively control stabilisation and decay of particular transcripts.

4.3.4 ERK signalling differs between 2D and 3D microenvironments

Transmembrane proteins, such as integrins or receptor tyrosine kinases, are able to sense changes in the extracellular environment and relay this information to cytoplasmic signalling circuits like the ERK-MAPK pathway. It is therefore not surprising that the microenvironment in which cells are cultured significantly influences cellular signalling pathways to change cellular features such as cell shape and migration [395, 451]. *Rab17* and *liprin- β 2* were suppressed in an ERK isoform-specific manner when cells were cultured on CDM, but to a lesser extent when cells were grown on plastic. This discrepancy in signalling may be the result of different subcellular localisations of the two isoforms in 2D and 3D. Indeed, Aplin *et al.* have demonstrated that integrin-mediated adhesions to fibronectin enhance nuclear ERK translocation via a mechanism that is dependent in the organisation of the actin cytoskeleton [451]. Thus, localising ERK to distinct subcellular compartments is likely to be altered by extracellular-matrix adhesions and contribute to isoform-specific signalling. Unfortunately, there are currently no ERK isoform-specific antibodies, which would allow comparison of the localisation of the two ERKs between 2D and 3D substrates. However, the use of photoactivatable ERK fusion proteins, which would allow the monitoring of isoform-specific trafficking and localisation, might provide a better understanding of how ERK localisation is regulated in 2D and 3D microenvironments.

4.3.5 Correlation between mRNA abundance and protein levels

Unfortunately, we were not able to confirm that the measured changes in Rab17 and Liprin- β 2 transcript levels were reflected in their protein levels, because the commercially available antibodies were not capable of specifically recognising the endogenous protein (data not shown). Moreover, we attempted to raise a Rab17 antibody by injecting purified Rab17 into rabbits. However, the resulting antiserum, although able to distinguish purified Rab17 from closely related Rab20 and Rab24, was insufficiently sensitive to specifically detect endogenous Rab17 in cell lysates.

4.3.6 *Other potentially interesting microarray hits*

Due to our primary interest in receptor trafficking and its role in regulating tumour cell migration, we chose to focus our validation studies on targets which have been implicated in receptor trafficking or integrin biology, i.e. Rab17 and Liprin-β2 [463, 464]. However, other candidate genes, which are up- or down-regulated in an ERK2-dependent manner, may also contribute to the invasive phenotype of MDA-MB-231 cells, and may therefore be discussed briefly in the following paragraphs.

One such gene encodes the proteoglycan serglycin (SRGN) and this has recently been implicated as a driver of metastasis. Serglycin is one of the most up-regulated genes during the invasion-metastasis cascade and its overexpression correlates with an enhanced migratory phenotype [480]. Given that ERK signalling is generally augmented during tumorigenesis and our data identified ERK2 as a driver of *srgn* transcription, it is conceivable, that both proteins are functionally linked to promote metastasis.

Sulfiredoxin is another interesting microarray hit, which has already been linked to the ERK-MAPK pathway as an AP-1 target gene by Wei *et al.* and was shown to be required for cellular transformation [481]. Moreover, sulfiredoxin has been implicated in promoting lung cancer progression by enhancing tumour cell motility and cellular invasion, which makes this protein an interesting target for anti-cancer treatment strategies [482]. Our microarray data suggests a transcriptional regulation comparable to CSF2, where knockdown of either ERK1 or ERK2 resulted in a significant decrease in sulfiredoxin mRNA levels, which could only be restored to control levels when ERK2 was re-expressed. Thus, our data adds to the current literature in that it identifies sulfiredoxin mRNA stability as a regulatory mechanism for gene expression, which may be exploited clinically.

Another candidate gene with interesting clinical implications is thioredoxin-interacting protein (TXNIP), whose expression according to our microarray screen was increased by ERK2 knockdown. Intriguingly, TXNIP is frequently down-regulated in ERBB2-positive breast cancer patients, which correlates with poor survival [483]. Moreover, an inverse relationship between TXNIP expression and carcinogenesis has been shown for bladder and prostate cancer [484, 485], indicating a tumour-suppressive function for this gene.

Mechanistically, TXNIP diminishes ERK activation by attenuating CXCR4 expression *in vitro* and *in vivo* [484]. Our work expands the current knowledge by suggesting an ERK-dependent inhibition of *txnip* expression, which warrants continuous signalling through the ERK-MAPK pathway and a pro-invasive phenotype.

The transcriptional regulation of the selenium-binding protein 1 (SELENBP1) by the ERK-MAPK pathway represents another interesting observation from our microarray screen. Various research groups have proposed a tumour-suppressive function for this protein, whose expression is frequently reduced in various cancer types [486-488]. Moreover, Pohl *et al.* have shown a clear inhibitory role for SELENBP1 in tumour cell migration and carcinogenesis [489]. Given that the highly motile phenotype of HCT116 cells is dependent on ERK signalling [490] and overexpression of SELENBP1 impairs HCT116 motility *in vitro*, it is possible that ERK2 drives invasion by suppressing a subset of anti-migratory genes including SELENBP1, Rab17 and Liprin-β2.

Taken together our microarray screen identified several interesting genes whose expression was regulated in an ERK2-dependent manner. Given that some of these have previously been shown to drive or suppress tumourigenesis, it would be interesting to determine their role in tumour cell migration and invasion in future experiments.

5 Rab17 and Liprin- β 2 are inhibitors of tumour cell migration and invasion

5.1 Introduction

In the previous chapter we have identified Ras-related protein 17 (Rab17) and LAR-interacting protein- β 2 (Liprin- β 2) as genes, whose expression is suppressed by ERK2 in 3D microenvironments. Given that both genes have been implicated in the regulation of vesicular transport and our primary research interest lies in receptor trafficking and cell migration, we chose to investigate a potential role for these two microarray hits in tumour cell motility.

5.1.1 *Rab17 - a member of the RAB family of GTPases*

Rab17 belongs to the RAS-superfamily of GTPases, which comprises over 170 members including oncogenic H-Ras, N-Ras and K-Ras. Most family members share the common feature of harbouring an intrinsic hydrolase activity, which converts GTP (guanosine triphosphate) to GDP (guanosine diphosphate). Thus, GTPases represent molecular switches, which cycle between an inactive, GDP-bound and an active, GTP-bound state [491]. Two groups of regulatory proteins, i.e. guanine nucleotide exchange factors (GEFs) and GTPase activating proteins (GAPs), act to influence the GTP-loading of GTPases. GEFs promote GDP dissociation and subsequent GTP binding to activate the GTPases; which unmask protein interaction domains; while GAPs enhance the intrinsic hydrolase activity to accelerate the formation of an inactive, GDP-bound state. Moreover, GDP-dissociation inhibitors (GDIs) prevent GTPase activation by locking the enzyme in an inactive conformation [491].

Rab proteins are peripheral membrane proteins, which are anchored to destination membranes via a covalently linked prenyl group at their C-terminus. Rab escort proteins (REPs) accompany newly synthesised GTPases through the cytoplasm by binding to and shielding the hydrophobic prenyl group. Once Rab proteins reach the destination membrane, they insert into it using their prenyl group. Notably, REPs only carry inactive GDP-bound Rabs. Thus, the GTPases require activation following membrane insertion in order for them to bind to Rab effector proteins, through which the GTPases function. Following membrane fusion, Rab proteins are recycled through GDIs, which like REPs bind

to the prenyl group of inactive GTPases and deliver Rabs to their destination membrane [492].

The RAS-superfamily of GTPases can be subdivided into five subfamilies; i.e. the RAS family (due to their homology with the rat sarcoma genes), the RHO family (Ras homologs), the RAB family (Ras-related proteins), the ARF family (ADP ribosylation factors) and the RAN family (Ras-related nuclear proteins) [491]. The RAB family represents the largest of the five subclasses with over 70 members and it controls multiple stages of vesicular transport, such as vesicle formation, movement and fusion [493]. Although endocytic vesicles are thought of as highly plastic structures, there is evidence that functionally distinct compartments exist, and that these can be characterised by specific Rabs. For example, Rab4 and Rab5 are known to associate with early endosomes [494, 495], while Rab11 serves as a marker for recycling endosomes [496]. Moreover, Rab7 has been shown to localise to late endosomes [495].

Rab17 was identified as a cell type-specific GTPase, whose expression was thought to be restricted to epithelial cells. Northern blot analysis of various tissues demonstrated Rab17 transcripts to be present in kidney, liver and intestine, but not in organs lacking epithelial cells [497]. Interestingly, mesenchymal kidney precursor cells do not express Rab17, yet its expression is induced during differentiation into epithelial cells, suggesting a role for this GTPase in establishing and maintaining epithelial characteristics. In polarised cells with distinct basolateral and apical surfaces, such as Madin-Darby Canine Kidney (MDCK) cells, ectopically expressed Rab17 is localised to both basolateral and apical structures, which suggests a role for this protein in cellular transcytosis [497]. Indeed, subsequent work showed that overexpression of mutant forms of Rab17 (defective in GTP-binding or hydrolysis) resulted in an increase in transferrin receptor transcytosis in polarised Eph4 cells [462]. This finding was further supported by Hunziker *et al.* who showed that ectopic overexpression of wild type Rab17 impaired transcytosis of dimeric immunoglobulin A in MDCK cells [498]. Moreover, inactive GDP-loaded Rab17 mutants were shown to stimulate receptor recycling from apical endosomes to the apical surface [462]. Thus, the current evidence suggests an inhibitory role of Rab17 on transcellular transport of proteins and lipids as well as receptor recycling.

Phylogenetically, Rab17 belongs to the Rab5 subfamily and shares an overall sequence identity of approximately 40% with Rab5, Rab22, Rab24 and Rab20 [497, 499]. Rab5 is one of the best-studied Rab proteins, which mainly associates with early endosomes when activated. Rab5's function in vesicle trafficking is likely multifarious, as the GTPase is thought to be involved in processes such as generating endocytic vesicles at the plasma membrane, regulating membrane fusion events and controlling vesicle transport by recruiting microtubule motor proteins [500]. Like Rab5, Rab22 associates with early endosomes. Intriguingly, its ectopic expression results in an enlargement of endocytic vesicles in the perinuclear compartment and a decrease in endocytosis as measured by fluid phase markers [501]. In contrast, Rab24 is an unusual GTPase in that its GTPase activity is impaired due to a serine in codon 61 rather than a glutamine. Because the enzyme primarily exists in a switched-on state, Rab24 does not associate with GDIs and may employ novel mechanisms in regulating vesicular trafficking [502]. Rab20 is also unusual in that it contains a 40 amino acid insertion of unknown function and an atypical codon 61 [503].

Several putative interaction partners for Rab17 have been identified through yeast two-hybrid and large scale proteomic screens (Table 5-1), yet none of these have been validated by co-immunoprecipitation or co-localisation experiments. Interestingly, three of the proposed binding partners (Rab7A, Chmp6, and Smurf2) are involved in receptor degradation. Thus, it is likely that Rab17 may play a role in regulating the degradative pathway as well as modulating receptor internalisation and recycling. To add to this, Rab17 has been identified as a regulator of cilium formation, as overexpression of the Rab17-specific GAP, TBC1D7, impaired cilium development [504].

<i>Gene ID</i>	<i>Gene name</i>	<i>Gene function</i>	<i>Ref.</i>
TBC1D7	TBC1 domain family member 7	GTPase activating protein	[504]
RAB7A	Ras-related protein 7A	Late endosomal marker	[505]
NUDT3	Nudix type motif 3	Implicated in nucleoside phosphate metabolic pathways	[506]
CHMP6	Chromatin modifying protein 6	Involved in surface receptor degradation and the formation of endocytic multivesicular bodies	[507]
SMURF2	SMAD-specific E3 ubiquitin ligase 2	Involved in protein degradation	[508]
S100A8	S100 calcium binding protein A8	Versatile functions: implicated in differentiation and cell cycle progression amongst others	[506]
RABAC1	Rab acceptor protein 1	GDI displacement factor	[505]
ACVR1	Activin A receptor type 1	belong to the TGFβ superfamily	[508]

Table 5-1 Overview of known and putative Rab17 interaction partners as determined by high-throughput experiments

5.1.2 Liprins – a family of LAR-interacting proteins

Liprin- β 2 belongs to the family of LAR (leukocyte common antigen-related)-interacting proteins, which constitutes a class of cytoplasmic adaptor proteins involved in neuronal and non-neuronal processes. In humans there are six *liprin* genes, which are subdivided into two classes based on sequence similarities and binding characteristics, i.e. α -type (Liprin- α 1 to α 4) and β -type (Liprin- β 1 and - β 2) [464]. Members of the Liprin family demonstrate a high degree of sequence conservation over a 250 amino acid region in their C-termini. This region, designated the Liprin homology domain, is unique to this protein family and thought to play an important role in their function by mediating protein-protein interactions [464, 509]. Although the nomenclature suggests otherwise, only Liprin- α proteins can interact with LAR proteins (a family of transmembrane protein tyrosine phosphatases) via their C-terminal domain, indicating that the biological functions of the two subclasses may be different [464]. Recently, Kazrin, known for its role in desmosome assembly, was identified as a novel member of the Liprin family [510].

All family members share the same overall structure with an N-terminal coiled-coil domain and a distinct C-terminus comprising three consecutive SAM (steryl alpha motif) domains (Figure 5-1 A). Co-immunoprecipitation experiments have demonstrated that Liprins homodimerise via their N-terminal coiled-coil domain and heterodimerise via the C-terminal region [464, 509]. Notably, heterodimerisation of the two Liprin subclasses is still controversial, as subsequent work failed to isolate Liprin- α /Liprin- β complexes in co-immunoprecipitation experiments. However, direct interaction between α - and β -Liprins was recently demonstrated in co-crystallisation experiments by Wei *et al.*, arguing for the existence of heterodimers [511]. Interestingly, the central coiled coil domains of Liprin- β s form parallel homodimers and are predicted to bring all six SAM domains in close proximity [512]. Thus, the N-terminal regions intertwine to form rod-like structures, which may be organized into more complex molecular networks as reported for other coiled-coil proteins, such as myosin II heavy chains or intermediate filaments [513, 514]. In addition, recent computational analysis identified Liprin- β 's second SAM domain as a potential polymer forming module [515]. Thus, heterodimerisation of the two Liprin subclasses is believed to give rise to either closed or open scaffolds, which are thought to regulate the cytomatrix organisation of neuronal and non-neuronal cells (Figure 5-1 B) [512].

Studies on Liprins so far have focused on the function of Liprin- α 1 in neuronal and non-neuronal cells. In neurons, Liprin- α proteins play an important role in organizing the pre-synaptic site for rapid neurotransmitter release by localizing LAR proteins to the active zone [516]. Furthermore, Liprin- α and LAR proteins are expressed in post-synaptic sites, where they regulate dendrite development [517]. Non-neuronal functions are less studied, but there is some evidence for a role for Liprin- α 1 in cell motility [509, 518, 519]. Liprin- α 1 and LAR colocalise to focal adhesions at the cellular rear and may facilitate adhesion disassembly, a prerequisite for cell migration [509]. Moreover, overexpression of Liprin- α 1 induces cell spreading on fibronectin, while RNAi inhibits cell spreading and lamellipodia formation [519]. Intriguingly, Liprin- α 1 was shown to prevent internalisation of inactive β 1 integrin from the cell surface, thereby increasing the amount of integrin available for ECM binding and activation [520].

Liprin- β 1's biological functions are less well characterised, although recent evidence suggests a role for this protein in lymphatic vascular development [521]. Moreover, Liprin- β 1 has been identified as a novel binding partner for the metastasis-associated protein S100A4 (Mts1). The binding site for Mts1 resides within the C-terminal portion of Liprin- β 1, indicating the possibility that Mts1 association may interfere with Liprin- α /Liprin- β complex formation, thus releasing Liprin- α 1 from a heterodimeric complex to promote LAR function at focal adhesions [522].

Liprin- β s have been proposed to regulate Liprin- α s by masking the C-terminal protein-protein interaction domain via heterodimerisation. Thus, Liprin- β s may indirectly affect the biological functions of the α -types, by sequestering the adaptor molecules. To date, Liprin- α 1, -2 and -3 have been identified as Liprin- β 2 interaction partners in yeast two-hybrid experiments [464]. Furthermore, large scale proteomic screens have identified PTPRC, TSG101, PRNP, DTNB and 14-3-3 σ as putative Liprin- β 2 binding partners (Table 5-2), but none of these have been validated in co-immunoprecipitation or pull-down experiments. However, there is very few published studies that shine light on the biological functions of Liprin- β 2, and future work will have to determine the functional similarities and disparities between the β -type Liprins and their role in regulating Liprin- α s.

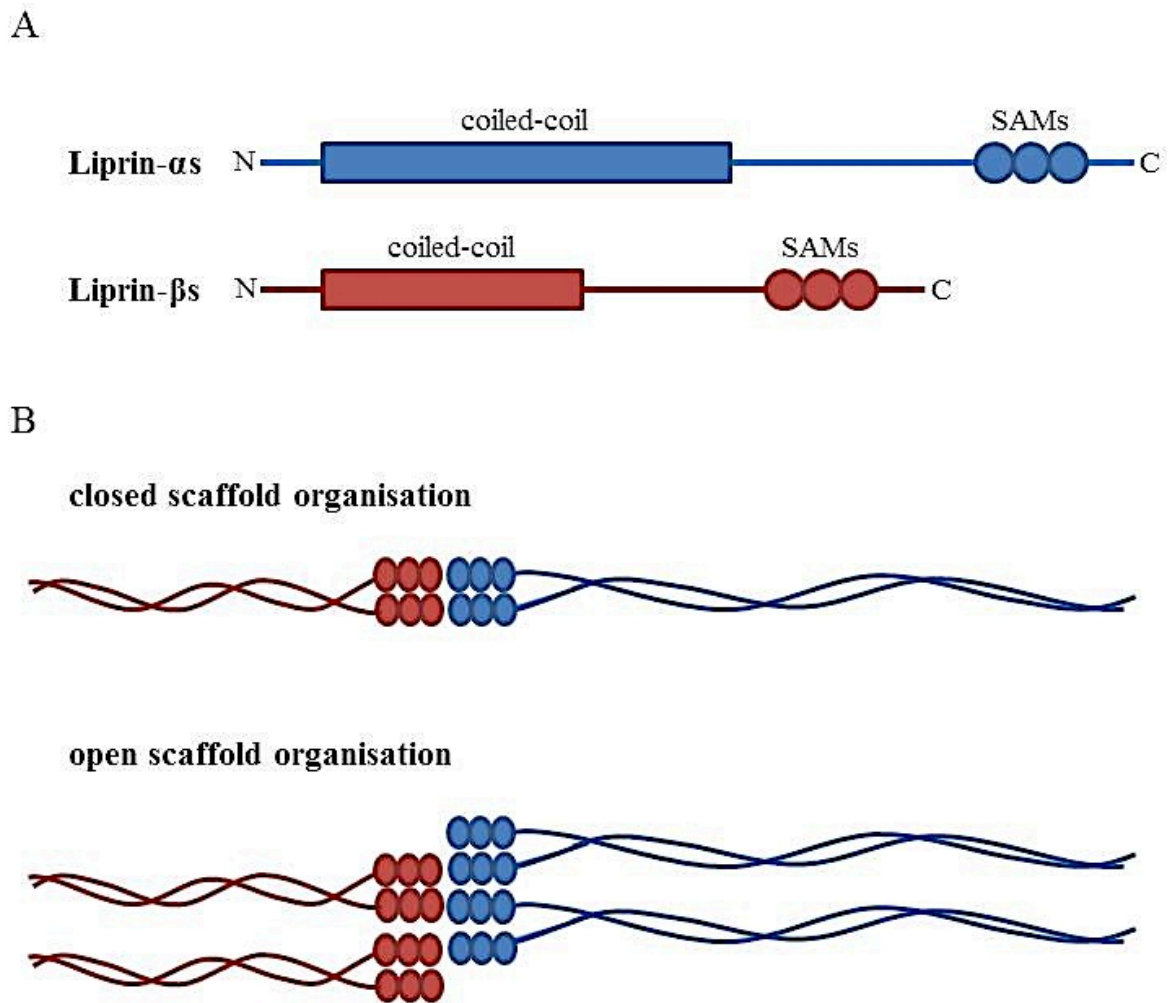


Figure 5-1 Schematic illustration of Liprin domain organisation and proposed complex formation
 A. The diagram shows the relative sizes and domain composition of Liprin- α s (blue) and Liprin- β s (red)
 B. Speculative scaffold organisations are depicted consisting of Liprin- α s and Liprin- β s. Interactions of the three tandem SAM domains can be arranged to form a “closed dimer” or an open scaffold consisting of multiple Liprin molecules.

<i>Gene ID</i>	<i>Gene name</i>	<i>Gene function</i>	<i>Ref.</i>
PPFIA1	Liprin-α1	Proposed scaffolding function for the recruitment and anchoring of LAR protein tyrosine phosphatases	[464]
PPFIA2	Liprin-α2		
PPFIA3	Liprin-α3		
PTPRC	Protein tyrosine phosphatase receptor type C	Essential regulator of B- and T-cell antigen receptor signalling	[464]
TSG101	Tumour susceptibility gene 101	Plays a role in late endosomal sorting as part of the ESCRT complex, frequently mutated in breast cancer	[523]
PRNP	Prion protein	Remains unclear	[415]
DTNB	Dystrobrevin beta	Component of the dystrophin-associated protein complex	[523]
14-3-3 σ		p53 effector, important in cell cycle control, expression frequently lost in cancer	[524]

Table 5-2 Overview of known and putative Liprin-β2 interaction partners as determined by high-throughput experiments

5.2 Results

5.2.1 *Knockdown of Rab17 and Liprin-β2 promotes tumour cell invasion of MDA-MB-231 cells*

To determine whether Rab17 and Liprin-β2 influence cell motility, we transiently knocked down their expression in MDA-MB-231 cells using siRNA SMARTpools (consisting of 4 individual short interfering RNA oligonucleotides). Using qRT-PCR we observed a 60% decrease in Rab17 mRNA levels (Figure 5-2 A) and an 80% reduction in Liprin-β2 transcript levels (Figure 5-2 B), suggesting an efficient knockdown of either gene.

Having confirmed the efficacy of Rab17 and Liprin-β2 suppression, we performed inverted invasion assays to test whether this change in gene expression would affect tumour cell invasion into fibronectin-containing Matrigel. Interestingly, knockdown of Rab17 increased the invasiveness by approximately 100% ($p \leq 0.01$). Likewise, silencing of Liprin-β2 significantly promoted invasion of MDA-MB-231 cells into Matrigel plugs ($p \leq 0.05$) (Figure 5-2 C/D). Taken together, this data suggests both Rab17 and Liprin-β2 act as inhibitors of invasive cell migration.

Next we wanted to investigate whether this increase in invasiveness was mirrored by changes in migration on CDM. To this end, MDA-MB-231 cells depleted for either Rab17 or Liprin-β2 were seeded onto CDM and their motility was monitored using a Nikon time-lapse microscope over the course of 16 hours. Interestingly, we observed a marginal but significant decrease in the overall migration velocity when Rab17 was depleted (Figure 5-3 B). In addition, the persistence of cell migration was strongly increased following Rab17 silencing ($p \leq 0.0001$) (Figure 5-3 C). In contrast, knockdown of Liprin-β2 did not have an effect on the overall migration velocity, but significantly increased the migration persistence ($p \leq 0.05$) when compared to NT siRNA-transfected cells (Figure 5-3 B/C).

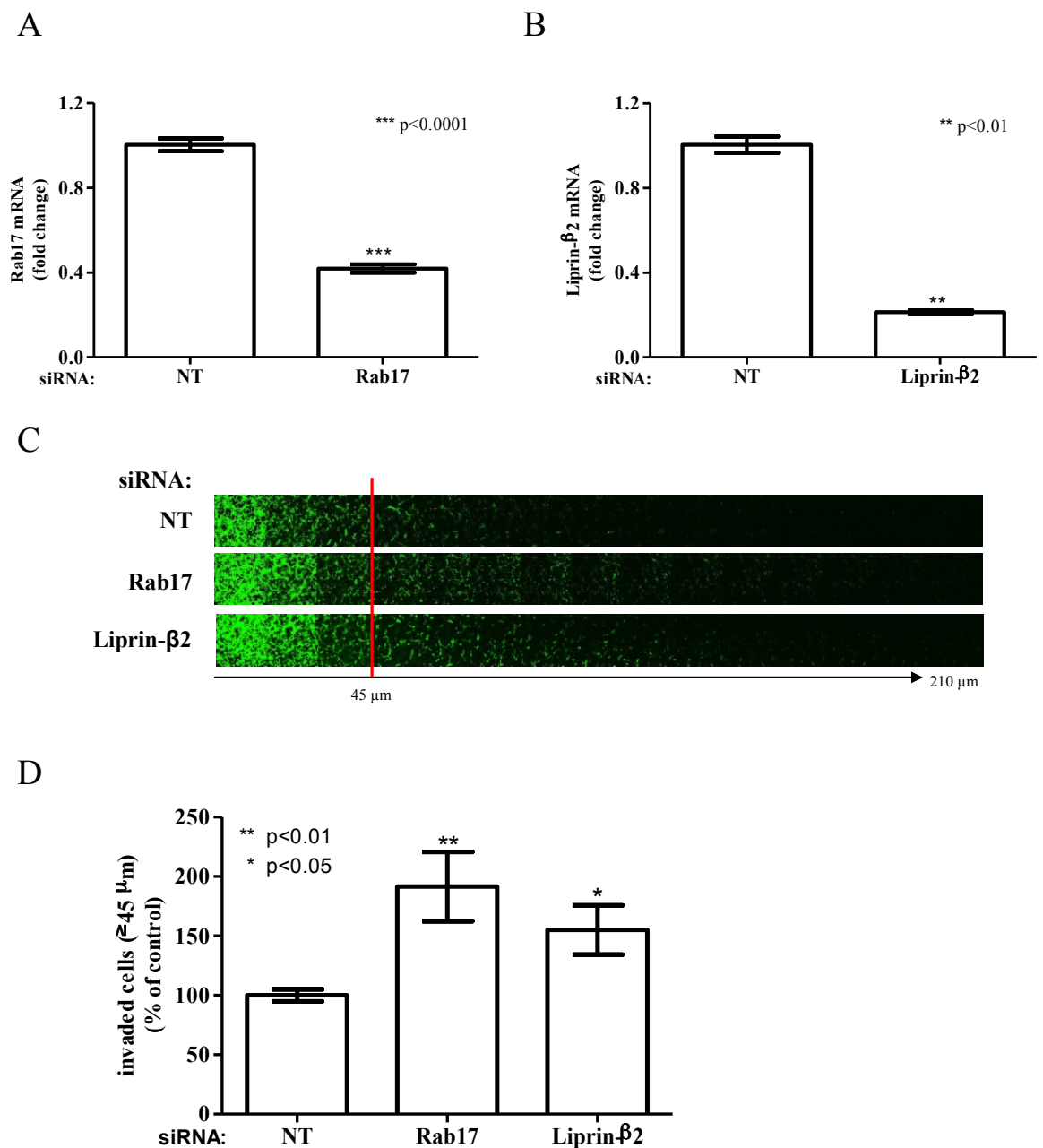


Figure 5-2 Suppression of Rab17 and Liprin-β2 promotes invasiveness of MDA-MB-231 cells

A-B. MDA-MB-231 cells were transfected with non-targeting siRNAs (NT), or SMARTpools targeting Rab17 or Liprin-β2. The effectiveness of the knockdown was assessed by qRT-PCR 48 hrs post transfection. Statistical significance of differences was determined by Mann-Whitney *U* test analysis.

C. Matrigel plugs were enriched with 25 μg/ml fibronectin and 4x10⁴ cells were plated onto the underside of each Transwell 24 hrs post nucleofection. 36 hrs following this, invading cells were visualized by Calcein-AM staining. Serial optical sections were captured every 15 μm and are presented as a sequence in which the depth increases from left to right.

D. Invasive migration was quantified by measuring the fluorescence intensity of cells penetrating the Matrigel plug to depths of ≥ 45 μm and expressed relative to cells transfected with non-targeting (NT) siRNA. Values are means ± standard error of the mean (SEM) of 18 replicates from three independent experiments. Statistical significance of differences was determined by Mann-Whitney *U* test analysis.

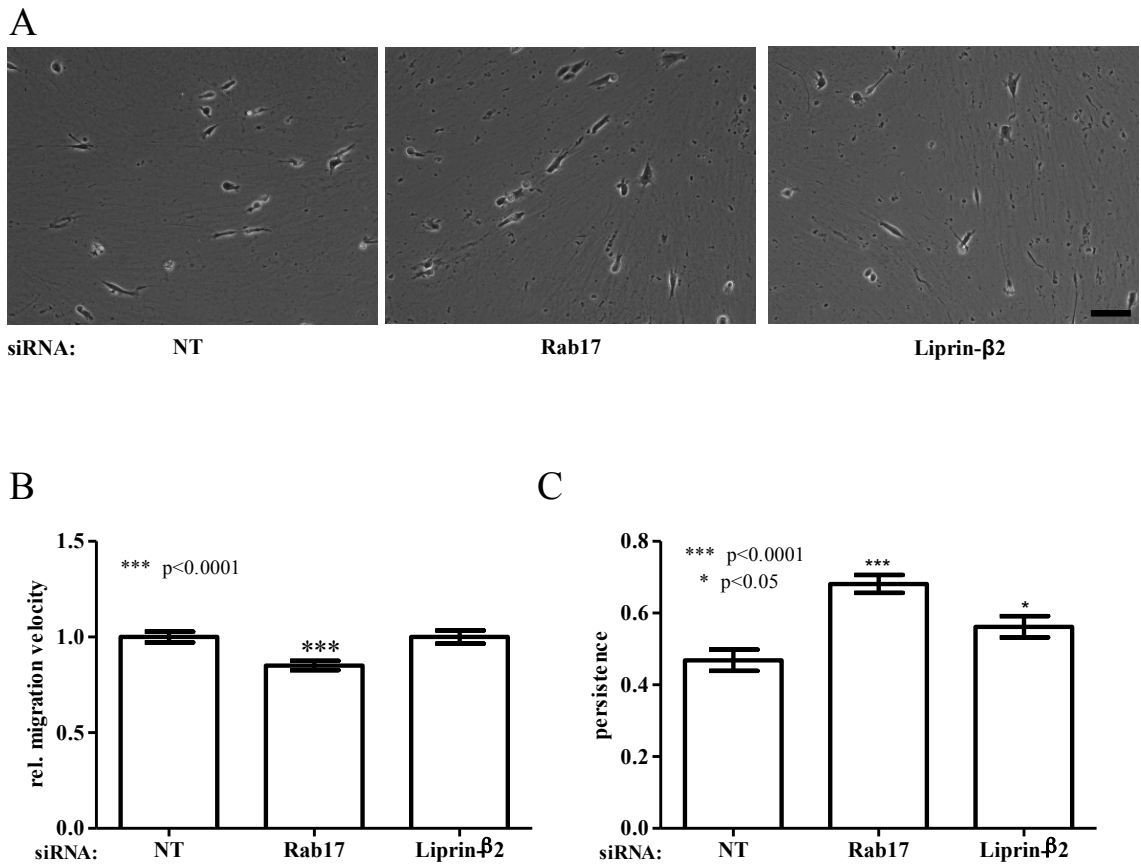


Figure 5-3 Knockdown of Rab17 and Liprin-β2 increases persistence of MDA-MB-231 cells on CDM
 A. MDA-MB-231 cells were transfected with non-targeting siRNAs (NT), or those targeting Rab17 or Liprin-β2 and plated onto cell-derived matrix. Images were captured every 10 minutes over a 16 hrs period using a Nikon time-lapse microscope. Still images from a representative movie are displayed. Scale bar, 100 μm.

B-C. The movement of individual cells was followed using the ImageJ cell tracking software. The overall migration velocity (B) and persistence (C) were extracted from the trackplots. Values are means ± SEM of >75 trackplots from three independent experiments. Statistical significance of differences was determined by Mann-Whitney *U* test analysis.

5.2.2 Depletion of Rab17 and Liprin- β 2 promote invasion of A2780-Rab25 and BE cells

To assess whether Rab17's and Liprin- β 2's inhibitory role on invasive cell migration was specific to MDA-MB-231 cells or more generally applicable, we decided to also perform invasion assays in two additional cell lines: (i) A2780 ovarian carcinoma cells stably transfected with Rab25 and (ii) BE colon carcinoma cells. A2780-Rab25 and BE cells were transfected with non-targeting siRNA oligos, or those targeting Rab17 and Liprin- β 2. qRT-PCR revealed a 50% and 60% knockdown of Rab17 mRNA levels in A2780-Rab25 and BE cells, respectively ($p \leq 0.01$) (Figure 5-4 A). Likewise, Liprin- β 2 transcript levels were significantly diminished by siRNA in both cell lines (Figure 5-4 B). Silencing of Rab17 in either A2780-Rab25 or BE cells significantly increased the invasiveness by 50% ($p \leq 0.01$) or 200% ($p \leq 0.0001$), respectively (Figure 5-4 C/D). Similarly, suppression of Liprin- β 2 by RNAi significantly increased the propensity of A2780-Rab25 (increase of 50%, $p < 0.001$) and BE cells (increase of 300%, $p < 0.01$) to invade into Matrigel (Figure 5-4 C/D). Taken together, these data suggest that Rab17 and Liprin- β 2 act as inhibitors of invasive cell migration into fibronectin-supplemented Matrigel plugs.

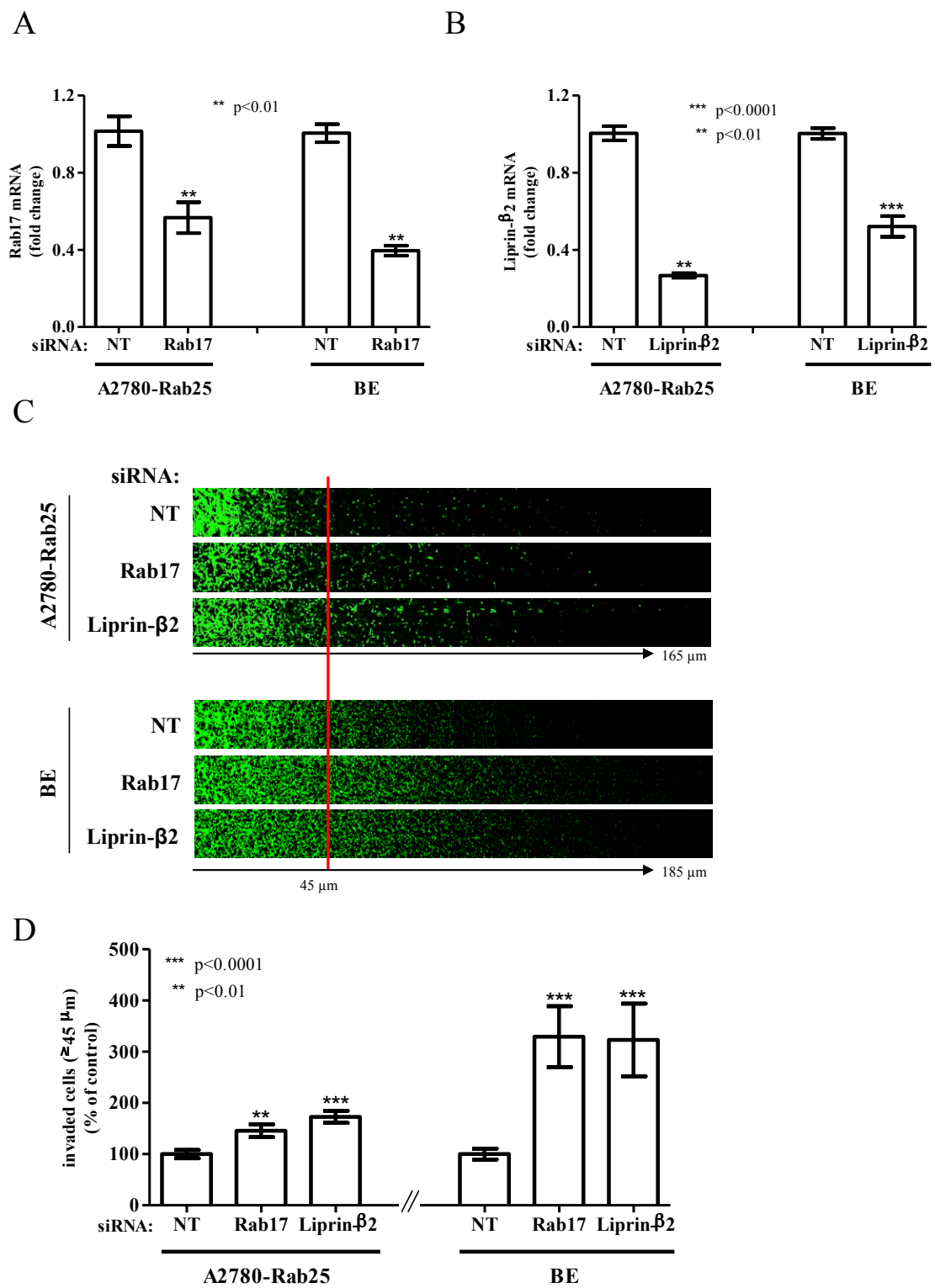


Figure 5-4 Depletion of Rab17 and Liprin-β2 promotes invasiveness of A2780-Rab25 and BE cells

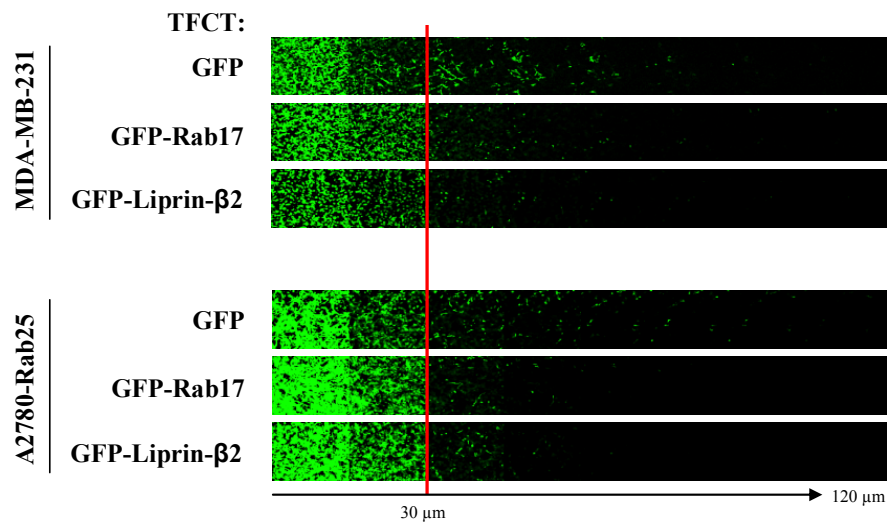
A-B. A2780-Rab25 and BE cells were transfected with non-targeting siRNAs (NT), or SMARTpools targeting Rab17 or Liprin-β2. Efficiency of the knockdown was assessed by qRT-PCR 48 hrs post transfection. Statistical significance of differences was determined by Mann-Whitney *U* test analysis. C. Matrigel plugs were enriched with 25 μg/ml fibronectin and 3×10⁴ cells were plated onto the underside of each Transwell 24 hrs post nucleofection. 36 hrs following this, invading cells were visualized by Calcein-AM staining. Serial optical sections were captured every 15 μm and are presented as a sequence in which the depth increases from left to right.

D. Invasive migration was quantified by measuring the fluorescence intensity of cells penetrating the Matrigel plug to depths of ≥ 45 μm and expressed relative to cells transfected with non-targeting (NT) siRNA. Values are means ± standard error of the mean (SEM) of 18 replicates from three independent experiments. Statistical significance of differences was determined by Mann-Whitney *U* test analysis.

5.2.3 Overexpression of Rab17 and Liprin-β2 impairs invasion into Matrigel and migration on cell-derived matrix

Given that knockdown of either Rab17 or Liprin-β2 promoted invasiveness, we wanted to investigate whether their overexpression would decrease the propensity of MDA-MB-231 or A2780-Rab25 cells to invade into Matrigel plugs or to migrate on CDM. To do this, cells were transfected with an empty vector control (pEGFP-C1), pEGFP-Rab17 and pCMV6-AC-GFP-Liprin-β2. Ectopic expression of all plasmids was ensured by visual inspection of the cells on a fluorescent microscope prior to setting up inverted invasion assays. Expression of GFP alone reduced the invasive potential of both cancer cell lines and prompted us to compare the relative percentage of cells that migrated beyond 30 μm rather than 45 μm. Recombinant expression of GFP-Rab17 or GFP-Liprin-β2 significantly reduced invasion of MDA-MB-231 cells by ≥ 50% ($p \leq 0.0001$) when compared to GFP alone (Figure 5-5). Consistent with this, we observed a 68% decrease in invasion ($p \leq 0.0001$), when the GFP-tagged proteins were overexpressed in A2780-Rab25 cells. We also observed a significant decrease in the overall migration velocity of MDA-MB-231 cells plated onto CDM following expression of either ectopic Rab17 or Liprin-β2 when compared to GFP alone (data not shown), and this was owing to both a decrease in the momentary velocity of moving cells (Figure 5-6 B) and an increase in cellular resting (Figure 5-6 C). Thus, our data indicates that Rab17 and Liprin-β2 act to restrict carcinoma cell migration in 3D microenvironments in much the same way as does knockdown of ERK2.

A



B

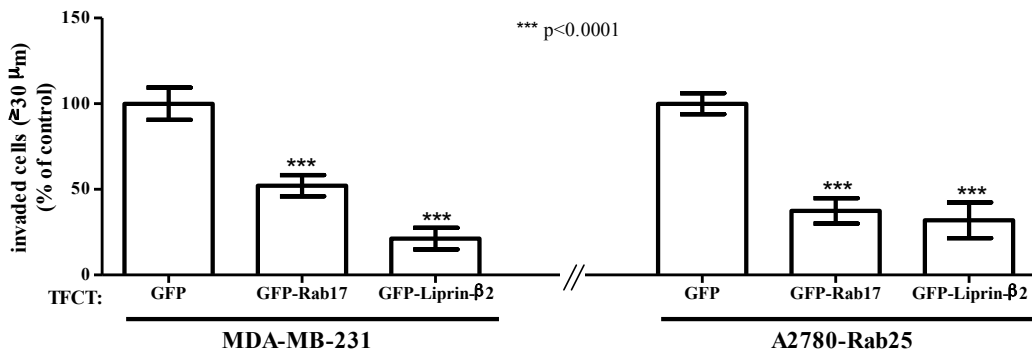


Figure 5-5 Ectopic expression of Rab17 or Liprin-β2 suppresses invasiveness MDA-MB-231 and A2780-Rab25 cells

MDA-MB-231 and A2780-Rab25 cells were transfected with GFP alone, GFP-Rab17 or GFP-Liprin-β2. Expression of various constructs was verified by eye on a fluorescent microscope 24 hrs post nucleofection. A. Respective cells were plated onto plugs of fibronectin-supplemented Matrigel. 36 hrs following this, invading cells were visualized by Calcein-AM staining. Serial optical sections were captured every 15 μm and are presented as a sequence in which the depth increases from left to right. B. Invasive migration was quantified by measuring the fluorescence intensity of cells penetrating the Matrigel plug to depths of $\geq 30 \mu\text{m}$ and expressed relative to cells transfected with empty vector control. Values are means \pm standard error of the mean (SEM) of 18 replicates from three independent experiments. Statistical significance of differences was determined by Mann-Whitney *U* test analysis.

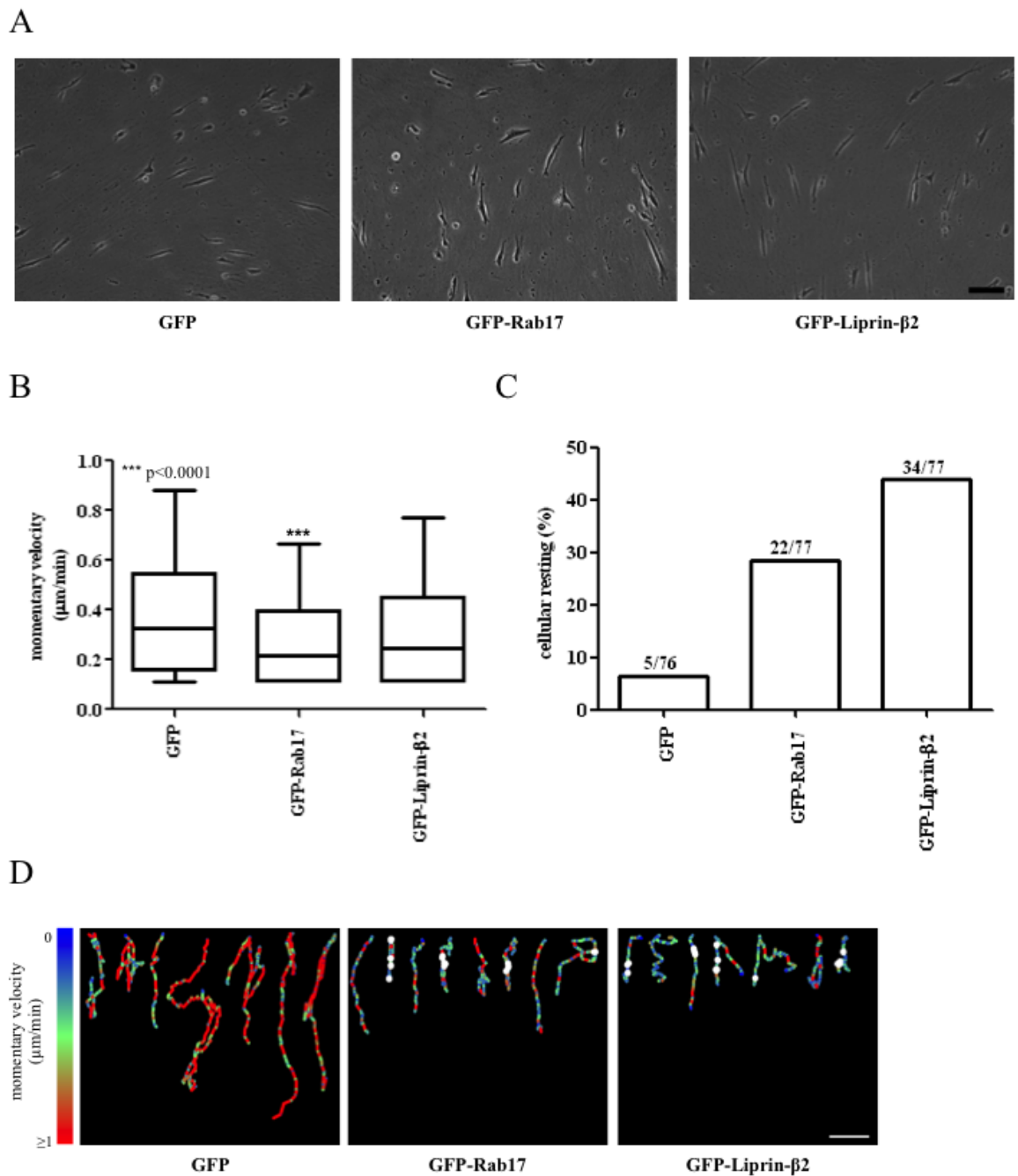


Figure 5-6 Ectopic expression of Rab17 or Liprin-β2 decreases the momentary velocity and increases cellular resting in MDA-MB-231 cells

MDA-MB-231 cells were transfected with empty vector control (GFP alone), GFP-Rab17 or Liprin-β2, and plated onto cell-derived matrix. Images were captured every 10 minutes over a 16 hrs period. Cell movement was followed using cell-tracking software.

A. Still images from a representative movie are displayed. Scale bar, 100 μm.

B. Momentary migration velocities were calculated for each timeframe of the time-lapse experiment giving rise to over 7,000 values for each condition. Values are represented as box and whisker plots (whiskers: 10-90 percentile) and represent three independent experiments. Statistical significance of differences was determined by Mann-Whitney *U* test analysis.

C. Cellular resting was extracted from manual cell tracking and represents means ± SEM of three independent experiments. Percentage of resting cells is displayed with absolute numbers for each condition above each column.

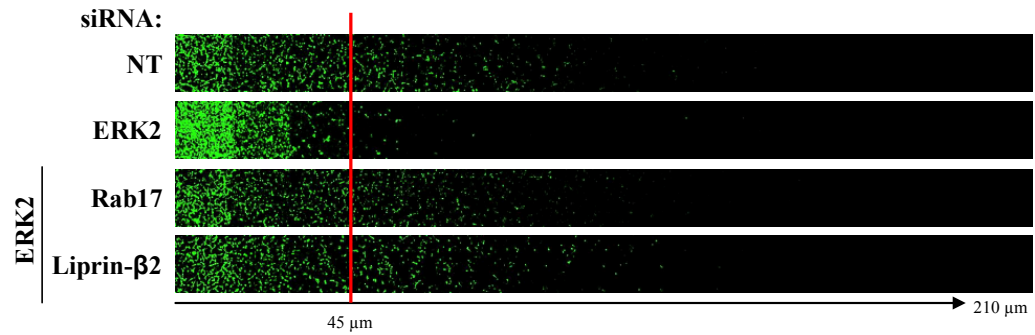
D. Representative migration trackplots are displayed. The migration speed is denoted by a colour code, the scale of which is indicated on the left side of the panels. The points at which cells moved less than 2 μm in 90 min (cellular resting) are indicated by white dots. Scale bar 100 μm.

5.2.4 ERK2 drives invasive cell migration of MDA-MB-231 cells by suppressing expression of Rab17 and Liprin-β2

Having established that Rab17 and Liprin-β2 act to restrict tumour cell invasion into Matrigel plugs and migration on CDM, we wished to determine to what extent ERK2's suppression of Rab17 and Liprin-β2 was responsible for the kinase's ability to drive invasion. To do this, we silenced ERK2 in combination with knockdown of either Rab17 or Liprin-β2 and carried out invasion assays. Interestingly, siRNA of Rab17 restored invasion of ERK2 knockdown cells to levels comparable to control cells (Figure 5-7). In addition, concomitant silencing of Liprin-β2 with ERK2 not only restored the invasive phenotype of MDA-MB-231 cells, but also enhanced the invasive capacity when compared to control transfected cells ($p \leq 0.05$) (Figure 5-7). Consistent with this, we found that concomitant knockdown of Rab17 or Liprin-β2 with ERK2 increased the momentary velocity and reduced the tendency of ERK2 knockdown cells to pause (cellular resting), whilst migrating on CDM (Figure 5-8). To strengthen these observations made using SMARTpool siRNAs, we repeated the motility studies on CDM with two independent oligos to target Rab17 and Liprin-β2. Firstly, we examined the knockdown efficiency of the four RNA duplexes constituting the SMARTpool and chose two RNA duplexes, which demonstrated the most efficient knockdown (data not shown). Indeed, both of the duplexes chosen to suppress Rab17 and Liprin-β2 were able to reverse the effect that ERK2 knockdown had on momentary velocity and cellular resting on CDM (Figure 5-8).

Taken together these data indicate that *rab17* or *liprin-β2* are novel motility suppressor genes, and in order to drive invasion and migration of carcinoma cells in 3D microenvironments, ERK2 must reduce the expression of at least one of these genes.

A



B

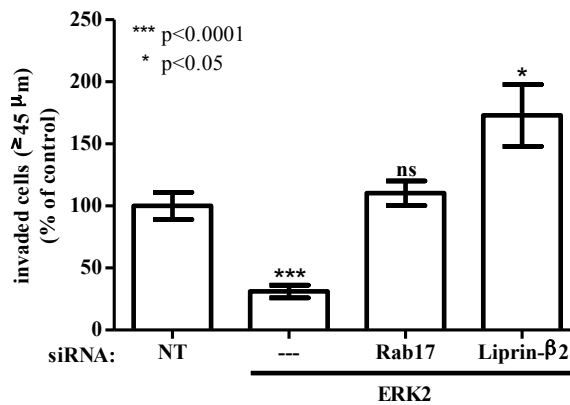


Figure 5-7 siRNA of Rab17 or Liprin-β2 restores the invasiveness of ERK2 knockdown cells

MDA-MB-231 cells were transfected with non-targeting siRNAs (NT), or siRNAs targeting ERK2 in combination those targeting Rab17 or Liprin-β2.

A. Cells were plated onto plugs of fibronectin-supplemented Matrigel. 36 hrs following this, invading cells were visualized by Calcein-AM staining. Serial optical sections were captured every 15 μm and are presented as a sequence in which the depth increases from left to right.

B. Invasive migration was quantified by measuring the fluorescence intensity of cells penetrating the Matrigel plug to depths of ≥ 45 μm and expressed relative to cells transfected with non-targeting (NT) siRNA. Values are means ± standard error of the mean (SEM) of 18 replicates from three independent experiments. Statistical significance of differences was determined by Mann-Whitney *U* test analysis.

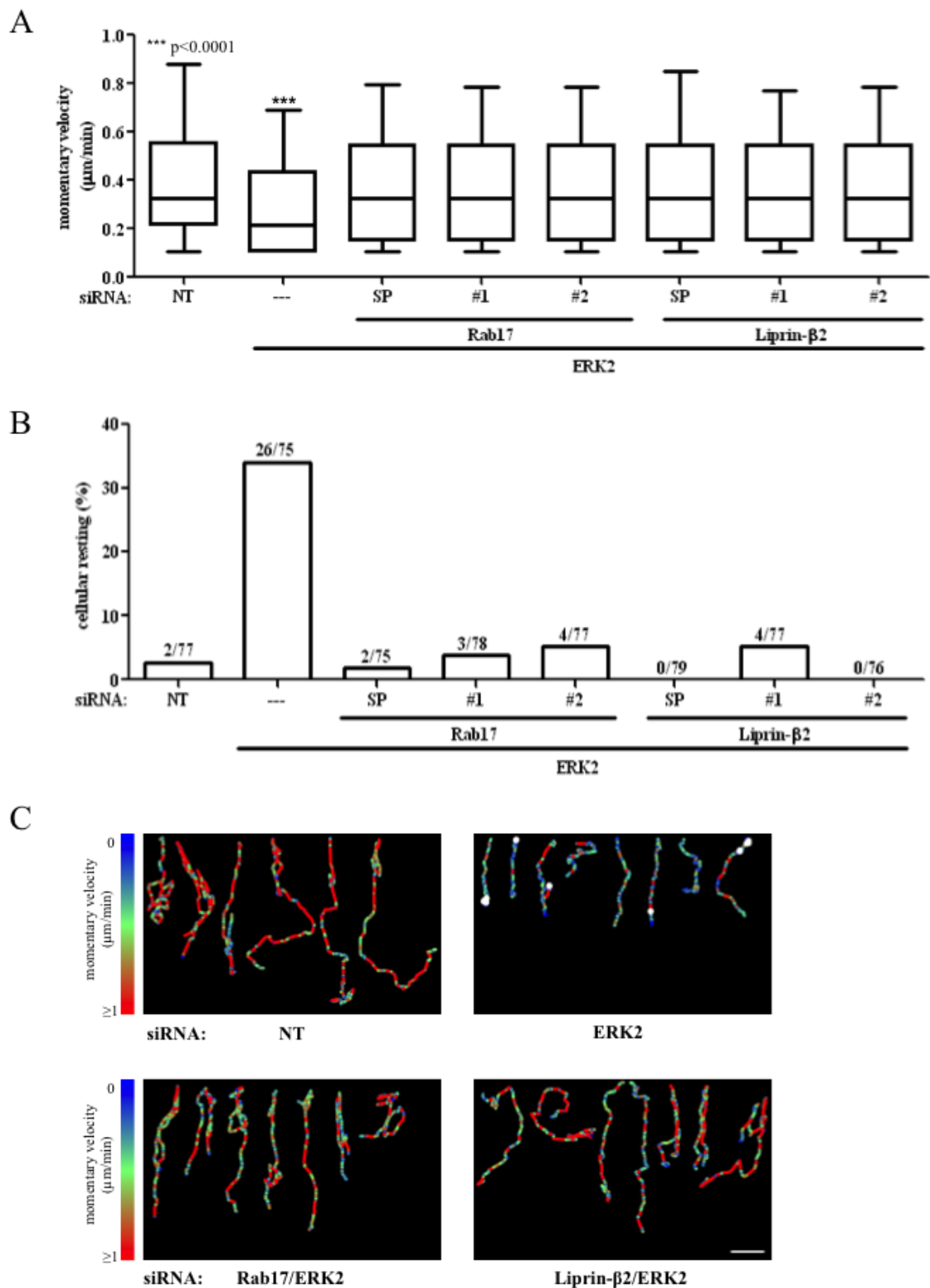


Figure 5-8 Suppression of Rab17 and Liprin- β 2 restores the migratory characteristics of ERK2 knockdown cells

MDA-MB-231 cells were transfected with non-targeting siRNAs (NT), or siRNAs targeting ERK2 in combination those targeting Rab17 or Liprin- β 2 and plated onto cell-derived matrix. Images were captured every 10 minutes over a 16 hrs period. Cell movement was followed using cell-tracking software. (see next page also)

A. Momentary migration velocities were calculated for each timeframe of the time-lapse experiment giving rise to over 7,000 values for each condition. Values are represented as box and whisker plots (whiskers: 10-90 percentile) and represent three independent experiments. “SP” denotes SMARTpool. Statistical significance of differences was determined by Mann-Whitney U test analysis.

B. Cellular resting was extracted from manual cell tracking and represents means \pm SEM of three independent experiments. Percentage of resting cells is displayed with absolute numbers for each condition above each column.

C. Representative migration trackplots are displayed. The migration speed is denoted by a colour code, the scale of which is indicated on the left side of the panels. The points at which cells moved less than 2 μ m in 90 min (cellular resting) are indicated by white dots. Scale bar 100 μ m.

5.2.5 ERK2 drives migration on plastic surfaces but not through Rab17 and Liprin- β 2

In chapter 3 we established that silencing of ERK2 (but not ERK1) in MDA-MB-231 cells impaired cell migration on CDM and plastic surfaces. Thus, motility of these cells is dependent on ERK2 signalling irrespective of the microenvironment. Moreover, in chapter 4 we demonstrated that ERK2 suppressed expression of Rab17 and Liprin- β 2 on CDM as well as on plastic surfaces. We, therefore, wished to investigate the requirement for suppression of Rab17 and Liprin- β 2 in ERK2-dependent cell migration into scratch wounds. To do this, we silenced Rab17 and Liprin- β 2 in ERK2 knockdown cells and measured the speed, persistence and FMI of cell migration into scratch wounds. As before, knockdown of ERK2 (but not ERK1) significantly reduced the migratory speed of cells closing the scratch wound (Figure 5-9 A). However, by contrast with the situation in 3D microenvironments, siRNA of Rab17 and Liprin- β 2 in combination with ERK2 was not sufficient to restore the migration velocity of ERK2 knockdown cells (Figure 5-9 A), although the persistence of Rab17 and Liprin- β 2 knockdown cells was marginally increased (Figure 5-9 B/C). Taken together, these data indicate that although ERK2 controls cell movement in 3D microenvironments by suppressing Rab17 and Liprin- β 2, the pathways by which ERKs control cell migration on plastic do not involve these two novel ERK2 effectors.

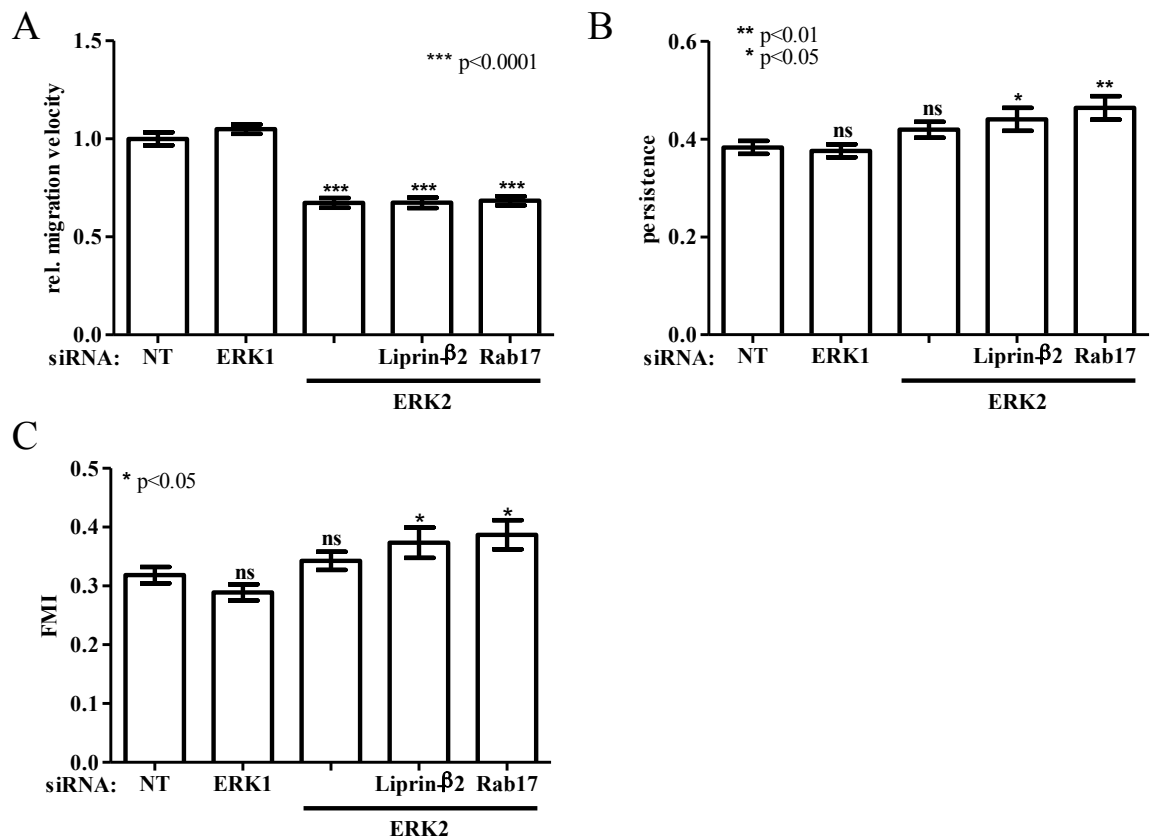


Figure 5-9 RNAi of Rab17 and Liprin-β2 does not restore motility defects of ERK2 knockdown cells on plastic

A-C. MDA-MB-231 cells were transfected with non-targeting siRNAs (NT), or siRNAs targeting ERK2 in combination those targeting Rab17 or Liprin-β2. Subsequently, cells were seeded into a 6-well dish, so that they were confluent 48 hrs post nucleofection. After scratching, wound closure was monitored and the movement of individual cells was followed using ImageJ cell tracking software. The overall migration velocity (A), persistence (B) and forward migration index (FMI) (C) were extracted from the trackplots. Values are means ± SEM of >75 trackplots from three independent experiments. Statistical significance of differences was determined by Mann-Whitney *U* test analysis.

5.2.6 Rab17 localises to early and recycling endosomes

Rab17 is thought to play a role in vesicular transport. To characterise vesicles to which Rab17 localises in tumour cell lines, we ectopically expressed the GTPase tagged to either mCherry or GFP in both MDA-MB-231 and A2780-Rab25 cells. Live cell imaging indicated that Rab17 (irrespective of the tag) localised to vesicular-type structures that were dynamic and in constant movement (data not shown). Intriguingly, small Rab17-positive vesicles localised mainly to the peripheral cytoplasm, while larger vesicles were found in the perinuclear region. Next, we overexpressed Rab17, plated cells on fibronectin-coated, collagen-coated or uncoated coverslips and fixed cells with 4% paraformaldehyde. Fixation did not alter the distribution of the Rab17-positive vesicles, nor did the addition of fibronectin or collagen affect the distribution of Rab17 vesicles (data not shown). We then stained for endogenous protein (such as EEA1) or overexpressed fluorescently labelled marker proteins, such as Rab11, Rab7 and Sialin in combination with Rab17. Confocal imaging identified Rab17 on all EEA1 positive early endosomes. Moreover, Rab17 partially co-localised with recycling endosomes as marked by GFP-Rab11. In contrast we observed no co-localisation of Rab17 with late endosomes as marked by Rab7, or with Sialin-positive lysosomes (Figure 5-10). Thus, Rab17 localises predominantly to early endosomes, but also to some centrally located recycling compartments.

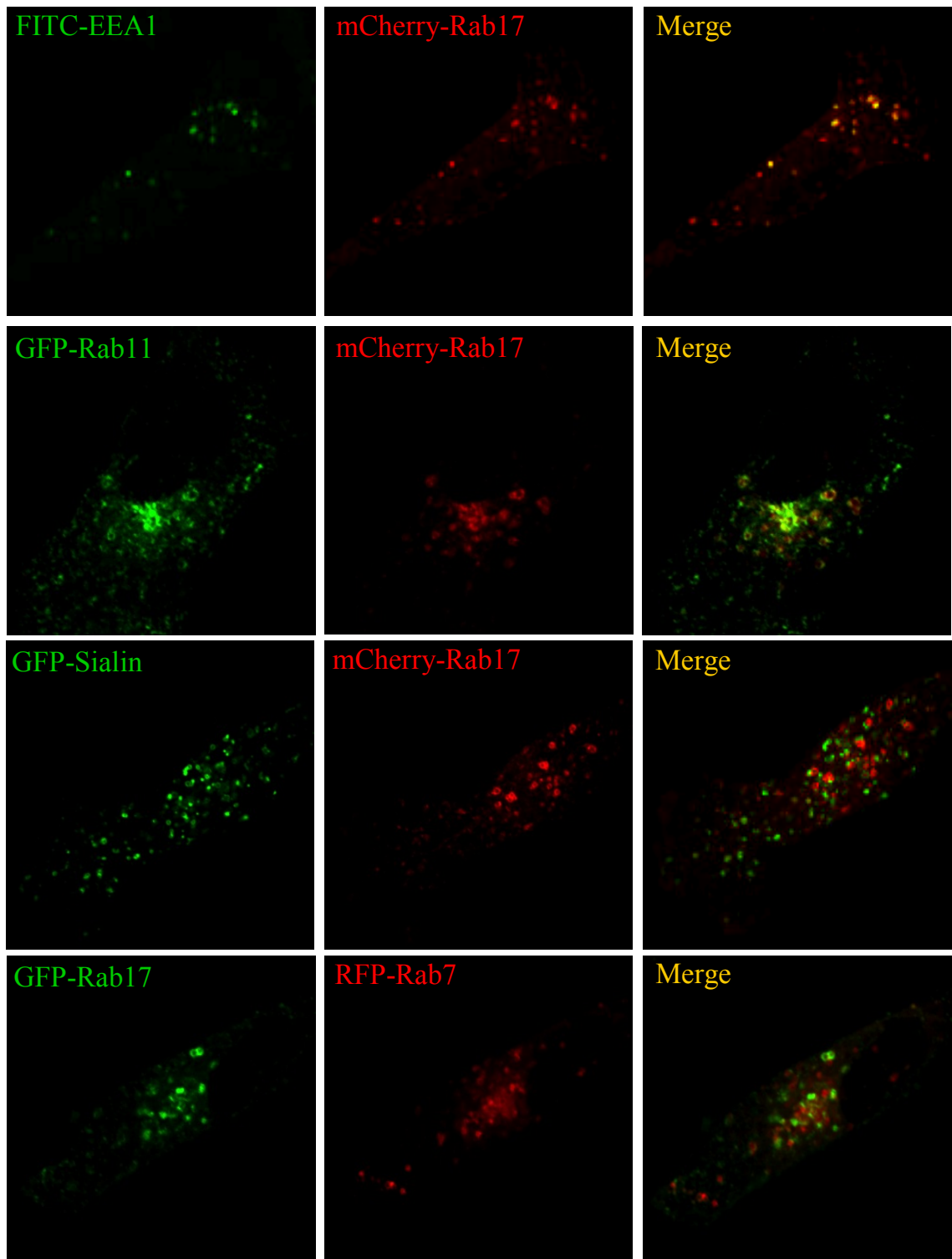


Figure 5-10 Rab17 associates with early and recycling endosomes

MDA-MB-231 cells were transfected as stated below, seeded onto coverslips and fixed with 4% paraformaldehyde 24 hrs after transfection. Co-localisation was examined using a confocal microscope. Scale bars, 10 μ m.

- A. Fixed cells were permeabilised and stained for endogenous early endosome antigen 1 (EEA1) (green).
- B. GFP-Rab11 (green) and mCherry-Rab17 (red) were co-transfected.
- C. GFP-Rab17 (green) and RFP-Rab7 (red) were co-transfected.
- D. GFP-Sialin (green) and mCherry-Rab17 (red) were co-transfected.

5.2.7 Rab17 vesicles are positive for β 1 integrin

Enhanced β 1 integrin recycling is known to be associated with the invasiveness of cancer cell lines [380, 525]. To initiate studies to determine whether Rab17 expression affected β 1 integrin trafficking, we expressed mCherry-Rab17 and stained for endogenous β 1 integrin. Rab17 was associated with a subset of vesicles, whose lumen stained positive for β 1 integrin (Figure 5-11 A), indicating that the GTPase may be involved in sorting and/or recycling of this integrin receptor.

A previous study by Pellinen et al. identified the small GTPase Rab21 as a regulator of cell adhesion and endosomal trafficking of β 1 integrin. Moreover, Rab21 was shown to directly interact with β 1 integrin's cytoplasmic tail in co-immunoprecipitation studies [526]. Given that Rab21, like Rab17, belongs to the Rab5 family of small GTPases, we postulated that Rab17 may compete with Rab21 for β 1 integrin binding. To test this idea, we nucleofected MDA-MB-231 cells with an empty vector control (GFP alone) or GFP-Rab17, harvested cells 24 hours post transfection and co-immunoprecipitated with an antibody recognising GFP. We were not able to demonstrate a physical interaction between Rab17 and β 1 integrin (Figure 5-11), suggesting that Rab17 associates to β 1 integrin-containing vesicles by binding to other cargo molecules or adaptor proteins.

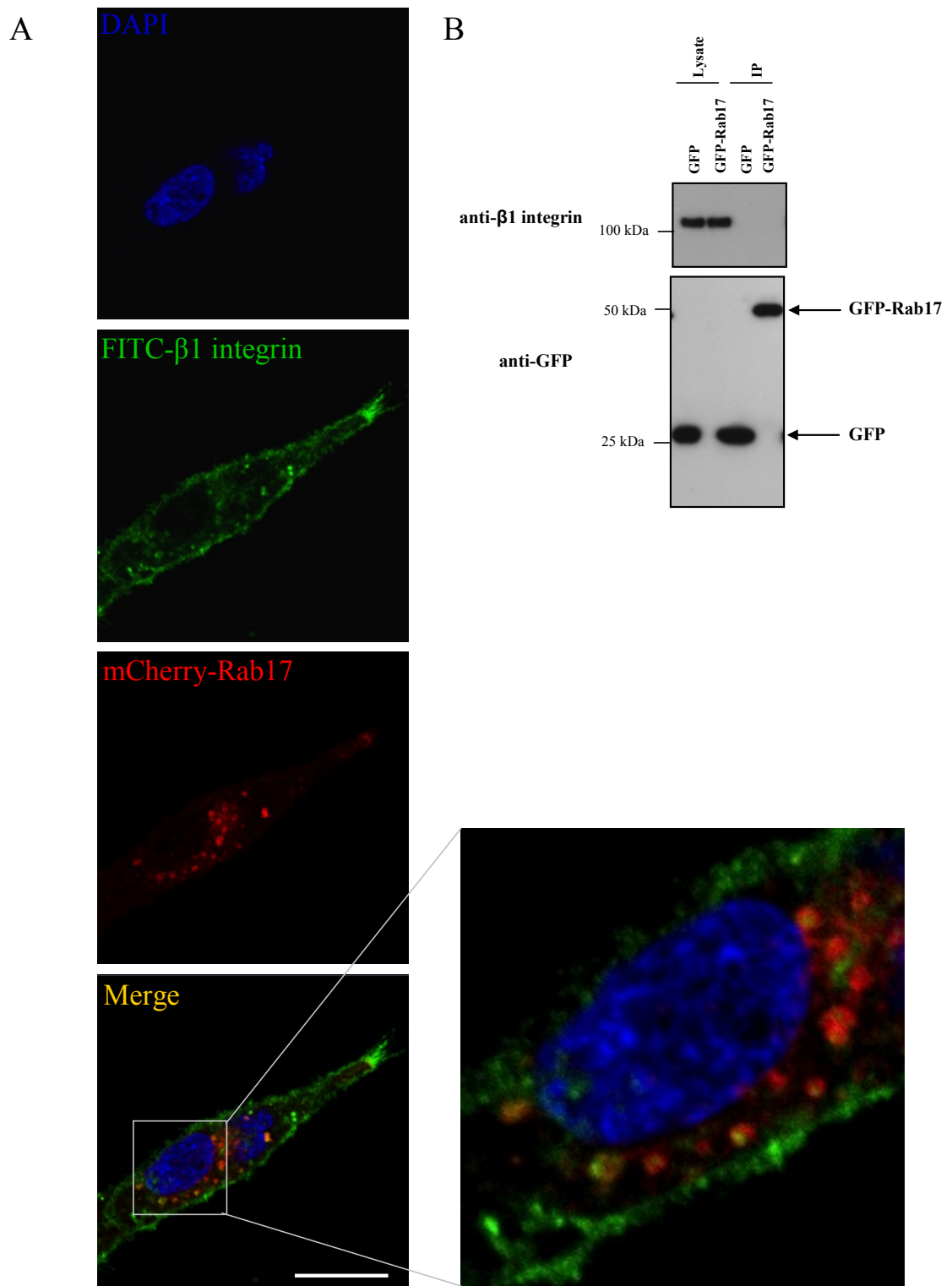


Figure 5-11 Rab17 associates with $\beta 1$ integrin-positive vesicles

A. MDA-MB-231 cells were transfected with mCherry-Rab17, seeded onto coverslips and fixed with 4% paraformaldehyde 24 hrs after transfection. Cells were permeabilised with 0.02% Triton-X 100 and stained for endogenous $\beta 1$ integrin. Co-localisation was examined using a confocal microscope. Scale bars, 20 μm .
 B. MDA-MB-231 cells were transfected with empty vector control (GFP alone) or GFP-Rab17, immunoprecipitated using a GFP-antibody (mouse) and blotted with anti-GFP (rabbit) and anti- $\beta 1$ integrin (mouse) antibodies.

5.3 Discussion

5.3.1 Summary

Here, we show that knockdown of Rab17 or Liprin- β 2 enhances invasiveness of three cancer cell lines, while their overexpression has the opposite effect. This suggests a role for both proteins in restricting carcinoma cell motility in 3D microenvironments. Importantly, knockdown of either Rab17 or Liprin- β 2 restores invasiveness of ERK2-depleted MDA-MB-231 cells, indicating that ERK2 drives invasion by suppressing expression of these genes. Characterisation of Rab17-positive vesicles demonstrated a potential role for this GTPase in regulating early endocytic events. Moreover, co-localisation of β 1 integrin within Rab17 vesicles, suggests a function of this GTPase in integrin trafficking.

5.3.2 Rab17 – a novel suppressor of cell motility

Rab17 has been shown to influence receptor-mediated transcytosis and recycling of receptors to the apical membrane in non-transformed epithelial cells [462, 498]. Recently, a study by Singh *et al.* found that Rab17 was one of many genes to be up-regulated in cancer cell lines exhibiting a more epithelial morphology, whereas the GTPase was down-regulated in cells displaying a more mesenchymal morphology [527]. This indicates that Rab17 is associated with the maintenance of a polarised epithelial morphology and might provide an explanation as to why Rab17 levels must be reduced in order for metastatic tumour cells to migrate with mesenchymal characteristics.

Given that Rab17 would be expected to control membrane trafficking, it is interesting to speculate as to how it might suppress cell migration. Recycling of α 5 β 1 integrin is known to be key to tumour cell migration and invasion [380, 525, 528] and our data suggests that overexpression of Rab17 leads to the accumulation of β 1 integrin within large endosomes to which Rab17 itself is localised. Taken together with reports suggesting that Rab17 opposes the return of receptors to the plasma membrane [462, 498], this moots that Rab17 may be an integrin recycling suppressor, whose expression must be reduced for cells to migrate efficiently. Moreover, as Rab17 has been proposed to interact with signalling molecules involved in receptor degradation, such as Rab7a, CHMP6 and Smurf2

(see Table 5-1), it is conceivable that the GTPase feeds receptors into the degradative pathway, thereby decreasing their recycling and ultimately inhibiting cell migration.

5.3.3 Liprin- β 2 – a novel inhibitor of cell motility

The role of Liprin family members, in particular the α -Liprins, has been well established in synaptic transmission. It is clear from reverse genetic studies in vertebrates, *Drosophila* and *C. elegans* that Liprin mutants have defects in synaptic vesicle transport, in which synaptic vesicles accumulate in axons [516]. Thus, Liprins control vesicular transport, and this is due to their ability to act as scaffolds to recruit and stabilise a number of different proteins to the sites of exocytosis [516].

Heterodimerisation of the two Liprin subclasses is thought to modify the biological functions of α -Liprins, who have been implicated in promoting tumour cell migration and invasion [518]. In fact, Liprin- α 1 is part of the human 11q13 chromosomal region that is frequently amplified in malignant tumours [529, 530] and was shown to regulate receptor clustering at neuronal plasma membranes by interacting with GIT1 (G protein-coupled receptor kinase interacting ArfGAP 1) [531]. Moreover, Liprin- α 1 binds to neuron-specific kinesin motor proteins, thereby regulating synaptic vesicle trafficking [532]. Consistent with this, Liprin- α 1 was shown to alter integrin trafficking, which may provide a means by which it contributes to cell migration [519]. In contrast to this pro-invasive function of Liprin- α 1, we identify Liprin- β 2 is a novel suppressor of cell migration and invasion downstream of ERK2. Thus, the question arises as to how two structurally related proteins can have such opposing functions. We may only speculate on this matter, as apart from structural data very little is known about the β -Liprins. Firstly, β -Liprins may act to antagonise the biological functions of α -Liprins by masking protein-protein interaction domains during heterodimerisation. Indeed, studies indicating that the C-terminal SAM domains also serve as docking platforms for protein kinases (e.g. calcium/calmodulin-dependent serine protein kinase) and phosphatases (e.g. LAR, PTP α and PTP δ) suggest that this is a possibility [464, 531]. Alternatively, heterodimerisation might introduce a conformational change in the N-terminal coiled-coil domain, thereby altering association with proteins such as GIT and the kinesin motor KIF1A [531, 532]. Furthermore, it is also possible that Liprin- β 2 might act to sequester α -Liprins to impair its function.

Interestingly, Liprin- α 1 is required for the correct subcellular localisation of ING4 (inhibitor of growth 4), a suppressor of cell spreading and cell migration, which impairs actin polymerisation at the cellular front [533]. Thus, Liprin- α 1 may represent a double-edged sword that can either promote or inhibit cell migration depending on its binding partners. Consistent with this idea, a recent report identified Liprin- α 1 as an inhibitor of cell invasion in head and neck squamous carcinoma cells [534]. As Liprin- β 2 may form a scaffold to organise α -Liprins, increased expression of Liprin- β 2 could promote the localisation of motility suppressors at the cellular front. Thus, depending on the molecular signature of the cell type Liprin- β 2 may enhance or decrease cell motility by organising Liprin- α s.

5.3.4 Rab17 and Liprin- β 2 - members of the same signalling circuit

In this chapter we showed that knockdown of either Rab17 or Liprin- β 2 was sufficient to restore invasiveness of ERK2-depleted MDA-MB-231 cells, which suggests that both proteins are part of the same signalling circuit. Given that Rab17 is expected to regulate membrane trafficking and Liprins have also been shown to control these processes, we would like to speculate as to how the two proteins may cooperate to inhibit receptor recycling and thereby inhibit cell migration.

We propose a role for Rab17 in vesicle sorting. Thus, increased expression of Rab17 may either promote receptor degradation, which ultimately reduces the amount of recycled receptors, or alter the recycling route from a short to a long loop. This means that silencing of Rab17 would decrease receptor degradation or change the recycling route, and ultimately stimulate cell migration. Liprin- β 2 may either act upstream or downstream of Rab17. One possibility is that the scaffold could impair receptor clustering at the plasma membrane, which would result in a decrease in endocytosis and diminish the internal receptor pool, which can be recycled back to the plasma membrane. If this was true, RNAi of Liprin- β 2 would promote cell motility by enhancing endocytosis and thus stimulating receptor cycling. Alternatively, Liprin- β 2 may also act downstream of the GTPase. Given that Liprins were shown to recruit and stabilise signalling molecules at the sites of exocytosis, augmented expression of Liprin- β 2 may slow the trafficking of recycling endosomes or impair fusion events at the plasma membrane (Figure 5-12). Taken together, we believe that knockdown of either Rab17 or Liprin- β 2 may change the

dynamics of receptor recycling to promote cell motility. Future work studying receptor internalisation, recycling and degradation when either proteins are depleted or overexpressed should shed light on the signalling hierarchy and molecular mechanism with which both Rab17 and Liprin- β 2 impair cell motility.

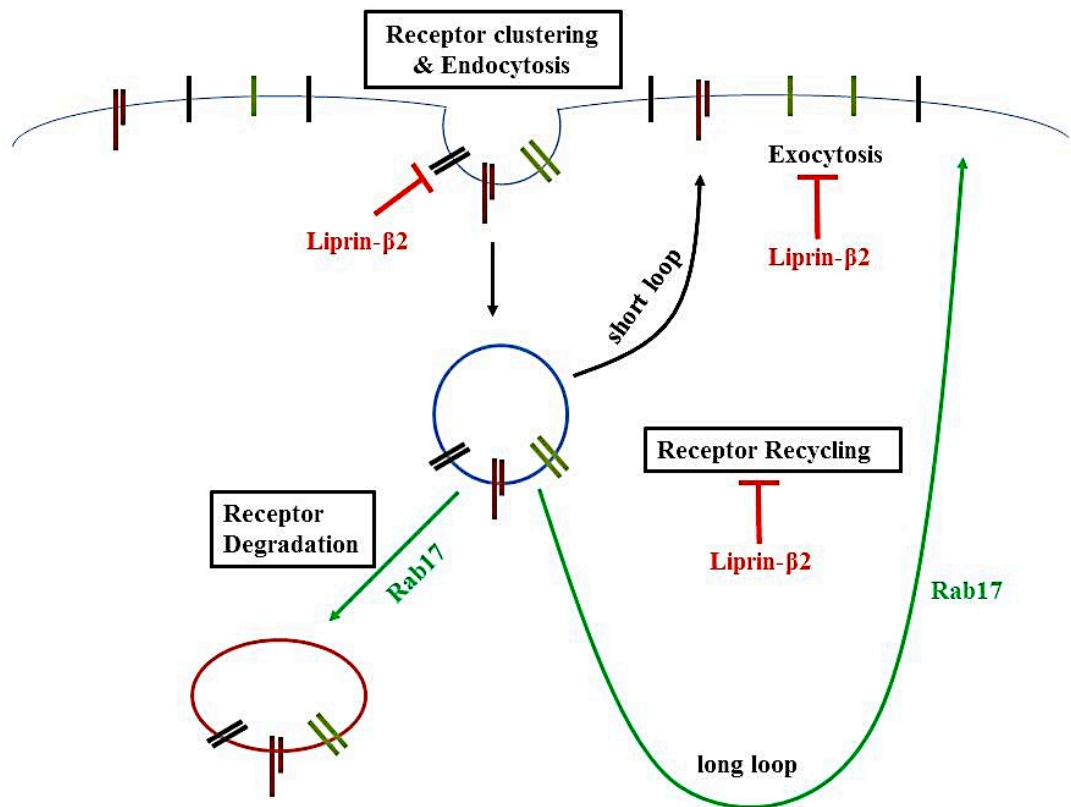


Figure 5-12 Working paradigm

Schematic illustration on how Liprin-β2 and Rab17 may cooperate to impair receptor recycling. Liprin-β2 may act upstream of Rab17 by impairing receptor clustering or internalisation. Alternatively, Liprin-β2 may affect receptor recycling by slowing down vesicle trafficking or preventing exocytosis of recycling vesicles. Rab17 may act to impair cell motility by either promoting receptor degradation or changing the recycling route from a short to a long loop.

5.3.5 Rab17 and Liprin- β 2 and their potential roles in cancer

We have demonstrated an inhibitory role for Rab17 and Liprin- β 2 in tumour cell invasion in three independent carcinoma cell lines, suggesting that this suppressive function may be generally applicable in cancer. Indeed, when assessing the expression profile of both proteins in cancer (using the oncomine database [535]), we found a frequent decrease of Rab17 and Liprin- β 2 transcript levels in tumour tissues (Figure 5-13). However, changes in mRNA levels do not necessarily correlate with changes in respective protein levels [536]. Thus, loss of expression of these proteins should ideally be determined by immunohistochemical profiling of tissue microarrays. Yet, the current lack of antibodies recognising the endogenous protein prevented us from addressing this issue. Future studies will have to determine whether loss of Rab17 and/or Liprin- β 2 correlates with poor prognosis and overall survival and whether there are certain subtypes of cancer, which are more or less dependent on the expression of both proteins. Given that Rab17 is highly expressed in the kidney and expression levels are markedly reduced in all kidney tumour samples assessed in the oncomine database (Figure 5-13 A), the GTPase may play an important role in kidney homeostasis.



Figure 5-13 Expression profiles of Rab17 and Liprin-β2 across various cancer types

Depicted are mRNA expression profiles of Rab17 (A) and Liprin-β2 (B) across various cancer types, which were gathered using the online Oncomine database [535]. Red signifies the gene's overexpression or copy gain, while blue represents the gene's underexpression or copy loss. Intensity of colour signifies whether the gene was in the top 1%, 5%, or 10% of all genes measured. The number in each cell represents the number of studies, which met the search criteria as follows fold change ≥ 1.5 , $p \leq 0.05$, data type: mRNA and DNA.

6 Summary and future directions

6.1 Final summary

The ERK pathway is hyperactivated in many human cancers as a consequence of increased expression or activating mutations of upstream components [314]. Although the canonical role of aberrant ERK signalling is its positive influence on cell survival and proliferation [283, 537], more and more evidence suggests a link between this pathway and tumour cell migration and invasion [277, 314, 377-379]. Given that the predominant two ERK kinases (ERK1 and ERK2) are highly homologous and have indistinguishable kinase activities *in vitro*, both enzymes were believed to be redundant and interchangeable [357].

To contrast with this view, here we show that ERK2 silencing inhibits invasive cell migration, and re-expression of ERK2 (but not ERK1) restores the normal invasive phenotype; arguing that true functional disparities do exist between these kinases which are not just a consequence of different gene dosage. A detailed quantitative analysis of cell movement on 3D matrices revealed that ERK2 depletion impairs cellular motility by decreasing the migration velocity as well as increasing the time that cells remain stationary (cellular resting). Thus, invasiveness of cancer cells is directly dependent on the speed with which the migration machinery propels the cell forward and the ability of cells to retain a motile phenotype.

To search for ERK2-specific effectors, which influence cell migration and invasion, we performed a microarray study using the rescue paradigm as an experimental set-up. Interestingly, knockdown of ERK2 altered the expression of a large number of genes, and in most cases expression of these was restored to normal levels by ectopic expression of either ERK1 or -2. However, we identified a subset of 27 genes whose expression was altered by knockdown of ERK2, but restored to normal levels following re-expression of siRNA-resistant ERK2 but not ERK1. Prominent amongst these were CSF2 (reduced expression following ERK2 depletion), Rab17 and Liprin- β 2 (increased expression following ERK2 depletion), which we validated by qRT-PCR. Rab17 and Liprin- β 2 play inhibitory roles in the invasive behaviour of three independent cancer cell lines. Importantly, knockdown of either Rab17 or Liprin- β 2 restores invasiveness of ERK2-depleted cells, indicating that ERK2 drives invasion of MDA-MB-231 cells by

suppressing expression of these genes. Given that Rab17 and Liprin- β 2 are indirect effectors of ERK2 and silencing of CSF2 induces transcription of Rab17 and Liprin- β 2, we propose a model in which ERK2 drives tumour cell migration by promoting CSF2 transcription and translation, which in turn suppresses expression of the motility inhibitors Rab17 and Liprin- β 2 (Figure 6-1).

6.2 Future directions

The identification of true functional differences between ERK1 and ERK2 poses many open questions with regard to tumourigenesis and we would like to discuss the ones we believe to be most pressing. Firstly, do their functional differences arise from distinct substrate profiles between the two kinases or do they bind to the same substrates with differing binding affinities? To answer these questions it would be necessary to compare the respective interactomes of ERK1 and ERK2 using SILAC (stable isotope labelling with amino acids in cell culture) mass spectrometry. However, a meaningful comparison of ERK1 and ERK2 substrate profiles requires the same amount of bait protein, which on an endogenous level is difficult to achieve due to different expression levels of ERK1 and ERK2. Thus, we propose using a combination of mass spectrometry and the rescue paradigm that we have developed for the present study. As both constructs are tagged, recombinant kinases could be immunoprecipitated using FLAG-beads, thus avoiding problems arising from different expression levels and circumventing the limitation of there currently being no suitable antibody for immunoprecipitation of endogenous ERK2.

The present work has identified an ERK2-specific expression profile and suggests ERK2 as a regulator of transcriptional and translational events. Intriguingly, ERK2 has recently been identified as an unconventional DNA-binding protein, which can directly bind to a G/CAAAG/C consensus motif [468]. Our data raise the question whether this is unique to ERK2 and if so, whether this might induce expression of ERK2-specific genes, such as *csf2*. ERK1 binding to the G/CAAG/C motif can be investigated by electromobility shift assays *in vitro* and chromatin immunoprecipitation *in vivo*. If both ERK isoforms were able to bind to DNA, it would also be interesting to compare genome-wide DNA binding sites using chromatin immunoprecipitation sequencing (ChIP-Seq). Additionally, one could

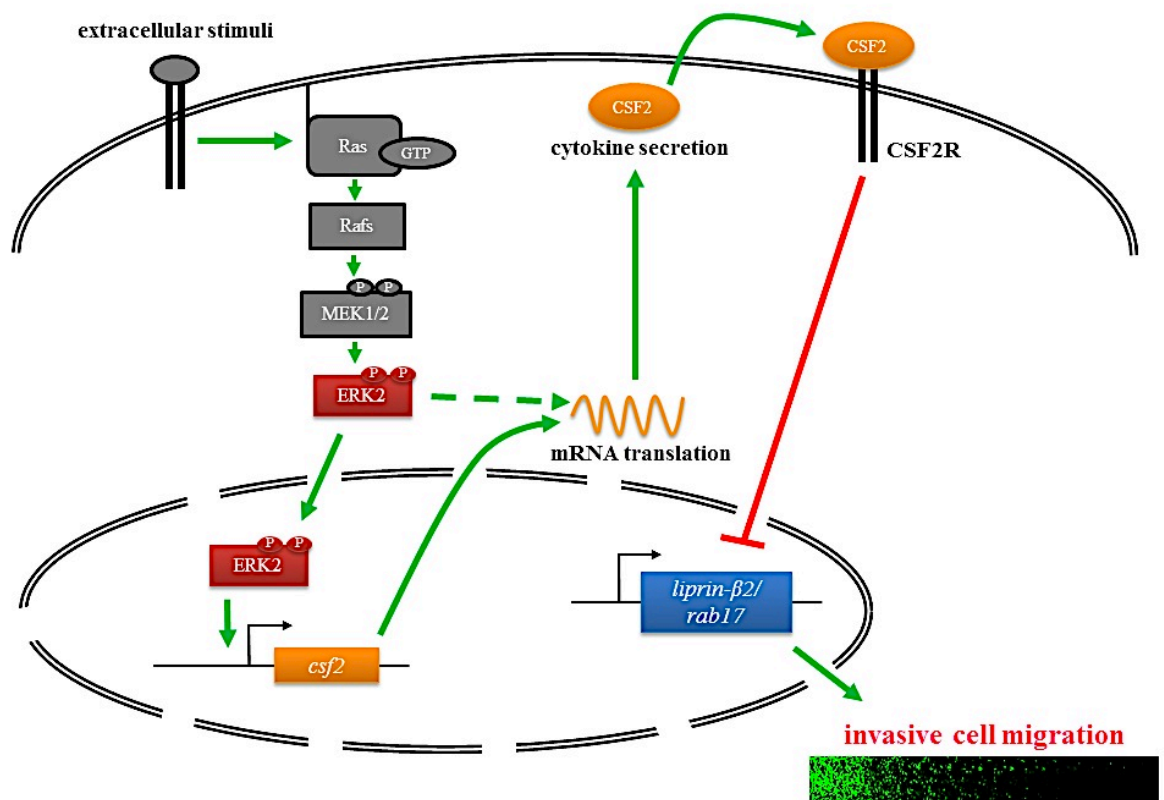


Figure 6-1 Working model demonstrating how ERK2 drives invasive cell migration

investigate whether ERK2 recruits transcription factors to the promoter regions it binds, and thereby controls transcriptional events.

Given the published role of the N-terminal region of ERK1 in controlling nuclear shuttling frequencies, which in turn may influence its capacity to regulate transcription, it would be interesting to determine whether ERK2's function in driving tumour cell migration could be localised to a specific domain of the kinases, such as the N-terminal domain. This could be achieved by generating ERK chimeras and performing rescue experiments. Indeed, we have already made two chimeras, one containing the N-terminal region of ERK2 fused to the C-terminal portion of ERK1 (E2>E1) and another corresponding chimera of the N-terminal region of ERK1 fused to the C-terminal portion of ERK2 (E1>E2). When both chimeras were expressed to similar levels on an ERK2 knockdown background, both were similarly phosphorylated at the TEY motif, suggesting an intact tertiary structure (data not shown). Analysis of cell migration on CDM indicated that although expression of E1>E2 restored the migratory defects caused by ERK2 knockdown, E2>E1 was ineffective in this regard (data not shown). These data indicate that the information conferring ERK2's capacity to drive migration is not located within the divergent N-terminal portion of the kinase. However, there are other regions of significant divergences between ERK1 and ERK2 (for example a 20 amino acid region close to the C-terminus) and future work will be necessary to evaluate their role in tumour cell migration and invasion.

Our gene expression data suggests a role for ERK2 in stabilising and destabilising mRNA transcripts. So far, ERK has only been implicated in regulating the destabilising factor tristetraprolin post-translationally [476, 477]. Yet, ERK2 is likely to phosphorylate other RNA-binding proteins and future work will have to investigate this. It is possible that our microarray data hold information which could be used to identify novel ERK2-regulated RNA-stabilising or destabilising factors. By comparing the 5' and 3' UTRs of our ERK2-regulated genes we hope to identify known regulatory elements involved in the recruitment of RNA-binding proteins. In follow-up studies, we would like to test whether these stabilising or destabilising factor were regulated by the ERK-MAPK pathway and whether this was linked to the gene expression signature we observed in this present study.

One of the strengths of this study is the identification of Rab17 and Liprin- β 2 as ERK targets that are novel motility suppressors. The fact that invasiveness of three independent cell lines is augmented following knockdown of either of these proteins, suggests that their function in inhibiting cell migration is generally applicable. However, whether or not loss of Rab17 and/or Liprin- β 2 expression is a general phenomenon during tumourigenesis will have to be examined by immunohistochemical staining of various cancer tissues. To date, we do not know how ERK2 suppresses Rab17 and Liprin- β 2 in MDA-MB-231 cells, but the rate at which they are upregulated following ERK inhibition, suggests that the *rab17* and *liprin β 2* genes are targeted indirectly. Moreover, silencing of ERK2 in A2780-Rab25 cells does not alter expression of Rab17 and Liprin- β 2 (data not shown), indicating that ERK2 drives tumour cell invasion differently in these cells and that the link between Rab17/Liprin- β 2 and ERK2 is not generally applicable. The current literature suggests a role for both proteins in receptor trafficking, yet the molecular mechanism by which Rab17 and Liprin- β 2 reduce tumour cell motility will have to be elucidated in the future. Firstly, what are the biological functions of both proteins? What drives and suppresses expression of Rab17 and Liprin- β 2? Moreover, what are the main interacting partners of Rab17 and Liprin- β 2? Do both proteins impair receptor internalisation or recycling? Alternatively, do they promote receptor degradation? What is the cargo of Rab17-positive vesicles and what is its function in tumour cell migration? Future studies may want to determine the interactome of Rab17 and Liprin- β 2 using mass spectrometry. Given that the commercial antibodies we have tested did not recognise endogenous Rab17 or Liprin- β 2 we suggest overexpression of the tagged proteins which can be immunoprecipitated using a GFP antibody. To shine light on how Rab17 signalling suppresses tumour cell motility, it would be interesting to investigate if knockdown or overexpression of Rab17 changes the surface proteome using surface labelling approaches followed by quantitative mass spectrometry. Moreover, one could develop new techniques based on the use of cleavable surface-labelling reagents to measure changes in the internalome (all of the internalised surface proteins) and recyclome (all of the recycled proteins), which may give insight on trafficking events regulated by Rab17.

In conclusion, this study has identified Rab17 and Liprin- β 2 as novel inhibitors of cell motility whose expression is regulated by ERK2 in MDA-MB-231 cells. Moreover, we have demonstrated that suppression of either Rab17 or Liprin- β 2 can completely compensate for loss of ERK2. Thus, we propose one way for ERK2 to drive invasiveness is by

suppressing Rab17 and/or Liprin- β 2. The potential for inhibitors of the MAPK pathway to be used as anticancer agents is now being assessed in the clinic, and our finding that ERK2-mediated suppression of Rab17 and Liprin- β 2 drives cancer invasiveness will be important in the interpretation of data from these studies.

List of references

1. Hanahan, D. and R.A. Weinberg, *The hallmarks of cancer*. Cell, 2000. **100**(1): p. 57-70.
2. Kinzler, K.W. and B. Vogelstein, *Lessons from hereditary colorectal cancer*. Cell, 1996. **87**(2): p. 159-70.
3. Bergers, G., D. Hanahan, and L.M. Coussens, *Angiogenesis and apoptosis are cellular parameters of neoplastic progression in transgenic mouse models of tumorigenesis*. Int J Dev Biol, 1998. **42**(7): p. 995-1002.
4. Bergers, G., et al., *Effects of angiogenesis inhibitors on multistage carcinogenesis in mice*. Science, 1999. **284**(5415): p. 808-12.
5. Foulds, L., *The Experimental Study of Tumor Progression*. Vol. I-III. 1954: London: Academic Press.
6. Weinberg, R.A., *The Nature of Cancer*, in *The Biology of Cancer*. 2007, Garland Science, Taylor & Francis group. p. 24.
7. Weinberg, R.A., *The Nature of Cancer*, in *The Biology of Cancer*. 2007, Garland Science, Taylor & Francis group. p. 28-35.
8. Hanahan, D. and R.A. Weinberg, *Hallmarks of cancer: the next generation*. Cell, 2011. **144**(5): p. 646-74.
9. Colotta, F., et al., *Cancer-related inflammation, the seventh hallmark of cancer: links to genetic instability*. Carcinogenesis, 2009. **30**(7): p. 1073-81.
10. Tennant, D.A., et al., *Metabolic transformation in cancer*. Carcinogenesis, 2009. **30**(8): p. 1269-80.
11. Wilczynski, J.R. and M. Duechler, *How do tumors actively escape from host immunosurveillance?* Arch Immunol Ther Exp (Warsz), 2010. **58**(6): p. 435-48.
12. Leber, M.F. and T. Efferth, *Molecular principles of cancer invasion and metastasis (review)*. Int J Oncol, 2009. **34**(4): p. 881-95.
13. Mareel, M., M.J. Oliveira, and I. Madani, *Cancer invasion and metastasis: interacting ecosystems*. Virchows Arch, 2009. **454**(6): p. 599-622.
14. Christofori, G. and H. Semb, *The role of the cell-adhesion molecule E-cadherin as a tumour-suppressor gene*. Trends Biochem Sci, 1999. **24**(2): p. 73-6.
15. Hazan, R.B., et al., *N-cadherin promotes adhesion between invasive breast cancer cells and the stroma*. Cell Adhes Commun, 1997. **4**(6): p. 399-411.
16. Kawamura-Kodama, K., et al., *N-cadherin expressed on malignant T cell lymphoma cells is functional, and promotes heterotypic adhesion between the lymphoma cells and mesenchymal cells expressing N-cadherin*. J Invest Dermatol, 1999. **112**(1): p. 62-6.
17. Coussens, L.M. and Z. Werb, *Matrix metalloproteinases and the development of cancer*. Chem Biol, 1996. **3**(11): p. 895-904.
18. Smets, F.N., et al., *Loss of cell anchorage triggers apoptosis (anoikis) in primary mouse hepatocytes*. Mol Genet Metab, 2002. **75**(4): p. 344-52.
19. Bromberg, M.E., et al., *Role of tissue factor in metastasis: functions of the cytoplasmic and extracellular domains of the molecule*. Thromb Haemost, 1999. **82**(1): p. 88-92.
20. Semeraro, N. and M. Colucci, *Tissue factor in health and disease*. Thromb Haemost, 1997. **78**(1): p. 759-64.
21. Mueller, B.M., et al., *Expression of tissue factor by melanoma cells promotes efficient hematogenous metastasis*. Proc Natl Acad Sci U S A, 1992. **89**(24): p. 11832-6.
22. Enns, A., et al., *Integrins can directly mediate metastatic tumor cell adhesion within the liver sinusoids*. J Gastrointest Surg, 2004. **8**(8): p. 1049-59; discussion 1060.

23. Enns, A., et al., *Alphavbeta5-integrins mediate early steps of metastasis formation*. Eur J Cancer, 2005. **41**(7): p. 1065-72.
24. Rinker-Schaeffer, C.W., et al., *Metastasis suppressor proteins: discovery, molecular mechanisms, and clinical application*. Clin Cancer Res, 2006. **12**(13): p. 3882-9.
25. Steeg, P.S., et al., *Evidence for a novel gene associated with low tumor metastatic potential*. J Natl Cancer Inst, 1988. **80**(3): p. 200-4.
26. Steeg, P.S., et al., *Altered expression of NM23, a gene associated with low tumor metastatic potential, during adenovirus 2 Ela inhibition of experimental metastasis*. Cancer Res, 1988. **48**(22): p. 6550-4.
27. Lauffenburger, D.A. and A.F. Horwitz, *Cell migration: a physically integrated molecular process*. Cell, 1996. **84**(3): p. 359-69.
28. Pankov, R., et al., *A Rac switch regulates random versus directionally persistent cell migration*. J Cell Biol, 2005. **170**(5): p. 793-802.
29. Friedl, P. and B. Weigelin, *Interstitial leukocyte migration and immune function*. Nat Immunol, 2008. **9**(9): p. 960-9.
30. Giebel, B., et al., *Segregation of lipid raft markers including CD133 in polarized human hematopoietic stem and progenitor cells*. Blood, 2004. **104**(8): p. 2332-8.
31. Binaime, F., et al., *What makes cells move: requirements and obstacles for spontaneous cell motility*. Mol Biosyst, 2010. **6**(4): p. 648-61.
32. Friedl, P., et al., *CD4+ T lymphocytes migrating in three-dimensional collagen lattices lack focal adhesions and utilize beta1 integrin-independent strategies for polarization, interaction with collagen fibers and locomotion*. Eur J Immunol, 1998. **28**(8): p. 2331-43.
33. Brakebusch, C., et al., *Beta1 integrin is not essential for hematopoiesis but is necessary for the T cell-dependent IgM antibody response*. Immunity, 2002. **16**(3): p. 465-77.
34. Sahai, E. and C.J. Marshall, *Differing modes of tumour cell invasion have distinct requirements for Rho/ROCK signalling and extracellular proteolysis*. Nat Cell Biol, 2003. **5**(8): p. 711-9.
35. Friedl, P. and K. Wolf, *Tumour-cell invasion and migration: diversity and escape mechanisms*. Nat Rev Cancer, 2003. **3**(5): p. 362-74.
36. Falcioni, R., et al., *Expression of beta 1, beta 3, beta 4, and beta 5 integrins by human lung carcinoma cells of different histotypes*. Exp Cell Res, 1994. **210**(1): p. 113-22.
37. Jaspars, L.H., et al., *Extracellular matrix and beta 1 integrin expression in nodal and extranodal T-cell lymphomas*. J Pathol, 1996. **178**(1): p. 36-43.
38. Cukierman, E., et al., *Taking cell-matrix adhesions to the third dimension*. Science, 2001. **294**(5547): p. 1708-12.
39. Maaser, K., et al., *Functional hierarchy of simultaneously expressed adhesion receptors: integrin alpha2beta1 but not CD44 mediates MV3 melanoma cell migration and matrix reorganization within three-dimensional hyaluronan-containing collagen matrices*. Mol Biol Cell, 1999. **10**(10): p. 3067-79.
40. Friedl, P., *Prespecification and plasticity: shifting mechanisms of cell migration*. Curr Opin Cell Biol, 2004. **16**(1): p. 14-23.
41. Keely, P.J., et al., *Cdc42 and Rac1 induce integrin-mediated cell motility and invasiveness through PI(3)K*. Nature, 1997. **390**(6660): p. 632-6.
42. Nobes, C.D. and A. Hall, *Rho GTPases control polarity, protrusion, and adhesion during cell movement*. J Cell Biol, 1999. **144**(6): p. 1235-44.
43. Friedl, P., S. Borgmann, and E.B. Brocker, *Amoeboid leukocyte crawling through extracellular matrix: lessons from the Dictyostelium paradigm of cell movement*. J Leukoc Biol, 2001. **70**(4): p. 491-509.

44. Davidson, L.A. and R.E. Keller, *Neural tube closure in Xenopus laevis involves medial migration, directed protrusive activity, cell intercalation and convergent extension*. Development, 1999. **126**(20): p. 4547-56.
45. Jacques, T.S., et al., *Neural precursor cell chain migration and division are regulated through different beta1 integrins*. Development, 1998. **125**(16): p. 3167-77.
46. Simian, M., et al., *The interplay of matrix metalloproteinases, morphogens and growth factors is necessary for branching of mammary epithelial cells*. Development, 2001. **128**(16): p. 3117-31.
47. Hegerfeldt, Y., et al., *Collective cell movement in primary melanoma explants: plasticity of cell-cell interaction, beta1-integrin function, and migration strategies*. Cancer Res, 2002. **62**(7): p. 2125-30.
48. Friedl, P., et al., *Migration of coordinated cell clusters in mesenchymal and epithelial cancer explants in vitro*. Cancer Res, 1995. **55**(20): p. 4557-60.
49. Nabeshima, K., et al., *Cohort migration of carcinoma cells: differentiated colorectal carcinoma cells move as coherent cell clusters or sheets*. Histol Histopathol, 1999. **14**(4): p. 1183-97.
50. Kraus, A.C., et al., *In vitro chemo- and radio-resistance in small cell lung cancer correlates with cell adhesion and constitutive activation of AKT and MAP kinase pathways*. Oncogene, 2002. **21**(57): p. 8683-95.
51. Friedl, P. and K. Wolf, *Plasticity of cell migration: a multiscale tuning model*. J Cell Biol, 2010. **188**(1): p. 11-9.
52. Moll, R., et al., *Differential loss of E-cadherin expression in infiltrating ductal and lobular breast carcinomas*. Am J Pathol, 1993. **143**(6): p. 1731-42.
53. Thiery, J.P., *Epithelial-mesenchymal transitions in tumour progression*. Nat Rev Cancer, 2002. **2**(6): p. 442-54.
54. Byers, S.W., et al., *Role of E-cadherin in the response of tumor cell aggregates to lymphatic, venous and arterial flow: measurement of cell-cell adhesion strength*. J Cell Sci, 1995. **108 (Pt 5)**: p. 2053-64.
55. Boulton, T.G., et al., *An insulin-stimulated protein kinase similar to yeast kinases involved in cell cycle control*. Science, 1990. **249**(4964): p. 64-7.
56. Courchesne, W.E., R. Kunisawa, and J. Thorner, *A putative protein kinase overcomes pheromone-induced arrest of cell cycling in S. cerevisiae*. Cell, 1989. **58**(6): p. 1107-19.
57. Elion, E.A., P.L. Grisafi, and G.R. Fink, *FUS3 encodes a cdc2+/CDC28-related kinase required for the transition from mitosis into conjugation*. Cell, 1990. **60**(4): p. 649-64.
58. Boulton, T.G., et al., *ERKs: a family of protein-serine/threonine kinases that are activated and tyrosine phosphorylated in response to insulin and NGF*. Cell, 1991. **65**(4): p. 663-75.
59. Pearson, G., et al., *Mitogen-activated protein (MAP) kinase pathways: regulation and physiological functions*. Endocr Rev, 2001. **22**(2): p. 153-83.
60. Gonzalez, F.A., et al., *Heterogeneous expression of four MAP kinase isoforms in human tissues*. FEBS Lett, 1992. **304**(2-3): p. 170-8.
61. Bogoyevitch, M.A. and N.W. Court, *Counting on mitogen-activated protein kinases--ERKs 3, 4, 5, 6, 7 and 8*. Cell Signal, 2004. **16**(12): p. 1345-54.
62. Dhillon, A.S., et al., *MAP kinase signalling pathways in cancer*. Oncogene, 2007. **26**(22): p. 3279-90.
63. Raman, M., W. Chen, and M.H. Cobb, *Differential regulation and properties of MAPKs*. Oncogene, 2007. **26**(22): p. 3100-12.
64. Conrad, P.W., D.E. Millhorn, and D. Beitner-Johnson, *Hypoxia differentially regulates the mitogen- and stress-activated protein kinases. Role of Ca2+/CaM in*

- the activation of MAPK and p38 gamma*. Adv Exp Med Biol, 2000. **475**: p. 293-302.
65. Efimova, T., et al., *Novel protein kinase C isoforms regulate human keratinocyte differentiation by activating a p38 delta mitogen-activated protein kinase cascade that targets CCAAT/enhancer-binding protein alpha*. J Biol Chem, 2002. **277**(35): p. 31753-60.
 66. Henrich, L.M., et al., *Extracellular signal-regulated kinase 7, a regulator of hormone-dependent estrogen receptor destruction*. Mol Cell Biol, 2003. **23**(17): p. 5979-88.
 67. Ishitani, T., et al., *The TAK1-NLK-MAPK-related pathway antagonizes signalling between beta-catenin and transcription factor TCF*. Nature, 1999. **399**(6738): p. 798-802.
 68. Smit, L., et al., *Wnt activates the Tak1/Nemo-like kinase pathway*. J Biol Chem, 2004. **279**(17): p. 17232-40.
 69. Xia, L., et al., *Identification of human male germ cell-associated kinase, a kinase transcriptionally activated by androgen in prostate cancer cells*. J Biol Chem, 2002. **277**(38): p. 35422-33.
 70. Abe, S., et al., *Molecular cloning of a novel serine/threonine kinase, MRK, possibly involved in cardiac development*. Oncogene, 1995. **11**(11): p. 2187-95.
 71. Miyata, Y., M. Akashi, and E. Nishida, *Molecular cloning and characterization of a novel member of the MAP kinase superfamily*. Genes Cells, 1999. **4**(5): p. 299-309.
 72. Meyerson, M., et al., *A family of human cdc2-related protein kinases*. EMBO J, 1992. **11**(8): p. 2909-17.
 73. Taglienti, C.A., M. Wylk, and R.J. Davis, *Molecular cloning of the epidermal growth factor-stimulated protein kinase p56 KKIAMRE*. Oncogene, 1996. **13**(12): p. 2563-74.
 74. Manning, G., et al., *The protein kinase complement of the human genome*. Science, 2002. **298**(5600): p. 1912-34.
 75. Coulombe, P. and S. Meloche, *Atypical mitogen-activated protein kinases: structure, regulation and functions*. Biochim Biophys Acta, 2007. **1773**(8): p. 1376-87.
 76. Kyriakis, J.M. and J. Avruch, *pp54 microtubule-associated protein 2 kinase. A novel serine/threonine protein kinase regulated by phosphorylation and stimulated by poly-L-lysine*. J Biol Chem, 1990. **265**(28): p. 17355-63.
 77. Hibi, M., et al., *Identification of an oncoprotein- and UV-responsive protein kinase that binds and potentiates the c-Jun activation domain*. Genes Dev, 1993. **7**(11): p. 2135-48.
 78. Kyriakis, J.M., et al., *The stress-activated protein kinase subfamily of c-Jun kinases*. Nature, 1994. **369**(6476): p. 156-60.
 79. Ip, Y.T. and R.J. Davis, *Signal transduction by the c-Jun N-terminal kinase (JNK)--from inflammation to development*. Curr Opin Cell Biol, 1998. **10**(2): p. 205-19.
 80. Wu, G.S., *The functional interactions between the p53 and MAPK signaling pathways*. Cancer Biol Ther, 2004. **3**(2): p. 156-61.
 81. Hui, L., et al., *Proliferation of human HCC cells and chemically induced mouse liver cancers requires JNK1-dependent p21 downregulation*. J Clin Invest, 2008. **118**(12): p. 3943-53.
 82. Sakurai, T., et al., *Loss of hepatic NF-kappa B activity enhances chemical hepatocarcinogenesis through sustained c-Jun N-terminal kinase 1 activation*. Proc Natl Acad Sci U S A, 2006. **103**(28): p. 10544-51.
 83. Ke, H., et al., *The c-Jun NH2-terminal kinase 2 plays a dominant role in human epidermal neoplasia*. Cancer Res, 2010. **70**(8): p. 3080-8.

84. Das, M., et al., *The role of JNK in the development of hepatocellular carcinoma*. Genes Dev, 2011. **25**(6): p. 634-45.
85. Feng, Q., et al., *Apoptosis induced by genipin in human leukemia K562 cells: involvement of c-Jun N-terminal kinase in G(2)/M arrest*. Acta Pharmacol Sin, 2011.
86. Lee, J.C., et al., *A protein kinase involved in the regulation of inflammatory cytokine biosynthesis*. Nature, 1994. **372**(6508): p. 739-46.
87. Brancho, D., et al., *Mechanism of p38 MAP kinase activation in vivo*. Genes Dev, 2003. **17**(16): p. 1969-78.
88. Iyoda, K., et al., *Involvement of the p38 mitogen-activated protein kinase cascade in hepatocellular carcinoma*. Cancer, 2003. **97**(12): p. 3017-26.
89. Bulavin, D.V., et al., *Loss of oncogenic H-ras-induced cell cycle arrest and p38 mitogen-activated protein kinase activation by disruption of Gadd45a*. Mol Cell Biol, 2003. **23**(11): p. 3859-71.
90. Lee, J.D., R.J. Ulevitch, and J. Han, *Primary structure of BMK1: a new mammalian map kinase*. Biochem Biophys Res Commun, 1995. **213**(2): p. 715-24.
91. Zhou, G., Z.Q. Bao, and J.E. Dixon, *Components of a new human protein kinase signal transduction pathway*. J Biol Chem, 1995. **270**(21): p. 12665-9.
92. Kondoh, K., et al., *Regulation of nuclear translocation of extracellular signal-regulated kinase 5 by active nuclear import and export mechanisms*. Mol Cell Biol, 2006. **26**(5): p. 1679-90.
93. Kasler, H.G., et al., *ERK5 is a novel type of mitogen-activated protein kinase containing a transcriptional activation domain*. Mol Cell Biol, 2000. **20**(22): p. 8382-9.
94. Nishimoto, S. and E. Nishida, *MAPK signalling: ERK5 versus ERK1/2*. EMBO Rep, 2006. **7**(8): p. 782-6.
95. Kato, Y., et al., *Bmk1/Erk5 is required for cell proliferation induced by epidermal growth factor*. Nature, 1998. **395**(6703): p. 713-6.
96. Arnoux, V., et al., *Erk5 controls Slug expression and keratinocyte activation during wound healing*. Mol Biol Cell, 2008. **19**(11): p. 4738-49.
97. Regan, C.P., et al., *Erk5 null mice display multiple extraembryonic vascular and embryonic cardiovascular defects*. Proc Natl Acad Sci U S A, 2002. **99**(14): p. 9248-53.
98. Nishimoto, S., M. Kusakabe, and E. Nishida, *Requirement of the MEK5-ERK5 pathway for neural differentiation in Xenopus embryonic development*. EMBO Rep, 2005. **6**(11): p. 1064-9.
99. Kato, Y., et al., *BMK1/ERK5 regulates serum-induced early gene expression through transcription factor MEF2C*. EMBO J, 1997. **16**(23): p. 7054-66.
100. English, J.M., et al., *Identification of substrates and regulators of the mitogen-activated protein kinase ERK5 using chimeric protein kinases*. J Biol Chem, 1998. **273**(7): p. 3854-60.
101. Kamakura, S., T. Moriguchi, and E. Nishida, *Activation of the protein kinase ERK5/BMK1 by receptor tyrosine kinases. Identification and characterization of a signaling pathway to the nucleus*. J Biol Chem, 1999. **274**(37): p. 26563-71.
102. Mehta, P.B., et al., *MEK5 overexpression is associated with metastatic prostate cancer, and stimulates proliferation, MMP-9 expression and invasion*. Oncogene, 2003. **22**(9): p. 1381-9.
103. Esparis-Ogando, A., et al., *Erk5 participates in neuregulin signal transduction and is constitutively active in breast cancer cells overexpressing ErbB2*. Mol Cell Biol, 2002. **22**(1): p. 270-85.

104. Turgeon, B., B.F. Lang, and S. Meloche, *The protein kinase ERK3 is encoded by a single functional gene: genomic analysis of the ERK3 gene family*. Genomics, 2002. **80**(6): p. 673-80.
105. Hunter, T. and G.D. Plowman, *The protein kinases of budding yeast: six score and more*. Trends Biochem Sci, 1997. **22**(1): p. 18-22.
106. Plowman, G.D., et al., *The protein kinases of Caenorhabditis elegans: a model for signal transduction in multicellular organisms*. Proc Natl Acad Sci U S A, 1999. **96**(24): p. 13603-10.
107. Zhang, J., et al., *Activity of the MAP kinase ERK2 is controlled by a flexible surface loop*. Structure, 1995. **3**(3): p. 299-307.
108. Rowles, J., et al., *Purification of casein kinase I and isolation of cDNAs encoding multiple casein kinase I-like enzymes*. Proc Natl Acad Sci U S A, 1991. **88**(21): p. 9548-52.
109. Cheng, M., T.G. Boulton, and M.H. Cobb, *ERK3 is a constitutively nuclear protein kinase*. J Biol Chem, 1996. **271**(15): p. 8951-8.
110. Julien, C., P. Coulombe, and S. Meloche, *Nuclear export of ERK3 by a CRM1-dependent mechanism regulates its inhibitory action on cell cycle progression*. J Biol Chem, 2003. **278**(43): p. 42615-24.
111. Zhu, A.X., et al., *Cloning and characterization of p97MAPK, a novel human homolog of rat ERK-3*. Mol Cell Biol, 1994. **14**(12): p. 8202-11.
112. Cheng, M., et al., *Characterization of a protein kinase that phosphorylates serine 189 of the mitogen-activated protein kinase homolog ERK3*. J Biol Chem, 1996. **271**(20): p. 12057-62.
113. Sauma, S. and E. Friedman, *Increased expression of protein kinase C beta activates ERK3*. J Biol Chem, 1996. **271**(19): p. 11422-6.
114. Coulombe, P., et al., *Rapid turnover of extracellular signal-regulated kinase 3 by the ubiquitin-proteasome pathway defines a novel paradigm of mitogen-activated protein kinase regulation during cellular differentiation*. Mol Cell Biol, 2003. **23**(13): p. 4542-58.
115. Abe, M.K., et al., *Extracellular signal-regulated kinase 7 (ERK7), a novel ERK with a C-terminal domain that regulates its activity, its cellular localization, and cell growth*. Mol Cell Biol, 1999. **19**(2): p. 1301-12.
116. Abe, M.K., et al., *ERK8, a new member of the mitogen-activated protein kinase family*. J Biol Chem, 2002. **277**(19): p. 16733-43.
117. Kuo, W.L., et al., *ERK7 expression and kinase activity is regulated by the ubiquitin-proteasome pathway*. J Biol Chem, 2004. **279**(22): p. 23073-81.
118. Qian, Z., et al., *Molecular cloning and characterization of a mitogen-activated protein kinase-associated intracellular chloride channel*. J Biol Chem, 1999. **274**(3): p. 1621-7.
119. Kumar, S., J. Boehm, and J.C. Lee, *p38 MAP kinases: key signalling molecules as therapeutic targets for inflammatory diseases*. Nat Rev Drug Discov, 2003. **2**(9): p. 717-26.
120. Kaminska, B., *MAPK signalling pathways as molecular targets for anti-inflammatory therapy--from molecular mechanisms to therapeutic benefits*. Biochim Biophys Acta, 2005. **1754**(1-2): p. 253-62.
121. Kim, E.K. and E.J. Choi, *Pathological roles of MAPK signaling pathways in human diseases*. Biochim Biophys Acta, 2010. **1802**(4): p. 396-405.
122. Rubinfeld, H., T. Hanoch, and R. Seger, *Identification of a cytoplasmic-retention sequence in ERK2*. J Biol Chem, 1999. **274**(43): p. 30349-52.
123. Tanoue, T., et al., *A conserved docking motif in MAP kinases common to substrates, activators and regulators*. Nat Cell Biol, 2000. **2**(2): p. 110-6.

124. Tanoue, T. and E. Nishida, *Docking interactions in the mitogen-activated protein kinase cascades*. Pharmacol Ther, 2002. **93**(2-3): p. 193-202.
125. Xie, X., et al., *Crystal structure of JNK3: a kinase implicated in neuronal apoptosis*. Structure, 1998. **6**(8): p. 983-91.
126. Wilson, K.P., et al., *Crystal structure of p38 mitogen-activated protein kinase*. J Biol Chem, 1996. **271**(44): p. 27696-700.
127. Sharrocks, A.D., S.H. Yang, and A. Galanis, *Docking domains and substrate-specificity determination for MAP kinases*. Trends Biochem Sci, 2000. **25**(9): p. 448-53.
128. Smith, J.A., et al., *Creation of a stress-activated p90 ribosomal S6 kinase. The carboxyl-terminal tail of the MAPK-activated protein kinases dictates the signal transduction pathway in which they function*. J Biol Chem, 2000. **275**(41): p. 31588-93.
129. Chang, C.I., et al., *Crystal structures of MAP kinase p38 complexed to the docking sites on its nuclear substrate MEF2A and activator MKK3b*. Mol Cell, 2002. **9**(6): p. 1241-9.
130. Zhou, T., et al., *Docking interactions induce exposure of activation loop in the MAP kinase ERK2*. Structure, 2006. **14**(6): p. 1011-9.
131. Lee, T., et al., *Docking motif interactions in MAP kinases revealed by hydrogen exchange mass spectrometry*. Mol Cell, 2004. **14**(1): p. 43-55.
132. Jacobs, D., et al., *Multiple docking sites on substrate proteins form a modular system that mediates recognition by ERK MAP kinase*. Genes Dev, 1999. **13**(2): p. 163-75.
133. Seidel, J.J. and B.J. Graves, *An ERK2 docking site in the Pointed domain distinguishes a subset of ETS transcription factors*. Genes Dev, 2002. **16**(1): p. 127-37.
134. Molina, D.M., S. Grewal, and L. Bardwell, *Characterization of an ERK-binding domain in microphthalmia-associated transcription factor and differential inhibition of ERK2-mediated substrate phosphorylation*. J Biol Chem, 2005. **280**(51): p. 42051-60.
135. Akella, R., T.M. Moon, and E.J. Goldsmith, *Unique MAP Kinase binding sites*. Biochim Biophys Acta, 2008. **1784**(1): p. 48-55.
136. Dudley, D.T., et al., *A synthetic inhibitor of the mitogen-activated protein kinase cascade*. Proc Natl Acad Sci U S A, 1995. **92**(17): p. 7686-9.
137. Wroblewski, S.T. and A.M. Doweyko, *Structural comparison of p38 inhibitor-protein complexes: a review of recent p38 inhibitors having unique binding interactions*. Curr Top Med Chem, 2005. **5**(10): p. 1005-16.
138. Ohren, J.F., et al., *Structures of human MAP kinase kinase 1 (MEK1) and MEK2 describe novel noncompetitive kinase inhibition*. Nat Struct Mol Biol, 2004. **11**(12): p. 1192-7.
139. Nagar, B., et al., *Crystal structures of the kinase domain of c-Abl in complex with the small molecule inhibitors PD173955 and imatinib (STI-571)*. Cancer Res, 2002. **62**(15): p. 4236-43.
140. Ramos, J.W., *The regulation of extracellular signal-regulated kinase (ERK) in mammalian cells*. Int J Biochem Cell Biol, 2008. **40**(12): p. 2707-19.
141. McCubrey, J.A., et al., *Roles of the Raf/MEK/ERK pathway in cell growth, malignant transformation and drug resistance*. Biochim Biophys Acta, 2007. **1773**(8): p. 1263-84.
142. Fang, J.Y. and B.C. Richardson, *The MAPK signalling pathways and colorectal cancer*. Lancet Oncol, 2005. **6**(5): p. 322-7.
143. Kohno, M. and J. Pouyssegur, *Targeting the ERK signaling pathway in cancer therapy*. Ann Med, 2006. **38**(3): p. 200-11.

144. Vigneri, R., S. Squatrito, and L. Sciacca, *Insulin and its analogs: actions via insulin and IGF receptors*. Acta Diabetol, 2010. **47**(4): p. 271-8.
145. Petkova, S.B., et al., *Cell cycle molecules and diseases of the cardiovascular system*. Front Biosci, 2000. **5**: p. D452-60.
146. Wellbrock, C., M. Karasarides, and R. Marais, *The RAF proteins take centre stage*. Nat Rev Mol Cell Biol, 2004. **5**(11): p. 875-85.
147. Morrison, D.K. and R.E. Cutler, *The complexity of Raf-1 regulation*. Curr Opin Cell Biol, 1997. **9**(2): p. 174-9.
148. Kolch, W., *Coordinating ERK/MAPK signalling through scaffolds and inhibitors*. Nat Rev Mol Cell Biol, 2005. **6**(11): p. 827-37.
149. Diaz, B., et al., *Phosphorylation of Raf-1 serine 338-serine 339 is an essential regulatory event for Ras-dependent activation and biological signaling*. Mol Cell Biol, 1997. **17**(8): p. 4509-16.
150. Morrison, D.K., *Mechanisms regulating Raf-1 activity in signal transduction pathways*. Mol Reprod Dev, 1995. **42**(4): p. 507-14.
151. Fabian, J.R., I.O. Daar, and D.K. Morrison, *Critical tyrosine residues regulate the enzymatic and biological activity of Raf-1 kinase*. Mol Cell Biol, 1993. **13**(11): p. 7170-9.
152. Alessi, D.R., et al., *Identification of the sites in MAP kinase kinase-1 phosphorylated by p74raf-1*. EMBO J, 1994. **13**(7): p. 1610-9.
153. Zheng, C.F. and K.L. Guan, *Properties of MEKs, the kinases that phosphorylate and activate the extracellular signal-regulated kinases*. J Biol Chem, 1993. **268**(32): p. 23933-9.
154. Shaul, Y.D., et al., *Specific phosphorylation and activation of ERK1c by MEK1b: a unique route in the ERK cascade*. Genes Dev, 2009. **23**(15): p. 1779-90.
155. Ferrell, J.E., Jr. and R.R. Bhatt, *Mechanistic studies of the dual phosphorylation of mitogen-activated protein kinase*. J Biol Chem, 1997. **272**(30): p. 19008-16.
156. Yoon, S. and R. Seger, *The extracellular signal-regulated kinase: multiple substrates regulate diverse cellular functions*. Growth Factors, 2006. **24**(1): p. 21-44.
157. Gonzalez, F.A., D.L. Raden, and R.J. Davis, *Identification of substrate recognition determinants for human ERK1 and ERK2 protein kinases*. J Biol Chem, 1991. **266**(33): p. 22159-63.
158. Aebersold, D.M., et al., *Extracellular signal-regulated kinase 1c (ERK1c), a novel 42-kilodalton ERK, demonstrates unique modes of regulation, localization, and function*. Mol Cell Biol, 2004. **24**(22): p. 10000-15.
159. Yung, Y., et al., *ERK1b, a 46-kDa ERK isoform that is differentially regulated by MEK*. J Biol Chem, 2000. **275**(21): p. 15799-808.
160. Shaul, Y.D. and R. Seger, *ERK1c regulates Golgi fragmentation during mitosis*. J Cell Biol, 2006. **172**(6): p. 885-97.
161. Marshall, C.J., *Specificity of receptor tyrosine kinase signaling: transient versus sustained extracellular signal-regulated kinase activation*. Cell, 1995. **80**(2): p. 179-85.
162. Ebisuya, M., K. Kondoh, and E. Nishida, *The duration, magnitude and compartmentalization of ERK MAP kinase activity: mechanisms for providing signaling specificity*. J Cell Sci, 2005. **118**(Pt 14): p. 2997-3002.
163. Pouyssegur, J., V. Volmat, and P. Lenormand, *Fidelity and spatio-temporal control in MAP kinase (ERKs) signalling*. Biochem Pharmacol, 2002. **64**(5-6): p. 755-63.
164. Raman, M. and M.H. Cobb, *MAP kinase modules: many roads home*. Curr Biol, 2003. **13**(22): p. R886-8.

165. Sontag, E., et al., *The interaction of SV40 small tumor antigen with protein phosphatase 2A stimulates the map kinase pathway and induces cell proliferation.* Cell, 1993. **75**(5): p. 887-97.
166. Alessi, D.R., et al., *Inactivation of p42 MAP kinase by protein phosphatase 2A and a protein tyrosine phosphatase, but not CL100, in various cell lines.* Curr Biol, 1995. **5**(3): p. 283-95.
167. Ory, S., et al., *Protein phosphatase 2A positively regulates Ras signaling by dephosphorylating KSR1 and Raf-1 on critical 14-3-3 binding sites.* Curr Biol, 2003. **13**(16): p. 1356-64.
168. Cho, U.S. and W. Xu, *Crystal structure of a protein phosphatase 2A heterotrimeric holoenzyme.* Nature, 2007. **445**(7123): p. 53-7.
169. Xu, Y., et al., *Structure of the protein phosphatase 2A holoenzyme.* Cell, 2006. **127**(6): p. 1239-51.
170. McCright, B., et al., *The B56 family of protein phosphatase 2A (PP2A) regulatory subunits encodes differentiation-induced phosphoproteins that target PP2A to both nucleus and cytoplasm.* J Biol Chem, 1996. **271**(36): p. 22081-9.
171. Letourneux, C., G. Rocher, and F. Porteu, *B56-containing PP2A dephosphorylate ERK and their activity is controlled by the early gene IEX-1 and ERK.* EMBO J, 2006. **25**(4): p. 727-38.
172. Saxena, M., et al., *Crosstalk between cAMP-dependent kinase and MAP kinase through a protein tyrosine phosphatase.* Nat Cell Biol, 1999. **1**(5): p. 305-11.
173. Paul, S., et al., *NMDA-mediated activation of the tyrosine phosphatase STEP regulates the duration of ERK signaling.* Nat Neurosci, 2003. **6**(1): p. 34-42.
174. Saxena, M. and T. Mustelin, *Extracellular signals and scores of phosphatases: all roads lead to MAP kinase.* Semin Immunol, 2000. **12**(4): p. 387-96.
175. Patterson, K.I., et al., *Dual-specificity phosphatases: critical regulators with diverse cellular targets.* Biochem J, 2009. **418**(3): p. 475-89.
176. Marchetti, S., et al., *Extracellular signal-regulated kinases phosphorylate mitogen-activated protein kinase phosphatase 3/DUSP6 at serines 159 and 197, two sites critical for its proteasomal degradation.* Mol Cell Biol, 2005. **25**(2): p. 854-64.
177. Brondello, J.M., J. Pouyssegur, and F.R. McKenzie, *Reduced MAP kinase phosphatase-1 degradation after p42/p44MAPK-dependent phosphorylation.* Science, 1999. **286**(5449): p. 2514-7.
178. Kamata, H., et al., *Reactive oxygen species promote TNFalpha-induced death and sustained JNK activation by inhibiting MAP kinase phosphatases.* Cell, 2005. **120**(5): p. 649-61.
179. Fukuda, M., Y. Gotoh, and E. Nishida, *Interaction of MAP kinase with MAP kinase kinase: its possible role in the control of nucleocytoplasmic transport of MAP kinase.* EMBO J, 1997. **16**(8): p. 1901-8.
180. Hsiao, K.M., et al., *Evidence that inactive p42 mitogen-activated protein kinase and inactive Rsk exist as a heterodimer in vivo.* Proc Natl Acad Sci U S A, 1994. **91**(12): p. 5480-4.
181. Therrien, M., et al., *KSR, a novel protein kinase required for RAS signal transduction.* Cell, 1995. **83**(6): p. 879-88.
182. Kornfeld, K., D.B. Hom, and H.R. Horvitz, *The ksr-1 gene encodes a novel protein kinase involved in Ras-mediated signaling in C. elegans.* Cell, 1995. **83**(6): p. 903-13.
183. Morrison, D.K. and R.J. Davis, *Regulation of MAP kinase signaling modules by scaffold proteins in mammals.* Annu Rev Cell Dev Biol, 2003. **19**: p. 91-118.
184. Yu, W., et al., *Regulation of the MAP kinase pathway by mammalian Ksr through direct interaction with MEK and ERK.* Curr Biol, 1998. **8**(1): p. 56-64.

185. Therrien, M., et al., *KSR modulates signal propagation within the MAPK cascade*. Genes Dev, 1996. **10**(21): p. 2684-95.
186. Roy, F., et al., *KSR is a scaffold required for activation of the ERK/MAPK module*. Genes Dev, 2002. **16**(4): p. 427-38.
187. Schaeffer, H.J., et al., *MPI: a MEK binding partner that enhances enzymatic activation of the MAP kinase cascade*. Science, 1998. **281**(5383): p. 1668-71.
188. Teis, D., W. Wunderlich, and L.A. Huber, *Localization of the MPI-MAPK scaffold complex to endosomes is mediated by p14 and required for signal transduction*. Dev Cell, 2002. **3**(6): p. 803-14.
189. Wunderlich, W., et al., *A novel 14-kilodalton protein interacts with the mitogen-activated protein kinase scaffold mp1 on a late endosomal/lysosomal compartment*. J Cell Biol, 2001. **152**(4): p. 765-76.
190. Pullikuth, A., et al., *The MEK1 scaffolding protein MPI regulates cell spreading by integrating PAK1 and Rho signals*. Mol Cell Biol, 2005. **25**(12): p. 5119-33.
191. Vomastek, T., et al., *Modular construction of a signaling scaffold: MORGI interacts with components of the ERK cascade and links ERK signaling to specific agonists*. Proc Natl Acad Sci U S A, 2004. **101**(18): p. 6981-6.
192. Luttrell, L.M. and R.J. Lefkowitz, *The role of beta-arrestins in the termination and transduction of G-protein-coupled receptor signals*. J Cell Sci, 2002. **115**(Pt 3): p. 455-65.
193. Daaka, Y., et al., *Essential role for G protein-coupled receptor endocytosis in the activation of mitogen-activated protein kinase*. J Biol Chem, 1998. **273**(2): p. 685-8.
194. DeFea, K.A., et al., *The proliferative and antiapoptotic effects of substance P are facilitated by formation of a beta -arrestin-dependent scaffolding complex*. Proc Natl Acad Sci U S A, 2000. **97**(20): p. 11086-91.
195. DeFea, K.A., et al., *beta-arrestin-dependent endocytosis of proteinase-activated receptor 2 is required for intracellular targeting of activated ERK1/2*. J Cell Biol, 2000. **148**(6): p. 1267-81.
196. Tohgo, A., et al., *beta-Arrestin scaffolding of the ERK cascade enhances cytosolic ERK activity but inhibits ERK-mediated transcription following angiotensin AT1a receptor stimulation*. J Biol Chem, 2002. **277**(11): p. 9429-36.
197. Minden, A., et al., *Differential activation of ERK and JNK mitogen-activated protein kinases by Raf-1 and MEKK*. Science, 1994. **266**(5191): p. 1719-23.
198. Lu, Z., et al., *The PHD domain of MEKK1 acts as an E3 ubiquitin ligase and mediates ubiquitination and degradation of ERK1/2*. Mol Cell, 2002. **9**(5): p. 945-56.
199. Xu, S., et al., *Cloning of rat MEK kinase 1 cDNA reveals an endogenous membrane-associated 195-kDa protein with a large regulatory domain*. Proc Natl Acad Sci U S A, 1996. **93**(11): p. 5291-5.
200. Karandikar, M., S. Xu, and M.H. Cobb, *MEKK1 binds raf-1 and the ERK2 cascade components*. J Biol Chem, 2000. **275**(51): p. 40120-7.
201. Yujiri, T., et al., *Role of MEKK1 in cell survival and activation of JNK and ERK pathways defined by targeted gene disruption*. Science, 1998. **282**(5395): p. 1911-4.
202. Therrien, M., A.M. Wong, and G.M. Rubin, *CNK, a RAF-binding multidomain protein required for RAS signaling*. Cell, 1998. **95**(3): p. 343-53.
203. Lanigan, T.M., et al., *Human homologue of Drosophila CNK interacts with Ras effector proteins Raf and Rlf*. FASEB J, 2003. **17**(14): p. 2048-60.
204. Rabizadeh, S., et al., *The scaffold protein CNK1 interacts with the tumor suppressor RASSF1A and augments RASSF1A-induced cell death*. J Biol Chem, 2004. **279**(28): p. 29247-54.

205. Jaffe, A.B., P. Aspenstrom, and A. Hall, *Human CNK1 acts as a scaffold protein, linking Rho and Ras signal transduction pathways*. *Mol Cell Biol*, 2004. **24**(4): p. 1736-46.
206. Ziogas, A., K. Moelling, and G. Radziwill, *CNK1 is a scaffold protein that regulates Src-mediated Raf-1 activation*. *J Biol Chem*, 2005. **280**(25): p. 24205-11.
207. Sieburth, D.S., Q. Sun, and M. Han, *SUR-8, a conserved Ras-binding protein with leucine-rich repeats, positively regulates Ras-mediated signaling in C. elegans*. *Cell*, 1998. **94**(1): p. 119-30.
208. Li, W., M. Han, and K.L. Guan, *The leucine-rich repeat protein SUR-8 enhances MAP kinase activation and forms a complex with Ras and Raf*. *Genes Dev*, 2000. **14**(8): p. 895-900.
209. Roy, M., Z. Li, and D.B. Sacks, *IQGAP1 is a scaffold for mitogen-activated protein kinase signaling*. *Mol Cell Biol*, 2005. **25**(18): p. 7940-52.
210. Ren, J.G., Z. Li, and D.B. Sacks, *IQGAP1 modulates activation of B-Raf*. *Proc Natl Acad Sci U S A*, 2007. **104**(25): p. 10465-9.
211. Roy, M., Z. Li, and D.B. Sacks, *IQGAP1 binds ERK2 and modulates its activity*. *J Biol Chem*, 2004. **279**(17): p. 17329-37.
212. Marais, R., et al., *Differential regulation of Raf-1, A-Raf, and B-Raf by oncogenic ras and tyrosine kinases*. *J Biol Chem*, 1997. **272**(7): p. 4378-83.
213. Bos, J.L., *ras oncogenes in human cancer: a review*. *Cancer Res*, 1989. **49**(17): p. 4682-9.
214. Hagel, M., et al., *The adaptor protein paxillin is essential for normal development in the mouse and is a critical transducer of fibronectin signaling*. *Mol Cell Biol*, 2002. **22**(3): p. 901-15.
215. Ishibe, S., et al., *Phosphorylation-dependent paxillin-ERK association mediates hepatocyte growth factor-stimulated epithelial morphogenesis*. *Mol Cell*, 2003. **12**(5): p. 1275-85.
216. Liu, Z.X., et al., *Hepatocyte growth factor induces ERK-dependent paxillin phosphorylation and regulates paxillin-focal adhesion kinase association*. *J Biol Chem*, 2002. **277**(12): p. 10452-8.
217. Schmalzigaug, R., et al., *GIT1 utilizes a focal adhesion targeting-homology domain to bind paxillin*. *Cell Signal*, 2007. **19**(8): p. 1733-44.
218. Zhang, N., et al., *GIT1 is a novel MEK1-ERK1/2 scaffold that localizes to focal adhesions*. *Cell Biol Int*, 2010. **34**(1): p. 41-7.
219. Yin, G., et al., *GIT1 functions as a scaffold for MEK1-extracellular signal-regulated kinase 1 and 2 activation by angiotensin II and epidermal growth factor*. *Mol Cell Biol*, 2004. **24**(2): p. 875-85.
220. Yujiri, T., et al., *MEK kinase 1 interacts with focal adhesion kinase and regulates insulin receptor substrate-1 expression*. *J Biol Chem*, 2003. **278**(6): p. 3846-51.
221. Araujo, H., et al., *Characterization of PEA-15, a major substrate for protein kinase C in astrocytes*. *J Biol Chem*, 1993. **268**(8): p. 5911-20.
222. Hill, J.M., et al., *Recognition of ERK MAP kinase by PEA-15 reveals a common docking site within the death domain and death effector domain*. *EMBO J*, 2002. **21**(23): p. 6494-504.
223. Vaidyanathan, H., et al., *ERK MAP kinase is targeted to RSK2 by the phosphoprotein PEA-15*. *Proc Natl Acad Sci U S A*, 2007. **104**(50): p. 19837-42.
224. Formstecher, E., et al., *PEA-15 mediates cytoplasmic sequestration of ERK MAP kinase*. *Dev Cell*, 2001. **1**(2): p. 239-50.
225. Whitehurst, A.W., et al., *The death effector domain protein PEA-15 prevents nuclear entry of ERK2 by inhibiting required interactions*. *J Biol Chem*, 2004. **279**(13): p. 12840-7.

226. Yeung, K., et al., *Mechanism of suppression of the Raf/MEK/extracellular signal-regulated kinase pathway by the raf kinase inhibitor protein*. Mol Cell Biol, 2000. **20**(9): p. 3079-85.
227. Robinson, M.J., et al., *A constitutively active and nuclear form of the MAP kinase ERK2 is sufficient for neurite outgrowth and cell transformation*. Curr Biol, 1998. **8**(21): p. 1141-50.
228. Tsang, M., et al., *Identification of Sef, a novel modulator of FGF signalling*. Nat Cell Biol, 2002. **4**(2): p. 165-9.
229. Bivona, T.G., et al., *Phospholipase Cgamma activates Ras on the Golgi apparatus by means of RasGRP1*. Nature, 2003. **424**(6949): p. 694-8.
230. Torii, S., et al., *Sef is a spatial regulator for Ras/MAP kinase signaling*. Dev Cell, 2004. **7**(1): p. 33-44.
231. Casar, B., et al., *Mxi2 promotes stimulus-independent ERK nuclear translocation*. EMBO J, 2007. **26**(3): p. 635-46.
232. Sanz, V., I. Arozarena, and P. Crespo, *Distinct carboxy-termini confer divergent characteristics to the mitogen-activated protein kinase p38alpha and its splice isoform Mxi2*. FEBS Lett, 2000. **474**(2-3): p. 169-74.
233. Sanz-Moreno, V., B. Casar, and P. Crespo, *p38alpha isoform Mxi2 binds to extracellular signal-regulated kinase 1 and 2 mitogen-activated protein kinase and regulates its nuclear activity by sustaining its phosphorylation levels*. Mol Cell Biol, 2003. **23**(9): p. 3079-90.
234. Karlsson, M., et al., *Both nuclear-cytoplasmic shuttling of the dual specificity phosphatase MKP-3 and its ability to anchor MAP kinase in the cytoplasm are mediated by a conserved nuclear export signal*. J Biol Chem, 2004. **279**(40): p. 41882-91.
235. Mandl, M., D.N. Slack, and S.M. Keyse, *Specific inactivation and nuclear anchoring of extracellular signal-regulated kinase 2 by the inducible dual-specificity protein phosphatase DUSP5*. Mol Cell Biol, 2005. **25**(5): p. 1830-45.
236. Caunt, C.J., et al., *Spatiotemporal regulation of ERK2 by dual specificity phosphatases*. J Biol Chem, 2008. **283**(39): p. 26612-23.
237. Traverse, S., et al., *Sustained activation of the mitogen-activated protein (MAP) kinase cascade may be required for differentiation of PC12 cells. Comparison of the effects of nerve growth factor and epidermal growth factor*. Biochem J, 1992. **288** (Pt 2): p. 351-5.
238. Eblen, S.T., et al., *Mitogen-activated protein kinase feedback phosphorylation regulates MEK1 complex formation and activation during cellular adhesion*. Mol Cell Biol, 2004. **24**(6): p. 2308-17.
239. Sundberg-Smith, L.J., et al., *Adhesion stimulates direct PAK1/ERK2 association and leads to ERK-dependent PAK1 Thr212 phosphorylation*. J Biol Chem, 2005. **280**(3): p. 2055-64.
240. Coles, L.C. and P.E. Shaw, *PAK1 primes MEK1 for phosphorylation by Raf-1 kinase during cross-cascade activation of the ERK pathway*. Oncogene, 2002. **21**(14): p. 2236-44.
241. Dougherty, M.K., et al., *Regulation of Raf-1 by direct feedback phosphorylation*. Mol Cell, 2005. **17**(2): p. 215-24.
242. Balan, V., et al., *Identification of novel in vivo Raf-1 phosphorylation sites mediating positive feedback Raf-1 regulation by extracellular signal-regulated kinase*. Mol Biol Cell, 2006. **17**(3): p. 1141-53.
243. Corbalan-Garcia, S., et al., *Identification of the mitogen-activated protein kinase phosphorylation sites on human Sos1 that regulate interaction with Grb2*. Mol Cell Biol, 1996. **16**(10): p. 5674-82.

244. Owens, D.M. and S.M. Keyse, *Differential regulation of MAP kinase signalling by dual-specificity protein phosphatases*. *Oncogene*, 2007. **26**(22): p. 3203-13.
245. Kucharska, A., et al., *Regulation of the inducible nuclear dual-specificity phosphatase DUSP5 by ERK MAPK*. *Cell Signal*, 2009. **21**(12): p. 1794-805.
246. Hoshino, R., et al., *Constitutive activation of the 41-/43-kDa mitogen-activated protein kinase signaling pathway in human tumors*. *Oncogene*, 1999. **18**(3): p. 813-22.
247. Stommel, J.M., et al., *Coactivation of receptor tyrosine kinases affects the response of tumor cells to targeted therapies*. *Science*, 2007. **318**(5848): p. 287-90.
248. Chrysogelos, S.A., et al., *Mechanisms of EGF receptor regulation in breast cancer cells*. *Breast Cancer Res Treat*, 1994. **31**(2-3): p. 227-36.
249. Liu, E., et al., *The HER2 (c-erbB-2) oncogene is frequently amplified in in situ carcinomas of the breast*. *Oncogene*, 1992. **7**(5): p. 1027-32.
250. Cirisano, F.D. and B.Y. Karlan, *The role of the HER-2/neu oncogene in gynecologic cancers*. *J Soc Gynecol Investig*, 1996. **3**(3): p. 99-105.
251. Di Fiore, P.P., et al., *erbB-2 is a potent oncogene when overexpressed in NIH/3T3 cells*. *Science*, 1987. **237**(4811): p. 178-82.
252. Grandis, J.R. and J.C. Sok, *Signaling through the epidermal growth factor receptor during the development of malignancy*. *Pharmacol Ther*, 2004. **102**(1): p. 37-46.
253. Tong, L.A., et al., *Crystal structures at 2.2 Å resolution of the catalytic domains of normal ras protein and an oncogenic mutant complexed with GDP*. *J Mol Biol*, 1991. **217**(3): p. 503-16.
254. Scheffzek, K., et al., *The Ras-RasGAP complex: structural basis for GTPase activation and its loss in oncogenic Ras mutants*. *Science*, 1997. **277**(5324): p. 333-8.
255. Davies, H., et al., *Mutations of the BRAF gene in human cancer*. *Nature*, 2002. **417**(6892): p. 949-54.
256. Libra, M., et al., *Analysis of BRAF mutation in primary and metastatic melanoma*. *Cell Cycle*, 2005. **4**(10): p. 1382-4.
257. Franssen, K., et al., *Mutation analysis of the BRAF, ARAF and RAF-1 genes in human colorectal adenocarcinomas*. *Carcinogenesis*, 2004. **25**(4): p. 527-33.
258. Garnett, M.J. and R. Marais, *Guilty as charged: B-RAF is a human oncogene*. *Cancer Cell*, 2004. **6**(4): p. 313-9.
259. Wan, P.T., et al., *Mechanism of activation of the RAF-ERK signaling pathway by oncogenic mutations of B-RAF*. *Cell*, 2004. **116**(6): p. 855-67.
260. Waskiewicz, A.J., et al., *Mitogen-activated protein kinases activate the serine/threonine kinases Mnk1 and Mnk2*. *EMBO J*, 1997. **16**(8): p. 1909-20.
261. Waskiewicz, A.J., et al., *Phosphorylation of the cap-binding protein eukaryotic translation initiation factor 4E by protein kinase Mnk1 in vivo*. *Mol Cell Biol*, 1999. **19**(3): p. 1871-80.
262. Mamane, Y., et al., *Epigenetic activation of a subset of mRNAs by eIF4E explains its effects on cell proliferation*. *PLoS One*, 2007. **2**(2): p. e242.
263. Long, X., et al., *Rheb binds and regulates the mTOR kinase*. *Curr Biol*, 2005. **15**(8): p. 702-13.
264. Ma, L., et al., *Phosphorylation and functional inactivation of TSC2 by Erk implications for tuberous sclerosis and cancer pathogenesis*. *Cell*, 2005. **121**(2): p. 179-93.
265. Roux, P.P., et al., *Tumor-promoting phorbol esters and activated Ras inactivate the tuberous sclerosis tumor suppressor complex via p90 ribosomal S6 kinase*. *Proc Natl Acad Sci U S A*, 2004. **101**(37): p. 13489-94.

266. Stefanovsky, V.Y., et al., *An immediate response of ribosomal transcription to growth factor stimulation in mammals is mediated by ERK phosphorylation of UBF*. Mol Cell, 2001. **8**(5): p. 1063-73.
267. Zhao, J., et al., *ERK-dependent phosphorylation of the transcription initiation factor TIF-IA is required for RNA polymerase I transcription and cell growth*. Mol Cell, 2003. **11**(2): p. 405-13.
268. Kim, D.W. and B.H. Cochran, *Extracellular signal-regulated kinase binds to TFII-I and regulates its activation of the c-fos promoter*. Mol Cell Biol, 2000. **20**(4): p. 1140-8.
269. Felton-Edkins, Z.A., et al., *The mitogen-activated protein (MAP) kinase ERK induces tRNA synthesis by phosphorylating TFIIIB*. EMBO J, 2003. **22**(10): p. 2422-32.
270. Markowitz, R.B., et al., *Phosphorylation of the C-terminal domain of RNA polymerase II by the extracellular-signal-regulated protein kinase ERK2*. Biochem Biophys Res Commun, 1995. **207**(3): p. 1051-7.
271. Suzuki, T., et al., *Phosphorylation of three regulatory serines of Tob by Erk1 and Erk2 is required for Ras-mediated cell proliferation and transformation*. Genes Dev, 2002. **16**(11): p. 1356-70.
272. Alvarez, E., et al., *Pro-Leu-Ser/Thr-Pro is a consensus primary sequence for substrate protein phosphorylation. Characterization of the phosphorylation of c-myc and c-jun proteins by an epidermal growth factor receptor threonine 669 protein kinase*. J Biol Chem, 1991. **266**(23): p. 15277-85.
273. Yang, J.Y., et al., *ERK promotes tumorigenesis by inhibiting FOXO3a via MDM2-mediated degradation*. Nat Cell Biol, 2008. **10**(2): p. 138-48.
274. Biswas, S.C. and L.A. Greene, *Nerve growth factor (NGF) down-regulates the Bcl-2 homology 3 (BH3) domain-only protein Bim and suppresses its proapoptotic activity by phosphorylation*. J Biol Chem, 2002. **277**(51): p. 49511-6.
275. Allan, L.A., et al., *Inhibition of caspase-9 through phosphorylation at Thr 125 by ERK MAPK*. Nat Cell Biol, 2003. **5**(7): p. 647-54.
276. Hunger-Glaser, I., et al., *Bombesin, lysophosphatidic acid, and epidermal growth factor rapidly stimulate focal adhesion kinase phosphorylation at Ser-910: requirement for ERK activation*. J Biol Chem, 2003. **278**(25): p. 22631-43.
277. Klemke, R.L., et al., *Regulation of cell motility by mitogen-activated protein kinase*. J Cell Biol, 1997. **137**(2): p. 481-92.
278. Martinez-Quiles, N., et al., *Erk/Src phosphorylation of cortactin acts as a switch on-switch off mechanism that controls its ability to activate N-WASP*. Mol Cell Biol, 2004. **24**(12): p. 5269-80.
279. Marklund, U., et al., *Multiple signal transduction pathways induce phosphorylation of serines 16, 25, and 38 of oncoprotein 18 in T lymphocytes*. J Biol Chem, 1993. **268**(34): p. 25671-80.
280. Mitsushima, M., et al., *Extracellular signal-regulated kinase activated by epidermal growth factor and cell adhesion interacts with and phosphorylates vinexin*. J Biol Chem, 2004. **279**(33): p. 34570-7.
281. Glading, A., et al., *Epidermal growth factor activates m-calpain (calpain II), at least in part, by extracellular signal-regulated kinase-mediated phosphorylation*. Mol Cell Biol, 2004. **24**(6): p. 2499-512.
282. Graves, L.M., et al., *Regulation of carbamoyl phosphate synthetase by MAP kinase*. Nature, 2000. **403**(6767): p. 328-32.
283. Torii, S., et al., *ERK MAP kinase in G cell cycle progression and cancer*. Cancer Sci, 2006. **97**(8): p. 697-702.

284. Balmanno, K. and S.J. Cook, *Sustained MAP kinase activation is required for the expression of cyclin D1, p21Cip1 and a subset of AP-1 proteins in CCL39 cells.* Oncogene, 1999. **18**(20): p. 3085-97.
285. Yoshida, Y., et al., *Mice lacking a transcriptional corepressor Tob are predisposed to cancer.* Genes Dev, 2003. **17**(10): p. 1201-6.
286. Garnovskaya, M.N., et al., *Mitogen-induced rapid phosphorylation of serine 795 of the retinoblastoma gene product in vascular smooth muscle cells involves ERK activation.* J Biol Chem, 2004. **279**(23): p. 24899-905.
287. Murphy, L.O., J.P. MacKeigan, and J. Blenis, *A network of immediate early gene products propagates subtle differences in mitogen-activated protein kinase signal amplitude and duration.* Mol Cell Biol, 2004. **24**(1): p. 144-53.
288. Bouchard, C., et al., *Direct induction of cyclin D2 by Myc contributes to cell cycle progression and sequestration of p27.* EMBO J, 1999. **18**(19): p. 5321-33.
289. Hermeking, H., et al., *Identification of CDK4 as a target of c-MYC.* Proc Natl Acad Sci U S A, 2000. **97**(5): p. 2229-34.
290. Gartel, A.L. and K. Shchors, *Mechanisms of c-myc-mediated transcriptional repression of growth arrest genes.* Exp Cell Res, 2003. **283**(1): p. 17-21.
291. Staller, P., et al., *Repression of p15INK4b expression by Myc through association with Miz-1.* Nat Cell Biol, 2001. **3**(4): p. 392-9.
292. Claassen, G.F. and S.R. Hann, *A role for transcriptional repression of p21CIP1 by c-Myc in overcoming transforming growth factor beta -induced cell-cycle arrest.* Proc Natl Acad Sci U S A, 2000. **97**(17): p. 9498-503.
293. Adhikary, S. and M. Eilers, *Transcriptional regulation and transformation by Myc proteins.* Nat Rev Mol Cell Biol, 2005. **6**(8): p. 635-45.
294. Hann, S.R. and R.N. Eisenman, *Proteins encoded by the human c-myc oncogene: differential expression in neoplastic cells.* Mol Cell Biol, 1984. **4**(11): p. 2486-97.
295. Sears, R., et al., *Multiple Ras-dependent phosphorylation pathways regulate Myc protein stability.* Genes Dev, 2000. **14**(19): p. 2501-14.
296. Liu, Y., et al., *Regulation of p21WAF1/CIP1 expression through mitogen-activated protein kinase signaling pathway.* Cancer Res, 1996. **56**(1): p. 31-5.
297. Pumiglia, K.M. and S.J. Decker, *Cell cycle arrest mediated by the MEK/mitogen-activated protein kinase pathway.* Proc Natl Acad Sci U S A, 1997. **94**(2): p. 448-52.
298. Harrington, E.A., A. Fanidi, and G.I. Evan, *Oncogenes and cell death.* Curr Opin Genet Dev, 1994. **4**(1): p. 120-9.
299. Kerr, J.F., A.H. Wyllie, and A.R. Currie, *Apoptosis: a basic biological phenomenon with wide-ranging implications in tissue kinetics.* Br J Cancer, 1972. **26**(4): p. 239-57.
300. Adams, J.M. and S. Cory, *The Bcl-2 apoptotic switch in cancer development and therapy.* Oncogene, 2007. **26**(9): p. 1324-37.
301. Puthalakath, H. and A. Strasser, *Keeping killers on a tight leash: transcriptional and post-translational control of the pro-apoptotic activity of BH3-only proteins.* Cell Death Differ, 2002. **9**(5): p. 505-12.
302. Ewings, K.E., et al., *ERK1/2-dependent phosphorylation of BimEL promotes its rapid dissociation from Mcl-1 and Bcl-xL.* EMBO J, 2007. **26**(12): p. 2856-67.
303. Ley, R., et al., *Activation of the ERK1/2 signaling pathway promotes phosphorylation and proteasome-dependent degradation of the BH3-only protein, Bim.* J Biol Chem, 2003. **278**(21): p. 18811-6.
304. Ley, R., et al., *Extracellular signal-regulated kinases 1/2 are serum-stimulated "Bim(EL) kinases" that bind to the BH3-only protein Bim(EL) causing its phosphorylation and turnover.* J Biol Chem, 2004. **279**(10): p. 8837-47.

305. Fang, X., et al., *Regulation of BAD phosphorylation at serine 112 by the Ras-mitogen-activated protein kinase pathway*. *Oncogene*, 1999. **18**(48): p. 6635-40.
306. Datta, S.R., et al., *Akt phosphorylation of BAD couples survival signals to the cell-intrinsic death machinery*. *Cell*, 1997. **91**(2): p. 231-41.
307. Lizcano, J.M., N. Morrice, and P. Cohen, *Regulation of BAD by cAMP-dependent protein kinase is mediated via phosphorylation of a novel site, Ser155*. *Biochem J*, 2000. **349**(Pt 2): p. 547-57.
308. Datta, S.R., et al., *14-3-3 proteins and survival kinases cooperate to inactivate BAD by BH3 domain phosphorylation*. *Mol Cell*, 2000. **6**(1): p. 41-51.
309. Fueller, J., et al., *C-RAF activation promotes BAD poly-ubiquitylation and turnover by the proteasome*. *Biochem Biophys Res Commun*, 2008. **370**(4): p. 552-6.
310. Boucher, M.J., et al., *MEK/ERK signaling pathway regulates the expression of Bcl-2, Bcl-X(L), and Mcl-1 and promotes survival of human pancreatic cancer cells*. *J Cell Biochem*, 2000. **79**(3): p. 355-69.
311. Shaywitz, A.J. and M.E. Greenberg, *CREB: a stimulus-induced transcription factor activated by a diverse array of extracellular signals*. *Annu Rev Biochem*, 1999. **68**: p. 821-61.
312. Arthur, J.S., et al., *Mitogen- and stress-activated protein kinase 1 mediates cAMP response element-binding protein phosphorylation and activation by neurotrophins*. *J Neurosci*, 2004. **24**(18): p. 4324-32.
313. Domina, A.M., et al., *MCL1 is phosphorylated in the PEST region and stabilized upon ERK activation in viable cells, and at additional sites with cytotoxic okadaic acid or taxol*. *Oncogene*, 2004. **23**(31): p. 5301-15.
314. Reddy, K.B., S.M. Nabha, and N. Atanaskova, *Role of MAP kinase in tumor progression and invasion*. *Cancer Metastasis Rev*, 2003. **22**(4): p. 395-403.
315. Pullikuth, A.K. and A.D. Catling, *Scaffold mediated regulation of MAPK signaling and cytoskeletal dynamics: a perspective*. *Cell Signal*, 2007. **19**(8): p. 1621-32.
316. Lovric, J., et al., *Activated raf induces the hyperphosphorylation of stathmin and the reorganization of the microtubule network*. *J Biol Chem*, 1998. **273**(35): p. 22848-55.
317. Chiariello, M., C.B. Bruni, and C. Bucci, *The small GTPases Rab5a, Rab5b and Rab5c are differentially phosphorylated in vitro*. *FEBS Lett*, 1999. **453**(1-2): p. 20-4.
318. Mizutani, K., et al., *Essential roles of ERK-mediated phosphorylation of vinexin in cell spreading, migration and anchorage-independent growth*. *Oncogene*, 2007. **26**(50): p. 7122-31.
319. Carragher, N.O., et al., *A novel role for FAK as a protease-targeting adaptor protein: regulation by p42 ERK and Src*. *Curr Biol*, 2003. **13**(16): p. 1442-50.
320. Cortesio, C.L., et al., *Calpain-mediated proteolysis of paxillin negatively regulates focal adhesion dynamics and cell migration*. *J Biol Chem*, 2011. **286**(12): p. 9998-10006.
321. Franco, S.J., et al., *Calpain-mediated proteolysis of talin regulates adhesion dynamics*. *Nat Cell Biol*, 2004. **6**(10): p. 977-83.
322. Cortesio, C.L., et al., *Calpain 2 and PTP1B function in a novel pathway with Src to regulate invadopodia dynamics and breast cancer cell invasion*. *J Cell Biol*, 2008. **180**(5): p. 957-71.
323. Cruzalegui, F.H., E. Cano, and R. Treisman, *ERK activation induces phosphorylation of Elk-1 at multiple S/T-P motifs to high stoichiometry*. *Oncogene*, 1999. **18**(56): p. 7948-57.
324. Gille, H., A.D. Sharrocks, and P.E. Shaw, *Phosphorylation of transcription factor p62TCF by MAP kinase stimulates ternary complex formation at c-fos promoter*. *Nature*, 1992. **358**(6385): p. 414-7.

325. Tanimura, S., et al., *Prolonged nuclear retention of activated extracellular signal-regulated kinase 1/2 is required for hepatocyte growth factor-induced cell motility*. J Biol Chem, 2002. **277**(31): p. 28256-64.
326. Murphy, L.O., et al., *Molecular interpretation of ERK signal duration by immediate early gene products*. Nat Cell Biol, 2002. **4**(8): p. 556-64.
327. Steeg, P.S., *Tumor metastasis: mechanistic insights and clinical challenges*. Nat Med, 2006. **12**(8): p. 895-904.
328. Hanahan, D. and J. Folkman, *Patterns and emerging mechanisms of the angiogenic switch during tumorigenesis*. Cell, 1996. **86**(3): p. 353-64.
329. Jiang, B.H. and L.Z. Liu, *AKT signaling in regulating angiogenesis*. Curr Cancer Drug Targets, 2008. **8**(1): p. 19-26.
330. Mukhopadhyay, D., et al., *Hypoxic induction of human vascular endothelial growth factor expression through c-Src activation*. Nature, 1995. **375**(6532): p. 577-81.
331. Bancroft, C.C., et al., *Effects of pharmacologic antagonists of epidermal growth factor receptor, PI3K and MEK signal kinases on NF-kappaB and AP-1 activation and IL-8 and VEGF expression in human head and neck squamous cell carcinoma lines*. Int J Cancer, 2002. **99**(4): p. 538-48.
332. Tarkkonen, K., J. Ruohola, and P. Harkonen, *Fibroblast growth factor 8 induced downregulation of thrombospondin 1 is mediated by the MEK/ERK and PI3K pathways in breast cancer cells*. Growth Factors, 2010. **28**(4): p. 256-67.
333. Ebrahim, Q., et al., *Cross-talk between vascular endothelial growth factor and matrix metalloproteinases in the induction of neovascularization in vivo*. Am J Pathol, 2010. **176**(1): p. 496-503.
334. Hawinkels, L.J., et al., *VEGF release by MMP-9 mediated heparan sulphate cleavage induces colorectal cancer angiogenesis*. Eur J Cancer, 2008. **44**(13): p. 1904-13.
335. Versteeg, H.H., M.P. Peppelenbosch, and C.A. Spek, *Tissue factor signal transduction in angiogenesis*. Carcinogenesis, 2003. **24**(6): p. 1009-13.
336. Zhou, J.N., et al., *Activation of tissue-factor gene expression in breast carcinoma cells by stimulation of the RAF-ERK signaling pathway*. Mol Carcinog, 1998. **21**(4): p. 234-43.
337. Kasid, U., *Raf-1 protein kinase, signal transduction, and targeted intervention of radiation response*. Exp Biol Med (Maywood), 2001. **226**(7): p. 624-5.
338. Weinstein-Oppenheimer, C.R., et al., *Role of the Raf signal transduction cascade in the in vitro resistance to the anticancer drug doxorubicin*. Clin Cancer Res, 2001. **7**(9): p. 2898-907.
339. Kim, S.H., et al., *Effect of the activated Raf protein kinase on the human multidrug resistance 1 (MDR1) gene promoter*. Cancer Lett, 1996. **98**(2): p. 199-205.
340. Garcia, R., R.A. Franklin, and J.A. McCubrey, *EGF induces cell motility and multi-drug resistance gene expression in breast cancer cells*. Cell Cycle, 2006. **5**(23): p. 2820-6.
341. Roberts, P.J. and C.J. Der, *Targeting the Raf-MEK-ERK mitogen-activated protein kinase cascade for the treatment of cancer*. Oncogene, 2007. **26**(22): p. 3291-310.
342. Ng, M. and D. Cunningham, *Cetuximab (Erbiximab)--an emerging targeted therapy for epidermal growth factor receptor-expressing tumours*. Int J Clin Pract, 2004. **58**(10): p. 970-6.
343. Bonner, J.A., et al., *Radiotherapy plus cetuximab for squamous-cell carcinoma of the head and neck*. N Engl J Med, 2006. **354**(6): p. 567-78.
344. Cunningham, D., et al., *Cetuximab monotherapy and cetuximab plus irinotecan in irinotecan-refractory metastatic colorectal cancer*. N Engl J Med, 2004. **351**(4): p. 337-45.

345. Gibson, T.B., A. Ranganathan, and A. Grothey, *Randomized phase III trial results of panitumumab, a fully human anti-epidermal growth factor receptor monoclonal antibody, in metastatic colorectal cancer*. Clin Colorectal Cancer, 2006. **6**(1): p. 29-31.
346. Kainuma, O., et al., *Inhibition of growth and invasive activity of human pancreatic cancer cells by a farnesyltransferase inhibitor, manumycin*. Pancreas, 1997. **15**(4): p. 379-83.
347. Wilhelm, S.M., et al., *BAY 43-9006 exhibits broad spectrum oral antitumor activity and targets the RAF/MEK/ERK pathway and receptor tyrosine kinases involved in tumor progression and angiogenesis*. Cancer Res, 2004. **64**(19): p. 7099-109.
348. Chapman, P.B., et al., *Improved survival with vemurafenib in melanoma with BRAF V600E mutation*. N Engl J Med, 2011. **364**(26): p. 2507-16.
349. Davies, S.P., et al., *Specificity and mechanism of action of some commonly used protein kinase inhibitors*. Biochem J, 2000. **351**(Pt 1): p. 95-105.
350. Rinehart, J., et al., *Multicenter phase II study of the oral MEK inhibitor, CI-1040, in patients with advanced non-small-cell lung, breast, colon, and pancreatic cancer*. J Clin Oncol, 2004. **22**(22): p. 4456-62.
351. Cheng, K.W., et al., *The RAB25 small GTPase determines aggressiveness of ovarian and breast cancers*. Nat Med, 2004. **10**(11): p. 1251-6.
352. Hennigan, R.F., K.L. Hawker, and B.W. Ozanne, *Fos-transformation activates genes associated with invasion*. Oncogene, 1994. **9**(12): p. 3591-600.
353. Bass, M.D., et al., *Syndecan-4-dependent Rac1 regulation determines directional migration in response to the extracellular matrix*. J Cell Biol, 2007. **177**(3): p. 527-38.
354. Livak, K.J. and T.D. Schmittgen, *Analysis of relative gene expression data using real-time quantitative PCR and the 2(-Delta Delta C(T)) Method*. Methods, 2001. **25**(4): p. 402-8.
355. Papkoff, J., et al., *p42 mitogen-activated protein kinase and p90 ribosomal S6 kinase are selectively phosphorylated and activated during thrombin-induced platelet activation and aggregation*. Mol Cell Biol, 1994. **14**(1): p. 463-72.
356. Sarbassov, D.D., L.G. Jones, and C.A. Peterson, *Extracellular signal-regulated kinase-1 and -2 respond differently to mitogenic and differentiative signaling pathways in myoblasts*. Mol Endocrinol, 1997. **11**(13): p. 2038-47.
357. Lefloch, R., J. Pouyssegur, and P. Lenormand, *Single and combined silencing of ERK1 and ERK2 reveals their positive contribution to growth signaling depending on their expression levels*. Mol Cell Biol, 2008. **28**(1): p. 511-27.
358. Lee, S.J., T. Zhou, and E.J. Goldsmith, *Crystallization of MAP kinases*. Methods, 2006. **40**(3): p. 224-33.
359. Lefloch, R., J. Pouyssegur, and P. Lenormand, *Total ERK1/2 activity regulates cell proliferation*. Cell Cycle, 2009. **8**(5): p. 705-11.
360. Pages, G., et al., *Defective thymocyte maturation in p44 MAP kinase (Erk 1) knockout mice*. Science, 1999. **286**(5443): p. 1374-7.
361. Hatano, N., et al., *Essential role for ERK2 mitogen-activated protein kinase in placental development*. Genes Cells, 2003. **8**(11): p. 847-56.
362. Saba-EI-Leil, M.K., et al., *An essential function of the mitogen-activated protein kinase Erk2 in mouse trophoblast development*. EMBO Rep, 2003. **4**(10): p. 964-8.
363. Yao, Y., et al., *Extracellular signal-regulated kinase 2 is necessary for mesoderm differentiation*. Proc Natl Acad Sci U S A, 2003. **100**(22): p. 12759-64.
364. Mazzucchelli, C., et al., *Knockout of ERK1 MAP kinase enhances synaptic plasticity in the striatum and facilitates striatal-mediated learning and memory*. Neuron, 2002. **34**(5): p. 807-20.

365. Satoh, Y., et al., *Extracellular signal-regulated kinase 2 (ERK2) knockdown mice show deficits in long-term memory; ERK2 has a specific function in learning and memory.* J Neurosci, 2007. **27**(40): p. 10765-76.
366. Samuels, I.S., et al., *Deletion of ERK2 mitogen-activated protein kinase identifies its key roles in cortical neurogenesis and cognitive function.* J Neurosci, 2008. **28**(27): p. 6983-95.
367. Bost, F., et al., *The extracellular signal-regulated kinase isoform ERK1 is specifically required for in vitro and in vivo adipogenesis.* Diabetes, 2005. **54**(2): p. 402-11.
368. Krens, S.F., et al., *Characterization and expression patterns of the MAPK family in zebrafish.* Gene Expr Patterns, 2006. **6**(8): p. 1019-26.
369. Krens, S.F., et al., *Distinct functions for ERK1 and ERK2 in cell migration processes during zebrafish gastrulation.* Dev Biol, 2008. **319**(2): p. 370-83.
370. Li, J. and S.E. Johnson, *ERK2 is required for efficient terminal differentiation of skeletal myoblasts.* Biochem Biophys Res Commun, 2006. **345**(4): p. 1425-33.
371. Vantaggiato, C., et al., *ERK1 and ERK2 mitogen-activated protein kinases affect Ras-dependent cell signaling differentially.* J Biol, 2006. **5**(5): p. 14.
372. Fremin, C., et al., *ERK2 but not ERK1 plays a key role in hepatocyte replication: an RNAi-mediated ERK2 knockdown approach in wild-type and ERK1 null hepatocytes.* Hepatology, 2007. **45**(4): p. 1035-45.
373. Bourcier, C., et al., *p44 mitogen-activated protein kinase (extracellular signal-regulated kinase 1)-dependent signaling contributes to epithelial skin carcinogenesis.* Cancer Res, 2006. **66**(5): p. 2700-7.
374. Liu, X., et al., *The MAP kinase pathway is required for entry into mitosis and cell survival.* Oncogene, 2004. **23**(3): p. 763-76.
375. Zeng, P., et al., *RNA interference (RNAi) for extracellular signal-regulated kinase 1 (ERK1) alone is sufficient to suppress cell viability in ovarian cancer cells.* Cancer Biol Ther, 2005. **4**(9): p. 961-7.
376. Voisin, L., et al., *Genetic demonstration of a redundant role of extracellular signal-regulated kinase 1 (ERK1) and ERK2 mitogen-activated protein kinases in promoting fibroblast proliferation.* Mol Cell Biol, 2010. **30**(12): p. 2918-32.
377. Adeyinka, A., et al., *Activated mitogen-activated protein kinase expression during human breast tumorigenesis and breast cancer progression.* Clin Cancer Res, 2002. **8**(6): p. 1747-53.
378. Chen, H., et al., *Extracellular signal-regulated kinase signaling pathway regulates breast cancer cell migration by maintaining slug expression.* Cancer Res, 2009. **69**(24): p. 9228-35.
379. Bessard, A., et al., *MEK/ERK-dependent uPAR expression is required for motility via phosphorylation of P70S6K in human hepatocarcinoma cells.* J Cell Physiol, 2007. **212**(2): p. 526-36.
380. Caswell, P.T., et al., *Rab25 associates with alpha5beta1 integrin to promote invasive migration in 3D microenvironments.* Dev Cell, 2007. **13**(4): p. 496-510.
381. Nagata, S., *Apoptosis by death factor.* Cell, 1997. **88**(3): p. 355-65.
382. Soldani, C. and A.I. Scovassi, *Poly(ADP-ribose) polymerase-1 cleavage during apoptosis: an update.* Apoptosis, 2002. **7**(4): p. 321-8.
383. Gao, J., et al., *Significant anti-proliferation of human endometrial cancer cells by combined treatment with a selective COX-2 inhibitor NS398 and specific MEK inhibitor U0126.* Int J Oncol, 2005. **26**(3): p. 737-44.
384. Lind, C.R., et al., *The mitogen-activated/extracellular signal-regulated kinase kinase 1/2 inhibitor U0126 induces glial fibrillary acidic protein expression and reduces the proliferation and migration of C6 glioma cells.* Neuroscience, 2006. **141**(4): p. 1925-33.

385. Marampon, F., et al., *MEK/ERK inhibitor U0126 affects in vitro and in vivo growth of embryonal rhabdomyosarcoma*. *Mol Cancer Ther*, 2009. **8**(3): p. 543-51.
386. Wang, W., et al., *Identification and testing of a gene expression signature of invasive carcinoma cells within primary mammary tumors*. *Cancer Res*, 2004. **64**(23): p. 8585-94.
387. Beningo, K.A., M. Dembo, and Y.L. Wang, *Responses of fibroblasts to anchorage of dorsal extracellular matrix receptors*. *Proc Natl Acad Sci U S A*, 2004. **101**(52): p. 18024-9.
388. Hay, E.D., *The mesenchymal cell, its role in the embryo, and the remarkable signaling mechanisms that create it*. *Dev Dyn*, 2005. **233**(3): p. 706-20.
389. Zamir, E., et al., *Molecular diversity of cell-matrix adhesions*. *J Cell Sci*, 1999. **112** (Pt 11): p. 1655-69.
390. Gloeckner, C.J., K. Boldt, and M. Ueffing, *Strep/FLAG tandem affinity purification (SF-TAP) to study protein interactions*. *Curr Protoc Protein Sci*, 2009. **Chapter 19**: p. Unit19 20.
391. Ge, X., Y.M. Fu, and G.G. Meadows, *U0126, a mitogen-activated protein kinase kinase inhibitor, inhibits the invasion of human A375 melanoma cells*. *Cancer Lett*, 2002. **179**(2): p. 133-40.
392. Kornyei, Z., et al., *Proliferative and migratory responses of astrocytes to in vitro injury*. *J Neurosci Res*, 2000. **61**(4): p. 421-9.
393. Coomber, B.L. and A.I. Gotlieb, *In vitro endothelial wound repair. Interaction of cell migration and proliferation*. *Arteriosclerosis*, 1990. **10**(2): p. 215-22.
394. Friedl, P., K.S. Zanker, and E.B. Brocker, *Cell migration strategies in 3-D extracellular matrix: differences in morphology, cell matrix interactions, and integrin function*. *Microsc Res Tech*, 1998. **43**(5): p. 369-78.
395. Li, S., et al., *Genomic analysis of smooth muscle cells in 3-dimensional collagen matrix*. *FASEB J*, 2003. **17**(1): p. 97-9.
396. Coso, O.A., et al., *The small GTP-binding proteins Rac1 and Cdc42 regulate the activity of the JNK/SAPK signaling pathway*. *Cell*, 1995. **81**(7): p. 1137-46.
397. Minden, A., et al., *Selective activation of the JNK signaling cascade and c-Jun transcriptional activity by the small GTPases Rac and Cdc42Hs*. *Cell*, 1995. **81**(7): p. 1147-57.
398. Postma, M., et al., *Chemotaxis: signalling modules join hands at front and tail*. *EMBO Rep*, 2004. **5**(1): p. 35-40.
399. Kimura, K., et al., *Regulation of myosin phosphatase by Rho and Rho-associated kinase (Rho-kinase)*. *Science*, 1996. **273**(5272): p. 245-8.
400. Szczur, K., et al., *Rho GTPase CDC42 regulates directionality and random movement via distinct MAPK pathways in neutrophils*. *Blood*, 2006. **108**(13): p. 4205-13.
401. Eblen, S.T., et al., *Rac-PAK signaling stimulates extracellular signal-regulated kinase (ERK) activation by regulating formation of MEK1-ERK complexes*. *Mol Cell Biol*, 2002. **22**(17): p. 6023-33.
402. Zang, M., C. Hayne, and Z. Luo, *Interaction between active Pak1 and Raf-1 is necessary for phosphorylation and activation of Raf-1*. *J Biol Chem*, 2002. **277**(6): p. 4395-405.
403. Fincham, V.J., et al., *Active ERK/MAP kinase is targeted to newly forming cell-matrix adhesions by integrin engagement and v-Src*. *EMBO J*, 2000. **19**(12): p. 2911-23.
404. Brahmabhatt, A.A. and R.L. Klemke, *ERK and RhoA differentially regulate pseudopodia growth and retraction during chemotaxis*. *J Biol Chem*, 2003. **278**(15): p. 13016-25.

405. Fujishiro, S.H., et al., *ERK1/2 phosphorylate GEF-H1 to enhance its guanine nucleotide exchange activity toward RhoA*. *Biochem Biophys Res Commun*, 2008. **368**(1): p. 162-7.
406. Bisel, B., et al., *ERK regulates Golgi and centrosome orientation towards the leading edge through GRASP65*. *J Cell Biol*, 2008. **182**(5): p. 837-43.
407. Ochieng, J., et al., *Increased invasive, chemotactic and locomotive abilities of c-Ha-ras-transformed human breast epithelial cells*. *Invasion Metastasis*, 1991. **11**(1): p. 38-47.
408. Rodier, J.M., et al., *pp60c-src is a positive regulator of growth factor-induced cell scattering in a rat bladder carcinoma cell line*. *J Cell Biol*, 1995. **131**(3): p. 761-73.
409. Ueoka, Y., et al., *Hepatocyte growth factor modulates motility and invasiveness of ovarian carcinomas via Ras-mediated pathway*. *Br J Cancer*, 2000. **82**(4): p. 891-9.
410. Satoh, Y., et al., *ERK2 dependent signaling contributes to wound healing after a partial-thickness burn*. *Biochem Biophys Res Commun*, 2009. **381**(1): p. 118-22.
411. Krens, S.F., et al., *ERK1 and ERK2 MAPK are key regulators of distinct gene sets in zebrafish embryogenesis*. *BMC Genomics*, 2008. **9**: p. 196.
412. Shin, S., et al., *ERK2 but not ERK1 induces epithelial-to-mesenchymal transformation via DEF motif-dependent signaling events*. *Mol Cell*. **38**(1): p. 114-27.
413. Gee, J.M., et al., *Phosphorylation of ERK1/2 mitogen-activated protein kinase is associated with poor response to anti-hormonal therapy and decreased patient survival in clinical breast cancer*. *Int J Cancer*, 2001. **95**(4): p. 247-54.
414. Milde-Langosch, K., et al., *Expression and prognostic relevance of activated extracellular-regulated kinases (ERK1/2) in breast cancer*. *Br J Cancer*, 2005. **92**(12): p. 2206-15.
415. Satoh, J., et al., *Protein microarray analysis identifies human cellular prion protein interactors*. *Neuropathol Appl Neurobiol*, 2009. **35**(1): p. 16-35.
416. Marchi, M., et al., *The N-terminal domain of ERK1 accounts for the functional differences with ERK2*. *PLoS One*, 2008. **3**(12): p. e3873.
417. Lakka, S.S., et al., *Downregulation of MMP-9 in ERK-mutated stable transfectants inhibits glioma invasion in vitro*. *Oncogene*, 2002. **21**(36): p. 5601-8.
418. McCawley, L.J., et al., *Sustained activation of the mitogen-activated protein kinase pathway. A mechanism underlying receptor tyrosine kinase specificity for matrix metalloproteinase-9 induction and cell migration*. *J Biol Chem*, 1999. **274**(7): p. 4347-53.
419. Nguyen, D.H., et al., *Myosin light chain kinase functions downstream of Ras/ERK to promote migration of urokinase-type plasminogen activator-stimulated cells in an integrin-selective manner*. *J Cell Biol*, 1999. **146**(1): p. 149-64.
420. Alblas, J., et al., *The role of MAP kinase in TPA-mediated cell cycle arrest of human breast cancer cells*. *Oncogene*, 1998. **16**(1): p. 131-9.
421. Chu, B., et al., *Sequential phosphorylation by mitogen-activated protein kinase and glycogen synthase kinase 3 represses transcriptional activation by heat shock factor-1*. *J Biol Chem*, 1996. **271**(48): p. 30847-57.
422. Yehia, G., et al., *Mitogen-activated protein kinase phosphorylates and targets inducible cAMP early repressor to ubiquitin-mediated destruction*. *J Biol Chem*, 2001. **276**(38): p. 35272-9.
423. Feng, J. and B. Villeponteau, *High-resolution analysis of c-fos chromatin accessibility using a novel DNase I-PCR assay*. *Biochim Biophys Acta*, 1992. **1130**(3): p. 253-8.
424. Allegra, P., et al., *Affinity chromatographic purification of nucleosomes containing transcriptionally active DNA sequences*. *J Mol Biol*, 1987. **196**(2): p. 379-88.

425. Chen, T.A. and V.G. Allfrey, *Rapid and reversible changes in nucleosome structure accompany the activation, repression, and superinduction of murine fibroblast protooncogenes c-fos and c-myc*. Proc Natl Acad Sci U S A, 1987. **84**(15): p. 5252-6.
426. Sassone-Corsi, P., et al., *Requirement of Rsk-2 for epidermal growth factor-activated phosphorylation of histone H3*. Science, 1999. **285**(5429): p. 886-91.
427. Thomson, S., et al., *The nucleosomal response associated with immediate-early gene induction is mediated via alternative MAP kinase cascades: MSK1 as a potential histone H3/HMG-14 kinase*. EMBO J, 1999. **18**(17): p. 4779-93.
428. Soloaga, A., et al., *MSK2 and MSK1 mediate the mitogen- and stress-induced phosphorylation of histone H3 and HMG-14*. EMBO J, 2003. **22**(11): p. 2788-97.
429. Clayton, A.L., et al., *Phosphoacetylation of histone H3 on c-fos- and c-jun-associated nucleosomes upon gene activation*. EMBO J, 2000. **19**(14): p. 3714-26.
430. Weg-Remers, S., et al., *Regulation of alternative pre-mRNA splicing by the ERK MAP-kinase pathway*. EMBO J, 2001. **20**(15): p. 4194-203.
431. Habelhah, H., et al., *ERK phosphorylation drives cytoplasmic accumulation of hnRNP-K and inhibition of mRNA translation*. Nat Cell Biol, 2001. **3**(3): p. 325-30.
432. Chen, L.C., et al., *Thymidine phosphorylase mRNA stability and protein levels are increased through ERK-mediated cytoplasmic accumulation of hnRNP K in nasopharyngeal carcinoma cells*. Oncogene, 2009. **28**(17): p. 1904-15.
433. Mikula, M. and K. Bomsztyk, *Direct recruitment of ERK cascade components to inducible genes is regulated by heterogeneous nuclear ribonucleoprotein (hnRNP) K*. J Biol Chem, 2011. **286**(11): p. 9763-75.
434. Paroo, Z., et al., *Phosphorylation of the human microRNA-generating complex mediates MAPK/Erk signaling*. Cell, 2009. **139**(1): p. 112-22.
435. Filipowicz, W., S.N. Bhattacharyya, and N. Sonenberg, *Mechanisms of post-transcriptional regulation by microRNAs: are the answers in sight?* Nat Rev Genet, 2008. **9**(2): p. 102-14.
436. Nigg, E.A., *Nucleocytoplasmic transport: signals, mechanisms and regulation*. Nature, 1997. **386**(6627): p. 779-87.
437. Stewart, M., *Molecular mechanism of the nuclear protein import cycle*. Nat Rev Mol Cell Biol, 2007. **8**(3): p. 195-208.
438. Lange, A., et al., *Classical nuclear localization signals: definition, function, and interaction with importin alpha*. J Biol Chem, 2007. **282**(8): p. 5101-5.
439. Christophe, D., C. Christophe-Hobertus, and B. Pichon, *Nuclear targeting of proteins: how many different signals?* Cell Signal, 2000. **12**(5): p. 337-41.
440. Adachi, M., M. Fukuda, and E. Nishida, *Two co-existing mechanisms for nuclear import of MAP kinase: passive diffusion of a monomer and active transport of a dimer*. EMBO J, 1999. **18**(19): p. 5347-58.
441. Wolf, I., et al., *Involvement of the activation loop of ERK in the detachment from cytosolic anchoring*. J Biol Chem, 2001. **276**(27): p. 24490-7.
442. Casar, B., A. Pinto, and P. Crespo, *Essential role of ERK dimers in the activation of cytoplasmic but not nuclear substrates by ERK-scaffold complexes*. Mol Cell, 2008. **31**(5): p. 708-21.
443. Lidke, D.S., et al., *ERK nuclear translocation is dimerization-independent but controlled by the rate of phosphorylation*. J Biol Chem, 2010. **285**(5): p. 3092-102.
444. Chuderland, D., A. Konson, and R. Seger, *Identification and characterization of a general nuclear translocation signal in signaling proteins*. Mol Cell, 2008. **31**(6): p. 850-61.
445. Matsubayashi, Y., M. Fukuda, and E. Nishida, *Evidence for existence of a nuclear pore complex-mediated, cytosol-independent pathway of nuclear translocation of ERK MAP kinase in permeabilized cells*. J Biol Chem, 2001. **276**(45): p. 41755-60.

446. Kosako, H., et al., *Phosphoproteomics reveals new ERK MAP kinase targets and links ERK to nucleoporin-mediated nuclear transport*. Nat Struct Mol Biol, 2009. **16**(10): p. 1026-35.
447. Lin, T.H., et al., *Cell anchorage permits efficient signal transduction between ras and its downstream kinases*. J Biol Chem, 1997. **272**(14): p. 8849-52.
448. Aplin, A.E., S.M. Short, and R.L. Juliano, *Anchorage-dependent regulation of the mitogen-activated protein kinase cascade by growth factors is supported by a variety of integrin alpha chains*. J Biol Chem, 1999. **274**(44): p. 31223-8.
449. Miyamoto, S., et al., *Integrins can collaborate with growth factors for phosphorylation of receptor tyrosine kinases and MAP kinase activation: roles of integrin aggregation and occupancy of receptors*. J Cell Biol, 1996. **135**(6 Pt 1): p. 1633-42.
450. Short, S.M., J.L. Boyer, and R.L. Juliano, *Integrins regulate the linkage between upstream and downstream events in G protein-coupled receptor signaling to mitogen-activated protein kinase*. J Biol Chem, 2000. **275**(17): p. 12970-7.
451. Aplin, A.E., et al., *Integrin-mediated adhesion regulates ERK nuclear translocation and phosphorylation of Elk-1*. J Cell Biol, 2001. **153**(2): p. 273-82.
452. Bolstad, B.M., et al., *A comparison of normalization methods for high density oligonucleotide array data based on variance and bias*. Bioinformatics, 2003. **19**(2): p. 185-93.
453. Schmid, R., et al., *Comparison of normalization methods for Illumina BeadChip HumanHT-12 v3*. BMC Genomics, 2010. **11**: p. 349.
454. Churchill, G.A., *Using ANOVA to analyze microarray data*. Biotechniques, 2004. **37**(2): p. 173-5, 177.
455. Scheffe, J.H., et al., *Quantitative real-time RT-PCR data analysis: current concepts and the novel "gene expression's CT difference" formula*. J Mol Med (Berl), 2006. **84**(11): p. 901-10.
456. Arezi, B., et al., *Amplification efficiency of thermostable DNA polymerases*. Anal Biochem, 2003. **321**(2): p. 226-35.
457. Pfaffl, M.W., *A new mathematical model for relative quantification in real-time RT-PCR*. Nucleic Acids Res, 2001. **29**(9): p. e45.
458. Bussolino, F., et al., *Granulocyte- and granulocyte-macrophage-colony stimulating factors induce human endothelial cells to migrate and proliferate*. Nature, 1989. **337**(6206): p. 471-3.
459. Gutschalk, C.M., et al., *Granulocyte colony-stimulating factor and granulocyte-macrophage colony-stimulating factor promote malignant growth of cells from head and neck squamous cell carcinomas in vivo*. Cancer Res, 2006. **66**(16): p. 8026-36.
460. Lederle, W., et al., *IL-6 promotes malignant growth of skin SCCs by regulating a network of autocrine and paracrine cytokines*. Int J Cancer, 2011. **128**(12): p. 2803-14.
461. Gasson, J.C., *Molecular physiology of granulocyte-macrophage colony-stimulating factor*. Blood, 1991. **77**(6): p. 1131-45.
462. Zacchi, P., et al., *Rab17 regulates membrane trafficking through apical recycling endosomes in polarized epithelial cells*. J Cell Biol, 1998. **140**(5): p. 1039-53.
463. McMurtrie, E.B., et al., *Rab17 and rab18, small GTPases with specificity for polarized epithelial cells: genetic mapping in the mouse*. Genomics, 1997. **45**(3): p. 623-5.
464. Serra-Pages, C., et al., *Liprins, a family of LAR transmembrane protein-tyrosine phosphatase-interacting proteins*. J Biol Chem, 1998. **273**(25): p. 15611-20.
465. Jackson, A.L., et al., *Expression profiling reveals off-target gene regulation by RNAi*. Nat Biotechnol, 2003. **21**(6): p. 635-7.

466. Scacheri, P.C., et al., *Short interfering RNAs can induce unexpected and divergent changes in the levels of untargeted proteins in mammalian cells*. Proc Natl Acad Sci U S A, 2004. **101**(7): p. 1892-7.
467. Williams, B.R.G., et al., *Activation of the interferon system by short-interfering RNAs*. Nature Cell Biology, 2003. **5**(9): p. 834-839.
468. Hu, S., et al., *Profiling the human protein-DNA interactome reveals ERK2 as a transcriptional repressor of interferon signaling*. Cell, 2009. **139**(3): p. 610-22.
469. Wang, X., et al., *RAF may induce cell proliferation through hypermethylation of tumor suppressor gene promoter in gastric epithelial cells*. Cancer Sci, 2009. **100**(1): p. 117-25.
470. Shapiro, P.S., et al., *Extracellular signal-regulated kinase activates topoisomerase IIalpha through a mechanism independent of phosphorylation*. Mol Cell Biol, 1999. **19**(5): p. 3551-60.
471. Karin, M., *Too many transcription factors: positive and negative interactions*. New Biol, 1990. **2**(2): p. 126-31.
472. Morton, S., et al., *A reinvestigation of the multisite phosphorylation of the transcription factor c-Jun*. EMBO J, 2003. **22**(15): p. 3876-86.
473. Manabe, A., et al., *Transcriptional repression activity of N-MYC protein requires phosphorylation by MAP kinase*. Biochem Biophys Res Commun, 1996. **219**(3): p. 813-23.
474. Guhaniyogi, J. and G. Brewer, *Regulation of mRNA stability in mammalian cells*. Gene, 2001. **265**(1-2): p. 11-23.
475. Proudfoot, N.J., A. Furger, and M.J. Dye, *Integrating mRNA processing with transcription*. Cell, 2002. **108**(4): p. 501-12.
476. Brook, M., et al., *Posttranslational regulation of tristetraprolin subcellular localization and protein stability by p38 mitogen-activated protein kinase and extracellular signal-regulated kinase pathways*. Mol Cell Biol, 2006. **26**(6): p. 2408-18.
477. Essafi-Benkhadir, K., et al., *Tristetraprolin inhibits Ras-dependent tumor vascularization by inducing vascular endothelial growth factor mRNA degradation*. Mol Biol Cell, 2007. **18**(11): p. 4648-58.
478. Carballo, E., W.S. Lai, and P.J. Blackshear, *Evidence that tristetraprolin is a physiological regulator of granulocyte-macrophage colony-stimulating factor messenger RNA deadenylation and stability*. Blood, 2000. **95**(6): p. 1891-9.
479. Raught, B. and A.C. Gingras, *eIF4E activity is regulated at multiple levels*. Int J Biochem Cell Biol, 1999. **31**(1): p. 43-57.
480. Li, X.J., et al., *Serglycin is a theranostic target in nasopharyngeal carcinoma that promotes metastasis*. Cancer Res, 2011. **71**(8): p. 3162-72.
481. Wei, Q., et al., *Sulfiredoxin is an AP-1 target gene that is required for transformation and shows elevated expression in human skin malignancies*. Proc Natl Acad Sci U S A, 2008. **105**(50): p. 19738-43.
482. Wei, Q., et al., *Sulfiredoxin-Peroxiredoxin IV axis promotes human lung cancer progression through modulation of specific phosphokinase signaling*. Proc Natl Acad Sci U S A, 2011. **108**(17): p. 7004-9.
483. Cadenas, C., et al., *Role of thioredoxin reductase 1 and thioredoxin interacting protein in prognosis of breast cancer*. Breast Cancer Res, 2010. **12**(3): p. R44.
484. Nishizawa, K., et al., *Thioredoxin interacting protein suppresses bladder carcinogenesis*. Carcinogenesis, 2011.
485. Dunn, T.A., et al., *A novel role of myosin VI in human prostate cancer*. Am J Pathol, 2006. **169**(5): p. 1843-54.

486. Silvers, A.L., et al., *Decreased selenium-binding protein 1 in esophageal adenocarcinoma results from posttranscriptional and epigenetic regulation and affects chemosensitivity*. Clin Cancer Res, 2010. **16**(7): p. 2009-21.
487. Kim, H., et al., *Suppression of human selenium-binding protein 1 is a late event in colorectal carcinogenesis and is associated with poor survival*. Proteomics, 2006. **6**(11): p. 3466-76.
488. Chen, G., et al., *Reduced selenium-binding protein 1 expression is associated with poor outcome in lung adenocarcinomas*. J Pathol, 2004. **202**(3): p. 321-9.
489. Pohl, N.M., et al., *Transcriptional regulation and biological functions of selenium-binding protein 1 in colorectal cancer in vitro and in nude mouse xenografts*. PLoS One, 2009. **4**(11): p. e7774.
490. Pollock, C.B., et al., *Oncogenic K-RAS is required to maintain changes in cytoskeletal organization, adhesion, and motility in colon cancer cells*. Cancer Res, 2005. **65**(4): p. 1244-50.
491. Colicelli, J., *Human RAS superfamily proteins and related GTPases*. Sci STKE, 2004. **2004**(250): p. RE13.
492. Stenmark, H. and V.M. Olkkonen, *The Rab GTPase family*. Genome Biol, 2001. **2**(5): p. REVIEWS3007.
493. Pfeffer, S. and D. Aivazian, *Targeting Rab GTPases to distinct membrane compartments*. Nat Rev Mol Cell Biol, 2004. **5**(11): p. 886-96.
494. van der Sluijs, P., et al., *The small GTP-binding protein rab4 controls an early sorting event on the endocytic pathway*. Cell, 1992. **70**(5): p. 729-40.
495. Chavrier, P., et al., *Localization of low molecular weight GTP binding proteins to exocytic and endocytic compartments*. Cell, 1990. **62**(2): p. 317-29.
496. Ullrich, O., et al., *Rab11 regulates recycling through the pericentriolar recycling endosome*. J Cell Biol, 1996. **135**(4): p. 913-24.
497. Lutcke, A., et al., *Rab17, a novel small GTPase, is specific for epithelial cells and is induced during cell polarization*. J Cell Biol, 1993. **121**(3): p. 553-64.
498. Hunziker, W. and P.J. Peters, *Rab17 localizes to recycling endosomes and regulates receptor-mediated transcytosis in epithelial cells*. J Biol Chem, 1998. **273**(25): p. 15734-41.
499. Fukuda, M., *Regulation of secretory vesicle traffic by Rab small GTPases*. Cell Mol Life Sci, 2008. **65**(18): p. 2801-13.
500. Woodman, P.G., *Biogenesis of the sorting endosome: the role of Rab5*. Traffic, 2000. **1**(9): p. 695-701.
501. Mesa, R., et al., *Rab22a affects the morphology and function of the endocytic pathway*. J Cell Sci, 2001. **114**(Pt 22): p. 4041-9.
502. Erdman, R.A., et al., *Rab24 is an atypical member of the Rab GTPase family. Deficient GTPase activity, GDP dissociation inhibitor interaction, and prenylation of Rab24 expressed in cultured cells*. J Biol Chem, 2000. **275**(6): p. 3848-56.
503. Amillet, J.M., et al., *Characterization of human Rab20 overexpressed in exocrine pancreatic carcinoma*. Hum Pathol, 2006. **37**(3): p. 256-63.
504. Yoshimura, S., et al., *Functional dissection of Rab GTPases involved in primary cilium formation*. J Cell Biol, 2007. **178**(3): p. 363-9.
505. Bucci, C., et al., *Interaction cloning and characterization of the cDNA encoding the human prenylated rab acceptor (PRA1)*. Biochem Biophys Res Commun, 1999. **258**(3): p. 657-62.
506. Stelzl, U., et al., *A human protein-protein interaction network: a resource for annotating the proteome*. Cell, 2005. **122**(6): p. 957-68.
507. Ewing, R.M., et al., *Large-scale mapping of human protein-protein interactions by mass spectrometry*. Mol Syst Biol, 2007. **3**: p. 89.

508. Barrios-Rodiles, M., et al., *High-throughput mapping of a dynamic signaling network in mammalian cells*. Science, 2005. **307**(5715): p. 1621-5.
509. Serra-Pages, C., et al., *The LAR transmembrane protein tyrosine phosphatase and a coiled-coil LAR-interacting protein co-localize at focal adhesions*. EMBO J, 1995. **14**(12): p. 2827-38.
510. Nachat, R., et al., *KazrinE is a desmosome-associated liprin that colocalises with acetylated microtubules*. J Cell Sci, 2009. **122**(Pt 22): p. 4035-41.
511. Wei, Z., et al., *Liprin-Mediated Large Signaling Complex Organization Revealed by the Liprin-alpha/CASK and Liprin-alpha/Liprin-beta Complex Structures*. Mol Cell, 2011. **43**(4): p. 586-98.
512. Stafford, R.L., et al., *Crystal structure of the central coiled-coil domain from human liprin-beta2*. Biochemistry, 2011. **50**(18): p. 3807-15.
513. Parry, D.A., et al., *Towards a molecular description of intermediate filament structure and assembly*. Exp Cell Res, 2007. **313**(10): p. 2204-16.
514. Miroshnichenko, N.S., I.V. Balanuk, and D.N. Nozdrenko, *Packing of myosin molecules in muscle thick filaments*. Cell Biol Int, 2000. **24**(6): p. 327-33.
515. Meruelo, A.D. and J.U. Bowie, *Identifying polymer-forming SAM domains*. Proteins, 2009. **74**(1): p. 1-5.
516. Stryker, E. and K.G. Johnson, *LAR, liprin alpha and the regulation of active zone morphogenesis*. J Cell Sci, 2007. **120**(Pt 21): p. 3723-8.
517. Spangler, S.A. and C.C. Hoogenraad, *Liprin-alpha proteins: scaffold molecules for synapse maturation*. Biochem Soc Trans, 2007. **35**(Pt 5): p. 1278-82.
518. de Curtis, I., *Function of liprins in cell motility*. Exp Cell Res, 2011. **317**(1): p. 1-8.
519. Asperti, C., et al., *Liprin-alpha1 promotes cell spreading on the extracellular matrix by affecting the distribution of activated integrins*. J Cell Sci, 2009. **122**(Pt 18): p. 3225-32.
520. Asperti, C., E. Pettinato, and I. de Curtis, *Liprin-alpha1 affects the distribution of low-affinity beta1 integrins and stabilizes their permanence at the cell surface*. Exp Cell Res, 2010. **316**(6): p. 915-26.
521. Norrmen, C., et al., *Liprin (beta)1 is highly expressed in lymphatic vasculature and is important for lymphatic vessel integrity*. Blood, 2010. **115**(4): p. 906-9.
522. Kriajevska, M., et al., *Liprin beta 1, a member of the family of LAR transmembrane tyrosine phosphatase-interacting proteins, is a new target for the metastasis-associated protein S100A4 (Mts1)*. J Biol Chem, 2002. **277**(7): p. 5229-35.
523. Rual, J.F., et al., *Towards a proteome-scale map of the human protein-protein interaction network*. Nature, 2005. **437**(7062): p. 1173-8.
524. Benzinger, A., et al., *Targeted proteomic analysis of 14-3-3 sigma, a p53 effector commonly silenced in cancer*. Mol Cell Proteomics, 2005. **4**(6): p. 785-95.
525. Muller, P.A., et al., *Mutant p53 drives invasion by promoting integrin recycling*. Cell, 2009. **139**(7): p. 1327-41.
526. Pellinen, T., et al., *Small GTPase Rab21 regulates cell adhesion and controls endosomal traffic of beta1-integrins*. J Cell Biol, 2006. **173**(5): p. 767-80.
527. Singh, A., et al., *A gene expression signature associated with "K-Ras addiction" reveals regulators of EMT and tumor cell survival*. Cancer Cell, 2009. **15**(6): p. 489-500.
528. Caswell, P.T., et al., *Rab-coupling protein coordinates recycling of alpha5beta1 integrin and EGFR1 to promote cell migration in 3D microenvironments*. J Cell Biol, 2008. **183**(1): p. 143-55.
529. Jarvinen, A.K., et al., *Identification of target genes in laryngeal squamous cell carcinoma by high-resolution copy number and gene expression microarray analyses*. Oncogene, 2006. **25**(52): p. 6997-7008.

-
530. Jarvinen, A.K., et al., *High-resolution copy number and gene expression microarray analyses of head and neck squamous cell carcinoma cell lines of tongue and larynx*. *Genes Chromosomes Cancer*, 2008. **47**(6): p. 500-9.
 531. Ko, J., et al., *Interaction between liprin-alpha and GIT1 is required for AMPA receptor targeting*. *J Neurosci*, 2003. **23**(5): p. 1667-77.
 532. Shin, H., et al., *Association of the kinesin motor KIF1A with the multimodular protein liprin-alpha*. *J Biol Chem*, 2003. **278**(13): p. 11393-401.
 533. Shen, J.C., et al., *Inhibitor of growth 4 suppresses cell spreading and cell migration by interacting with a novel binding partner, liprin alpha1*. *Cancer Res*, 2007. **67**(6): p. 2552-8.
 534. Tan, K.D., et al., *Amplification and overexpression of PPF1A1, a putative 11q13 invasion suppressor gene, in head and neck squamous cell carcinoma*. *Genes Chromosomes Cancer*, 2008. **47**(4): p. 353-62.
 535. Rhodes, D.R., et al., *ONCOMINE: a cancer microarray database and integrated data-mining platform*. *Neoplasia*, 2004. **6**(1): p. 1-6.
 536. Chen, G., et al., *Discordant protein and mRNA expression in lung adenocarcinomas*. *Mol Cell Proteomics*, 2002. **1**(4): p. 304-13.
 537. Ewings, K.E., C.M. Wiggins, and S.J. Cook, *Bim and the pro-survival Bcl-2 proteins: opposites attract, ERK repels*. *Cell Cycle*, 2007. **6**(18): p. 2236-40.